Theory of

Molecular Auger Spectroscopy

by

Elzbieta Zofia Chelkowska, M.Sc.

Wroclaw University

submitted in fulfilment of the requirements

for the degree of

Doctor of Philosophy

University of Tasmania

April 1993.

Krzysiowi i Mirkowi

The important thing in science is not so much to obtain new facts as to discover new ways of thinking about them.

Sir William Lawrence Bragg

Statement

Except as stated herein, this thesis contains no material which has been accepted for the award of any other degree or diploma in any university, and to the best of my knowledge and belief, it contains no copy or paraphrase of material previously published or written by another person, except where due reference is made.

Elzbieta Chelkowska

Elzbieta Zofia Chelkowska
Department of Chemistry
University of Tasmania
April, 1993.

Acknowledgements

I would like to express my sincere thanks to my supervisors Professor Frank P. Larkins for his guidance. advice, encouragement, and enormous understanding and patience, and Doctor Brian F. Yates for critical reading and commenting on this work and also for his immense support in overcoming all obstacles during the final months.

I would like to thank very much Doctor Brad G. Armen for a "piece of code", valuable discussions, assistance and friendly *woof.*

Miss Cristina Tulea is acknowledged for making the results of her calculations available.

I am grateful to Professor Mike Schmidt for his instant help in getting access to GAMESS.

Financial support of Australian Research Council is greatly appreciated.

I would like to express my appreciation to all friends and colleagues from the Departments of Chemistry, Mathematics and Physics, too numerous to mention here, for their help and cheerful company.

I am indebted to all friends and colleagues from the Computing Centre and SciTech Library for their fantastic help and support in all near-catastrophic situations.

Very special thanks go to Doctors Sue Atkins and Steve Sonneveld together with Heather Gouldthorpe for their wonderful help and support in momentous, yet strenuous time.

I am very thankful to my parents - mother and late father for their love, support and understanding.

My friends Mila, Zosia, Helen and Neil are appreciated for their help and encouragement.

Finally, I would like to thank my husband Miroslaw Ryba for his generous support and tremendous patience, and little Christopher for just being there and making my life wonderful.

Abstract

Auger electron spectra of molecules are in general more complex than the spectra of the isolated constituent atoms because the increased number of valence electrons in molecules results in a significantly larger number of final double-hole states. *Ab initio* calculations are possible but their complexity restricts optimized studies to a limited number of relatively small molecules.

Alternative approaches are sought to simplify calculations. Semi-empirical methods are very promising since the results are often at least of the same level of accuracy as minimum basis *ab initio* calculations, yet the answer is obtained within a small fraction of effort required for *ab initio* computations.

In this work a semi-empirical method developed for atomic problems and adapted for molecules by Larkins is extended and appraised. All molecular Auger calculations are performed at the INDO or STO-3G level.

In the present approach the intensities of molecular Auger transitions are calculated using the intra-atomic model presented by Siegbahn. The exact expressions for intensity calculations depend upon the symmetry of the orbitals involved while the complexity of the calculations increases with the size of the basis set. For calculations within this project using first- or second-row atoms the smallest basis set *sp* is considered sufficient.

Molecular Auger energies are calculated as the difference in the experimental binding energies of the core and valence molecular orbitals involved in transitions corrected by a term which includes the hole-hole interaction energy. The correction term depends on the symmetry of the final double-hole state and is calculated as a simple function of Coulomb- and exchange-type integrals.

Using the above approach some KVV and LVV Auger spectra of molecules containing first- and second-row elements are calculated. In particular, the method is applied to interpret the KVV and LVV spectra of the first- and second-row hydrides respectively. Moreover, theoretical and experimental spectra of CH_3-X (where X=F, OH, NH_2, CH_3) are compared when the influence of the chemical environment on the carbon KVV Auger transitions is investigated. The theoretical results are in satisfactory agreement with the experiment . In addition, the theory is tested by comparison with the experimental spectra of the first- and second-row tetrafluorides. There are some discrepancies between theory and experiment for highly symmetric molecules.

On the basis of undertaken calculations C(KVV) molecular Auger spectra of XCHO (where X=F, OH, NH_2, CH_3) are predicted. The theory is also verified for an example of second-row polyatomic molecule - OCS. The intensity calculations of the molecular S(LVV) Auger spectrum are the first direct evaluation based upon the molecular wavefunction for this type of molecules. The calculations can be extended to the compounds containing the third row elements.

The overall agreement between theory and experiment is most encouraging nevertheless absolute energy calculation requires some minor refinement. It is concluded that this method represents an efficient approach for the interpretation of complex Auger spectra and may be extended to larger polyatomic systems with d orbitals.

Table of Contents

Glossary of Terms

ADC	algebraic diagrammatic construction method
AES	Auger electron spectroscopy
AO	atomic orbitals
CI	configuration interaction
CNDO	complete neglect of differential overlap
DIP	double hole ionisation potential
EC	equivalent cores
FWHM	full width at half maximum
INDO	intermediate neglect of differential overlap
LCAO	linear combination of atomic orbitals
mau	atomic unit*10^{-3}
MBS	minimal basis set
MO	molecular orbitals
NEC	non-equivalent cores
RHF	restricted Hartree-Fock
SCF	self consistent field
STO-3G	basis set where any Slater-type orbital is fit by 3 gaussian functions.

Chapter 1

INTRODUCTION

1.1. General Information

The excess of energy stored by a system as a consequence of the ejection of an electron from an inner orbital of an atom or a molecule can be released via radiation (fluorescence) or via emission of an electron (Auger effect). When an electronic vacancy W in the atom is filled by one electron from a less tightly bound state X with the simultaneous emission of a second electron from another less tightly bound state Y (Fig.1.1) then the process is called an Auger effect and the ejected electron is called an Auger electron.

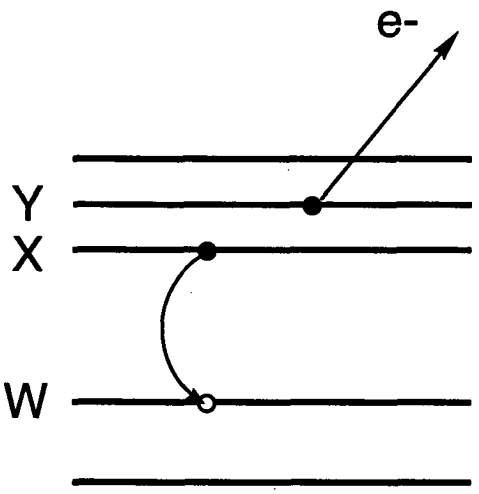

FIG.1.1 Schematic picture of an Auger process.

When the initial hole is in the core orbital K or L and the final state has vacancies in molecular valence orbitals X and Y the Auger spectrum is called KVV or LVV respectively. The Auger decay is a dominant path in a process of de-excitation of light element atoms with initial core holes.

The phenomenon of radiationless autoionization was observed by Barkla (in 1909), Sadler (in 1917), Kossel (in 1923), Dallas (in 1924) and Wilson (in 1923). The process was

investigated by Pierre Auger in 1923-1926 (Auger 1923, Auger 1925, Auger 1926) and named after him in 1926. One year later G. Wentzel (Wentzel 1927) developed the non-relativistic theory of the Auger effect explaining it as an autoionization process resulting from the electrostatic interaction between two electrons in an atom which is already singly ionized in an inner shell. Two reviews (Burhop 1952 and Bergström 1955) initiated a very rapid increase interest in the Auger spectroscopy. In 1960s several theoretical predictions of the K Auger spectrum were carried out to explain relativistic effects, intermediate coupling, and configuration interaction. As a result of progress in technology some further discoveries were possible. In the late 1960s satellite lines in the Auger spectrum of neon were first time reported after detailed observation and analysis by Körber and Mehlhorn (1966). Since 1970 the growth in number of applications of Auger electron spectroscopy (AES) reported in literature is very spectacular, mostly through a vast improvement in the UHV technology.

Recently molecular Auger spectroscopy has received a lot of attention because new experimental techniques (synchrotron radiation sources, coincidence spectroscopies) enable verification of existing, and prediction of new, phenomena in molecules.

The study of the dynamics of Auger processes in molecules reveals information about the dynamics of the excitation and decay process but calculations are limited to a very small molecules because a large number of different transitions is generally possible from any given initial state. The Auger electron spectra of molecules are far more complex than those of atoms since the increased number of available valence electrons yield many more possible final states. The complexity of the Auger transitions in the molecules is represented in the Fig.1.2 where several double hole final states of CO are shown.

The atomic selection rules for an Auger process require that the total angular momentum and the parity of the final-state system (ion plus emitted electron) must be the same as of the initial state. In general, there are no selection rules for Auger transition in molecules.

A typical atomic Auger spectrum contains three regions: outer-outer, outer-inner and inner-inner valency while molecular spectra are often broad and structureless. An Auger spectrum of an element in a molecule may shift with respect to changes in the chemical state. Additionally, the spectrum can be altered by presence of polarization or many body effects.

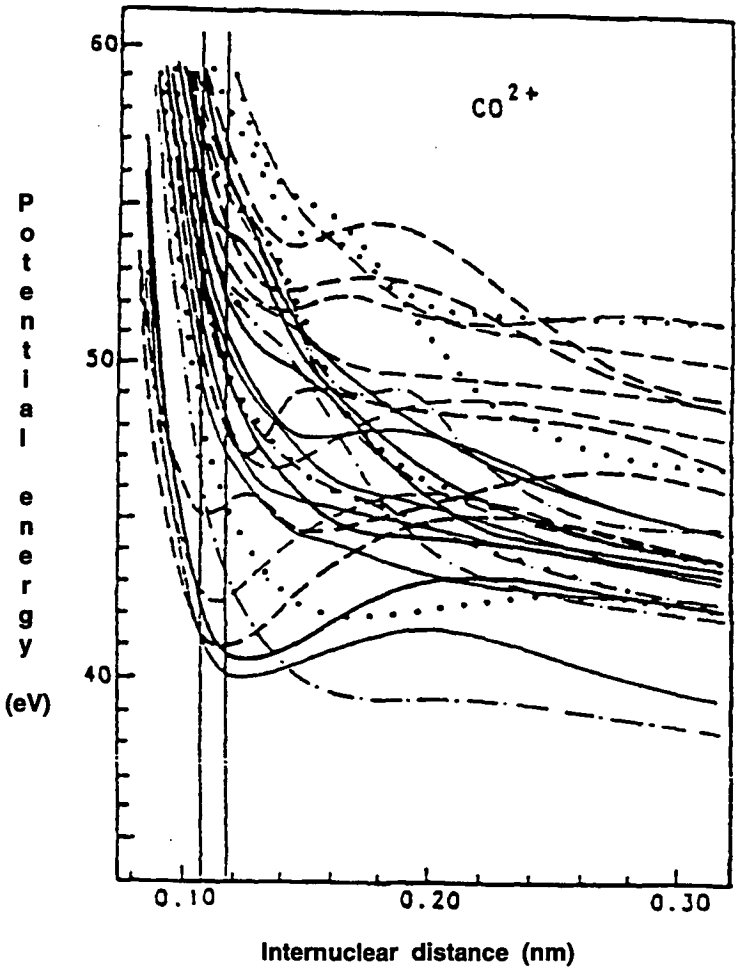

FIG.1.2 Calculated potential energy curves of the electronic states of CO^{2+} located between 35 and 60 eV (solid line $^{1,3}\Pi$; dashed line $^{1,3}\Sigma^{+}$; dotted line $^{1}\Delta$; dot-and-dash line $^{3}\Sigma^{-}$;) (Reproduced from Hubin-Franskin M-J and Delwiche J 1990).

Apart from normal Auger lines in a spectrum satellites can occur. A satellite line arises when the configuration shown in Fig. 1.1 is altered either for the initial or the final state, i.e. there is more than one initial hole or the core hole vacancy is formed without the electron going to the continuum or the final state does not contain exactly two holes in the valence orbitals. A chemical dependence of the satellite peaks will in general also be displayed when these involve valence electron excitations. The types of satellites which may be present in an Auger spectrum are illustrated in Fig.1.3.

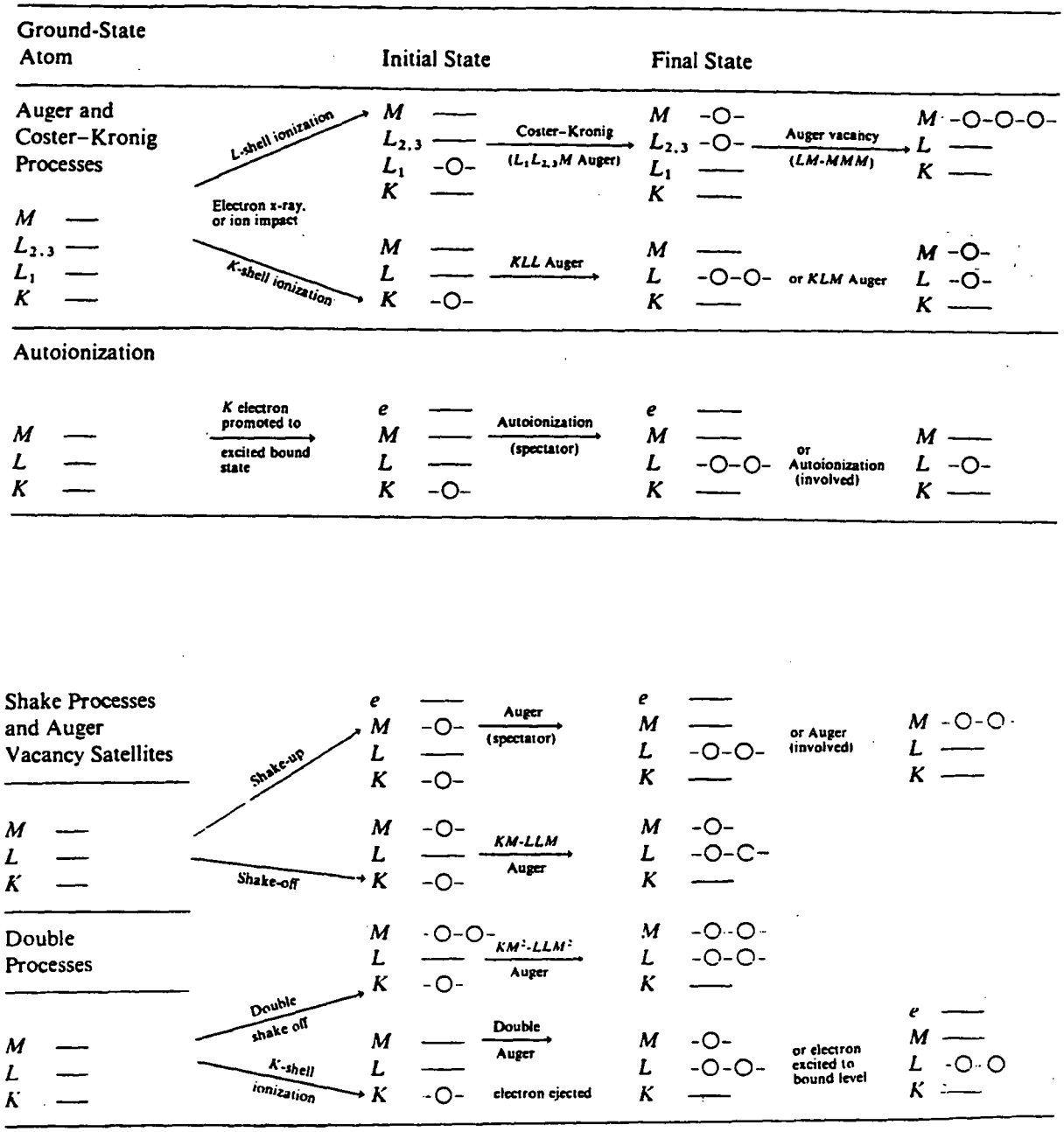

FIG.1.3 Summary of Auger and Related Processes. (The transitions shown in the diagram do not represent all possible transitions for an atom with full KLM shells, only representative examples are given.) (Reproduced from Thompson et al. 1985).

The above diagram does not include the final state shake off Auger satellite lines.

The Auger electron spectroscopy (AES) is used in fundamental studies of atomic and nuclear phenomena as well as being of relevance to surface physics, chemistry, materials science.

The application of Auger spectroscopy in molecules can be divided into two fields. Firstly, Auger spectra are used as a source of information on electronic structure of free molecules. The experimental and theoretical interest has been focused to those molecules which are small enough to yield well-resolved and structure-rich spectra and which are accessible to accurate computer analysis for interpretative purpose. The spectra of the molecules may reflect such parameters as symmetry, delocalization, bonding characteristic and lifetime effects, vibronic coupling. In a second application molecular Auger spectra are used for element identification and structural analysis of large composite systems.

The availability of a high resolution experimental profiles are crucial for testing any theoretical method. Hence, spectra obtained with tunable synchrotron sources and having ion beams with a desired ion charge are very important in better understanding the physics involved in an Auger process.

As shown in Fig.1.2 and 1.3, complexity of the Auger phenomenon in molecules precludes elaborate theoretical computation except for simple systems. Hence, other methods have to be considered (at least as a first approximation) for calculation of Auger spectra in other than typical model molecules (i.e. hydrides or small diatomics). This project is aimed at further addressing this problem.

1.2. Presentation of the Problem

The aim of the project is to develop a theory of calculation of molecular Auger spectra which can be used mainly for the interpretation of spectra for larger systems where *ab initio* calculations are not readily accomplished. The method of calculation evolved from the theory will first be tested on small molecules containing first row elements to establish its applicability. Then it will be extended to the molecules containing second row elements.

Hence, in the next chapter (Chapter 2) theoretical and experimental work on molecular Auger spectroscopy will be reviewed and in Chapter 3 the background of the applied theory will be presented. Evaluation of the method will be provided in a reference to the first row hydrides (Chapter 4) as examples of Ne - like molecules and to CH_3-X molecules (Chapter 5), where X=CH_3, NH_2, OH, F, with various symmetries but the same number of electrons. On the basis of acquired knowledge an attempt to predict Auger spectra of X-CHO molecules will be made in Chapter 6.

Subsequently, in Chapter 7 the appraisal of the method will be given in reference to second row hydrides as examples of Ar - like molecules. Auger spectra of tetrahedral hydrides and

fluorides containing first and second row elements will be also investigated in Chapter 9 following an analysis of Auger spectra of OCS - a polyatomic molecule containing second row elements in Chapter 8. All findings will be summarised in Chapter 10.

Chapter 2

LITERATURE REVIEW

2.1. Introduction

One of the first papers on the studies of Auger spectra of molecules was reported in 1960 (Mehlhorn 1960). Nonetheless, it was not until early 1970s when Auger decay in molecules became investigated more closely. Since then spectra of over two hundred volatile species have been reported. Interpretation of the spectra, however, has concentrated on small molecules containing first row atoms only and for larger systems a brief analysis of the molecular Auger spectra was usually presented. This is caused by the fact that the number of final double-hole electronic states in molecules increases dramatically with the number of valence electrons available thus increasing complexity of the spectra. Therefore the calculations of energy and intensity of Auger transitions in any polyatomic molecule represent considerably complicated tasks sometimes not feasible to achieve.

There are several monographs dedicated to the Auger spectroscopy. The theory of Auger transitions in atoms is presented by Chattarji (1976) and Åberg and Howat (1982), while the experimental aspects of the Auger effect can be found in Carlson (1975), Thompson *et al.* (1985), Briggs and Seah (1983) and Briant and Messmer (1988). A complete bibliography of Auger effect from 1925 till 1975 is compiled in Hawkins (1977). The latest developments in the Auger spectroscopy used for elucidation of electronic processes in atoms and molecules are presented in Wandelt *et al.* (1992) and in Mehlhorn (1990). Recently Ramaker (1991) and Ågren *et al.* (1992) reviewed theory for molecular spectra. The later review is focused on the implication of scattering theory formulation of Auger transitions in molecules, the one- and many-particle interpretation of Auger states and on computational schemes based on the one- and many particle approximations. An overview paper written by Ågren (1991) examines interaction between theory and experiment in molecular core spectroscopies. Another review (Tarantelli *et. al.* 1992) is dedicated to the Green's function and ADC formalisms in molecular calculations.

2.2. Experiments

Molecular Auger spectra have been examined in many experiments. Two- and three-atomic molecular systems containing first row elements have been studied most widely and the

spectra of molecules were obtained with a variety of energy sources (electrons, photons, ions) (Moddeman *et al.* 1971, Siegbahn *et al.* 1969, Stolterfoht *et al.* 1973).

Auger spectra of polyatomic molecules were recorded by various research groups. A comprehensive source of experiments reported by researchers from Uppsala, Oak Ridge, Albuquerque, Oregon, Oulu, Loughborough and others is published in Thompson *et al.* (1985) (up to 1980) and in Tulea (1987) (up to 1986).

KVV spectra of first row hydrides were measured by Shaw *et al.* (1977), Thompson *et al.* (1976), White *et al.* (1977), Camilloni *et al.* (1977), Appel and Horsley (1974), Shaw *et al.* (1975), Spohr *et al.* (1970), Siegbahn *et al.* (1969), Moddeman (1970), Asplund *et al.* (1977), Rye *et al.* (1978), Ariyasinghe *et al.* (1987), Aksela (private communication), Moddeman (1970), Rye *et al.* (1978), Connor *et al.* (1976) and Siegbahn *et al.* (1975) while KLL spectra of second row hydrides were reported by Asplund *et al.* (1977), Vayrynen *et al.* (1983) and Siegbahn (1978).

Auger spectra of molecules containing second row elements were obtained by de Souza *et al.* (1986, 1985, 1989) (SiH_4, $SiMe_4$, SiF_4), Aksela *et al.* (1986, 1988, 1990, 1992x) (SiF_4, $SiCl_4$, HCl, Cl_2, H_2S), Japanese group (Ueda *et al.* 1991) (BF_3, PX_3), Yagishita *et al.* (1986) (SiH_4), Asplund *et al.* (1976 and 1977) (sulphur compounds), Cesar *et al.* (1990) (H_2S), Carroll and Thomas (1990) (OCS), Platania *et al.* (1992) (PCl_3), Rosenberg *et al.* (1990) (SiF_4, $SiCl_4$), Suoninen *et al.* (1985) (gaseous xanthanes and related sulphur-containing compounds), Rye and Houston (1983) (SiH_4, CF_4, SiF_4, $SiCl_4$, CCl_4), Fournier *et al.* (1989)(CCl_4), Cini *et al.* (1986 and 1987) (BCl_3 and $Me_n SiCl_{4-n}$, respectively).

Systems containing molecules from third and higher row elements were also explored (GeH_4 - by Maracci *et al.* 1989, HBr and BBr_3 - by Cini *et al.* 1986).

Availability of tuneable synchrotron sources made possible more detailed studies of Auger phenomenon in molecules. Many molecular spectra have been re-run using the new more precise technique. Table 2.1 presents a list of experiments conducted since 1984, where synchrotron radiation sources have been used for studying molecules.

TABLE 2.1.

Synchrotron experiments with free molecules since 1984.

Molecule	Reference
BF_3	Ueda *et al.* 1991
C_2H_5I and C_2H_4IBr	Motte-Tollet *et al.* 1992
CaF_2	Tiedje *et al.* 1990

TABLE 2.1. Continuation

Synchrotron experiments with free molecules since 1984 .

Molecule	Reference
CCl_4, $CHCl_3$, CH_2Cl_2 and MeCl.	Carlson *et al.* 1988
CF_2Br_2 and CF_3Br	Novak *et al.* 1986
CF_4	Lapiano-Smith *et al.* 1989, Truesdale *et al.* 1984
CO	Truesdale *et al.* 1984
CO_2	Truesdale *et al.* 1984
CS_2	Hayes and Eberhardt 1990, Carlson *et al.* 1988
Fe_2O_3	Fujimori *et al.* 1986
Me_4Si	de Souza *et al.* 1985, Morin *et al.* 1986
N_2	Habenicht *et al.* 1990, Lindle *et al.* 1984
HCl	Aksela *et al.* 1990
NO	Lindle *et al.* 1984
O_2	Frasinski *et al.* 1986, Lapiano-Smith *et al.* 1990
OCS	Truesdale *et al.* 1984, Eland 1987, Carlson *et al.* 1988
PF_3	Vayrynen *et al.* 1992, Ueda *et al.* 1991
BF_3, PH_3 and PCl_3	Ueda *et al.* 1991
SF_6	Bancroft *et al.* 1990, Ferrett *et al.* 1988x, Frasinski *et al.* 1986, Eland 1987
$SiCl_4$	Carlson *et al.* 1988, Rosenberg *et al.* 1990, Aksela *et al.* 1988
SiF_4	Aksela *et al.* 1986, Ferrett *et al.* 1988, Lablanquie *et al.* 1989, Lapiano-Smith *et al.* 1989, Rosenberg *et al.* 1990, de Souza *et al.* 1989
H_2S, Cl_2	Aksela *et al.* 1992
SiH_4	de Souza *et al.* 1986, Yagishita *et al.* 1986
$SnCl_2$	Stranges *et al.* 1992

Coincidence studies reveal additional information about doubly charged states in molecules (see for example Eland 1987, Millie *et al.* 1986, Fournier*et al.* 1987 and 1989).

Observation of secondary processes following the excitation of a core electron (fragmentation into ions or electron emission or fluorescence) (in coincidence with Auger electron emission spectrum) provides further information about doubly charged states in gaseous molecules. Table 2.2 contains some references to molecules studied recently in coincidence experiments.

TABLE 2.2

Coincidence experiments with free molecules since 1986.

Molecule	Reference
arom. azabenzenes	Eberhardt *et al.* 1990
BF_3	Ueda *et al.* 1992
C_4H_4S, C_4H_8S	Hayes and Eberhardt 1991
CF_4	Lapiano-Smith *et al.* 1989
CH_4	Hatherly *et al.* 1989
CO	Hitchcock *et al.* 1988, Eberhardt 1987, Eberhardt *et al.* 1986
CO_2	Carroll and Thomas 1991
CS_2	Hayes and Eberhardt 1990, Eland 1987
N_2	Eberhardt *et al.* 1987, Habenicht *et al.* 1990
N_2O	Murphy and Eberhardt 1988, Hanson *et al.* 1990
NH_3	Stankiewicz *et al.* 1989
NO	Carroll and Thomas 1992
O_2	Frasinski *et al.* 1986, Carroll and Thomas 1990
SF_6	Sato *et al.* 1992, Eland 1987, Frasinski *et al.* 1986
SiF_4	Lablanquie *et al.* 1989, Lapiano-Smith *et al.* 1989
SO_2, CH_3I, OCS, NO_2	Eland 1987

2.3. Calculations

Interpretation of the spectra requires methods for evaluation of energies and intensities. The general theory of the prediction of the Auger decay rates has been completely developed (Aberg and Howat 1982). However in systems like molecules there are some difficulties:

- the non-spherical character of the potential to which the continuum electron is subjected inside the molecular region

- polycentric nature of the bound-free integrals for the transition matrix elements.

There are several ways of approximation used in molecules. One of them relies on use of one-centre potential and the continuum orbital in atom-like molecules. Faegri and Kelly (1979) calculated continuum orbitals as spherical waves in the monocentric expanded molecular potential. The nonsphericallity of the potential was taken into account using perturbation method. Higashi *et al.* 1982 also considered nonspherical potential in their calculations for methane. Carravetta and Ågren (1987) adopted Stieltjes imaging method to calculate Auger rates in non-isotropic potentials.

Faegri and Manne (1976) estimated methane rates from the experimental data obtained for Ne while Kvalheim (1983) calculated rates for HCl using McGuire's (1971, 1975) rates for Ar and modifying them appropriately.

Another approach based on variational techniques was used for calculations of continuum orbital in LiF (Colle and Simonucci 1989). In this method the continuum electron wavefunction was approximated by solution of the Lippman-Schwinger equation.

Manne and Ågren (1985) applied many-electron wavefunctions to calculate Auger transition amplitudes.

Liegener *et al.* (1991) introduced a least-squares method for calculating continuum orbitals for Auger electrons. Previously Liegener (1982, 1988 and references there) used Green's function approach to calculate relative transition rates.

Recently Zähringer *et al.* (1992) proposed a method for calculating Auger rates where molecular scattering wave functions were applied. This technique was utilised in calculation of an HF spectrum.

When the transition rates are estimated on the quasi-atomic model any satellites are difficult to assign in any reliable fashion. Tarantelli *et al.* (1985b) used a statistical approach where transition rates were approximated by two-hole strengths multiplied by a weighing factor for transitions for singlets or triplets. The method can incorporate 3-hole states, i.e. shake off satellites.

Complexity of Auger transitions in molecules makes the full *ab initio* calculations very rare. To this date there is only one known full MC SCF *ab initio* (frozen core) calculation for molecules (Larkins and Richards 1986).

All the above calculations were performed for small molecules where the density of doubly ionized final states is relatively small and the experimental spectra are strongly structured. The Auger transitions in these cases can be interpreted in terms of individual final states.

For large molecules, however, very often the number of final two-hole states is too large to make *ab initio* calculations possible. At the same time, the large number of final states together with their vibrational bands can give rise to overlapping bands in the experimental spectrum and the spectrum is not resolvable even if higher experimental resolution is employed. As a result, detailed analysis of an experimental spectrum is extremely difficult if achievable at all (Mehlhorn 1990). Because of complexity only Green's function *ab initio* based (Liegener 1982 and Tarantelli 1985b) or semi-empirical methods (Larkins 1990, Jennison 1980) are used for energy calculations of polyatomic molecular Auger spectra.

In general, intensity transition probabilities have been calculated semi-empirically according to an intra-atomic orbital-based model. In this approach the molecular orbitals involved in the final Auger state are expanded into their atomic components centred at the atom with

the initial core-hole. The Auger matrix elements are evaluated between the atomic orbitals and the Auger continuum orbital, where the latter is approximated as a spherical wave function centred at the primary ionization site.

Siegbahn *et al.* (1975) proposed a semi-empirical method of calculation of Auger transition rates and applied it to the water molecule calculations. In this method transition rates were calculated by expanding molecular orbitals into their components centred at the atom with the initial core and calculating Auger matrix elements between atomic orbitals and the Auger continuum orbital. An independent-particle method was introduced by Jennison (1980) and used for calculation of spectra of polyatomic carbon containing molecules. This method did not incorporate multiplet splittings. Larkins (1990 and references therein) used a method which was an extension of his work with atoms for energy calculations and a one-centre intra-atomic model based on Siegbahn's approach. Ramaker *et al.* (1979) used a simplified model where weighted electron-density populations were applied to estimate intensity of Auger transitions in some molecules. An alternative method was utilised by Rye and Houston (1983). These two methods were initially introduced for solids and then extended to calculations in molecules. Another approach (so called symmetry model, Økland *et al.* 1976) applied for estimation of relative Auger intensities in ammonia molecules adopted atomic transition rates of neon.

Energy calculations present a far lesser problem in Auger molecular spectroscopy, hence there is a number of *ab initio* calculations available. Different techniques are used to calculate energies of molecular Auger transitions. Nagy (1988) used X_α method for calculation of two hole final states energies in CO. However, singlet-triplet splitting were not resolved in the calculations. Gutsev (1986) calculated energies of a CO molecule by discrete variational method X_α. Tarantelli *et al.* (1985c) have applied the ADC(2) method for calculations of the double ionization energies of CH_4 and SiH_4. The ADC(2) method requires smaller configuration space than CI. Recently several complete-active-space self-consistent-field (CASSCF) calculations were carried out (see Cesar *et al.* 1990, Aksela *et al.* 1990) with excellent results. Liegener (1982, 1988) used a method based on Green's function to obtain DIP values in molecules. Hillier and Kendrick (1976) performed CI on basis of MO obtained using the SCF method for the first row hydrides. Kvalheim (1983) calculated energies for $L_{23}VV$ transitions in HCl using symmetry restricted configuration interaction.

Less rigorous semi-empirical methods are also employed, especially for larger systems. One of the approaches, proposed by Larkins (1987, 1990) and used in this project, has the advantage that the wave functions generated for energy calculations can also be used in the transition rate calculations and hence this method of Auger spectra calculations is very fast.

Chapter 3

METHOD OF CALCULATION

3.1. General Information

Calculation of molecular Auger spectra involves determination of energy and intensity of the transition for each element in a molecule. The existing techniques of calculation have been discussed in the previous chapter. While there are many well developed methods for energy assessment transition, rate evaluation represents a substantial problem.

The present method allows for absolute intensity calculation which is very rare among existing methods. Calculated Auger transition rates can be verified using available photoelectron lines (Coville and Thomas 1991, McColl and Larkins 1992).

The details of the present approach has been already published (Larkins 1987, Larkins *et al.* 1988, 1990). The method is based on assumptions that:

- generally the Frank-Condon principle is obeyed, i.e. there is no change in the inter-nuclear distances during an Auger transition

- the Born-Oppenheimer approximation is valid, i.e. nuclear motion is slow relative to electron motion and the nuclei can be considered to be fixed in space relative to electron motion.

Molecular wave functions required in this method for Auger calculations are generated at the *ab initio* or all-valence zero overlap level. Energy calculation requires determination of Coulomb and exchange integrals which can be obtained using *ab initio*-based wavefunctions for the ground state of a neutral molecule. However, for calculations of molecular transition rates, where the one-centre model is used, molecular orbitals expanded into a linear combination of atomic orbitals (LCAO) with relevant coefficients have to be employed. Hence minimal basis set (MBS) generated functions can also be used.

The selection rules for Auger transitions in atoms require that the total angular momentum and the parity of the final-state system (ion plus emitted electron) must be the same as of the initial state. These rules are applied in the present molecular calculations.

For simplicity of computation, the present method of molecular Auger calculations utilises a specially modified (Larkins 1987, Tulea 1987 Chelkowska and Larkins 1990) semiempirical

scheme of Pople *et al.* (1970) where wavefunctions and necessary integrals of a molecule containing first and second row elements are determined at the intermediate neglect of differential overlap (INDO) level within an *sp* basis set.

An input for the calculation of molecular Auger spectra contains:

1. ground state geometry of a considered molecule

2. experimental ionization energies

3. $R^k(\varepsilon)$ - radial atomic Auger matrix elements which contains the continuum orbital of outgoing electron.

3.2. Parametrisation

The original Pople *et al.* (1970) program was adapted and extended by Larkins and Tulea to enable it to calculate Auger spectra for the molecules containing first row atoms. For the second row atoms however only complete neglect of differential overlap (CNDO) calculations of KVV transitions were possible. KVV spectra were calculated within an *sp* basis on the assumption that the presence of d orbitals in the second row element basis set is not crucial and may be neglected. Within the CNDO approximation singlet-triplet features are not resolved because the CNDO method does not make adequate allowance for the different interactions that take place between two electrons with parallel or antiparallel spin. Hence, an extension of the existing program was necessary for calculations of KVV and LVV molecular Auger spectra of the second row elements in the INDO scheme. In the INDO approximation exchange terms are taken into account, but only in the simplest way. The monoatomic differental overlap is retained only in one-centre integrals G^1 and F^2.

The extension of the computer program included implementation of parametrisation for the second row elements and derivation of formulae in LS coupling required for molecular LVV transition calculations.

Four sets of optimised INDO parameters from Gordon *et al.* (1978) for molecules containing Na-Cl atoms were used. These parameters incorporate the orbital exponents ζ_A, the Slater-Condon factors F^2_A, G^1_A, the resonance or binding parameters β^0_A, and the Mulliken electronegativities $-1/2(I+A)_\mu$ where μ is *s* and *p*. They were implemented in the existing program.

The program was extensively tested for consistency for molecules containing first and the second row atoms. Subsequently energy parameters were calculated and substituted in the program. The full set of applied parameters is presented in Appendix A.

Formulae required for calculations of molecular LVV transitions using a one-centre intra-atomic approximation (Siegbahn *et al.* 1975) were calculated employing a simple Fortran

program and a fast symbolic computation package *Mathematica*™. The formulae (extended to the spd basis and *s*, *p*, and *d* initial hole states) are published elsewhere (Chelkowska and Larkins 1991a) while explicit molecular Auger intensity expressions applicable for *2p* initial hole and non-degenerate final states are presented in Appendix B.

3.3. Energy Calculations

Our method of energy calculations for molecular Auger transitions is based on the approach previously applied to atoms (Larkins 1976).

For the normal Auger transition, when the initial hole is in the core orbital, c and the final state has two vacancies in valence orbitals v and v' with total symmetry $^{2S+1}\Gamma$, the energy of the Auger electron $E(_{c\text{-}vv'}{}^{2S+1}\Gamma)$ can be estimated as:

$$E(c\text{-}vv'^{2S+1}\Gamma) = E[c] - E[vv']^{2S+1}\Gamma \qquad (3.1)$$

where E[c] denotes the energy of the initial N-1 core hole state and $E[vv']^{2S+1}\Gamma$ represents the energy of the final N-2 valence double hole state. Energies of initial and final states can be evaluated via *ab initio* calculations. However even for small molecules the number of final states may be very large. Hence alternative semiempirical methods have been developed to overcome the complexity of the calculations.

When the energy of the Auger electron is written as:

$$E(_{c\text{-}vv'}{}^{2S+1}\Gamma) = I_c - I_{vv'}(^{2S+1}\Gamma) \qquad (3.2)$$

where I_c is the ionization energy for a core electron and $I_{vv'}(^{2S+1}\Gamma)$ is the two-hole ionization energy of a $^{2S+1}\Gamma$ symmetry final state, the term $I_{vv'}(^{2S+1}\Gamma)$ can be substituted by molecular ionization energies I_v ,$I_{v'}$, and a special two-hole correction term $\Delta[vv']^{2S+1}\Gamma$, i.e. the Auger electron energy may be expressed as :

$$E(_{c\text{-}vv'}{}^{2S+1}\Gamma) = I_c - I_v - I_{v'} - \Delta[vv']^{2S+1}\Gamma \qquad (3.3)$$

Values of I_c, I_v, $I_{v'}$ are usually taken from photoelectron experiments.

Therefore, determination of the Auger electron energy in molecules is reduced to the computation of the $\Delta[vv']^{2S+1}\Gamma$ term. This can be achieved by using a method previously applied to atoms (Shirley 1973, Larkins 1976). The two-hole correction term $\Delta[vv']^{2S+1}\Gamma$ incorporates $<vv'>^{2S+1}\Gamma$, the interaction energy of a pair of holes in the orbitals v and v', and $R(vv')^{2S+1}\Gamma$, an adiabatic relaxation correction component, i.e.:

$$\Delta[vv']^{2S+1}\Gamma = <vv'>^{2S+1}\Gamma + R(vv')^{2S+1}\Gamma \qquad (3.4)$$

The hole-hole interaction energy $<vv'>^{2S+1}\Gamma$ for orbitals v and v' is calculated from the formula :

$$\langle vv' \rangle^{2S+1}\Gamma = \left\langle \Psi\ [vv']^{2S+1}\Gamma \left| \frac{1}{r_{12}} \right| \Psi\ [vv']^{2S+1}\Gamma \right\rangle \qquad (3.5)$$

where $\Psi[vv']^{2S+1}\Gamma$ is the double hole wavefunction of appropriate symmetry. The interaction term $\langle vv' \rangle^{2S+1}\Gamma$ is sometimes referred as U_{eff} (Jennison 1980) and for many molecules can be expressed in terms of Coulomb- and exchange-type integrals of the kind $J_{vv'}$ and $K_{vv'}$ where $J_{vv'} = Q(vv \mid v'v')$ and $K_{v'v} = Q(vv' \mid v'v)$, and

$$Q(ij \mid kl) = \left\langle \phi_i(1)\,\phi_k(2) \left| \frac{1}{r_{12}} \right| \phi_j(1)\,\phi_l(2) \right\rangle \qquad (3.5a)$$

with ϕ_v , $\phi_{v'}$ representing the one-electron molecular orbitals calculated using the SCF method.

In general, $\langle vv' \rangle = J_{vv'} \pm K_{vv'}$, when $v \neq v'$ or $\langle vv' \rangle = 2J_{vv'}$, when $v=v'$. In some cases of symmetry, however, modified expressions have to be applied (see Tulea 1987).

The values of $\langle vv' \rangle^{2S+1}\Gamma$ are usually determined for the neutral molecule in its ground state and are overestimated because the relaxation due to valence hole screening by valence electrons is neglected. However, an adiabatic relaxation correction term R(vv') is no longer well defined since the extent to which relaxation, correlation and other effects are accounted for in our calculations is not specified. Many-electron effects are more severe in molecules than in free atoms and an atomic value of R(vv') cannot be used even if the Auger process in some molecules is very atomic-like since an entire spectrum may shift with respect to changes in the chemical state of the element. The use of experimental ionization energies compensates to some extent effects associated with localization and hole-hole interaction, many body effect, and single hole polarization. Therefore, further evaluation of the role of the adiabatic relaxation correction term R(vv') in molecular calculations would be necessary. For the present, however, R(vv') will be set to zero and calculated spectra will be assigned by alignment with the experimental spectrum (if available).

Spin-orbit splitting is significant for the second row atoms and cannot be neglected in molecular Auger calculations. In our method values of spin-orbit splittings formerly determined for elements (Larkins 1977) are applied when energies of $L_{23}VV$ molecular spectra are computed.

3.4. Transition Rates Calculation

In the present approach the intensities of Auger transitions are calculated using the one-centre intra-atomic orbital-based model presented by Siegbahn *et al.* (1975). It is assumed that long-range effects within the molecule are of secondary importance in comparison with

the valence shell electron density of the atom in which the original core hole is localized (Matthew and Komninos 1975). This presumption has not been verified exhaustively yet, nevertheless, existing results indicate its corroboration.

The implementation of Auger theory for molecules has exclusively been restricted to the framework of Wentzel's ansatz (Wentzel 1927) . With this ansatz one assumes the Auger decay as part of a two-step process, i.e. with the decay uncoupled from the excitation of initial state, and independent of interaction between the primary photoelectron and the Auger electron, and that interaction with other collisional products is negligible (see Ågren and Cesar 1992). More references about intensity calculations using Wentzel's ansatz (Wentzel 1927) can be found in the previous chapter.

According to Wentzel's ansatz (Wentzel 1927) the normal transition probability expression from the initial core hole state $\Psi_i(N-1)$ to the final state $\Psi_f(N-1)$ with two holes in the valence orbital and an electron in the continuum, when first order non-relativistic perturbation theory is used, is given by:

$$I_{vv'} = 2\pi \left| \left\langle \Psi_f(N-1) \left| \sum_{ij} \frac{1}{r_{ij}} \right| \Psi_i(N-1) \right\rangle \right|^2 \qquad (3.6)$$

A large number of different transitions is generally possible from any given initial state. The selection rules for Auger transitions in atoms require that the total angular momentum and the parity of the final-state system (ion plus emitted electron) must be the same as of the initial state. These rules are applied for molecular calculations. When Hartree-Fock-type wavefunctions are used to describe a set of orthogonal one-electron orbitals, the above expression reduces to two-electron matrix elements, i.e.

$$I_{vv'} = 2\pi \left| \left\langle \Psi_f(c\varepsilon) \left| \sum_{ij} \frac{1}{r_{ij}} \right| \Psi_i(vv') \right\rangle \right|^2 \qquad (3.7)$$

where only electrons involved in the transition (c,ε - core hole and continuum orbital functions respectively and v, v' - generalised multicentre one-electron valence molecular functions) are included. The $\Psi_f(c\varepsilon)$ and $\Psi_i(vv')$ denote the two-electron wavefunctions of the appropriate symmetry. The matrix elements can be expressed in terms of integrals of the kind $J^{c\varepsilon}_{vv'}$ and $K^{c\varepsilon}_{v'v}$ where $J^{c\varepsilon}_{vv'} = Q(cv \mid \varepsilon v')$ and $K^{c\varepsilon}_{v'v} = Q(cv' \mid \varepsilon v)$ (see formula 3.5a). For the simplest non-degenerate case

$$I_{vv'} = 2\pi \frac{(2S+1)}{2} \left| J^{c\varepsilon}_{vv'} \pm K^{c\varepsilon}_{v'v} \right|^2 \qquad (3.8)$$

where S=0 and (+) are for the singlet, S=1 and (-) for the triplet.

When v=v' only a singlet state is possible. In this case $J_{vv'} = K_{v'v}$ and the intensity expression is reduced to

$$I_{vv'} = 2\pi \left| J^{c\varepsilon}_{vv'} \right|^2 \qquad (3.9)$$

i.e. half of the rate for non-equivalent orbitals.

Formulae for molecular Auger intensity calculations when degenerate orbitals are involved are far more complex and are presented elsewhere (see for example Larkins *et al.* 1990, Tulea 1987 or Chelkowska and Larkins 1991a). Intensity expressions would be extremely difficult to evaluate when a multicentre continuum function is used. The only full *ab initio* calculation has been reported for Li_2 (Larkins and Richards, 1986). The intra-atomic orbital-based model, which is applied in the present calculations, introduces a substantial simplification of the [above] expressions.

In the one-centre model, a non-radiative de-excitation process is expected to be localised around one atomic centre with the initial core hole. Therefore when molecular orbitals ϕc, ϕv, $\phi v'$ and $\phi \varepsilon$ are described by the LCAO approach only those components associated with the atom possessing the core hole are included in the evaluation.

Explicitly, if a core of atom A in the two-atomic molecule AB is ionized then:

the core hole wavefunction $\phi_c = \chi_c^A$ with quantum numbers $l_c m_c$

and the components of the delocalised molecular orbitals v,v' are selected as represented by

$\phi_v \approx \sum_i c_i^{v,A} \chi_i^A$ (with no contribution $\sum_i c_i^{v,B} \chi_i^B$ from the B atom included in the matrix element evaluation)

$\phi_{v'} \approx \sum_j c_j^{v',A} \chi_j^A$ (with no contribution $\sum_j c_j^{v',B} \chi_j^B$ from the B atom included in the matrix element evaluation)

where χ denotes an atomic wavefunction with quantum numbers lm.

ϕ_ε is expressed by all symmetry allowed atomic uncoupled continuum channels and is normalised to one electron per atomic unit of energy while χ_ε is described as a product of atomic Auger radial matrix element R^k and the spherical wave function, i.e.

$\chi_\varepsilon = R^k(l_i l_j, l_c l_\varepsilon)\, Y_{lm}(\Theta,\phi)$, where $_{lm}$ depends on the basis used.

Total transition intensity is expressed as a sum averaged over all initial states of all possible continuum states. Hence, for an initial core hole c with atomic quantum number l_c

$$I^{c\varepsilon}_{vv'} = \frac{f\pi}{(2l_c+1)} \sum_{m_c} \sum_{l_c} \sum_{m_\varepsilon} I^{l_c m_c,\, l_\varepsilon m_\varepsilon}_{vv'} \qquad (3.10)$$

where $l_\varepsilon m_\varepsilon$ are quantum numbers associated with the continuum orbitals. For equivalent non-degenerate orbitals (v=v'), f = 1/2; otherwise f = 1. The number of terms to be evaluated depends upon the symmetry of the core hole, c, and the size of the basis set. The relationship between these features is shown in the table below.

Number of $I_{vv'}^{l_c m_c, l_\varepsilon m_\varepsilon}$ terms

core hole	*sp* basis	*spd* basis
s	9	25
p	36	96
d	73	193

Expressions required for calculations of $I_{vv'}^{c\varepsilon}$ terms are presented elsewhere (Chelkowska and Larkins 1991a). However, for *1s* and *2p* initial holes, final intensity calculation formulae expressed in terms of the LCAO coefficients c_i (within an *sp* basis) for involved molecular valence orbitals, v and v', and atomic Auger integrals, R^k, are presented in Tulea (1987) and in Appendix B , respectively. The expressions in Appendix B were obtained by calculation of Coulomb and exchange-type integrals of kind $J_{vv'}^{2p\varepsilon}$ and $K_{v'v}^{2p\varepsilon}$ for each possible continuum channel ε, i.e. s,p,d,f using selection rules. Then the spherical wave functions were replaced by their equivalents in cartesian coordinates. Next step involved usage of formula (3.8) to obtain explicit intensity expressions for singlet and triplet transitions in terms of c_i and R^k. To achieve this step real and imaginary parts of appropriate expressions for singlet or triplet transitions were squared and added as in (3.8). The expressions for $I_{vv'}^{c\varepsilon}$ were thus summed for each channel separately according to expression (3.10) or (3.9) in the case of non-equivalent or equivalent orbitals, respectively. The above method of calculation along with an example is described in detail in Chelkowska and Larkins (1991a).

The c_i coefficients are calculated using the INDO approximation while atomic Auger matrix elements for the *s* core hole can be taken from McGuire (1969) or Walters and Bhalla (1971). Recently Chen *et al.* (1990) tabulated R^k integrals calculated with relativistic wavefunction for L subshells and Z up to 92. Values of R^k integrals for the initial *1s*, *2s* or *2p* hole and valence orbitals taken from Chen and normalised accordingly to Walters and Bhalla are presented in Appendix A. In the present work, however, only the R^k Auger matrix elements for the *2p* initial core hole are taken from Chen *et al.* (1990). The relevant Auger matrix elements used in calculations for the *1s* initial core hole are taken from Walters and Bhalla (1971) for historical reasons.

Spin-orbit splitting is important for the second row atoms and cannot be neglected in molecular Auger calculations of $L_{23}VV$ spectra. In the present method Auger transitions for $2p_{3/2}$ initial state were calculated and used in construction of a spectrum coming from $2p_{1/2}$

initial hole assuming statistical intensity ratio 2:1 for $2_{p3/2}$ and $2_{p1/2}$ initial states respectively. Then both spectra (i.e. initiated from $2_{p3/2}$ and $2_{p1/2}$) are superposed.

From a comparison of predicted theoretical and experimental linewidths of photoelectron spectra (Coville and Thomas 1991, McColl and Larkins 1992) it became apparent that equivalent cores representation is needed to provide appropriate description of polarisation of valence electrons by a core hole.

The finite lifetime of a core hole is a consequence of Heisenberg's uncertainty principle, i.e. $\Delta E \times \Delta\tau \geq 1$ (in atomic units), where ΔE represents inherent linewith and $\Delta\tau$ is the lifetime of a core hole state. The total rate of Auger decay can be estimated as $1/\Delta\tau$ from the linewidth of an experimental photoelectron spectrum assuming i) the Auger decay is dominant process ii) broadening associated with measuring procedure can be assessed. There is no certainty that experimental values available for photolines represent the true linewidths. However, it has been noticed that there is a discrepancy between the experimental 1s linewidths (inverse lifetimes) for carbon, nitrogen or oxygen atoms in molecules and the theoretical 1s linewidths predicted for the corresponding free atoms (Coville and Thomas 1991). Additionally, the same core-excited element in different compounds gives different linewidth values. Hence, it has been suggested that the lifetime may depend on the chemical environment. In the atom (say carbon) some of its valence orbitals are filled and some are completely empty, whereas in the molecule (such as methane) all of the same set of atomic orbitals are occupied but only partially. This (according to the one-centre model by Siegbahn *et al.* 1975) leads to faster Auger rate in molecules than in free atoms. Additionally, presence of a core hole introduces polarization of valence electrons. When the core hole is created in the atom (carbon, for example) its valence configuration does not change while for a compound such as methane as much as one electron may be withdrawn from the surrounding hydrogens to screen the core hole and the Auger rate will increase for methane (Coville and Thomas 1991).

An equivalent cores approach is introduced to mimic phenomena taking place in molecules during an Auger process. When an initial core hole is created in a core orbital of an atom with a nucleus Z then the valence electrons "see" the nucleus as one having the positive charge equal to Z+1. In the equivalent cores approach a molecule with an atom containing a core hole is replaced by a positive ion, in which an atom with a nucleus Z and a core vacancy is substituted by another atom with a nucleus Z+1, i.e. for the SiH_4 molecule the equivalent cores model is PH_4^+ ion.

In the present calculations the equivalent cores model is used unless stated differently.

Chapter 4

FIRST ROW HYDRIDES

4.1. Introduction

Hydrides form a bridge between well-established atomic Auger spectra and the complex Auger spectra of "electron rich" molecules to which even the first row diatomics belong. The relative simplicity of hydride spectra therefore makes them good models for a number of theoretical investigations concerning energies and intensities of molecular spectra (Cesar 1990).

The first row hydride molecules are isoelectronic with the Ne atom and their spectra can be interpreted in terms of perturbations to the energy structure of neon. Their Auger spectra should be atomic-like which means they should be structured, and three major groups of transitions should be easy to distinguish: inner-inner, inner-outer and outer-outer valence states. Some effects such as correlation, relaxation or polarization are common in larger and more complex molecules but they are also present in the hydrides. However, only the inner-inner transitions of the first row hydrides are seriously affected by the dynamic correlation effects and in the remaining major part of the spectra the MO picture is maintained. Additionally, the Auger spectra of the first row hydrides contain satellite lines similar to their isoelectronic atom counterpart.

In general, the complexity of the Auger spectrum depends on the degree of degeneracy, being the most complex for the lowest symmetry molecules (see Table 4.1). Furthermore, the decreasing symmetry of a molecule would result in increasing importance of configuration interaction between states of like symmetry.

The spectra of the hydrides have broad profiles in contrast to the atomic Ne spectrum (Körber and Mehlhorn 1966, Aksela 1988) due to lifetime and vibrational effects.

The span of the spectrum should increase gradually from methane to hydrogen fluoride due to the increasing value of ionization energies. A supplementary feature appearing in this group of molecules is the increasing number of lone-pairs which makes the Auger process more localised when proceeding from CH_4 to HF.

TABLE 4.1.

Symmetry and number of two-hole states for the first row hydrides isoelectronic with neon.

Molecule	Symmetry	[vv']Γ	Valence orbitals
CH_4	T_d	7	$2a_1,1t_2$
NH_3	C_{3v}	11	$2a_1,1e,3a_1$
OH_2	C_{2v}	16	$2a_1,1b_2,3a_1,1b_1$
FH	$C_{\infty v}$	11	$2\sigma,3\sigma,1\pi$
(Ne)		(6)	(2s,2p)

This study has been undertaken as a means to evaluate the strengths and weaknesses of the semi-empirical model which it is proposed to use for interpretation of the spectra of larger molecules for which *ab initio* procedures are not readily applicable. Auger spectra of the first row hydrides have been comprehensively studied by many authors. This fact additionally makes these molecules particularly good models for evaluation of the present procedure of calculation for the further application to the more complex compounds.

Some results of this study of the Auger spectra of the first row hydride molecules have been already published (Larkins *et al.* 1990).

In the following sections a discussion of experimental Auger spectra of the first row hydrides as well as comparison of the results obtained in the present and other studies will be given. On the basis of the above results, applicability of the present method will be evaluated.

4.2. Theoretical Considerations

Geometries used in the present studies were taken from Snyder and Basch (1972) while ionization energy values were obtained from Banna and Shirley (1975). Detailed information including experimental geometries and experimental ionization energies of the first row hydride molecules is provided in Appendix C.1. Fig.4.1 diagrammatically depicts ionization energy values for the valence orbitals used in the current calculations.

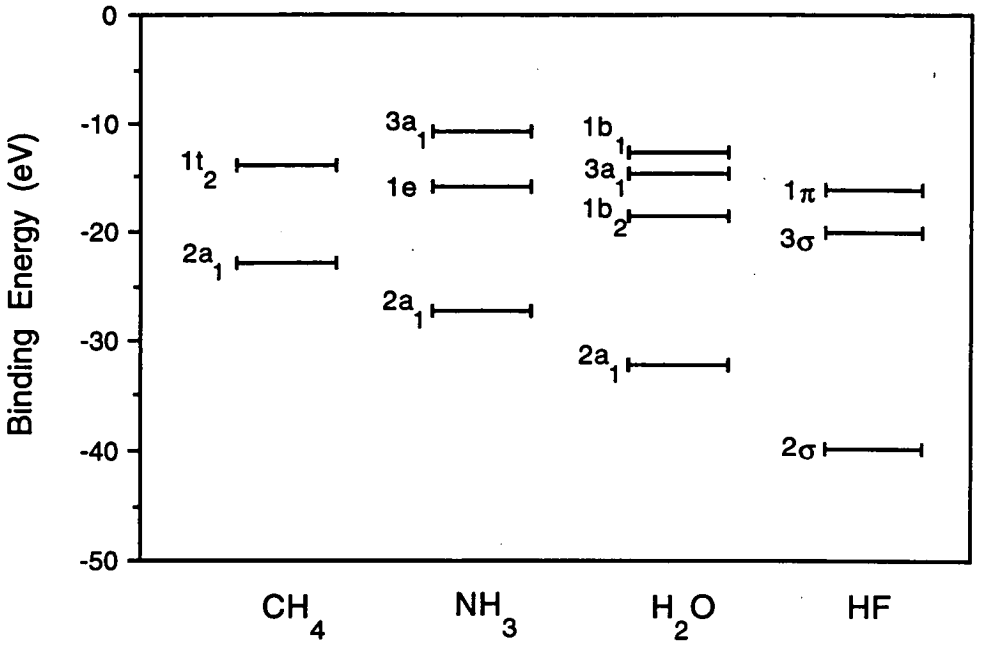

FIG.4.1. Valence ionization energies for the first row hydrides

The width of an Auger spectra can be nearly twice the difference in ionization energy range. Hence, from Fig.4.1 it becomes apparent that the KVV Auger spectra should increase in width when proceeding from CH_4 to HF.

Table 4.2 presents Mulliken population analysis electron populations and total Auger transition rates obtained for the first row hydrides using our method together with R^k atomic matrix elements from Walters and Bhalla (1971) for non-equivalent cores and equivalent cores approaches, respectively.

TABLE 4.2.

Calculated valence electron populations on the heavy atom and Auger rates for the first row hydrides isoelectronic with neon, using non-equivalent cores (NEC) and equivalent cores (EC) approaches.

Molecule	Atom	Valence -e^- population		Calc. Auger rate (mau)	
		NEC	EC	NEC	EC
CH_4	C^-	3.96	5.02	2.20	3.54
NH_3	N	5.25	6.09	3.88	5.22
H_2O	O	6.33	6.98	5.66	6.88
HF	F	7.28	7.64	7.40	8.15

With the equivalent cores model there is a substantial increase in the calculated valence electron populations of the atom with a core hole due to the polarisation introduced by the core hole. The effect can significantly modify the total Auger rate. The largest polarisation effect occurs when there are more polarisable nearest neighbour atoms present.

4.3. Experimental Findings

KVV experimental Auger spectra of Ne and all neon-like hydride molecules are presented in Fig.4.2 on a common scale representing negative values of double hole ionization potentials (DIP).

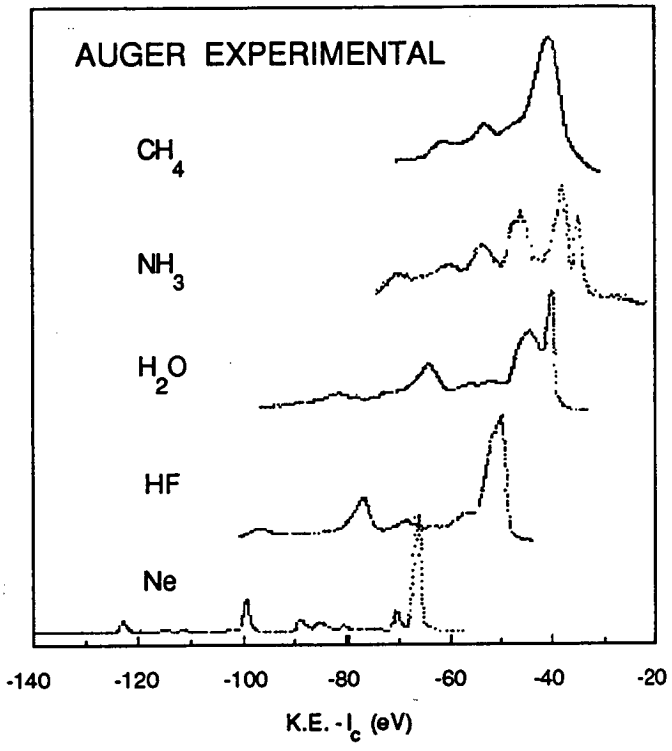

FIG. 4.2. Auger experimental spectra of the first row hydrides and atomic neon: CH_4 spectrum measured by Spohr *et al.* (1970), NH_3 spectrum by Shaw *et al.* (1977), H_2O spectrum by Siegbahn *et al.*(1975) , HF spectrum by Shaw and Thomas (1975) and Ne spectrum by Mehlhorn (1978).

4.3.1. CH_4

The spectrum of methane was one of the first published (Mehlhorn 1960). A decade later Spohr *et al.*(1970) and Siegbahn *et al.* (1969) reported X-ray excited spectra while Moddeman (1970) also measured electron excited Auger spectra of the CH_4 molecule. The Auger spectra of methane obtained using 2keV electron impact (Asplund *et al.* 1977, Rye *et al.*

1978), He^+ (1.8MeV) ions (Ariyasinghe *et al.* 1987) and synchrotron radiation (Aksela, private communication) are also available. All spectra induced with charged particles have different profiles since they show substantial satellite content which is enlarged with the increasing energy of the exciting particles. However, the Auger spectra of methane obtained by means of discrete line X-ray sources and synchrotron radiation are almost identical. They also include some satellite lines (by analogy to the Ne spectrum). The experimental spectrum of Spohr *et al.* (1970) is presented in Fig.4.2.

4.3.2. NH_3

Several authors independently published an ammonia spectrum obtained by using electron impact (Thompson *et al.* 1976 - 5eV electron impact -in nitrogen, Rye *et al.* 1978, Camilloni *et al.* 1977 - 2.4 keV electron impact, White *et al.* 1977- electron impact 1.5keV), proton impact (Appel and Horsley 1974) and X-rays (Shaw *et al.* 1977).

The profiles of the spectra are similar, however there are some discrepancies in absolute energies of the $3a^2\ ^1A_1$ state with values of 374.0 (Camilloni *et al.* 1977), 371.5 (White *et al.* 1977), and 370.2eV (Shaw *et al.* 1977) being reported.

The Auger spectrum obtained by Shaw *et al.* (1977) is considered to be the most accurate and is shown in Fig.4.2

4.3.3. H_2O

The electron impact induced Auger spectra of the water molecule have been reported by Moddeman *et al.* (1971), Rye *et al.*(1978) and Connor *et al.* (1976). Siegbahn *et al.*(1975) published a water spectrum obtained using Mg X-rays for core ionization. There are not any noteworthy distinctions between the spectra induced by different excitation sources. The X-ray induced spectrum of water measured by Siegbahn was chosen to be presented in Fig.4.2.

4.3.4. HF

There has been only one Auger spectrum of HF reported up to date (Shaw and Thomas 1975) and it is shown in Fig.4.2.

X-rays and a 8keV electron beam were used as excitation sources. The spectrum shows a broad background between 600 and 614 eV probably due to inelastic scattering of the Auger electrons in the sample gas.

4.4. Results and Discussion

Detailed results of calculations for the first row hydrides are presented in part D.1 of Appendix D. Theoretical spectra of first row hydrides generated using gaussians with FWHM=1.5 eV are shown in Fig.4.3. As with the experimental spectra, the theoretical shapes are displayed on a common scale representing the difference between the kinetic energy of the Auger electrons and the energy required to create an initial core hole. Total areas under the peaks are set to be the same for each molecule. In practice, vibrational broadening may result in transition lines having very different linewidths depending on the bonding characteristics of the molecular orbitals involved.

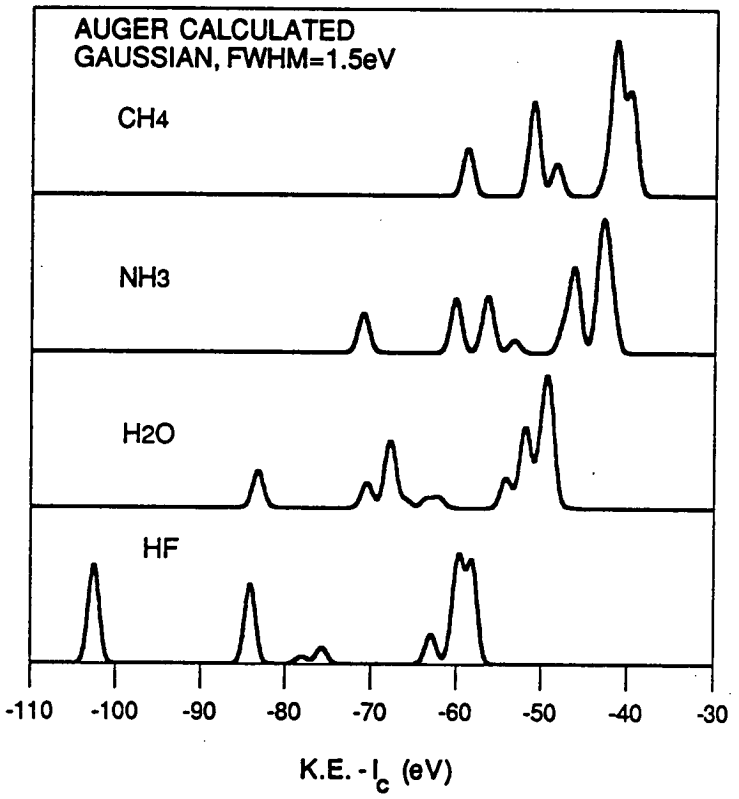

FIG. 4.3. Theoretical Auger spectra of the first row hydrides generated using gaussian shape with FWHM=1.5 eV.

The current level of calculations does not include correlation effects that are present in the ammonia and water molecules. Therefore, the theoretical shapes resemble the experimental ones better for methane and hydrogen fluoride than for ammonia or water. All generated spectra are too narrow when compared with the experimental ones. Additionally, in molecules the highest double hole ionization potential is typically around 30-40 eV (except in HF where the F(KVV) spectrum is atomic-like and the DIP (double hole ionization

potential) is higher) and theoretical spectra of the first row hydrides require some shift toward higher energy to align with the experiment. This shift also incorporates some relaxation effects which are site/orbital specific and cannot be assigned globally. In some cases the shift will be up to 10 eV.

4.4.1. CH_4

An experimental (Spohr *et al.* 1970) spectrum along with the calculated Auger transitions in methane are presented in Fig.4.4. The calculated spectrum is shifted 0.1eV toward higher energy.

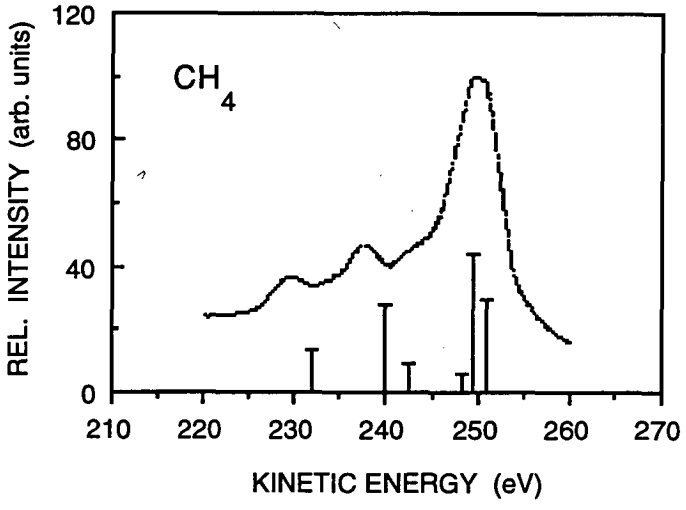

FIG. 4.4. An experimental (Spohr *et al.* 1970) and calculated (bars) Auger spectra for methane. The calculated spectrum is shifted 0.1 eV toward higher energy.

4.4.1.1. CH_4 Energies. There have been several *ab initio* calculations of the energies of doubly-ionized methane (Ortenburger 1975, Faegri, Manne 1976, Hillier, Kendrick 1976, Kvalheim 1982, Tarantelli 1985(a)). The agreement between them is within 2.1eV while absolute energies vary about 1.6 eV. Additional results of calculations performed by Jennison (1980), who has used a semi-empirical model, have been presented. Transition energies reported by other authors along with our calculations based on the INDO method are presented in Table 4.3. In Fig. 4.4 the calculated transitions are consistent with the experimental spectrum. A minimal shift (0.1 eV) is required to align the outer-outer regions of the experimental and calculated spectra. For the methane molecule, *ab initio* wavefunctions were also calculated with a STO-3G basis using Gamess (Schmidt *et al.*1991) and the program of Schaefer (Hehre *et al.* 1969). In general, semi-empirically based

calculations predict narrower spectra because correlation and some other effects are not considered. However, the discrepancies between calculated (using the present method) and experimental spectra of carbon in CH_4 are on the same level of accuracy as the optimised double-hole calculations (Table 4.3).

TABLE 4.3

Methane transition energies calculated by various models relative to the $[1t_21t_2]\ ^1T_2$ energy

Final state		HK /CI	K /RHF	K /CI	OB /SCF	FM	J	T /ADC	Present INDO CH_4	Present /MBS** /CH_4	Present /MBS***/ CH_4^{2+}	Expt P
$[1t_21t_2]$	$^3T_1$	-2.4			-3	-2.8	-2.6	-2.1	-1.9	-3.1	-2.6	
	^1E	-1.5	0.00	0.0	-2	-1.9		-1.3	-1.3	-2.3	-1.5	-2.0
	$^1T_2$	0	1.9	1.5	0	0.0	0.0	0.0	0.0	0.0	0.0	0.0
		252.7*			251.7*	253.3*	249.3*	251.8*	249.3*	251.0*	248.1*	249.4*
												(250.0)
	$^1A_1$	1.6	4.3	3.9	2.4	2.4		1.9	1.3	2.4	2.3	2.4
$[2a_11t_2]$	$^3T_1$	7.0	8.8	8.2	6.7	6.9	5.9	6.7	6.9	5.2	5.4	5.6
												(6.7)
	$^1T_2$	13.2	15.9	13.9	13.1	13.4	11.7	12.4	9.7	11.0	11.5	12.0
												(13.0)
$[2a_12a_1]$	$^1A_1$	21.2	23.2	21.6	21.3	21.5	18.7	20.1	17.5	17.6	18.0	20.0

*) Absolute energy.
**) using GAMESS (Schmidt *et al.*1991).
***) using PSI program of Schaefer (Hehre *et al.* 1969)
HK: Hillier and Kendrick (1976), K: Kvalheim (1982), OB: Ortenburger and Bagus (1975), FM: Faegri and Manne (1976), J: Jennison (1980), T: Tarantelli (1985a), P: Present fit using six gaussians to the experimental spectrum of Spohr *et al.*(1970); In parentheses are values from Thompson (1985) p.187.

The calculation of J and K based upon the *ab initio* derived wavefunctions represents better approximation of the multiplet splitting for the methane molecule.

4.4.1.2. CH_4 Transition Rates. The results of previous calculations by several authors (Kvalheim1982, Jennison 1980, Higashi 1982) along with Rye *et al.* (1978) relative intensities and the present results are given in Table 4.4. The relative rates are normalised to 100% for a total rate for the $[1t_21t_2]$ final state. All calculations except those of Higashi are based on one-centre approximations. Higashi's calculations were performed using explicit determination of the continuum orbital. The results of calculations of relative intensity

values employing the present method compare favourably with the results from previous studies. The theoretical shape of the C(KVV) spectrum in methane generated using FWHM=1.5 eV (Fig.4.3) emulates the experimental shape adequately. However, a larger FWHM (about 5-6 eV when accounting for satellites) is needed to obtain better resemblance of the experimental profile.

The differences between relative intensities obtained using the EC and NEC approaches (Table 4.4) are within 2% which suggests that the relative intensities are not sensitive to the EC or NEC methods. However, the reported absolute values of the total transition rates are not consistent (bottom of Table 4.4). Our absolute values estimated using atomic R^k values from Walters and Bhalla (1971) are 2.20 mau and 3.54 mau for the non-equivalent cores (NEC) and equivalent cores (EC) approaches, respectively, while Higashi's calculated transition rate is 79.9 mau (which is approximately 10 times larger than other values reported). This value must be incorrect since a total rate less than that for Ne (KLL) at 8.83 mau (Walters and Bhalla 1971) is to be expected. Total transition rates for carbon in methane reported by Kvalheim (1982), who used AO coefficients of the MO from *ab initio* gaussian calculations along with atomic R^k values from Walters and Bhalla (1971) within an RHF or semi-internal CI scheme, also appear to be too high. Recently Coville and Thomas (1991) reported a compilation of experimental and theoretical 1s linewidths in some compounds containing carbon, oxygen and nitrogen. The experimental value reported for methane is 94 meV, while our calculated value using the EC technique is 96 meV (60 meV when the NEC approach is used). The agreement is very encouraging and supports application of the EC method for the calculations of molecular Auger transition rates in carbon. The transition rate is associated with valence electron population and is better estimated in EC method (see Table 4.2).

By comparison to Ne, there can be some satellite lines present in the CH_4 spectrum. Kvalheim (1982) reported about 5% satellites present in the inner-inner orbital region of the methane Auger spectrum. The satellites are due to some configuration interaction.

It is also most likely that satellite lines will appear in a region between 240 and 250 eV (by analogy to the Ne (KLL) spectrum). Some authors (Hutson and Ramaker 1987) reported 49% of the intensity of the methane molecule coming from satellite lines (21% intensity was associated with the initial state and 20% with the final state satellite lines). Our calculations (Larkins *et al.* 1990) show the estimate for the initial satellite lines as approximately 16-20% which is in an excellent agreement with Hutson and Ramaker (1987) findings.

Additional coincidence experiments are necessary to get conclusive evidence on the contribution of satellites in the Auger spectrum.

TABLE 4.4

Methane relative and absolute transition intensities calculated by various models

Final state		K / RHF	K / CI	H	J	Present INDO NEC	Present INDO EC	Expt R
$[1t_2 1t_2]$	$^3T_1$			0	0		0	
$[1t_2 1t_2]$	^1E	37	30	0		37	37	
$[1t_2 1t_2]$	$^1T_2$	56	59	97	100	56	56	100
$[1t_2 1t_2]$	$^1A_1$	7	12	3		7	7	
$[2a_1 1t_2]$	$^3T_1$	12	9	12	18	12	12	18
$[2a_1 1t_2]$	$^1T_2$	35	11	43	28	37	35	29
$[2a_1 2a_1]$	$^1A_1$	18	6	4	21	19	17	24
Total absolute rate (mau)		**6.81**	**6.24**	**79.94**		**2.20**	**3.54**	

K: Kvalheim (1982), H: Higashi (1982), J: Jennison(1980), R: Rye et al (1978)

4.4.2. NH_3

An experimental (Shaw *et al.* 1977) spectrum along with the calculated Auger transitions in ammonia are presented in Fig.4.5. The calculated spectrum is shifted 6.7 eV toward higher energy.

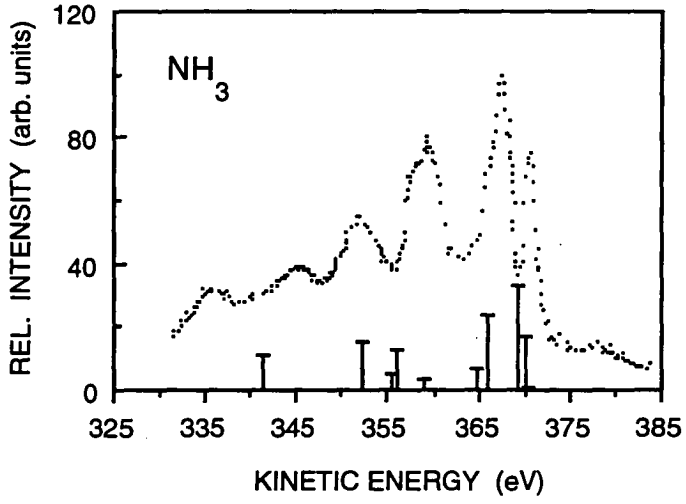

FIG. 4.5. An experimental (Shaw *et al.* 1977) and calculated (bars) Auger spectra for ammonia. The calculated spectrum is shifted 6.7 eV toward higher energy.

4.4.2.1. NH_3 Energies. Transition energies have been evaluated by several authors (Økland *et al.* 1976, Jennison 1981, Tarantelli *et al.* 1985). Økland et *al.* (1976) have used open-shell SCF calculations of double-zeta quality while Tarantelli *et al.* (1985) applied *ab initio* Green's functions and configuration interaction (CI) or second order algebraic diagrammatic construction (ADC) methods. Jennison (1981) used a modified version of HONDO 76 with double-zeta accuracy basis sets of Dunning.

The results are presented in Table 4.5. The experimental spectrum of ammonia is not appropriately predicted by the theory (Fig. 4.5). It is noticeable (Table 4.5) that *ab initio* calculated transition energies overestimate the width of the total Auger spectrum of ammonia while our INDO based calculations underestimate it. Moreover, even for the *ab initio* calculations there are differences between calculated and experimental Auger energies up to 4 eV. Separation of the experimental spectrum of ammonia into three regions: outer-outer, inner-outer and inner-inner is not possible. Correlation effects cause a splitting of the one electron states and hence an energy shift. Introduction of initial state correlations rectifies the energy span for the Auger transitions (see Jennison 1981). However, there are other effects (such as electronic relaxation) which are not compensated and energies of the Auger transitions in the ammonia molecule cannot be approximated very precisely using semi-empirical methods. Application of MBS wavefunctions improves multiplet splitting, however, it does not refine the overall spectrum significantly (Table 4.6).

The only satisfactory approximation of the experimental transition energies was achieved by Tarrantelli *et al.*(1985) who applied the ADC method. Yet, this method does not generate wavefunctions and hence requires special approaches for intensity calculations.

To advance the understanding of molecular Auger spectra more definitive spectrum of NH_3 (without satellite lines) need to be recorded.

TABLE 4.5

Ammonia transition energies calculated by various models relative to $[3a_1 3a_1]^1A_1$ energy.

Final	state	O	J	T /CI	T /ADC	Present /MBS*	Present /INDO	Expt S
$[3a_1 3a_1]$	$^1A_1$	0.0 (373.6)	0.0 (366.3)	0.0 **)	0.0 **)	0.0 (363.0)	0.0 (363.5)	0.0 (370.2)
$[1e 3a_1]$	^3E	2.2	0.6	2.3	2.5	-1.9	-0.3	
$[1e 3a_1]$	^1E	4.1	2.0	3.9	4.2	-0.3	0.9	4.7
[1e1e]	$^3A_2$	8.2	4.6	8.1	8.4	1.3	2.8	
[1e1e]	^1E	10.6	6.8	9.9	10.2	3.7	4.1	10.7
[1e1e]	$^1A_1$	12.8	9.0	11.8	11.8	6.1	5.4	13.4
$[2a_1 3a_1]$	$^3A_1$	14.9	12.4	14.0	13.9	9.6	11.2	

TABLE 4.5 Continuation

Ammonia transition energies calculated by various models relative to $[3a_1 3a_1]^1A_1$ energy.

Final	state	O	J	T /CI	T /ADC	Present /MBS*	Present /INDO	Expt S
$[2a_1 3a_1]$	$^1A_1$	20.8	17.3	19.3	19.1	14.9	14.2	19.3
$[2a_1 1e]$	^3E	20.9	16.4	19.7	19.7	12.8	14.6	19.3
$[2a_1 1e]$	^1E	28.6	23.2	26.1	25.6	19.6	18.0	26.5
$[2a_1 2a_1]$	$^1A_1$	39.7	33.6	37.4	36.4	29.6	28.8	35.6

*) Gamess (Schmidt *et al.* 1991) O: Økland *et al.* (1976), J: Jennison (1981), T: Tarrantelli *et al.* (1985/577), Present equivalent cores approach, S: Shaw et al (1977); In parentheses are absolute kinetic energies.

**) No absolute values of kinetic energy available.

4.4.2.2. NH_3 Transition Rates. Intensities of Auger transitions in the ammonia molecule have been calculated by Jennison (1981) who used an *ab initio* ground state orbital set and the intra-atomic transition model.

The theoretical profile generated using a gaussian curve with FWHM = 1.5 eV (Fig.4.3) is different from the experimental spectrum (Fig.4.2 or 4.5). Since the NH_3 spectrum cannot be easily separated into 3 independent parts (inner-inner, inner-outer, outer-outer) the assignment of peaks and intensity estimation varies for different researchers. The results of available calculations of intensities along with our EC results are presented in Table 4.6. The most intense transition is set to have 100 relative intensity. The total absolute rate of Auger transitions is 5.23 mau and is consistent with results obtained by Jennison. The NEC approach gives the total transition rate 26% smaller than the EC method. This is a consequence of different valence electron distribution for both (EC and NEC) approaches (see Table 4.2).

TABLE 4.6

Ammonia relative and absolute transition intensities, experimental and calculated by various models

Final	state	J	JA	Present /INDO	Expt W	Expt C	Expt S
$[3a_1 3a_1]$	$^1A_1$	53	85	52	55	52	54
$[1e3a_1]$	^3E	1		1			
$[1e3a_1]$	^1E	100	100	100	89	100	100
[1e1e]	$^3A_2$	0		0			
[1e1e]	^1E	63	40	74	100	73	68
[1e1e]	$^1A_1$	28	36	22	14	46	66
$[2a_1 3a_1]$	$^3A_1$	12		11		7	
$[2a_1 3a_1]$	$^1A_1$	44	65	38	45	63	52

TABLE 4.6 Continuation

Ammonia relative and absolute transition intensities, experimental and calculated by various models

Final	state	J	JA	Present /INDO	Expt W	Expt C	Expt S
$[2a_1 1e]$	^3E	16		16			
$[2a_1 1e]$	^1E	52	31	48	29	39	66
$[2a_1 2a_1]$	$^1A_1$	48	33	35	17	50	36

J: Jennison (1981), JA: Jennison (1981) - atomic matrix elements and a double zeta basis were used, W: White *et al.*(1977 - electron impact spectrum, C: Camilloni *et al.* (1977) - electron impact spectrum, S; Shaw *et al* (1977) - X-ray excited spectrum.

4.4.3. H_2O

An experimental (Siegbahn *et al.* 1975) spectrum along with the calculated Auger transitions in water are presented in Fig.4.6. The calculated spectrum is shifted 7.8 eV toward higher energy.

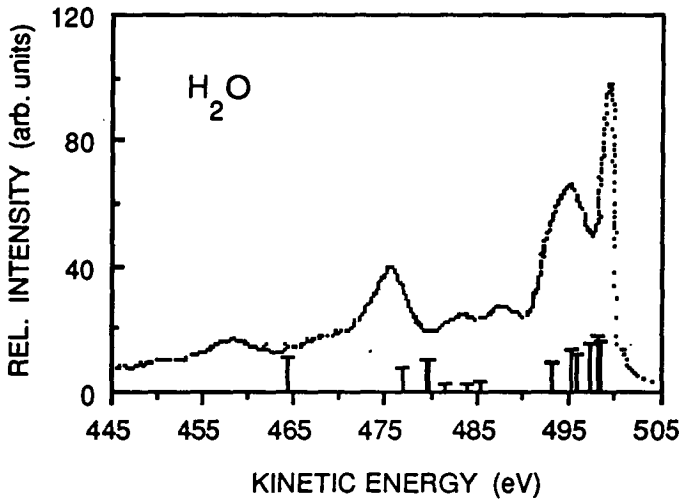

FIG. 4.6. An experimental (Siegbahn *et al.* 1975) and calculated (bars) Auger spectra for water. The calculated spectrum is shifted 7.8 eV toward higher energy.

4.4.3.1. H_2O Energies. The water molecule exhibits significant electron correlation effects and any calculations which omit this effect have not been very successful. Energies were calculated at the *ab initio* level by Hillier and Kendrick (1976), Ågren *et al.* (1975), Ågren and Siegbahn (1980) and Tarantelli (1985) and Carravetta and Ågren (1987). There are also results available from the use of the HAM/3 method for energy and intensity calculations (Chong 1981). Since our method cannot include semi-

internal correlations it does not compare favourably with *ab initio* methods. The results of energy calculations available for the water molecule are presented in Table 4.7. The experimental spectrum together with the results of our calculations are presented in Fig. 4.6. The calculated spectrum is too narrow and does not correspond well to the measured shape. When the experimental spectrum is compared with the results of various calculations, only those obtained by Carravetta and Ågren (1987) represent accurate energies of Auger transitions in the water molecule. The breakdown of the one-particle model is the principal source of the discrepancies.

TABLE 4.7

H_2O molecule transition energies calculated by various models relative to the $[1b_1 1b_1]^1A_1$ energy.

Final state		CH	A /SCF	A /CI	T /ADC	T /CI	H&K	T /CI opt	C&A /OSR HF	C&A /CI	Present /MBS* (NEC)	Present /INDO (NEC)	Expt S
$[3a_1 1b_1]$	$^3B_1$	1.1	-2.4		-1.9	2.1	-1.8	-2.1	-1.8	-1.3	-3.5	-1.9	-2.2
$[1b_1 1b_1]$	$^1A_1$	0	0	0	-0.8	-0.6	0	-0.7	0	0	0	0	0
		(498.8)	(500.2)	(500.8)			(501.1)		(500.8)	(499.4)	(490.5)	(490.8)	(498.6)
$[3a_1 1b_1]$	$^1B_1$	2.9	0.6	1.2	0.8	0.6	1.2	0.7	1.2	1.4	-0.5	0.5	0
$[1b_2 1b_1]$	$^3A_2$	3.7	2.5		2.5	2.2	3.1	2.3	3.1	3.0	-1.7	0.2	***
$[3a_1 1b_2]$	$^3B_2$	5.6	3.8		4.4	4.2	5.5	4.3	4.4	5.0	-0.9	1.2	)
$[3a_1 3a_1]$	$^1A_1$	3.6	3.9	4.4	4.0	3.4	5.4	4.3	4.4	4.8	1.6	2.9	4.8
$[1b_2 1b_1]$	$^1A_2$	5.1	4.5	5.1	4.4	4.1	5.2	4.3	5.1	5.0	-0.1	1.2	
$[3a_1 1b_2]$	$^1B_2$	7.2	6.4	7.0	6.6	6.4	8.1	6.6	7.0	7.3	1.7	3.3	)
$[1b_2 1b_2]$	$^1A_1$	8.6	11.9		11.7	11.9	13.3	11.7	12.5	12.0	5.2	5.4	11.9
$[2a_1 1b_1]$	$^3B_1$	16.8	18.2		16.6	16.7	18.8	16.4	18.7	17.3	12.1	13.3	)
													16.5
$[2a_1 3a_1]$	$^3A_1$	18.3	19.5		18.4	18.5	21.6	18.1	20.1	15.9	12.8	14.7	)
$[2a_1 3a_1]$	$^1A_1$	25.6	20.3	27.3	24.8	25.2	28.4	26.2	27.3	27.3	19.5	18.9	26.2
$[2a_1 1b_2]$	$^3B_2$	20.8	24.4		22.7	22.7	26.2	22.2	22.0	22.8	15.2	17.2	***
$[2a_1 1b_1]$	$^1B_1$	22.8	26.2	26.8	23.6	23.9	26.9	23.0	26.8	23.7	19.9	18.0	23.3
$[2a_1 1b_2]$	$^1B_2$	27.8	32.9	33.5	30.1	30.1	34.8	31.0	33.5	31.8	23.1	21.7	30.9
$[2a_1 2a_1]$	$^1A_1$	38.2	47.7	49.3	43.3	44.4	50.5	42.9	49.3	41.1	35.1	34.4	40.9

*) Gamess (Schmidt *et al.* 1991) CH: Chong(1981), A: Ågren *et al.* (1975), T: Tarantelli (1985/4683), H&K: Hillier and Kendrick (1976), C&A: Carravetta and Ågren (1987), S: Experimental spectrum of Siegbahn *et al.*(1975); In parentheses are absolute kinetic energies.

4.4.3.2. H_2O Transition Rates. The water molecule was used to test the one-centre model by Siegbahn *et al.* (1975) who applied *ab initio* wave functions to calculate Auger intensities. The values from our method based on the same model but with the use of the INDO

wavefunction are very similar in magnitude. The generated theoretical profile of the water Auger spectrum (Fig. 4.3) resembles the experimental shape (Fig.4.2 or 4.6), although, not very precisely. Recently Carravetta and Ågren (1987) presented calculations for the Auger spectrum of water based on Stieltjes imaging method which gives excellent results for the energy approximation. Both methods give very similar total transition rates : Carravetta - 5.52 mau , present work - 5.66 mau for H_2O or 6.88 mau when the equivalent cores model is used. The valence electron populations on the oxygen atom are 6.33 and 6.98 *e*, for NEC and EC models, respectively (Table 4.2). The experimental linewidth of 1s oxygen line in H_2O is not available, hence the theoretical result cannot be checked against experiment. However, for the O_2 molecule Coville and Thomas (1991) reported values 180 and 169 meV as experimental and calculated (using the EC model) linewidths, respectively. The theoretical values obtained from present study for oxygen in the water molecule are 154 and 187 meV for NEC and EC models, respectively. An additional experiment is needed to establish the lifetime of 1s hole in H_2O.

TABLE 4.8

H_2O molecule relative and absolute transition intensities calculated by various models

Final state		S	CH	C1	C2	Present /INDO
$[3a_1 1b_1]$	$^3B_1$	2	1	2	2	1
$[1b_1 1b_1]$	$^1A_1$	100	100	100	100	100
$[3a_1 1b_1]$	$^1B_1$	99	111	101	102	110
$[1b_2 1b_1]$	$^3A_2$	0	0	0	0	0
$[3a_1 1b_2]$	$^3B_2$	1	1	1	2	1
$[3a_1 3a_1]$	$^1A_1$	71	84	71	68	75
$[3a_1 1b_2]$	$^1B_2$	58	88	92	96	82
$[1b_2 1b_2]$	$^1A_1$	34	62	58	60	56
$[1b_2 1b_1]$	$^1A_2$	74	99	89	92	95
$[2a_1 1b_1]$	$^3B_1$	14	14	32	28	20
$[2a_1 3a_1]$	$^3A_1$	11	10	29	29	18
$[2a_1 3a_1]$	$^1A_1$	48	41	76	65	63
$[2a_1 1b_2]$	$^3B_2$	8	8	23	21	14
$[2a_1 1b_1]$	$^1B_1$	55	57	67	58	62
$[2a_1 1b_2]$	$^1B_2$	32	30	51	45	46
$[2a_1 2a_1]$	$^1A_1$	48	25	96	61	67
Total absolute rate (mau)				5.52	4.79	6.88

Siegbahn *et al.*(1975), CH: Chong(1981), C1: Carravetta (1987), mixed-wave calculations, C2: Carravetta (1987), hole-mixing calculations, Present - INDO equivalent cores approach.

Table 4.8 contains detailed results of calculations for the water molecule. The intensity coming via the $[1b_1 1b_1]\ ^1A_1$ final state is set to 100. It is encouraging that the INDO calculations yield relative intensities for every final state close to the values obtained by Carravetta, who used a far more complex method.

4.4.4. HF

An experimental (Shaw *et al.* 1975) spectrum along with the calculated Auger transitions in hydrogen fluoride are presented in Fig.4.7. The calculated spectrum is shifted 8.4 eV toward higher energy to align with the highest experimental peak.

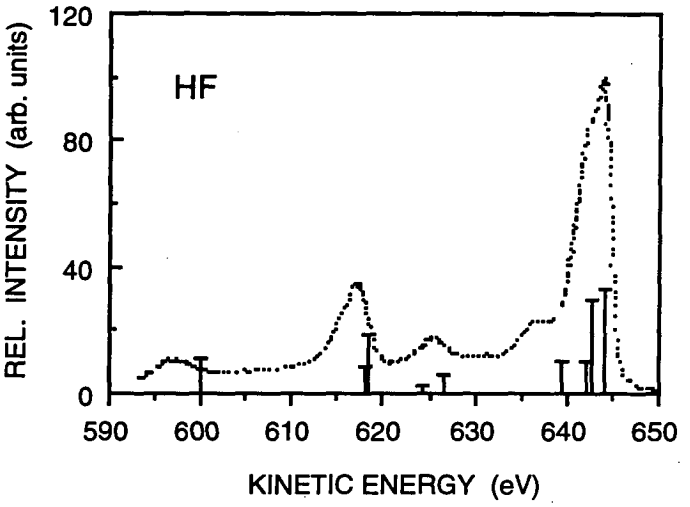

FIG. 4.7. An experimental (Shaw *et al.* 1975) and calculated (bars) Auger spectra for hydrogen fluoride. The calculated spectrum is shifted 8.4 eV toward higher energy.

4.4.4.1. HF Energies. Energy calculations of the Auger electron spectrum of HF were performed by several authors (Liegener 1982, Faegri and Kelly 1977, Kvalheim and Faegri 1979, Hillier and Kendrick 1976). Liegener (1982) has used renormalised Green's function theory while the other authors have used RHF formalism.

Results obtained via different methods vary by up to 8 eV and are presented in Table 4.9. There has been good agreement between the experimental (Shaw and Thomas 1975) and the calculated spectra. However detailed analysis is difficult because of ambiguity in curve fitting of the experimental spectrum. The present INDO method reproduces the experimental spectrum satisfactorily (Fig.4.7). Calculations performed using MBS wavefunctions improve the total width of the calculated transitions, however the overall

effect is not encouraging. Discrepancies appearing in the lower energy part of the spectrum can be attributed to inadequate description of the double-hole relaxation effect , which from comparison with atomic results can be of the order of 4 eV. For the INDO procedure, over-estimation of the size of the atomic Coulomb integrals is a major source of differences between experimental and calculated energies of Auger transitions in the HF molecule (Larkins 1990). When this fact is taken into account, no discrepancies are observed. Presence of three lone-pairs seem to be handled well. Nevertheless, caution should be exercised since our model - the HF molecule - is very simple.

TABLE 4.9

Hydrogen fluoride transition energies calculated by various models

Final	state	L	F&K	K&F	F	H&K	CH	Present /MBS*	Present /INDO	Expt S&T
$[1\pi 1\pi]$	$^1\Delta$	0	0	0	0	0	0	0	0	0
		(644.4)	(645.3)	**)	(645.7)	(646.0)	(644.8)	(636.2)	(635.9)	(644.3)
$[3\sigma 1\pi]$	$^3\Pi$	2.6	0.3	0.5	0.2	0.1	2.1	-2.4	-0.8	
$[1\pi 1\pi]$	$^1\Sigma^+$	1	2.9	1.7	2.9	1.2	2.1	3.0	2.0	1.9
$[3\sigma 1\pi]$	$^1\Pi$	4.3	3.4	3.4	3.4	3.4	4.1	0.3	1.5	1.9
$[3\sigma 3\sigma]$	$^1\Sigma^+$	9.5	8.3	8.4	8.3	8.3	5.2	3.2	4.8	7.4
$[2\sigma 1\pi]$	$^3\Pi$	20.4	20.8	19.7	21	20.8	19.6	16.9	17.6	19.2
$[2\sigma 3\sigma]$	$^3\Sigma^+$	24.7	24	23.1	24.2	24.1	22	18.2	19.9	19.2
$[2\sigma 1\pi]$	$^1\Pi$	26.6	30.7	29.4	31	31.3	28	26.7	25.9	28.1
$[2\sigma 3\sigma]$	$^1\Sigma^+$	31.1	34.7	33.2	33.3	33.6	29.7	26.8	26.1	30.2
$[2\sigma 2\sigma]$	$^1\Sigma^+$	49.6	53.05	55.1	54.6	57.0	46.5	44.9	44.4	48.7

*) Gamess (Schmidt *et al.* 1991) L: Liegener (1982), F&K: Faegri and Kelly (1977), K&F: Kvalheim and Faegri (1979), F: Faegri (1977), H&K: Hillier and Kendrick (1976), CH: Chong (1981), S&T: Experimental spectrum of Shaw and Thomas.(1975); In parentheses are absolute kinetic energies.

**) not stated.

4.4.4.2. HF Transition Rates. Total rates of Auger molecular transitions in hydrogen fluoride have been calculated by Liegener (1982), Kvalheim and Faegri (1979) using an *ab initio* based approach and by Chong (1981) on a semi-empirical level where the HAM/3 method has been used. Recently Zähringer *et al.* (1992) have applied molecular scattering wave functions to calculate Auger decay rates of hydrogen fluoride. The authors have concluded that transition rates are sensitive to the type of wave used for the continuum orbital (i.e. plane waves and Coulomb waves are not justified for computing rates). They have also found that the rate does not depend strongly on the interaction potential used to determine the continuum orbital and single potential is sufficient to calculate the molecular continuum waves for all final states. Ignoring the overlap matrix between initial and final

states had very small influence on the transition rates. Additionally, orthogonalization of the scattered wave with respect to the occupied orbitals of the initial state did not introduce any significant changes in the Auger transition rates unless the scattered wave was "poor quality" (i.e. plane or Coulomb waves). The above results were obtained with RHF (restricted Hartree-Fock) and SAHF (spin-averaged Hartree-Fock) approaches.

The agreement between different methods of calculation is most encouraging. Results obtained by Faegri and Kelly (1979) using the RHF approach are 8.65 mau, while incorporating CI for s states gives 8.27 mau. Our calculations for an equivalent cores model predict a total transition rate of 8.15 mau while the non-equivalent cores approach gives a value of 7.40 mau which is close to the results obtained by Zähringer *et al.* (1992) and Kvalheim and Faegri (1979). The population of valence electrons is 7.64 and 7.28 *e* for EC and NEC methods, respectively. The detailed results of calculations using various models are presented in Table 4.10. The relative intensity of the most intense transition $[1\pi 1\pi]^1\Delta$ is set to 100. The ratios between four major groups in the experimental spectrum of Shaw and Thomas (1975) have been estimated as 1.00/.05/0.18/.05 while most of the calculations (Table 4.10) predict 1.00/0.10/0.34/0.13. This discrepancy requires further investigation. It could be a gas scattering effect (Thomas, private communication). The theoretically generated profile using gaussian shapes with FWHM = 1.5 eV (Fig.4.3) compares favourably with the experimental shape (Fig.4.2 or 4.7).

TABLE 4.10

Hydrogen fluoride relative and absolute transition intensities calculated by various models

Final	state	L	F&K /RHF	F&K /RHF+CI	K&F /CI	CH	Z /SAHF	Present /INDO	Expt S&T
$[1\pi 1\pi]$	$^1\Delta$	100	100	100	100	100	100	100	100
$[3\sigma 1\pi]$	$^3\Pi$	1	1	1	0	0	1	1	1
$[1\pi 1\pi]$	$^1\Sigma^+$	30	30	36	30	29	30	29	
$[3\sigma 1\pi]$	$^1\Pi$	89	85	85	85	45	84	88	
$[3\sigma 3\sigma]$	$^1\Sigma^+$	31	28	20	29	16	27	30	
$[2\sigma 1\pi]$	$^3\Pi$	29	29	29	27	7	23	17	5
$[2\sigma 3\sigma]$	$^3\Sigma^+$	16	15	15	14	3	10	8	
$[2\sigma 1\pi]$	$^1\Pi$	59	65	65	55	26	56	55	18
$[2\sigma 3\sigma]$	$^1\Sigma^+$	29	32	26	21	12	28	26	
$[2\sigma 2\sigma]$	$^1\Sigma^+$	40	49	39	17	13	38	33	5
Total rate	absolute (mau)		**8.65**	**8.27**	**7.34**		**7.46**	**8.15**	
					only major contributions are summed				

L: Liegener (1982), F&K: Faegri and Kelly (1977), K&F: Kvalheim and Faegri (1979), CH: Chong (1981), Z; Zähringer et al. (1992) - Spin Averaged Hartree-Fock, Present: INDO equivalent cores approach, S&T: Experimental spectrum of Shaw and Thomas.(1975).

In Table 4.11, the results obtained by Faegri using SCF with a limited CI method for hydrogen fluoride are compared with our results where the equivalent cores model was used. There are small differences: Faegri's calculation predicts 11% intensity via triplet while it is only 6% with our model. Additionally, singlet transitions for the $2\sigma 1\pi$ final state are larger when calculated within an *ab initio* approach. Our calculation predicts larger intensities for the [3σ3σ] final state. The agreement in absolute transition rates is within 1%(!) and it is extremely encouraging since Faegri's calculations (Faegri 1977) are some of the most rigourous ones performed for molecules.

TABLE 4.11

Comparison of absolute transition rates (in mau) for hydrogen fluoride calculated using CI (Faegri 1977) and present methods.

								Total			
Channel	εs		εp		εd		Singlet		Triplet via εp	
Final state	F/CI	P/INDO	F/CI	P/INDO	F/CI	P/INDO	F/CI	P/INDO	F/CI	P/INDO
[2σ 2σ]	0.740	0.693	0.031	0.008	0.000	0.000	0.771	0.702		
[3σ 3σ]	0.083	0.082	0.033	0.033	0.288	0.521	0.404	0.636		
[1π 1π]	0.203	0.265	0.000	0.000	0.511	0.351	0.714	0.616		
[2σ 3σ]	0.014	0.065	0.506	0.479	0.002	0.009	0.522	0.552	0.269	0.157
[2σ 1π]	0.000	0.000	1.265	1.149	0.023	0.015	1.288	1.164	0.574	0.353
[3σ 1π]	0.000	0.000	0.049	0.038	1.643	1.815	1.692	1.853	0.021	0.012
[1π 1π]	0.000	0.000	0.000	0.000	1.986	2.107	1.986	2.107	0.000	0.000
						Total	**8.27*)**	**8.150**		

*)triplet 2σ3σ gives 0.033mau transition via d channel; F/CI - Faegri, P/INDO - present method.

4.5. Conclusions

The semi-empirical method is able to yield results comparable with *ab initio* methods in cases where many-electron effects are not too strong. The energies calculated using INDO formalism compare favourably with other (far more complex) methods in such cases. A special shift (incorporating relaxation effects and characteristic for the molecule) is needed to get better overall agreement of the experimental and calculated spectra.

The absolute transition rates are dependent on valence electron populations. The equivalent cores approach compensates for some relaxation and correlation effects and offers good approximation of transition rates in molecules. However, the relative intensities are substantially EC or NEC model independent.

The presence of dynamic and static correlation effects, transition dependent vibrational effects and satellite lines makes the quantitative interpretation of Auger spectra of molecules very difficult even in case of simple models as first row hydrides.

Inner valence orbitals require a description beyond the one-electron molecular picture. This feature is not available using the semi-empirical approach as presently formulated.

The effect of lone-pairs on the molecular Auger spectra has not been fully established since ammonia and water spectra experience correlation effects and lone-pair effect cannot be easily separated, while hydrogen fluoride seem to be too simple molecule for such exploration.

To fully evaluate this and other methods, results of more rigorous (coincidence) experiments are needed for all first hydride molecules. However on the basis of the available information, the present method appear to be provide a useful first order method for the calculation of molecular Auger spectra of larger molecules, on the condition, that correlation or relaxation effects are not too strong.

Chapter 5

CH_3X MOLECULES

5.1. Introduction

Auger spectra of molecules in the gas phase can reflect the local chemical environment of an atom in the corresponding molecule. Molecules described as CH_3X, where X = CH_3, NH_2, OH and F, are isoelectronic and the influence of symmetry or intra-molecular phenomena on their KVV Auger spectra can be studied. The carbon atoms in each of these molecules are in the same symmetrical environment. Nevertheless, CH_3X molecules possess low C_s symmetries (methanol and methyl amine) as well as higher 3-fold symmetries (ethane and methyl fluoride). The symmetry of a molecule affects the number of possible Auger transitions, being the highest for a molecule with the lowest symmetry. Additionally, the presence of X groups introduces different polarisation effects. The number of lone-pairs increases from one (for CH_3NH_2) to three (for CH_3F).

Analysis of the spectra in such a sequence should help to identify the trends of changes when progressing from ethane to methyl fluoride.

TABLE 5.1.

Symmetry and number of all possible two-hole states for the isoelectronic CH_3-X molecules.

Molecule	Symmetry	[vv']Γ	Valence orbitals
CH_3CH_3	D_{3d}	33	$2a_{1g}$,$2a_{2u}$,$1e_u$,$3a_{1g}$,$1e_g$
CH_3NH_2	C_s	49	3a',4a',1a",5a',6a',2a",7a'
CH_3OH	C_s	49	3a',4a',5a',1a",6a',7a',2a"
CH_3F	C_{3v}	33	$3a_1$,$4a_1$,1e,$5a_1$,2e

Several researchers reported calculations of Auger spectra for carbon and other elements in the CH_3X molecules (Ohrendorf *et al.* 1990, Liegener 1988, Larkins and Tulea 1987, Rye *et al.* 1978).

In the following sections comparison of experimental Auger spectra of carbon and other elements in the CH_3X molecules and the theoretical results obtained in the present and other studies will be given. The present method is based on the INDO formalism with non-equivalent cores (NEC) approach for energy and equivalent cores (EC) approach for intensity calculations, respectively. The results obtained for the CH_3X molecules using the above-mentioned approach will be compared and critically analysed.

5.2. Theoretical Considerations

Experimental geometries used in the present studies were taken from Landolt-Börnstein (1976) while experimental ionization energy values were obtained from various sources. Detailed information including geometries and ionization energies of the CH_3X molecules is provided in Appendix C.2. Fig.5.1 diagrammatically depicts ionization energy values for valence orbitals used in the current calculations. The width of Auger spectra is expected to increase from C_2H_6 to CH_3F, principally because of the increase in 2s-type ionization energies from C,N,O to F.

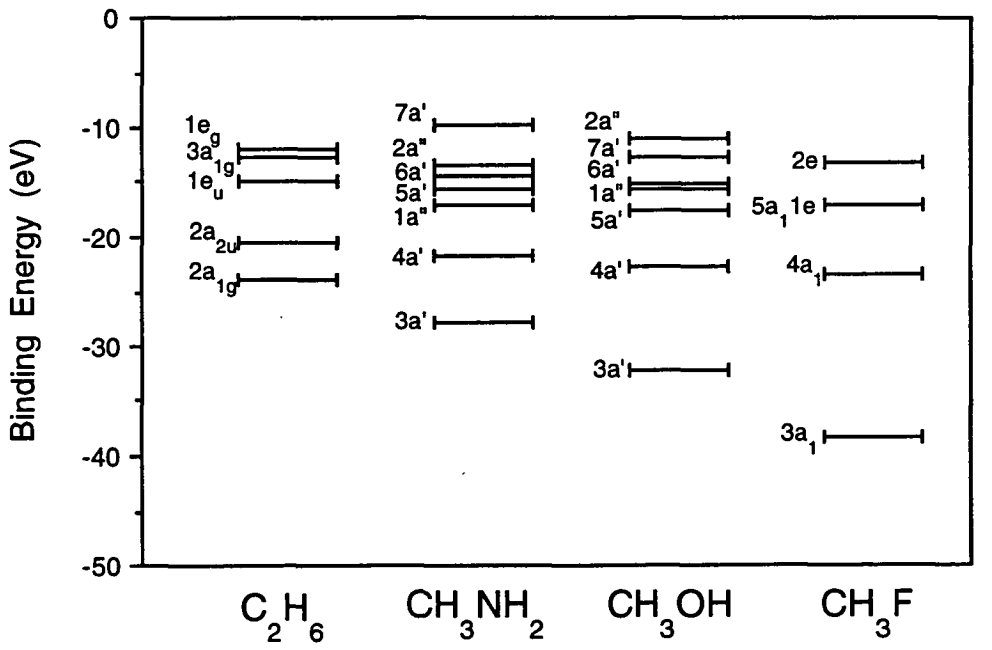

FIG.5.1. Experimental valence ionization energies of the CH_3X molecules.

In Table 5.2 valence electron populations and total Auger transition rates obtained for the CH_3X molecules using R^k atomic matrix elements from Walters and Bhalla (1971) for non-equivalent cores and equivalent cores approaches are presented.

TABLE 5.2.

Calculated valence electron populations and total Auger rates for the CH_3X molecules (X=CH_3, NH_2, OH and F), using non-equivalent cores (NEC) and equivalent cores (EC) approaches.

Molecule	Atom	Valence -e^- population		Calc. Auger rate (mau)	
		NEC	EC	NEC	EC
CH_3CH_3	C	3.88	4.96	2.18	3.45
	C	3.88	4.96	2.18	3.45
CH_3NH_2	C	3.80	4.89	2.05	3.36
	N	5.11	6.06	3.85	5.17
CH_3OH	C	3.74	4.85	1.97	3.30
	O	6.12	6.96	5.60	6.85
CH_3F	C	3.70	4.80	1.90	3.22
	F	6.99	7.65	7.22	8.19

As previously established (Chapter 4), the EC approach offers better approximation of the experimental linewidths than NEC approach. In Table 5.2 valence electron populations and total Auger transition rates calculated using both methods (NEC and EC) are presented to show the scale of changes.

5.3. Experimental Findings

Spohr *et al.*(1970) reported an X-ray induced Auger spectrum of ethane while Rye *et al.* (1980) applied an electron beam to obtain a KVV ethane spectrum. The former spectrum has a better resolution than the latter one. Additionally, the spectrum measured by Rye *et al.* (1980) has its background removed by a linear subtraction routine.

The experimental spectrum of a gaseous CH_3NH_2 molecule has not been reported yet.

Spectra of KVV Auger transitions in gaseous methanol have been recorded by Rye *et al.* (1978). The resolution of the spectra is claimed to be 2.4eV or better. The authors used a 2kV electron beam.

The only experimental spectrum of CH_3F reported to date has been measured by Moddeman (1970). The spectrum has a logarithmic intensity scale and cannot be used for detailed analysis of intensity of the KVV spectra in the CH_3F molecule.

The experimental KVV spectra of carbon and the X atom (X=C,O and F) in ethane (Spohr *et al.* 1970), methanol (Rye *et al.* 1978) and methyl fluoride (Moddeman 1970) are presented in Fig.5. 2 a and b, respectively.

The experimental spectrum of C(KVV) in methane (Spohr *et al.* 1970), is shown in Fig.5.2 a for comparison.

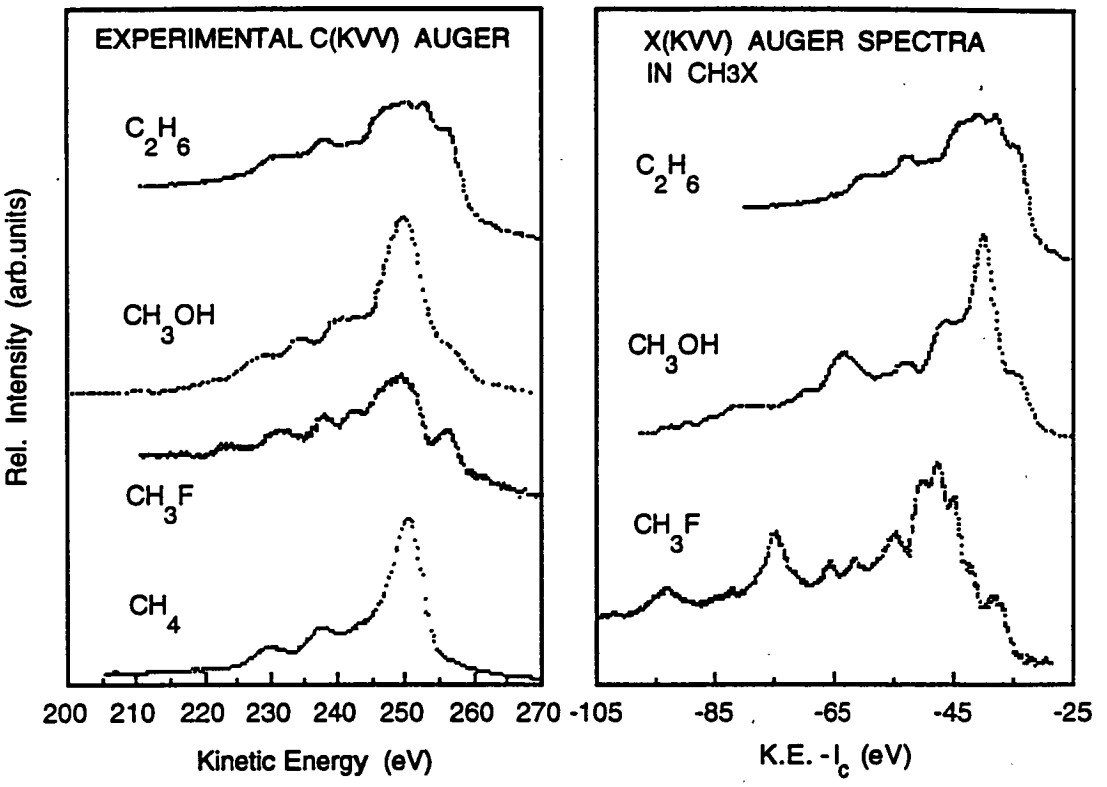

FIG. 5.2. Auger experimental spectra of carbon (a) and other elements (b) in the CH_3X molecules.
C_2H_6 spectrum measured by Spohr *et al.* (1970), CH_3OH spectrum by Rye *et al.* (1978), CH_3F spectrum by Moddeman (1970), CH_4 spectrum by Spohr *et al.* (1970).

5.4. Results and Discussion

Theoretically predicted Auger KVV spectra of C and X (where X=C, N, O and F) in C_2H_6, CH_3NH_2, CH_3OH and CH_3F, are presented in Figure 5.3 a and b, respectively.

The theoretical profiles were generated using gaussians with FWHM=1.5eV. As with the experimental spectra, the theoretical shapes for X element are displayed on a common scale

representing the difference between the kinetic energy of the Auger electrons and the energy required to create an initial core hole. Total areas under the peaks are set to be the same for each molecule. The generated profiles can be used as eye guides in spectra analysis. Additionally, for comparison purposes, the carbon Auger spectrum in methane is presented in Fig. 5.3 a.

Detailed results of calculations can be found in Appendix D.2.

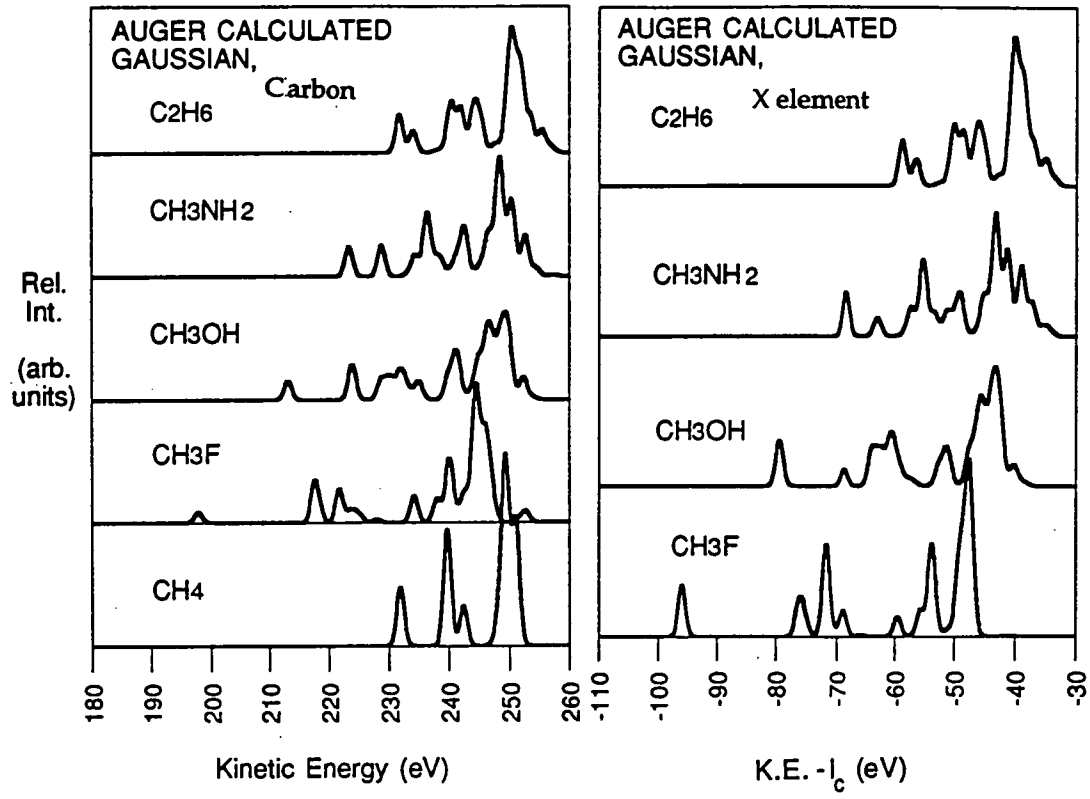

a b

FIG. 5.3. Theoretical Auger spectra of carbon (5.3 a) and X element (X=CH_3, NH_2, OH and F) (5.3 b) in the CH_3X molecules, generated using gaussian shape with FWHM=1.5 eV. Equivalent cores calculations.

Several calculations of energies at the *ab initio* level are available for carbon and other elements in CH_3X molecules (Ohrendorf *et al.* 1990, Liegener 1988). Semi-empirical (Larkins and Tulea 1987, Rye *et al.* 1978), statistical (Ohrendorf *et al.* 1990) or other (Liegener 1988) methods have been applied to intensity calculations for ethane and methyl fluoride.

5.4.1. C_2H_6

Results of energy and intensity calculations for the KVV spectrum of ethane together with available experimental assignments are presented in Table 5.3. The detailed assignment of Auger transitions is difficult because of broad structures in the experimental spectrum. The present theory predicts 33 final hole states (14 of them are triplets) in LS coupling where 8 of them have negligible intensity. The maximum intensity is assigned to the $[1e_u\ 3a_{1g}]^1E$ final hole state. The total transition rate for the KVV spectrum of carbon is calculated to be 3.45 mau, not too different from a result obtained for methane (3.54 mau). There is a good agreement between the calculated and the experimental spectrum. Some discrepancies are present for different methods of calculations.

Energies of transitions were calculated by Rye *et al.* (1978) who applied a one-particle model, and by Ohrendorf *et al.* (1990) who employed the two-particle Green's function method using the second order diagrammatic formalism ADC(2). The former results are comparable with our calculations and are presented in Table 5.3. The latter studies however cannot be directly compared with results of one-particle calculations and therefore are not shown in detail. Only a brief assignment of calculated groups of peaks to the experimental spectrum (Spohr *et al.* 1970) is presented in Table 5.3. In general, the energy calculation results obtained by Rye *et al.* (1978) are within 2 eV agreement with our results for the outer-outer region. Such discrepancies can be explained as due to slightly different values of the vertical ionization energies used by Rye *et al.* (1978) and in the present work.

TABLE 5.3

Ethane transition energies and intensities calculated by different authors

Final state		Sym-metry	Present Rel. En. (eV)	Rel.Int. C	Rye et al. (1978) Rel.En. (eV)	Rel.Int. C	Expt. mark	(Spohr) (eV)
$1e_g$	$1e_g$	$^3A_{2g}$	-32.7	0.0				
$1e_g$	$1e_g$	^1E_g	-33.5	6.8	-34.50	25.2	1	-34.8
$1e_u$	$1e_g$	$^3A_{1u}$	-33.7	0.0				
$1e_u$	$1e_g$	^3E_u	-33.8	0.0				
$1e_u$	$1e_g$	$^1A_{2u}$	-33.9	0.0				
$1e_g$	$1e_g$	$^1A_{1g}$	-34.3	2.0	-35.80	21.9		
$3a_{1g}$	$1e_g$	^3E_g	-34.4	0.1				
$3a_{1g}$	$1e_g$	^1E_g	-35.1	27.5	-36.20	81.3		
$3a_{1g}$	$3a_{1g}$	$^1A_{1g}$	-37.0	43.9	-39.10	54.1	2	-38.0
$1e_u$	$3a_{1g}$	^3E_u	-37.9	0.2				
$1e_u$	$1e_g$	$^3A_{2u}$	-38.3	0.0				

TABLE 5.3 Continuation

Ethane transition energies and intensities calculated by different authors

Final state		Sym-metry	Present Rel. En. (eV)	Rel.Int. C	Rye et al. (1978) Rel.En. (eV)	Rel.Int. C	Expt. mark	(Spohr) (eV)
$1e_u$	$3a_{1g}$	^1E_u	-38.6	100.0 (252.0 eV)	-39.60	74.8		
$1e_u$	$1e_u$	$^3A_{2g}$	-39.6	0.0				
$1e_u$	$1e_g$	^1E_u	-39.7	49.4	-37.50	40.2		
$1e_u$	$1e_u$	^1E_g	-40.2	89.9	-40.70	38.0	3	-41.0
$1e_u$	$1e_u$	$^1A_{1g}$	-40.7	26.4	-41.70	18.5		
$1e_u$	$1e_g$	$^1A_{1u}$	-41.1	14.5	-41.80	100.0* (248.8 eV)		
$2a_{2u}$	$1e_g$	^3E_u	-41.3	1.2	-44.30	38.0		
$2a_{2u}$	$3a_{1g}$	$^3A_{2u}$	-42.2	2.9	-42.20	6.8		
$2a_{2u}$	$1e_g$	^1E_u	-42.9	9.7	-47.00	25.4		
$2a_{2u}$	$1e_u$	^3E_g	-44.8	4.2	-40.80	7.0		
$2a_{2u}$	$3a_{1g}$	$^1A_{2u}$	-45.2	27.3	-46.30	28.7		
$2a_{1g}$	$1e_g$	^3E_g	-45.2	5.5	-48.10	10.7		
$2a_{2u}$	$1e_u$	^1E_g	-46.1	35.2	-44.50	27.6		
$2a_{1g}$	$1e_g$	^1E_g	-46.5	16.7	-51.80	31.2		
$2a_{1g}$	$3a_{1g}$	$^3A_{1g}$	-46.8	10.8	-47.00	10.7		
$2a_{1g}$	$3a_{1g}$	$^1A_{1g}$	-48.5	35.2	-51.40	31.6		
$2a_{1g}$	$1e_u$	^3E_u	-48.5	20.1	-45.40	11.7		
$2a_{1g}$	$1e_u$	^1E_u	-50.1	61.0	-47.70	33.9	6	-52.8
$2a_{2u}$	$2a_{2u}$	$^1A_{1g}$	-51.1	5.7	-51.30	16.3		
$2a_{1g}$	$2a_{2u}$	$^3A_{2u}$	-52.5	3.1	-51.80	1.9		
$2a_{1g}$	$2a_{2u}$	$^1A_{2u}$	-56.4	27.7	-57.80	96.0		
$2a_{1g}$	$2a_{1g}$	$^1A_{1g}$	-58.7	47.3	-59.90	49.1	8	-60.2
		Total	(mau)	3.45				

In parentheses - absolute energy values (in eV) of the most intense transitions.

*)There is an inconsistency in the Rye *et al.* (1980) paper: the most intense transition in ethane is assigned (in a table) to the $[1e_u\ 1e_g]^1A_{2u}$ final state, while in the text it is assigned to $[1e_u\ 1e_g]^1E_u$. However, the latest final state (according to the table (Rye *et al.* 1980) belongs to the previous feature (Rye *et al.* 1980). The only missing double hole configuration involving a $[1e_u\ 1e_g]$ final state seems to be $^1A_{1u}$.

However for transitions involving $2a_{2u}$, $1e_g$, $2a_{1g}$, $1e_u$ orbitals in final states variations are as large as 4.3-5.3 eV. Rye *et al.* (1978) have used the HONDO76 program with the Dunning basis set of double-zeta accuracy to calculate the spin dependent hole-hole repulsion term which has been used in energy calculations.

The total span of the KVV ethane spectrum is 26.0 eV using the semi-empirical method and 27.5eV when the Rye *et al.*(1978) approach is applied.

All zero-intensity transitions are assigned to the same transitions in both methods, i.e. in the present work and in Rye *et al.*(1978). The maximum intensity (reported as 100%) is assigned

by Rye *et al.* (1980) to the $[1e_u\ 1e_g]^1A_{1u}$ final double-hole state whereas for the present work the $[3a_{1g}\ 1eu]^1E_u$ transition is the strongest. One can notice differences between these two methods of calculations by comparison of results obtained for transitions involving $[3a_{1g}\ 1e_g]$, $[1e_u\ 1e_g]$, $[1e_u\ 1e_u]$, and $[2a_{2u}\ 2a_{1g}]$ singlet final states where discrepancies are 50% and more. Rye *et al.*(1978) claim that there is a strong non-orthogonality between initial and final state valence orbitals resulting from relaxation in the initial state to the presence of the core hole and it could be eliminated by performing separate RHF-SCF calculations upon the initial state and the ground state of the molecule. The above method does not give absolute transition rates.

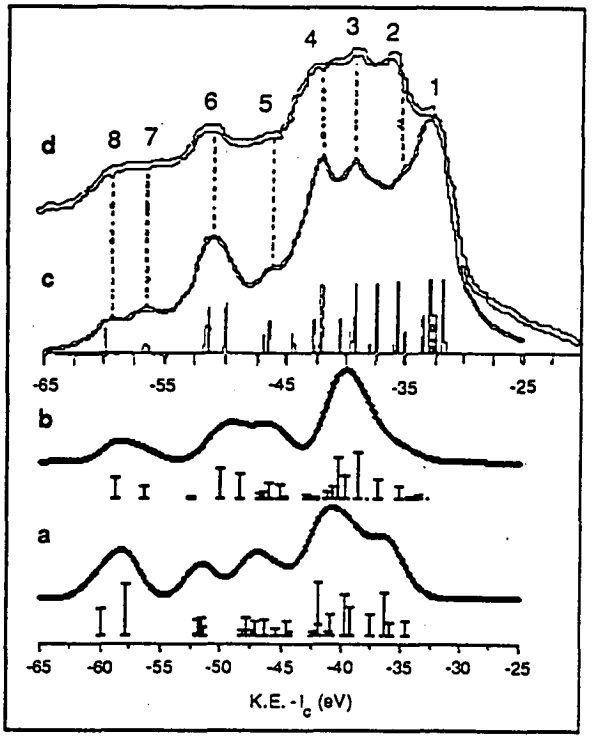

FIG. 5.4 Theoretical and experimental Auger spectra of ethane: (a) Rye *et al.* (1980)- gaussian profile, FWHM=3 eV, (b) present calculations- gaussian profile, FWHM=3 eV, (c) Ohrendorf *et al.* (1990) - lorentzian profile, FWHM=3 eV. The experimental spectrum (d) (Spohr *et al.* (1970) shifted towards higher energy 1.7 eV (as in Ohrendorf *et al.* 1990).

The ADC(2) (Ohrendorf *et al.* 1990) method predicts 30 doubly ionised main states (17 of them are singlets) and more than 25 doubly ionised satellites in an Auger spectrum of ethane. The main spectrum has a span of 28.3 eV and satellites appear mostly in the energy region of 240-244 eV, which is similar to methane. Some satellites could also be found at the energy 257 eV and below. The intensity of the carbon Auger spectrum in ethane arising

from satellite transitions was estimated by Hutson and Ramaker (1987) who used a self-fold of the one-electron DOS (density of states) with incorporated hole-hole correlation effects. The authors have predicted (similarly as for methane) about 50% of the carbon KVV intensity is yielded via satellites. Our calculations for methane (Larkins *et al.* 1990) have shown that the satellite component in the molecular Auger spectrum of methane is less than 20%. Therefore we assume that the above value also indicates the proportion of satellite present for ethane and it is 2-3 times lower than that suggested by Hutson and Ramaker (1987). Ohrendorf *et al.* (1990) used a statistical approach to calculate the intensities of Auger transitions. Every singlet transition contribution to the relative intensity is 3 times larger than that of the triplet. On that basis arbitrary intensities are assigned to calculated energy positions and the whole spectrum is generated by adding Gaussian or Lorentzian peaks. No absolute transition rate is available via this method. This method leads to extremely high peak at the beginning of the ethane spectrum (Fig.5.4). All presented calculation methods experience some problems in reproducing the experimental spectrum of ethane.

5.4.2. CH_3NH_2

The results of present method of calculations for this molecule are presented in Table 5.4.

TABLE 5.4

Transition energies and intensities of Auger spectra of methylamine calculated using present approach with equivalent cores.

Final state		Symmetry	Rel.energy (eV)	Rel.Int. Carbon	Rel.Int. Nitrogen
2a"	7a'	^{3}A"	-33.6	0.0	0.1
5a'	7a'	^{3}A'	-33.8	0.1	0.2
2a"	7a'	^{1}A"	-34.2	3.4	10.1
7a'	7a'	^{1}A'	-35.3	0.9	22.0
6a'	7a'	^{3}A'	-36.0	0.1	0.6
2a"	2a"	^{1}A'	-37.1	8.3	2.8
6a'	7a'	^{1}A'	-37.2	10.1	67.9
1a"	2a"	^{3}A'	-37.5	0.0	0.0
6a'	2a"	^{3}A"	-38.0	0.1	0.0
1a"	7a'	^{3}A"	-38.1	0.1	0.7
5a'	2a"	^{3}A"	-38.6	0.0	0.3
1a"	7a'	^{1}A"	-38.8	8.8	49.5
6a'	2a"	^{1}A"	-38.9	30.8	20.4
5a'	7a'	^{1}A'	-39.1	16.9	68.4
5a'	2a"	^{1}A"	-39.1	33.8	17.3
5a'	6a'	^{3}A'	-40.4	0.2	1.5
6a'	6a'	^{1}A'	-41.1	71.8	92.5
5a'	6a'	^{1}A'	-41.4	100.0 (250.2 eV)	99.2
4a'	7a'	^{3}A'	-42.0	0.9	1.7
1a"	6a'	^{3}A"	-42.3	0.2	0.1

TABLE 5.4 Continuation

Transition energies and intensities of Auger spectra of methylamine calculated using present approach with equivalent cores.

Final	state	Symmetry	Rel.energy (eV)	Rel.Int. Carbon	Rel.Int. Nitrogen
1a"	5a'	$^3A"$	-42.7	0.0	1.3
1a"	6a'	$^1A"$	-43.1	80.3	100.0 (362.0 eV)
1a"	5a'	$^1A"$	-43.2	88.2	85.0
4a'	7a'	$^1A'$	-43.2	4.9	17.8
5a'	5a'	$^1A'$	-43.3	86.9	64.9
1a"	2a"	$^1A'$	-44.6	43.2	27.9
4a'	2a"	$^3A"$	-44.6	2.4	0.5
1a"	1a"	$^1A'$	-45.2	56.4	68.4
4a'	6a'	$^3A'$	-45.8	8.2	2.5
4a'	2a"	$^1A"$	-46.5	13.8	6.0
4a'	5a'	$^3A'$	-47.5	7.8	3.8
4a'	1a"	$^3A"$	-48.8	6.3	2.5
4a'	6a'	$^1A'$	-49.0	52.6	42.8
4a'	5a'	$^1A'$	-49.1	45.1	35.6
3a'	7a'	$^3A'$	-49.4	1.7	11.6
4a'	1a"	$^1A"$	-50.3	36.1	29.5
3a'	7a'	$^1A'$	-51.3	6.3	40.6
3a'	2a"	$^3A"$	-51.3	5.6	4.0
3a'	2a"	$^1A"$	-52.8	17.6	12.4
3a'	6a'	$^3A'$	-53.3	15.8	23.4
3a'	5a'	$^3A'$	-53.6	18.1	19.3
4a'	4a'	$^1A'$	-54.8	19.3	7.7
3a'	5a'	$^1A'$	-55.1	57.3	70.0
3a'	6a'	$^1A'$	-55.3	54.5	73.2
3a'	1a"	$^3A"$	-55.5	14.6	19.7
3a'	1a"	$^1A"$	-57.2	46.0	60.8
3a'	4a'	$^3A'$	-58.5	5.6	5.6
3a'	4a'	$^1A'$	-62.8	67.2	39.7
3a'	3a'	$^1A'$	-68.2	64.2	95.0
	Total	rates	(mau)	3.36	5.17

In parentheses - absolute energy values (in eV) of the most intense transitions.

The calculated Auger spectra of carbon and nitrogen in methylamine along with theoretical profiles obtained using gaussian shapes with FWHM=1.5 eV are presented in Figure 5.5.

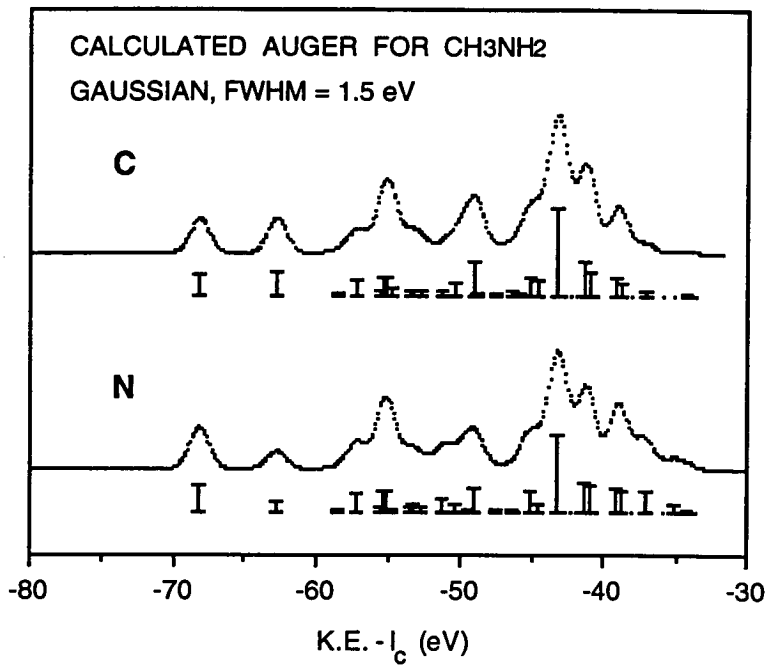

FIG. 5.5 Theoretical spectra of carbon and nitrogen in methylamine. Gaussian shape with FWHM = 1.5 eV was used to obtain theoretical profiles.

5.4.2.1. Carbon Spectrum. The symmetry of the methylamine molecule is lower than ethane and the number of possible final hole states increases to 37 non-zero states (49 total). The maximum intensity transition is assigned to the [5a' 6a']^{1}A' final state (Table 5.4). There are 4 more transitions with relative intensity over 70%: [1a" 5a']^{1}A'", [5a' 5a']^{1}A', [1a" 6a'],^{1}A'" and [6a' 6a']^{1}A'. The total absolute rate calculated using the equivalent cores model is 3.36 mau. The total span of the calculated spectrum is 34.6 eV which just reflects that the NH_2 group is more electronegative than CH_3. To obtain good agreement with experiment a shift of the calculated CH_3NH_2 spectrum toward higher energy would be needed on the basis of the trend observed in the calculated and experimental carbon spectra of the CH_3X group.

5.4.2.2 Nitrogen Spectrum. There are 40 non-zero final states in the Auger spectrum of nitrogen with the maximum intensity transition assigned to the [1a" 6a']^{1}A" final state. There are 4 more final double-hole states with relative intensity over 85%: [5a' 6a']^{1}A', [3a' 3a']^{1}A' [1a" 5a'],^{1}A", and [6a' 6a']^{1}A'. The total absolute rate calculated using the equivalent cores model is 5.17 mau. A shift of the calculated nitrogen spectrum toward higher energy would be necessary to achieve good alignment of calculated and experimental spectra. This has to be performed on the basis of the pattern observed in calculated and experimental X atom spectra of the CH_3X group. The theoretical profile does not resemble that of NH_3 which may suggest presence of effects which are not accounted for in the present method of calculation. The simulated spectrum of nitrogen is not much different from the carbon spectrum (Fig.5.5).

5.4.3. CH_3OH

The results of calculations of KVV spectra of carbon and oxygen in the methanol molecule are presented in Table 5.5.

TABLE 5.5

Transition energies and intensities of Auger spectra of methanol calculated using present approach with equivalent cores.

Final state		Symmetry	Rel.En.	Rel.Int.	Rel.Int.
			(eV)	Carbon	Oxygen
1a"	2a"	$^3A'$	-34.9	0.0	0.0
7a'	2a"	$^3A"$	-37.3	0.0	0.0
2a"	2a"	$^1A'$	-38.4	1.9	4.2
7a'	2a"	$^1A"$	-38.6	4.5	3.3
1a"	7a'	$^3A"$	-39.2	0.1	0.2
6a'	2a"	$^3A"$	-39.5	0.0	0.0
5a'	7a'	$^3A'$	-39.6	0.2	0.0
6a'	7a'	$^3A'$	-39.8	0.2	0.1
7a'	7a'	$^1A'$	-39.9	6.6	1.6
1a"	7a'	$^1A"$	-40.1	30.8	15.8
6a'	2a"	$^1A"$	-40.2	14.7	20.8
5a'	2a"	$^3A"$	-40.9	0.0	0.3
5a'	2a"	$^1A"$	-41.8	14.0	20.1
1a"	6a'	$^3A"$	-42.2	0.2	0.2
1a"	6a'	$^1A"$	-42.6	100.0 (249.8 eV)	100.0 (496.5 eV)
6a'	7a'	$^1A'$	-42.6	27.3	13.9
1a"	2a"	$^1A'$	-42.9	26.4	40.6
1a"	1a"	$^1A'$	-43.6	89.8	97.8
6a'	6a'	$^1A'$	-44.1	69.8	64.2
5a'	6a'	$^3A'$	-44.2	0.2	1.1
5a'	1a"	$^3A"$	-44.3	0.0	1.4
4a'	2a"	$^3A"$	-44.5	1.9	0.4
5a'	1a"	$^1A"$	-45.2	95.4	96.9
4a'	7a'	$^3A'$	-45.8	3.6	0.3
5a'	6a'	$^1A'$	-46.0	85.7	79.8
4a'	2a"	$^1A"$	-46.1	8.4	7.5
5a'	7a'	$^1A'$	-46.4	40.6	18.9
5a'	5a'	$^1A'$	-47.5	63.9	58.6
4a'	7a'	$^1A'$	-47.6	16.7	4.9
4a'	6a'	$^3A'$	-48.0	12.3	1.0
4a'	1a"	$^3A"$	-49.1	12.6	1.7
4a'	5a'	$^3A'$	-50.8	10.6	2.2
4a'	1a"	$^1A"$	-50.9	57.3	36.0
4a'	6a'	$^1A'$	-51.5	60.7	38.7
4a'	5a'	$^1A'$	-52.6	48.9	31.9
3a'	2a"	$^3A"$	-56.5	2.2	4.4
4a'	4a'	$^1A'$	-57.4	38.1	7.8
3a'	7a'	$^3A'$	-57.5	3.9	2.8
3a'	1a"	$^3A"$	-58.8	15.0	21.1
3a'	6a'	$^3A'$	-59.7	12.5	17.5
3a'	7a'	$^1A'$	-59.8	14.6	9.9
3a'	2a"	$^1A"$	-59.9	7.4	14.2

TABLE 5.5

Transition energies and intensities of Auger spectra of methanol calculated using present approach with equivalent cores.

Final	state	Symmetry	Rel.En. (eV)	Rel.Int. Carbon	Rel.Int. Oxygen
3a'	1a"	$^1A"$	-60.6	50.7	68.3
3a'	5a'	$^3A'$	-61.4	12.7	16.6
3a'	6a'	$^1A'$	-62.3	48.1	57.6
3a'	5a'	$^1A'$	-63.6	43.1	62.3
3a'	4a'	$^3A'$	-64.2	6.0	5.7
3a'	4a'	$^1A'$	-68.5	82.5	30.2
3a'	3a'	$^1A'$	-79.4	44.2	82.1
	Total	rate	(mau)	**3.30**	**6.85**

In parentheses - absolute energy values (in eV) of the most intense transitions.

The experimental spectra of carbon and oxygen are shown in Figure 5.6 a and b respectively.

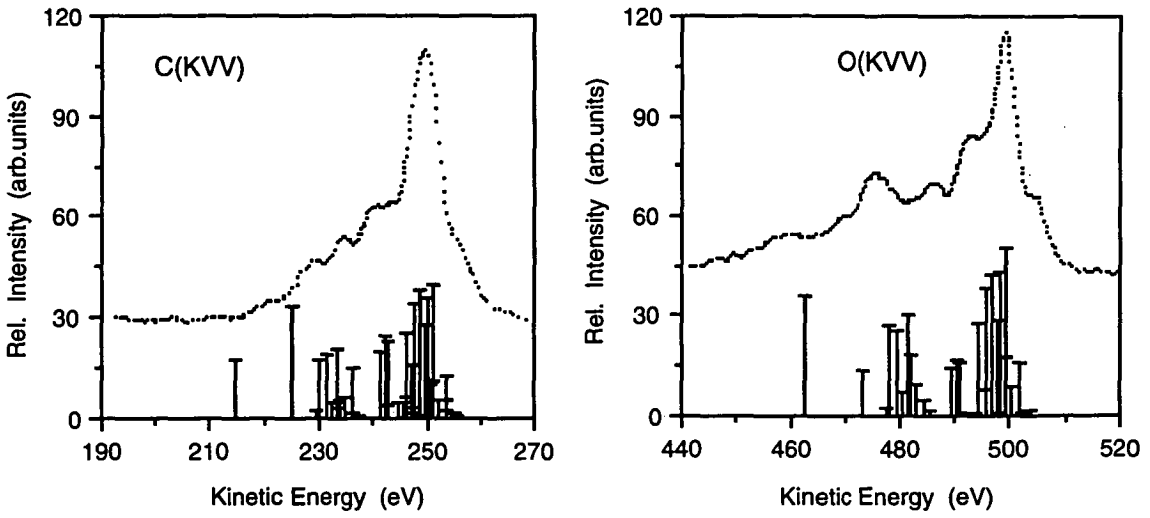

FIG. 5.6 The experimental (Rye *et al.* 1978) and calculated Auger spectra of carbon (a) and oxygen (b) in methanol. The calculated carbon and oxygen spectra are shifted toward higher energy by 1.4 and 3 eV, respectively.

5.4.3.1. Carbon Spectrum. The Auger spectrum of carbon contains 40 non-zero final states. The maximum intensity (100%) is assigned to the [1a" 6a']^{1}A" final state. There are 4 more transitions with relative intensity over 80%: [5a' 1a"]^{1}A", [1a" 1a"],^{1}A' [5a' 6a']^{1}A', and [3a' 4a']^{1}A'. The total absolute rate calculated using the equivalent cores model is 3.30 mau and the total span of the calculated spectrum is 44.5 eV (Table 5.5). A shift (1.4 eV) of the calculated carbon spectrum toward higher energy is necessary to align the calculated and experimental spectra. The calculated spectrum reproduces the experimental shape of carbon KVV in methanol satisfactorily (Fig.5.6a).

5.4.3.2. Oxygen Spectrum. There are 39 non-zero final states in the Auger spectrum of oxygen. The maximum intensity is assigned to the [1a" 6a']^{1}A" final state and four final states, [1a" 1a"]^{1}A', [5a' 1a"]^{1}A", [3a' 3a']^{1}A', and [5a' 6a']^{1}A', represent transitions with relative intensity over 75%. The total absolute rate calculated using the equivalent cores model is 6.85 mau. The total span of the calculated spectrum is 44.5 eV. The calculated spectrum is shifted 3 eV toward higher energy for better alignment with experimental oxygen KVV spectrum (Fig.5.6b). The experimental spectrum is adequately reproduced by the calculation.

5.4.4. CH_3F

Our results of Auger spectra calculations for the CH_3F molecule together with Liegener's results (Liegener 1988) from energy calculations and some assignments of an experimental spectrum by Moddeman (1970) are presented in Table 5. 6.

TABLE 5.6

Transition energies and intensities of the carbon Auger spectrum in methyl fluoride calculated using various approaches.

Final	state	Symmetry	Present			Liegener (1988)		
			Rel. En. (eV)	Rel.Int. C	Rel.Int F	Rel. En.*)	Rel.Int. C	Rel.Int F
1e	2e	^3E	-38.7	0.0	0.0			
1e	2e	$^3A_1$	-38.7	0.0	0.0			
1e	2e	$^1A_2$	-38.7	0.0	0.0			
2e	2e	$^3A_2$	-39.9	0.0	0.0			
2e	2e	^1E	-40.9	16.2	0.4	-35.8	24.9	6.2
2e	2e	$^1A_1$	-42.0	4.8	0.1	-36.3	9.1	3.0
$5a_1$	2e	^3E	-45.2	0.0	0.0			
$5a_1$	2e	^1E	-46.4	35.5	2.5	-39.7	47.1	14.5

TABLE 5.6 Continuation

Transition energies and intensities of the carbon Auger spectrum in methyl fluoride calculated using various approaches.

				Present		Liegener	(1988)	
Final	state	Symmetry	Rel. En.	Rel.Int.	Rel.Int	Rel. En.*)	Rel.Int.	Rel.Int
			(eV)	C	F	(eV)	C	F
1e	1e	$^3A_2$	-46.6	0.0	0.0			
1e	1e	^1E	-47.4	100.0 (246.2 eV)	100.0 (645.6 eV)	-49.5	100.0 (244.1 eV)	3.6
1e	2e	$^3A_2$	-47.4	0.0	0.0			
$4a_1$	2e	^3E	-47.5	7.3	0.1			
1e	$5a_1$	^3E	-48.0	0.0	0.0	-49.8	-	0.8
1e	1e	$^1A_1$	-48.1	29.4	29.2	-50.1- -50.8	50.1	1.8
1e	$5a_1$	^1E	-49.0	88.1	38.9	-43.3/ -46.8	52.3	7.6
1e	2e	^1E	-49.1	80.5	12.7	-41.4/ -41.7	96.8	3.5
$4a_1$	2e	^1E	-49.6	27.8	3.7	-52.1	76.5	100.0 (640.9 eV)
1e	2e	$^1A_1$	-50.8	23.7	3.7			
$4a_1$	$5a_1$	$^3A_1$	-50.9	8.3	0.3			
$4a_1$	1e	^3E	-51.6	18.0	1.3			
$5a_1$	$5a_1$	$^1A_1$	-53.2	30.8	6.0	-44.9/ -45.5	45.6	3.7
$4a_1$	1e	^1E	-53.7	68.9	58.6	-50.0- -54.3	35.2	7.0
$4a_1$	$5a_1$	$^1A_1$	-55.6	34.6	17.6	-56.3	18.3	13.4
$4a_1$	$4a_1$	$^1A_1$	-59.4	38.6	13.0	-55.6- -61.1	60.6	1.1
$3a_1$	2e	^3E	-65.6	4.7	1.1			
$3a_1$	1e	^3E	-68.6	11.6	17.1	-61.4	-	3.3
$3a_1$	2e	^1E	-69.8	17.7	3.6	-62.1	14.5	2.2
$3a_1$	$5a_1$	$^3A_1$	-71.0	4.9	3.3			
$3a_1$	$4a_1$	$^3A_1$	-71.7	3.5	5.0			
$3a_1$	1e	^1E	-71.9	43.9	56.8	-59.2- -75.7	-	63.1
$3a_1$	$5a_1$	$^1A_1$	-75.4	21.8	11.2	-68.4	8.8	1.9
$3a_1$	$4a_1$	$^1A_1$	-76.2	50.6	21.0	-77.2/ -79.2	9.8	12.8
$3a_1$	$3a_1$	$^1A_1$	-95.8	15.9	34.9	-96.8	-	21.3
	Total	rate	(mau)	3.22	8.19			

In parentheses - absolute energy values (in eV) of the most intense transitions.

*) There is not one-to-one equivalence between spectra calculated using the one particle method and the Green's function approach. Therefore, only the strongest components are listed. If there are 2 values of energies of states giving contribution to a certain final state, both values are listed as -77.2/-79.2. In a case when there are more than two participants to a final state, a range of energy is given (for example: -59.2 - -75.7).

In Figures 5.7 a and b experimental (Moddeman 1970) and theoretical (Liegener 1988 and present) spectra of carbon and fluorine, respectively, are presented.

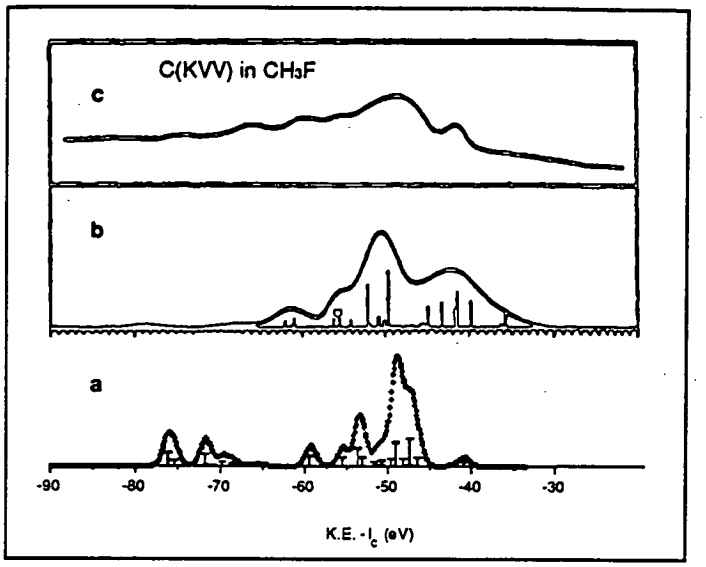

FIG. 5.7 The carbon spectra in CH_3F. (a) present calculations, gaussian profile, FWHM=1.5 eV, (b) Liegener (1988) - gaussian shape, FWHM not specified, (c) experimental (Moddeman 1970) shifted 4 eV.

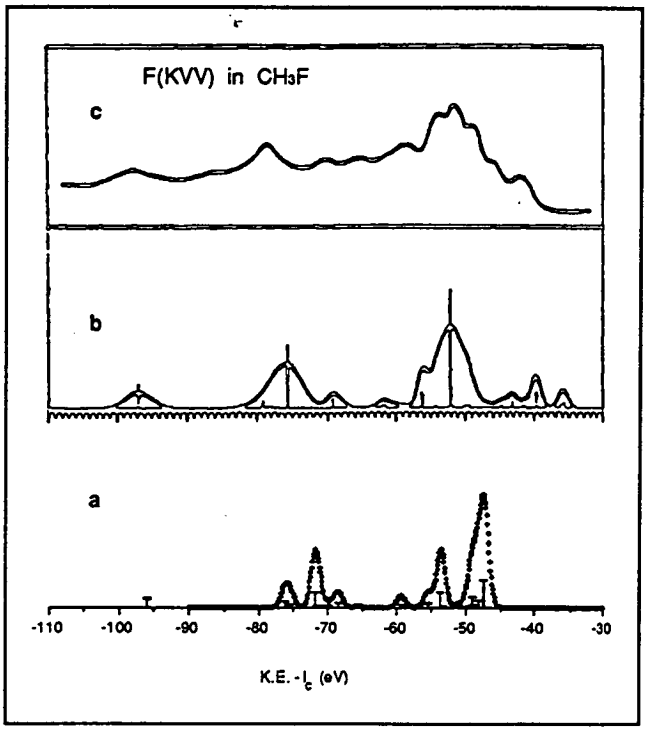

FIG. 5.8 The fluorine spectra in CH_3F. (a) present calculations, gaussian profile, FWHM=1.5 eV, (b) Liegener (1988) - gaussian shape, FWHM not specified, (c) experimental (Moddeman 1970) shifted 4 eV.

5.4.4.1. Carbon Spectrum. Only 25 final double-hole states have non-zero intensity (Table 5.6). The absolute total transition rate has a value of 3.22 mau. The most intense transition is assigned as 100% to the [1e 1e] ^1E final state, identical to Liegener's (1988) results obtained using a Green's function method. The next 2 transitions with relative intensities above 80% are [1e 5a']^1E and [1e 2e]^1E which also give strong lines in Liegener's calculations. However, any detailed comparison of present and Liegener's (1988) results is not possible since some transitions are not analogous in both methods.

The total span of the calculated carbon spectrum is 57.1 eV which is wider than the experimental counterpart. However, there is a possibility that the experimental spectrum is incomplete. A new measurement of the KVV carbon spectrum in CH_3F is needed to make the final comment. Overall, however, the presently calculated spectrum of carbon matches the experimental shape at least at the same level of accuracy as Liegener's results (Fig.5.7).

5.4.4.2. Fluorine Spectrum. The absolute transition rate through 23 non-zero final states is 8.19 mau when an equivalent cores approach is used and 7.22 mau otherwise. Almost one-third of the all possible double-hole states give relative intensities lower than 1%. The most intense transition is assigned to the [1e 1e]^1E final state while Liegener (1988) designated it to the [$4a_1$ 2e]^1E final state. The next most intense transition (59%) is assigned to the [$4a'_1$1e]^1E final state. (Table 5.6). The experimental spectrum is not accurately approximated by the theory. The feature from the high energy side is missing in the theoretical spectrum (Fig.5.8). This fact could be due to improper approximation of 1s core hole in fluorine by Ne^+ ion. A shift is required to align maxima of the calculated and the experimental spectra.

5.5. Comparison Between Molecules

As previously established (Chapter 4), the EC approach offers better approximation of the experimental linewidths than NEC approach. In Table 5.2 both values (NEC and EC) are presented to show the scale of changes. The most dramatic effect (when the NEC is replaced by EC method) is observed for carbon atoms. The changes are near 70% of the NEC calculated total transition rate for the most extreme case (C(KVV) in CH_3F). These changes are associated with redistribution of an electron charge when an initial hole is created and they suggest that the EC model provides a better physical approximation of the phenomenon of the presence of a core hole.

The differences in symmetries of the CH_3X molecules are not strongly manifested in the total Auger transition rates for carbon atoms (see Fig.5.9 and Table 5.2). The valence electron population changes from 4.96 e (for ethane) to 4.80 e (for methyl fluoride) while the calculated Auger rate decreases from 3.45 mau to 3.22 mau, respectively.

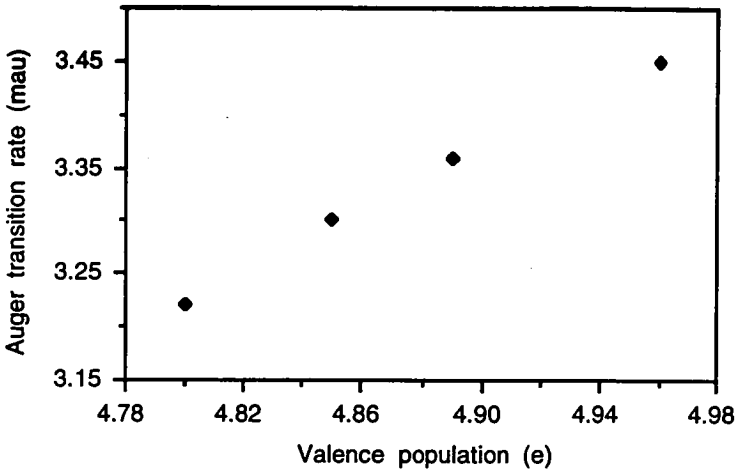

FIG. 5.9 Carbon Auger transition rates (EC) as a function of valence electron population on carbon atoms in CH_3X molecules.

There is a trend of decreasing electron population on the carbon atom in CH_3X molecules with increasing electronegativity of an X group. These changes are also reflected in the total transition rates. However, the overall effect is not as severe as the differences in total rates between the NEC and EC approaches (Table 5.2).

Figure 5.10 presents the calculated rates for KVV Auger transitions in CH_3X molecules as a function of valence electron population q represented as q(q-1). Similar statistical approach was suggested by Larkins (1971) for fluorescence yields in atoms and recently tested for molecules (Walsh *et al.* 1993) . In the original work (Larkins 1971) the intensity is expressed as

$$I[c] = 0.5\, n_s\, (n_s\text{-}1)\, R^A(c\text{-}ss) + n_s\, n_p\, R^A(c\text{-}sp) + 0.5\, n_p\, (n_p\text{-}1)\, R^A(c\text{-}pp) \qquad (5.1)$$

where n_s, n_p are the number of valence electrons associated with atom A (in the molecule - from Mulliken population analysis) and R^A are the reduced atomic rates expressed in LS coupling (taken for example from Chelkowska and Larkins 1991a). There is only weak dependence of the individual transition rates on atomic number. The primary source of diversity is associated with different number of valence electrons. Hence, it can be proven that an approximate expression of formula (5.1) can be written in terms of $q = n_s + n_p$ ($q > 1$) and some constant values (for the first row elements).

The application of this approach to molecules does not have a more rigourous theoretical basis.

In Fig.5.10 the solid line represents the equation $I = 0.45 + 0.15*q*(q\text{-}1)$, where I denotes the total Auger transition rate. The relationship is linear with the correlation coefficient equal to 1. Hence, the approach can serve as a brief estimate for calculated total Auger transition rates in the molecules containing the first row atoms.

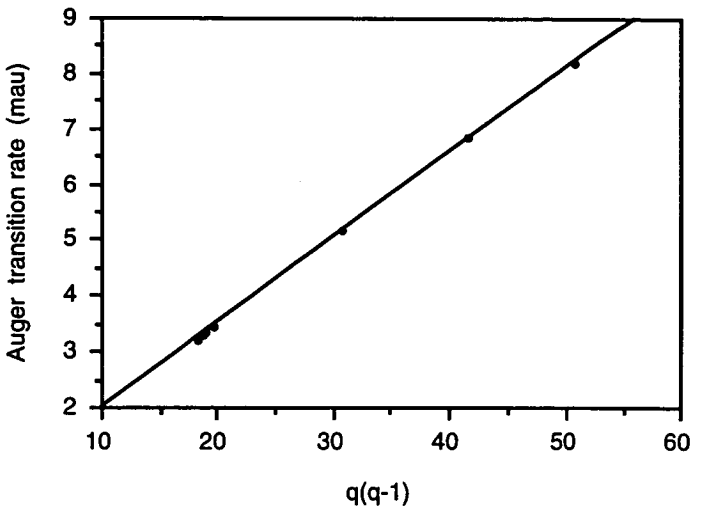

FIG. 5.10 Auger transition rates (EC) as a function of valence electron population q expressed as q*(q-1) relationship in CH_3X molecules.

5.6. Conclusions

The shift required to align calculated and experimental spectra of Y atoms (where Y=F, O, N and C) in the isoelectronic CH_3YH_n molecules is smaller than that which is required for the first row hydrides. The effect of proceeding from C_2H_6 to CH_3F can be observed for carbon and Y atom Auger spectra: more structure can be distinguished when moving from ethane to methyl fluoride. The basic structure of the KVV Auger spectrum in the CH_3-environment stays similar to that of methane. There is however a high energy peak which become more significant for CH_3OH and CH_3F carbon Auger spectra.

The total transition rates are also very similar for the carbon spectra of the whole CH_3YH_n family of molecules. It seems that polarisation introduced by an equivalent cores approach using CH_3Ne^+ as a model for the CH_3F molecule can be overestimated since approximation of core hole in a fluorine atom by Ne^+ may be too severe. Additionally, all parameters for Ne are extrapolated from values calculated for other elements with Z<10 (see Chapter 3.2) which could also introduce some inaccuracies.

Shifts of theoretical molecular spectra are required to achieve an agreement with experiments. The shift is important for compounds containing lone-pairs but not necessary for saturated molecules.

Chapter 6

XCHO MOLECULES

6.1. Introduction

Some of the experimental gas phase Auger spectra of the molecules described as XCHO, where X=F, OH, NH_2 and CH_3, have been recorded recently (Correia *et al.* 1991). However, formyl fluoride and formic acid Auger spectra have not been reported yet. The experience gained from the analysis of the first-row hydride and CH_3X spectra can be applied to predict KVV Auger spectra of carbon, oxygen and the heavy atom which is a part of the X group. The hypothesis about a molecular spectrum reflecting the local chemical environment of an atom in the corresponding molecule can be explored (since there are two molecules, acetaldehyde and formic acid where carbon atoms and oxygen atoms, respectively, are in different chemical environments).

The XCHO molecules, where X=F, OH, NH_2 and CH_3 are isoelectronic. They belong to the same low symmetry group, C_s and contain more electrons than their CH_3X counterparts. All molecules are planar except CH_3CHO. Theoretically there are 81 final states possible, some of them however have a zero or near zero intensity. For comparison purposes a KVV spectrum of formaldehyde, where 36 final double-hole states are possible will be considered. The XCHO notation for the molecules instead of conventional formulae will be retained in the present studies to highlight the influence of different X groups.

TABLE 6.1.

Symmetry and number of all possible two-hole states for the isoelectronic XCHO molecules.

XCHO Molecule	Symmetry	$[vv']\Gamma$	Valence orbitals
CH_3CHO	C_s	81	4a',5a',6a',7a',1a",8a',9a',2a",10a'
$HCONH_2$	C_s	81	4a',5a',6a',7a',8a',9a',1a",2a",10a'
HCOOH	C_s	81	4a',5a',6a',7a',8a',1a",9a',2a",10a'
FCHO	C_s	81	4a',5a',6a',7a',8a',1a",9a',2a",10a'
H_2CO	C_{2v}	36	$3a_1,4a_1,1b_2,5a_1,1b_1,2b_2$

Carbon and oxygen atoms (in the -CHO group) in all molecules are in the same symmetrical environment. However, the presence of X groups introduces different polarisation effects. Analysis of the spectra in such a sequence should help to identify the trends in changes when progressing from acetaldehyde to formyl fluoride.

In the following sections comparison of experimental Auger spectra of carbon, oxygen and other elements in the XCHO molecules and the theoretical results obtained in the present and Correia *et al.* (1991) studies will be given. The present method is based on the INDO formalism with non-equivalent cores (NEC) approach for energy and equivalent cores (EC) approach for intensity calculations, respectively. The results obtained for the XCHO molecules using the above-mentioned approach will be compared and analysed.

6.2. Theoretical Considerations

Geometries and ionization energies used in the present studies were taken from various sources. In the case of the FCHO molecule several ionization energy values were estimated from INDO calculations since experimental data were not available. Detailed information including experimental geometries and ionization energies of the XCHO molecules is provided in Appendix C.3. Fig.6.1 diagrammatically shows ionization energy values for valence orbitals used in the current calculations. The width of Auger spectra is expected to be similar for all molecules under consideration except for FCHO.

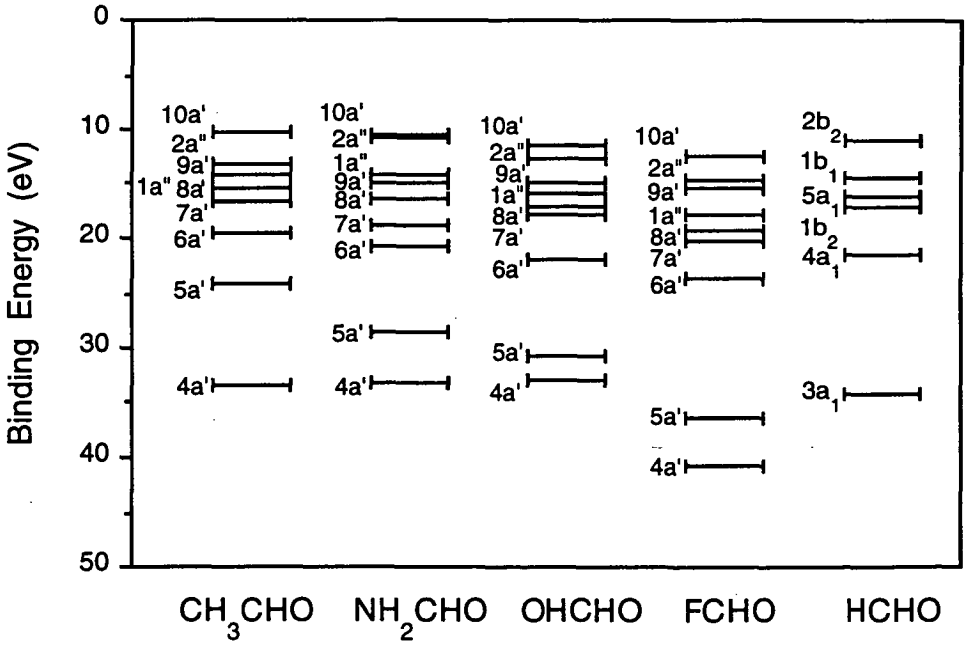

FIG.6.1. Experimental valence ionization energies of the XCHO molecules.

In Table 6.2 valence electron populations and total Auger transition rates obtained for the XCHO molecules using R^k atomic matrix elements from Walters and Bhalla (1971) for non-equivalent cores and equivalent cores approaches are presented.

TABLE 6.2.

Calculated valence electron populations and Auger rates for the XCHO molecules (X=CH_3, NH_2, OH, F and H), using non-equivalent cores (NEC) and equivalent cores (EC) approaches.

Molecule	Atom	Valence -e^- population		Calc. Auger rate (mau)	
		NEC	EC	NEC	EC
CH_3CHO	C	3.66	4.64	1.88	3.02
	O	6.28	6.99	5.55	6.89
	C (from CH_3)	4.02	5.02	2.97	3.54
NH_2CHO	C	3.56	4.53	1.77	2.87
	O	6.41	7.07	5.77	7.06
	N	5.22	6.08	3.87	5.24
OHCHO	C	3.48	4.50	1.70	2.83
	O	6.34	7.00	5.65	6.92
	O (from OH)	6.32	6.99	5.63	6.91
FCHO	C	3.41	4.44	1.63	2.76
	O	6.28	6.94	5.55	6.79
	F	6.25	7.64	7.35	8.25
HCHO	C	3.66	4.70	1.87	3.09
	O	6.23	6.90	5.47	6.72

As previously established (Chapter 4), the EC approach offers a better approximation of the experimental linewidths than the NEC approach. However, to show the scale of changes in electron populations and total Auger transition rates calculated results obtained via both methods (NEC and EC) are presented in Table 6.2.

6.3. Experimental Findings

Correia *et al.* (1991) reported X-ray induced (a monochromatised $Al_{K\alpha}$ source) Auger spectra of formaldehyde, acetaldehyde and formamide. These spectra are the only experimental Auger spectra in the gas phase reported to date for the XCHO molecules. Their C(KVV) and O(KVV) profiles are shown in Fig.6.2a and b, respectively. In Fig. 6.2 c the only available

experimental KVV spectrum of an X atom in XCHO molecules, i.e. N(KVV) in formamide, is presented.

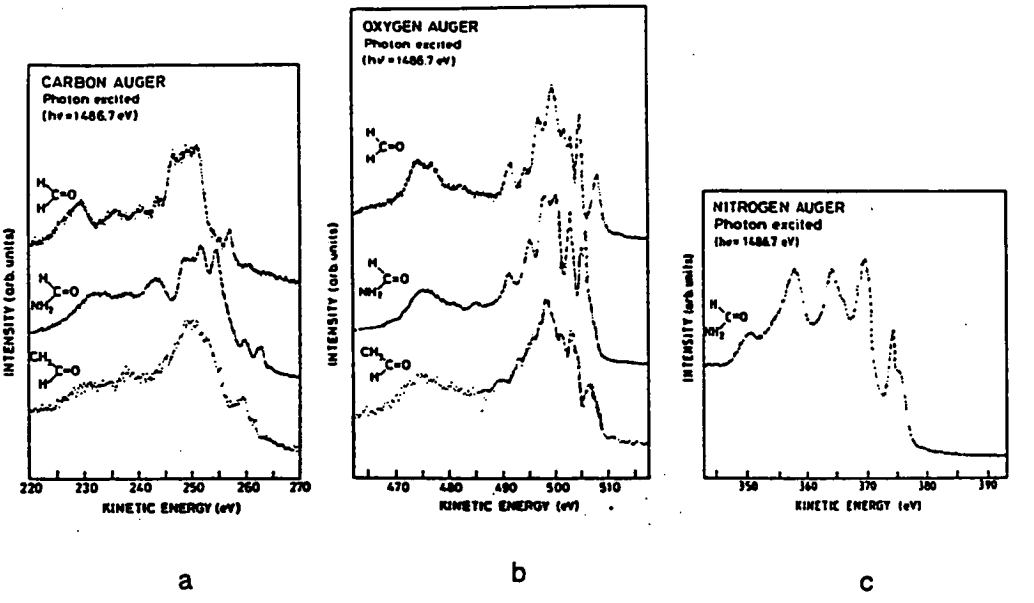

FIG. 6.2. Auger experimental spectra of carbon (a), oxygen (b) and nitrogen (c) in the XCHO molecules (Correia *et al.* 1991).

The Auger experimental spectra of the XCHO molecules lose their structural features and become more band-like when proceeding from formaldehyde to acetaldehyde.

6.4. Results and Discussion

Theoretically predicted Auger KVV spectra of C, O and X (where X=C, N, O and F) in CH_3CHO, NH_2CHO, OHCHO and FCHO are presented in Figure 6.3 a, b and c, respectively. Additionally, for comparison purposes calculated spectra of the simplest system containing the -CHO group, i.e. the HCHO molecule, are also shown in Fig.6.3a and b.

The theoretical profiles were generated using gaussians with FWHM=1.5eV and are displayed on a common scale representing the difference between the kinetic energy of the Auger electrons and the energy required to create an initial core hole. Total areas under the peaks are set to be the same for each molecule. The generated shapes can be used as eye guides in spectra analysis while detailed results of calculations can be found in Appendix D.3.

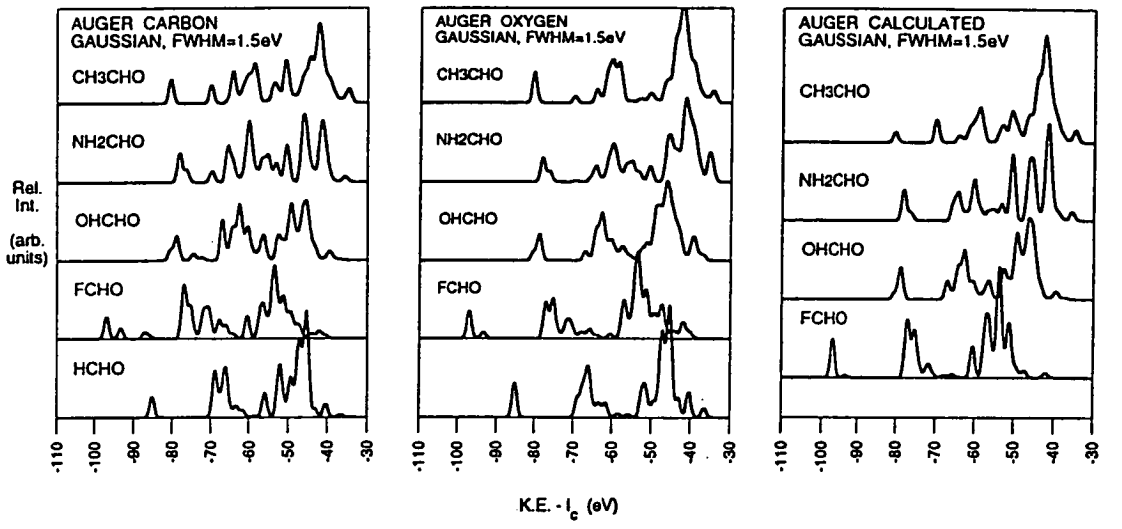

FIG. 6.3. Theoretical Auger spectra of carbon (a), oxygen (b) and X element (c) (X=CH_3, NH_2, OH and F) in the XCHO molecules, generated using gaussian shape with FWHM=0.5 eV. Equivalent cores calculations.

Correia *et al.* (1991) performed calculations of Auger spectra at several different levels: Hartree-Fock, Green's function and configuration interaction. The authors employed a common basis set (van Duijneveldt/Ross basis set with (5s,3p,1d) functions contracted from Huzinaga (9s,5p, 1d) for heavy atoms and (2s,1p) contracted from (4s,1p) for hydrogens) for all calculations. Additionally, they used experimental ground state geometries (as in the present calculations). The energy calculated by Correia *et al.* (1991) is presented as a double ionisation energy for the final states, while intensity analysis is based on ground state canonical Hartree-Fock orbitals. Unfortunately, detailed comparison of Correia *et al.* (1991) and the present calculations is not possible since only simulated spectra (with no specific information about each transition line) are available (Correia *et al.* 1991).

6.4.1. CH_3CHO

Results of energy and intensity calculations for the KVV spectrum of acetaldehyde are given in Table 6.3. The present theory predicts 81 final hole states, where 44 % of them are triplets in LS coupling. Many of the triplet final states have negligible intensity. Nevertheless, the

detailed assignment of Auger transitions is not achievable and, in general, several transitions are attributed to a group of peaks. The total width of the calculated spectra is 46.1 eV.

In Figures 6.4 a and b experimental spectra of acetaldehyde along with the theoretical profiles for carbon and oxygen, respectively, are shown. Bars represent calculated single transitions, while the theoretical shapes are generated using gaussians with FWHM=1.5 eV. The carbon spectrum of CH_3CHO consists of two spectra coming from carbon atoms from different chemical environments: methyl and carbonyl. The positions of these spectra is shifted 2.6 eV relative to each other, which corresponds to the shift between methyl and carbonyl carbon C 1s ionization energies used in the present calculations. There are some discrepancies in Auger energy values calculated by Correia *et al.* (1991) and in the present studies caused by the fact that Correia *et al.* (1991) have used 1s ionization energies values which are higher (by 0.2-0.8 eV) than the ones used here.

TABLE 6.3

Acetaldehyde transition energies and intensities calculated in the present studies.

Final	state	Symmetry	Rel.En. (eV)	Rel.Int. Carbon	Rel.Int. Oxygen	Rel.Int. C (-CH_3)
1a"	10a'	$^3A"$	-34.4	0.0	0.0	1.1
1a"	10a'	$^1A"$	-34.6	35.2	32.0	27.1
10a'	10a'	$^1A'$	-34.9	10.7	7.9	4.9
8a'	10a'	$^3A'$	-35.0	0.0	0.2	0.7
1a"	2a"	$^3A'$	-35.1	0.0	0.0	0.0
7a'	10a'	$^3A'$	-35.5	0.6	0.7	1.4
2a"	10a'	$^3A"$	-35.6	0.0	0.0	0.2
9a'	10a'	$^3A'$	-36.0	0.0	0.0	0.1
2a"	10a'	$^1A"$	-36.2	11.6	11.0	3.8
9a'	10a'	$^1A'$	-37.2	4.4	14.0	5.3
8a'	9a'	$^3A'$	-37.9	0.0	0.2	0.1
8a'	10a'	$^1A'$	-38.2	23.4	32.0	20.4
9a'	2a"	$^3A"$	-38.6	0.0	0.0	0.0
1a"	9a'	$^3A"$	-38.7	0.1	0.0	0.1
6a'	10a'	$^3A'$	-38.8	3.2	0.5	1.0
2a"	2a"	$^1A'$	-38.9	7.9	9.7	1.7
8a'	2a"	$^3A"$	-38.9	0.0	0.2	0.0
7a'	9a'	$^3A'$	-39.2	0.3	1.0	0.2
1a"	9a'	$^1A"$	-39.3	10.9	37.0	18.7
9a'	2a"	$^1A"$	-39.4	3.6	12.0	2.7
8a'	2a"	$^1A"$	-39.6	18.6	24.0	10.6
7a'	10a'	$^1A'$	-39.7	31.3	33.0	32.4
7a'	2a"	$^3A"$	-40.0	0.6	0.9	0.0
1a"	8a'	$^3A"$	-40.4	0.0	0.5	0.0
9a'	9a'	$^1A'$	-40.4	1.0	10.0	2.5
1a"	8a'	$^1A"$	-40.8	56.3	72.0	75.4
7a'	2a"	$^1A"$	-41.0	17.8	34.0	13.9
1a"	2a"	$^1A'$	-41.7	47.9	56.0	24.8
7a'	1a"	$^3A"$	-41.7	2.0	2.6	0.2
1a"	1a"	$^1A'$	-41.8	72.7	83.0	89.0
7a'	8a'	$^3A'$	-41.9	1.2	2.0	0.2

TABLE 6.3 Continuation

Acetaldehyde transition energies and intensities calculated in the present studies.

Final	state	Symmetry	Rel.En. (eV)	Rel.Int. Carbon	Rel.Int. Oxygen	Rel.Int. C (-CH_3)
6a'	10a'	^{1}A'	-42.0	37.7	22.0	16.4
8a'	8a'	^{1}A'	-42.3	27.5	38.0	40.4
6a'	2a"	^{3}A"	-42.4	2.4	0.5	0.1
7a'	8a'	^{1}A'	-42.6	33.9	69.0	68.2
6a'	8a'	^{3}A'	-42.6	4.5	0.3	0.5
6a'	9a'	^{3}A'	-42.7	0.7	0.5	0.1
7a'	1a"	^{1}A"	-42.8	54.1	100.0 (495.7 eV)	100.0 (248.4 eV)
6a'	2a"	^{1}A"	-42.9	24.3	16.0	7.2
8a'	9a'	^{1}A'	-43.4	9.2	26.0	14.2
5a'	10a'	^{3}A'	-43.6	1.0	0.6	3.0
7a'	9a'	^{1}A'	-43.8	7.2	53.0	25.1
6a'	1a"	^{3}A"	-43.9	7.4	1.4	0.7
6a'	1a"	^{1}A"	-44.3	73.6	49.0	51.4
7a'	7a'	^{1}A'	-44.3	23.9	71.0	70.6
6a'	9a'	^{1}A'	-44.6	10.6	19.0	8.6
5a'	10a'	^{1}A'	-44.9	23.0	3.1	14.1
6a'	7a'	^{3}A'	-45.3	9.0	2.5	0.6
6a'	7a'	^{1}A'	-45.8	64.6	48.0	47.0
6a'	8a'	^{1}A'	-46.8	45.5	51.0	51.8
5a'	2a"	^{3}A"	-46.9	0.9	0.7	1.9
5a'	9a'	^{3}A'	-47.7	0.2	0.8	2.3
5a'	2a"	^{1}A"	-48.2	18.0	3.2	5.6
5a'	8a'	^{3}A'	-49.1	1.6	1.5	9.0
5a'	9a'	^{1}A'	-49.2	8.4	3.9	7.1
5a'	1a"	^{3}A"	-49.4	2.8	2.2	13.3
5a'	7a'	^{3}A'	-49.7	1.9	1.3	11.6
6a'	6a'	^{1}A'	-50.4	46.8	17.	18.3
5a'	8a'	^{1}A'	-50.7	50.3	6.8	27.3
5a'	1a"	^{1}A"	-51.0	54.7	9.3	40.4
5a'	6a'	^{3}A'	-52.5	5.1	1.1	6.0
5a'	7a'	^{1}A'	-52.9	35.1	11.0	37.4
5a'	6a'	^{1}A'	-53.9	51.5	5.5	21.2
4a'	10a'	^{3}A'	-55.7	6.7	6.5	2.1
4a'	1a"	^{3}A"	-57.8	17.6	21.0	12.0
4a'	2a"	^{3}A"	-58.0	5.8	7.2	1.7
4a'	10a'	^{1}A'	-58.2	24.4	22.0	13.1
4a'	9a'	^{3}A'	-58.6	2.3	7.5	1.9
4a'	1a"	^{1}A"	-58.7	62.8	71.0	38.0
4a'	8a'	^{3}A'	-58.8	11.0	15.0	8.1
5a'	5a'	^{1}A'	-59.1	24.3	1.2	33.5
4a'	7a'	^{3}A'	-60.0	8.5	21.0	11.1
4a'	2a"	^{1}A"	-60.2	20.7	24.0	5.34
4a'	9a'	^{1}A'	-60.2	8.7	26.0	6.70
4a'	8a'	^{1}A'	-60.3	41.5	53.0	25.6
4a'	7a'	^{1}A'	-61.5	49.8	88.0	36.0
4a'	6a'	^{3}A'	-62.7	14.4	9.9	5.5
4a'	6a'	^{1}A'	-64.2	100.0 (229.6 eV)	43.0	20.1
4a'	5a'	^{3}A'	-65.5	12.0	0.9	0.6
4a'	5a'	^{1}A'	-70.0	58.4	21.0	61.0
4a'	4a'	^{1}A'	-80.5	77.5	98.0	27.5
	Total	rate	(mau)	**3.02**	**6.89**	**3.54**

In parentheses - absolute energy values (in eV) of the most intense transitions.

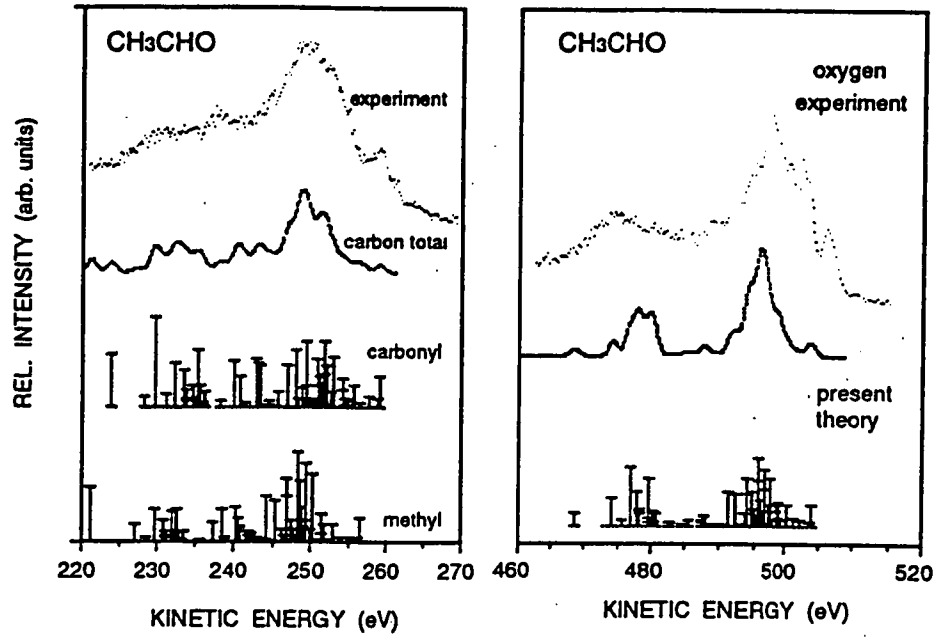

FIG. 6.4 Theoretical and experimental (Correia *et al.* 1991) Auger spectra of acetaldehyde: (a) carbon, (b) oxygen. A gaussian profile with FWHM=1.5 eV was used to generate theoretical shapes. The experimental spectrum of Correia *et al.* (1991) is not shifted.

6.4.1.1. Carbon Spectrum. The Auger spectrum of carbon in CH_3CHO incorporates transitions coming from 1s initial holes created in a methyl carbon atom as well as in a carbonyl carbon atom and hence the spectrum is very complex. The two theoretical shapes (i.e. corresponding to the carbonyl and methyl carbon atoms in CH_3CHO) can be compared in Fig.6.3 a and c, respectively. The overall profiles are similar despite differences in symmetry sites of the two carbon atoms. However, there is a shift of 2.6 eV between them which (when included) leads to the final theoretical profile for C(KVV) in the CH_3CHO molecule shown in Fig.6.4 a. The theoretical shape resembles the experimental spectrum very well. Using information from Table 6.3, one can assign the right-most peak in the experimental carbon spectrum (Fig.6.4 a) to the [1a" 10a'] ^{1}A" and [10a' 10a'] ^{1}A' final states. Therefore, this peak would be associated with carbonyl rather than methyl carbon (opposite to that suggested by Correia *et al.* 1991). Any further detailed analysis of the carbon spectra is impossible since there are many final double hole states very close to each other (Table 6.3). The main broad experimental peak in the carbon spectrum can be associated with final states involving several molecular orbitals including even 5a'. The maximum of the experimental spectrum (about 248-249 eV) consists of several transitions involving mostly 6a', 7a', 1a" and 8a' orbitals. In particular, the most intense transitions in this energy region

are assigned to final states [6a' 1a"] ^{1}A", [6a' 7a'] ^{1}A', [6a' 8a'] ^{1}A', [7a' 7a'] ^{1}A', [5a' 10a'] ^{1}A' from the carbonyl carbon atom and [7a' 1a"] ^{1}A", [1a" 1a"] ^{1}A', [7a' 8a'] ^{1}A', [8a' 78'] ^{1}A', [1a" 2a"] ^{1}A', [6a' 7a'] ^{1}A' from the methyl atom (Table 6.3).

The total transition rate from the carbonyl carbon atom is 85 % of the rate calculated for the methyl carbon and reflects changes in charge distribution (Table 6.2) for these two carbon atoms located in different symmetry sites. The positions of the carbon atoms also influence intensities arising from certain final double-hole states. Hence, the maximum theoretical intensity coming from the methyl carbon atom is associated with the [7a' 1a"] ^{1}A" final state while for carbonyl carbon the most intense transition is assigned to [4a' 6a'] ^{1}A' (Table 6.3). Nevertheless, the final shapes of carbonyl carbon and methyl carbon spectra are very similar (which is not true for simulated spectra obtained from Hartree-Fock calculations by Correia *et al.* 1991). The overall reproduction of the experimental spectrum of carbon in the CH_3CHO molecule in the present calculations is excellent. The claim by Correia *et al.* (1991) that discrepancies in their intensity calculation can possibly be attributed to the one-centre decomposition scheme (which neglects two-centre contribution and relaxation effects) does not seem to be justified.

6.4.1.2. Oxygen Spectrum. The experimental Auger spectrum of oxygen in the CH_3CHO molecule incorporates two broad features. The one on the higher energy side includes several peaks while the other one is structureless (Fig. 6.2 b). The theoretical profile of the Auger spectrum of oxygen in CH_3CHO simulated using gaussians with FWHM=1.5 eV (Fig. 6.3 b) contains three characteristic regions, two of them well reproduce the shape of the experimental spectrum and the third one (assigned to the single transition [4a' 4a']^{1}A') is beyond the region of the measured spectrum. The total transition rate is 6.89 mau for the EC approach (Table 6.2). The calculated maximum intensity corresponds to the [7a' 1a"] ^{1}A" final state, i.e. the same as for the carbonyl carbon. The next most intense transitions are related to [4a' 4a'] ^{1}A', [4a' 7a'] ^{1}A', [1a" 1a"] ^{1}A', [1a" 8a'] ^{1}A", [1a" 4a']^{1}A", and [7a' 7a'] ^{1}A' (Table 6.3). The first distinctive peak on the high energy side in the experimental spectrum (Fig. 6.4 b) is assigned to the [1a" 10a'] ^{1}A" final state, while the maximum of the experimental spectrum (about 497-498 eV) is associated with several double hole final states involving mostly 7a', 1a" and 9a', 8a', 6a' molecular orbitals. The broad structureless feature in the experimental spectrum with a maximum of about 475 eV contains transitions coming from the final states containing a hole in the 4a' molecular orbital (Table 6.3). The theoretical profile has to be shifted about 2.6-2.9 eV to achieve better alignment with the experimental Auger spectrum of oxygen. Intensities of the transitions are very satisfactorily reproduced by calculations (Fig.6.4 b). However, in the case where inner-inner orbitals are involved in the Auger transitions, correlation and relaxation effects become more significant and the experimental energy is not reproduced very precisely by calculations. Nevertheless, the overall agreement between theory and experiment is very good.

6.4.2. NH_2CHO

The results of calculations of the KVV spectra of carbon, oxygen and nitrogen in the formamide molecule as well as available assignments of transitions from Correia *et al.* (1991) are presented in Table 6.4. Among 81 final hole states 36 of them are triplets, mostly with small intensities. The intensities of triplet transitions become more significant for the final states involving inner-inner molecular orbitals. The total width of the calculated spectra is 45.4 eV which is similar to acetaldehyde.

In Figures 6.5 a and b experimental and theoretical Auger spectra (respectively) of oxygen, nitrogen and carbon are shown. The theoretical shapes are generated using gaussians with FWHM=1.5 eV. All spectra are presented on one common scale representing double ionization energy or a difference between the kinetic energy of the Auger electrons and the core hole energy (which is equal to the negative value of the double ionization energy). The calculated spectra require a shift of several eV to align with the experimental spectra (see Fig. 6.5 a,b).

The differences in 1s ionization energies values used by Correia *et al.* (1991) and in the present studies are smaller than 0.3 eV.

TABLE 6.4

Transition energies and intensities of Auger spectra of formamide calculated using present approach with equivalent cores along with available assignments from other studies (Correia *et al. 1991).*

Final	state	Symmetry	Rel.En. (eV)	Rel.Int. Carbon	Rel.Int. Oxygen	Rel.Int. Nitrogen	Correia *et al.* assignment	Energy (eV)
1a"	2a"	^{3}A'	-32.8	0.0	0.0	0.0		
2a"	10a'	^{3}A"	-33.9	0.0	0.0	0.2		
2a"	10a'	^{1}A"	-34.7	0.7	42.0	2.6	1	-30.0
1a"	10a'	^{3}A"	-35.3	0.0	0.0	0.8		
8a'	10a'	^{3}A'	-35.4	0.1	1.1	0.2		
2a"	2a"	^{1}A'	-35.4	0.2	26.4	6.0	2	-31.5
1a"	10a'	^{1}A"	-35.6	14.7	79.4	10.6	4	-34.5
7a'	10a'	^{3}A'	-37.5	0.3	2.1	0.7		
10a'	10a'	^{1}A'	-37.7	1.4	42.1	0.7	3	-32.4
9a'	2a"	^{3}A"	-37.9	0.0	0.2	0.0		
8a'	2a"	^{3}A"	-37.9	0.0	0.9	0.0		
8a'	2a"	^{1}A"	-38.6	2.0	47.3	8.7		
9a'	2a"	^{1}A"	-38.9	2.1	49.5	2.1		
9a'	10a'	^{3}A'	-39.1	0.0	0.2	0.0		

TABLE 6.4 Continuation

Transition energies and intensities of Auger spectra of formamide calculated using present approach with equivalent cores along with available assignments from other studies (Correia *et al. 1991).*

Final	state	Symmetry	Rel.En. (eV)	Rel.Int. Carbon	Rel.Int. Oxygen	Rel.Int. Nitrogen	Correia *et al.* assignment	Energy (eV)
8a'	10a'	^{1}A'	-39.5	6.0	85.9	3.6		
6a'	10a'	^{3}A'	-39.6	0.8	0.6	0.6		
7a'	10a'	^{1}A'	-39.7	10.4	43.8	10.1		
1a"	9a'	^{3}A"	-39.9	0.1	0.3	0.1		
1a"	9a'	^{1}A"	-40.3	45.7	93.6	8.5		
8a'	9a'	^{3}A'	-40.4	0.2	1.5	0.0		
7a'	2a"	^{3}A"	-40.6	0.1	1.7	0.1		
9a'	10a'	^{1}A'	-40.8	6.2	69.5	0.8		
1a"	1a"	^{1}A'	-41.2	100.0 (253.2 eV)	94.6	100.0 (365.2 eV)		
7a'	2a"	^{1}A"	-41.3	2.7	33.0	23.2		
8a'	1a"	^{3}A"	-41.5	0.8	1.7	0.0		
6a'	2a"	^{3}A"	-41.5	0.4	0.5	0.1		
7a'	9a'	^{3}A'	-41.7	0.5	1.4	0.1		
6a'	10a'	^{1}A'	-41.7	12.6	23.0	7.3		
8a'	1a"	^{1}A"	-41.9	44.1	89.4	35.5		
6a'	2a"	^{1}A"	-41.9	3.7	12.3	16.8		
1a"	2a"	^{1}A'	-42.0	9.2	100.0 (495.9 eV)	48.9		
8a'	9a'	^{1}A'	-43.5	17.8	70.5	2.6		
8a'	8a'	^{1}A'	-43.8	11.8	51.2	8.0		
7a'	1a"	^{3}A"	-44.5	1.6	3.2	0.2		
6a'	9a'	^{3}A'	-44.6	3.7	0.9	0.1		
9a'	9a'	^{1}A'	-44.9	13.1	58.0	0.4		
6a'	8a'	^{3}A'	-45.0	3.0	0.1	0.3		
7a'	1a"	^{1}A"	-45.1	58.0	62.4	94.9		
7a'	8a'	^{3}A'	-45.5	1.4	2.6	0.1		
6a'	1a"	^{3}A"	-45.8	8.4	0.9	0.5		
6a'	9a'	^{1}A'	-45.9	38.5	18.8	4.9		
7a'	9a'	^{1}A'	-45.9	22.5	72.8	9.6		
7a'	8a'	^{1}A'	-46.3	25.5	48.7	26.9		
6a'	1a"	^{1}A"	-46.4	81.3	23.2	68.6		
6a'	7a'	^{3}A'	-49.9	6.8	1.0	0.5		
6a'	7a'	^{1}A'	-50.3	50.8	13.1	52.1		
7a'	7a'	^{1}A'	-50.6	20.1	24.3	56.9		
5a'	10a'	^{3}A'	-50.6	0.0	3.3	0.2		
6a'	8a'	^{1}A'	-50.7	30.3	25.7	30.5		
5a'	2a"	^{3}A"	-50.7	0.0	2.6	0.6		
5a'	2a"	^{1}A"	-53.1	2.8	8.7	2.4		
6a'	6a'	^{1}A'	-53.1	41.7	3.4	29.4		
5a'	10a'	^{1}A'	-53.3	7.3	11.3	1.3		
4a'	10a'	^{3}A'	-53.6	2.6	15.1	1.1		
5a'	1a"	^{3}A"	-53.7	0.0	5.0	2.3		
5a'	9a'	^{3}A'	-54.6	0.0	3.7	0.2		
5a'	8a'	^{3}A'	-54.8	0.3	3.8	0.6		
4a'	2a"	^{3}A"	-54.8	1.0	12.0	4.7		
5a'	1a"	^{1}A"	-55.2	60.3	16.4	9.7		
4a'	10a'	^{1}A'	-55.3	8.6	51.3	8.9		
5a'	8a'	^{1}A'	-56.5	31.6	15.0	2.8		

TABLE 6.4 Continuation

Transition energies and intensities of Auger spectra of formamide calculated using present approach with equivalent cores along with available assignments from other studies (Correia *et al. 1991).*

Final	state	Symmetry	Rel.En. (eV)	Rel.Int. Carbon	Rel.Int. Oxygen	Rel.Int. Nitrogen	Correia *et al.* assignment	Energy (eV)
4a'	2a"	^{1}A"	-56.6	3.2	40.6	14.5		
5a'	7a'	^{3}A'	-56.6	0.8	1.9	1.5		
5a'	9a'	^{1}A'	-56.9	28.5	13.6	0.8		
4a'	9a'	^{3}A'	-58.3	7.4	18.5	1.2		
4a'	1a"	^{3}A"	-58.5	21.5	22.6	19.4		
5a'	6a'	^{3}A'	-58.9	4.1	1.0	1.3		
4a'	9a'	^{1}A'	-59.4	26.3	64.5	4.5		
4a'	8a'	^{3}A'	-59.7	7.3	17.5	5.4		
5a'	7a'	^{1}A'	-60.0	30.1	13.2	8.6		
5a'	6a'	^{1}A'	-60.0	39.9	4.6	5.6		
4a'	1a"	^{1}A"	-60.2	68.9	76.8	59.4		
4a'	8a'	^{1}A'	-61.2	28.7	69.9	17.0		
4a'	7a'	^{3}A'	-62.5	7.9	12.3	14.9		
4a'	6a'	^{3}A'	-63.9	13.6	4.3	10.7		
4a'	7a'	^{1}A'	-64.3	41.3	62.9	46.6		
4a'	6a'	^{1}A'	-65.6	94.0	21.2	35.3		
5a'	5a'	^{1}A'	-69.6	22.9	4.7	1.0		
4a'	5a'	^{3}A'	-70.1	10.3	0.5	0.6		
4a'	5a'	^{1}A'	-76.4	33.1	43.5	16.1		
4a'	4a'	^{1}A'	-78.2	79.3	99.7	62.8		
	Transition	rate	(mau)	**2.87**	**7.06**	**5.24**		

In parentheses - absolute energy values (in eV) of the most intense transitions.

*6.4.2.1. **Carbon Spectrum.*** The experimental spectrum of carbon contains several broad peaks with the maximum intensity above 38 eV (Fig. 6.5 a). The calculated total transition rate is 2.87 mau (Table 6.2) which is 5% lower than for carbonyl carbon in acetaldehyde. An assignment of theoretical transitions was done by Correia *et al.* (1991) for the first four peaks only (Table 6.4). In our calculations, transitions associated with peaks 2 and 3 (Fig.6.5 a) have insignificant intensities. However, assignment of peak 4 to the [1a" 10a'] ^{1}A" final state is consistent with Correia *et al.* (1991). There is 1.3 eV discrepancy in energy value for this transition calculated by Correia *et al.* (1991) and in the present study.

Peaks 8, 9 and 10 in the experimental spectrum are related to over 30 final states. The most intense of them are: [1a" 1a"] ^{1}A', [6a' 1a"]^{1}A", [7a' 1a"]^{1}A", [6a' 7a']^{1}A', [1a" 9a']^{1}A" and [1a" 8a']^{1}A" (Table 6.4). Peak 12 consists mostly of intensities arising from transitions involving double-hole final states: [5a' 1a"]^{1}A", [6a' 6a']^{1}A', [5a' 8a']^{1}A', [5a' 9a']^{1}A'. The overall reproduction of the experimental spectrum is not very accurate however it compares favourably with far more computationally intensive methods used by Correia *et al.* (1991).

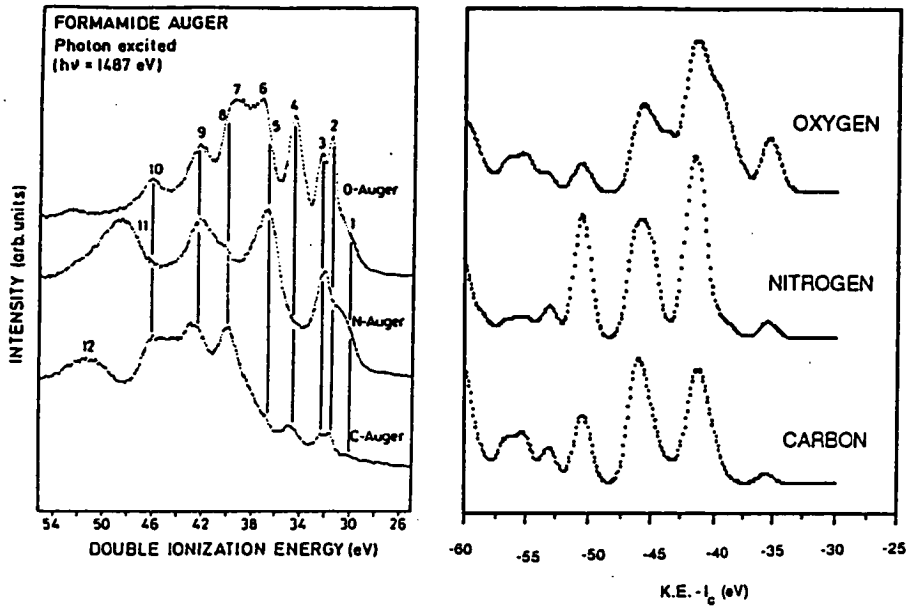

FIG. 6.5 Experimental (a) (Correia *et al.* 1991) and theoretical (b) spectra of oxygen, carbon and nitrogen in formamide. Gaussian shape with FWHM = 1.5 eV was used to obtain theoretical profiles.

6.4.2.2. Oxygen Spectrum. The experimental spectrum of oxygen is the most structured of all Auger spectra for formamide. Correia *et al.* (1991) assigned peak 1 to the [2a" 10a']^{1}A" final state, peak 2 to [2a" 2a"]^{1}A' and peak 3 to [10a' 10a']^{1}A' (Fig.6.5 a and Table 6.4). Present calculations do not reproduce the energies of the outermost part of the formamide spectra very well. Our assignment of the first four peaks in Auger oxygen spectrum is consistent with Correia *et al.* (1991). The experimental peaks 6 and 7 consist of over 20 final states. The most intense of them (over 80 % of relative intensity) are associated with [1a" 2a"]^{1}A', [1a" 1a"]^{1}A', [1a" 9a']^{1}A", [1a" 8a']^{1}A", [8a' 10a']^{1}A' (Table 6.4). Experimental peak 9 (Fig.6.5 a) is also assigned to a group of transitions with the strongest (over 60 % of relative intensity) related to [7a' 9a']^{1}A', [8a' 9a']^{1}A', [7a' 1a"]^{1}A" (Table 6.4). Peak 10 contains several transitions. The most intense of them are [6a' 8a']^{1}A' and [7a' 7a']^{1}A' (relative intensities are slightly above 20%). The calculated absolute transition rate is 7.06 mau which is only 2% higher than for acetaldehyde. The simulation of the experimental shape of the Auger oxygen spectrum by the theoretical profile is at least at the similar level of accuracy as that presented by Correia *et al.* (1991).

6.4.2.3. Nitrogen Spectrum. The experimental spectrum of nitrogen consists of five broad peaks (Fig.6.2 c) and four of them are presented in Fig.6.5 a. The calculated profile of the

nitrogen spectrum approximates the experimental shape satisfactorily, except the outermost energy region where intensities are underestimated. Detailed assignment of transitions in peaks 6,9 and 11 (Fig.6.5 a) is not achievable, nevertheless the dominating intensities can be identified. Hence, a transition to the [1a" 1a"]^{1}A' final state gives maximum intensity in the region of peak 6, transitions to the [7a' 1a"]^{1}A" and [6a' 1a"]^{1}A" final states give the greatest intensity in the region of peak 9 while transitions to the [7a' 7a']^{1}A' and [6a' 7a']^{1}A' final states give most intensity in the region of peak 11 (Table 6.4). When the initial hole appears in N1s the charge distribution changes to such an extent that the maximum electron population appears on 1a" then 4a', 7a' and 6a' molecular orbitals. This is reflected in the maximum intensities for the Auger nitrogen spectrum. The calculated absolute transition rate for formamide is 5.24 mau and is almost identical to result obtained for ammonia.

6.4.3. OHCHO

The formic acid molecule contains two differently located atoms of oxygen: one in a carbonyl group and one in a hydroxyl group. There are no experimental spectra available yet. Hence, only theoretical profiles of carbon and oxygen Auger spectra are shown in Fig. 6.6 a,b, respectively. Bars represent calculated single transitions. The calculated spectra are 44.2 eV wide. The separate theoretical shapes of oxygen spectra in OHCHO can be compared using Fig.6.3 b and c whereas the overall Auger oxygen spectrum is provided in Fig.6.6 b. All theoretical profiles were generated using gaussians with FWHM=1.5 eV. The detailed results of the calculations of KVV spectra of carbon and oxygen in the formic acid molecule are presented in Table 6.5.

TABLE 6.5

Transition energies and intensities of Auger spectra of formic acid calculated using present approach with equivalent cores.

Final state		Symmetry	Rel.En. (eV)	Rel.Int. Carbon	Rel.Int. O (-CHO)	Rel.Int. O (-OH)
2a"	10a'	^{3}A"	-36.3	0.0	0.0	0.1
1a"	2a"	^{3}A'	-36.4	0.0	0.0	0.0
2a"	10a'	^{1}A"	-36.9	2.0	14.7	2.0
7a'	10a'	^{3}A'	-37.5	0.2	1.1	1.0
9a'	10a'	^{3}A'	-37.6	0.0	0.0	0.1
10a'	10a'	^{1}A'	-38.4	2.5	17.3	1.1
9a'	10a'	^{1}A'	-39.0	3.6	14.9	1.7
1a"	10a'	^{3}A"	-39.0	0.0	0.0	0.5
1a"	10a'	^{1}A"	-39.5	18.1	47.3	13.7
8a'	9a'	^{3}A'	-39.7	0.4	0.2	0.0
2a"	2a"	^{1}A'	-39.9	1.1	7.8	2.0
9a'	2a"	^{3}A"	-40.0	0.0	0.0	0.0
9a'	2a"	^{1}A"	-40.9	2.3	8.7	1.8
8a'	10a'	^{3}A'	-40.9	0.1	0.5	0.2

TABLE 6.5 Continuation

Transition energies and intensities of Auger spectra of formic acid calculated using present approach with equivalent cores.

Final state		Symmetry	Rel.En. (eV)	Rel.Int. Carbon	Rel.Int. O (-CHO)	Rel.Int. O (-OH)
8a'	2a"	^{3}A"	-42.3	0.1	0.3	0.1
8a'	10a'	^{1}A'	-42.5	6.6	46.3	4.3
1a"	9a'	^{3}A"	-42.7	0.3	0.0	0.0
9a'	9a'	^{1}A'	-42.8	2.9	6.1	1.1
6a'	10a'	^{3}A'	-42.9	1.7	0.6	0.4
7a'	2a"	^{3}A"	-43.0	0.1	0.7	0.2
1a"	9a'	^{1}A"	-43.4	20.0	28.1	12.8
8a'	2a"	^{1}A'	-43.7	4.1	20.6	5.4
7a'	2a"	^{1}A"	-43.8	7.1	31.0	14.4
7a'	9a'	^{3}A'	-44.1	0.5	0.7	0.1
7a'	10a'	^{1}A'	-44.5	16.9	48.2	14.6
1a"	8a'	^{3}A"	-45.0	0.6	0.8	0.4
1a"	1a"	^{1}A'	-45.1	83.4	81.7	98.0
6a'	2a"	^{3}A"	-45.3	1.2	0.4	0.0
6a'	10a'	^{1}A'	-45.4	15.7	21.1	10.9
6a'	2a"	^{1}A"	-45.8	8.8	9.7	11.0
7a'	1a"	^{3}A"	-46.0	1.0	2.4	1.6
1a"	8a'	^{1}A"	-46.0	36.6	66.6	37.5
7a'	9a'	^{1}A'	-46.2	12.8	41.4	15.9
7a'	1a"	^{1}A"	-46.6	62.9	100.0 (492.4) eV	100.0 (494.0 eV)
7a'	8a'	^{3}A'	-46.6	0.8	2.2	0.4
6a'	9a'	^{3}A'	-46.8	1.1	0.3	0.0
1a"	2a"	^{1}A'	-47.8	18.9	50.6	28.3
7a'	8a'	^{1}A'	-47.8	22.7	65.4	33.8
6a'	8a'	^{3}A'	-48.5	4.6	0.2	0.5
8a'	8a'	^{1}A'	-48.8	9.8	33.2	8.8
6a'	9a'	^{1}A'	-48.9	19.5	8.7	7.9
7a'	7a'	^{1}A'	-49.0	28.9	73.5	62.1
6a'	1a"	^{3}A"	-49.0	10.2	1.3	0.1
6a'	1a"	^{1}A"	-49.6	78.2	31.4	75.9
6a'	7a'	^{3}A'	-49.7	8.8	1.7	1.0
8a'	9a'	^{1}A'	-51.1	9.8	18.6	4.7
6a'	8a'	^{1}A'	-51.2	31.7	30.5	31.8
6a'	7a'	^{1}A'	-52.6	59.7	31.5	62.3
5a'	10a'	^{3}A'	-53.8	0.0	1.3	0.2
5a'	2a"	^{3}A"	-55.3	0.0	0.9	0.3
4a'	10a'	^{3}A'	-55.4	2.9	8.4	1.6
6a'	6a'	^{1}A'	-56.3	50.6	7.1	37.0
5a'	10a'	^{1}A'	-56.6	9.7	5.2	1.1
5a'	9a'	^{3}A'	-56.9	0.2	0.8	0.2
4a'	2a"	^{3}A"	-57.5	1.9	5.7	2.8
4a'	10a'	^{1}A'	-57.5	10.2	28.9	9.9
5a'	2a"	^{1}A"	-57.9	5.4	3.3	1.0
5a'	1a"	^{3}A"	-58.4	0.0	2.9	1.9
5a'	9a'	^{1}A'	-59.0	11.4	3.1	0.8
5a'	8a'	^{3}A'	-59.0	0.2	2.1	0.5
4a'	9a'	^{3}A'	-59.1	3.5	5.0	2.0
5a'	7a'	^{3}A'	-59.6	0.5	2.3	1.2
4a'	2a"	^{1}A"	-59.7	6.5	19.4	9.0

TABLE 6.5 Continuation

Transition energies and intensities of Auger spectra of formic acid calculated using present approach with equivalent cores.

Final	state	Symmetry	Rel.En. (eV)	Rel.Int. Carbon	Rel.Int. O (-CHO)	Rel.Int. O (-OH)
5a'	1a"	^{1}A"	-60.3	47.9	10.7	6.9
4a'	1a"	^{3}A"	-60.6	16.7	18.3	19.1
4a'	9a'	^{1}A'	-60.6	13.2	17.5	6.6
4a'	8a'	^{3}A'	-61.4	5.0	12.2	5.8
5a'	8a'	^{1}A'	-62.1	25.3	8.1	2.4
4a'	7a'	^{3}A'	-62.2	8.5	19.0	16.1
5a'	7a'	^{1}A'	-62.3	32.5	13.0	6.8
4a'	1a"	^{1}A"	-62.6	57.3	62.5	62.4
4a'	8a'	^{1}A'	-63.0	23.3	46.4	21.4
5a'	6a'	^{3}A'	-63.0	4.7	1.0	1.2
4a'	7a'	^{1}A'	-64.2	40.6	78.3	60.7
5a'	6a'	^{1}A'	-64.4	36.4	4.7	4.3
4a'	6a'	^{3}A'	-65.4	13.1	5.5	11.7
4a'	6a'	^{1}A'	-67.0	100.0 (228.9 eV)	27.3	39.1
4a'	5a'	^{3}A'	-72.4	7.6	0.5	0.3
5a'	5a'	^{1}A'	-74.6	17.3	2.0	0.7
4a'	4a'	^{1}A'	-78.9	59.4	76.0	67.3
4a'	5a'	^{1}A'	-80.5	26.4	24.9	13.9
	Transition	rate	(mau)	**2.83**	**6.92**	**6.91**

In parentheses - absolute energy values (in eV) of the most intense transitions.

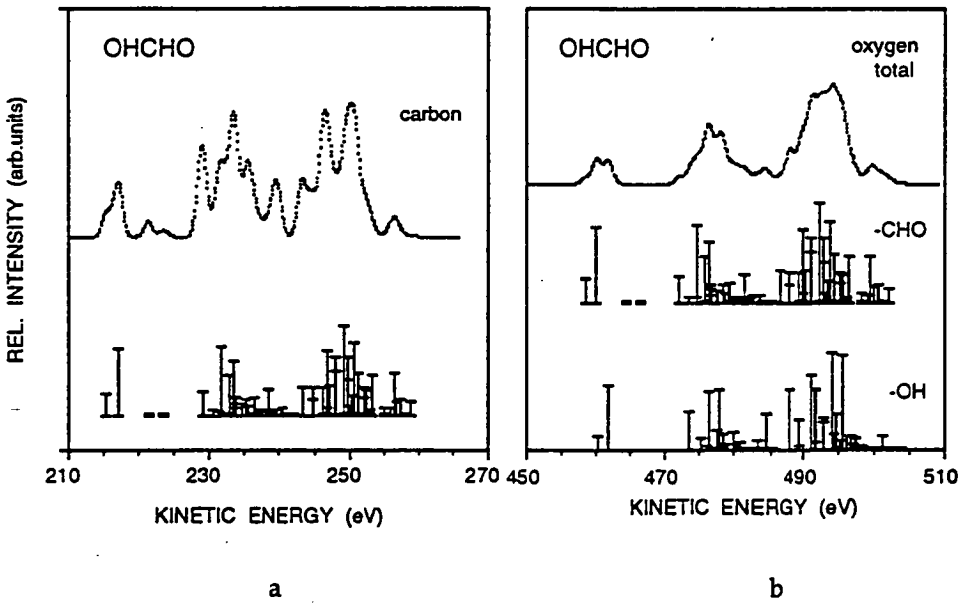

a b

FIG. 6.6 The theoretical (gaussian shape with FWHM=1.5 eV) Auger spectra of carbon (a) and oxygen (b) in formic acid.

6.4.3.1. Carbon Spectrum. The theoretical Auger spectrum contains almost 25% of negligible (below 1%) intensity transitions. Molecular population analysis shows that orbitals 4a' and 1a" should be the most important for the KVV spectrum of carbon in OHCHO. Indeed, the most intense transitions are assigned to the [4a' 6a']^{1}A', [1a" 1a"]^{1}A', [1a" 6a']^{1}A" and [1a" 7a']^{1}A" final states (Table 6.5). The total transition rate is 2.83 mau which is only 2% lower than for formamide. Additionally, the shape of the theoretical spectrum of carbon in OHCHO resembles the shape of the carbon spectrum in NH_2CHO. Hence, the effects introduced by presence of -OH group instead of -NH_2 do not seem to be significant. However, experimental results are needed to verify this finding.

6.4.3.2. Oxygen Spectrum. Each of the theoretical profiles (Fig. 6.3 b and c) contain almost 60 transitions with relative intensities above 1%. There is 1.6 eV difference between the energy of the same final states in carbonyl and hydroxyl group. However, the total transition rates are almost identical (6.92 and 6.91 mau for -CHO and -OH, respectively). The theoretical profiles obtained for both types of oxygen differ to a degree only in the highest kinetic energy region where the carbonyl oxygen spectrum contains more intense transitions than the hydroxyl oxygen spectrum. The maximum intensity transition is assigned to the [1a" 7a']^{1}A" final state for both oxygen atoms although the next most intense transitions (above 65%) vary for these two atoms. For the carbonyl oxygen the important transitions are: [1a" 1a"]^{1}A', [4a' 7a']^{1}A' , [4a' 4a']^{1}A', [7a' 7a']^{1}A', [1a" 8a']^{1}A' and [7a' 8a']^{1}A' while for the hydroxyl oxygen only [1a" 1a"]^{1}A', [6a' 1a"]^{1}A" , [4a' 4a']^{1}A' final states have relative intensities above 65%. Despite the above dissimilarities there seems to be no evidence for different symmetry sites, i.e. carbonyl and hydroxyl, resulting in different oxygen Auger spectra.

6.4.4. FCHO

The formyl fluoride molecule is the least studied one in the series of XCHO compounds. There are no experimental values of ionization energies available. Therefore, the required data were estimated using extrapolation of existing experimental values and results from several theoretical calculations. It was found that the most consistent results were obtained by means of the INDO technique. Hence, ionization energy values obtained this way were used in further calculations. The width of the theoretical spectra is 57.2 eV. The calculated Auger spectra of formyl fluoride are wider than any others of the previously studied molecules of the XCHO family, yet they are very close to the results obtained for the CH_3F molecule. The simulated Auger spectra (gaussian profile with FWHM = 1.5 eV) are shown in Fig. 6.3 a, b, c, while in Fig.6.7 the same spectra along with the bars representing single transitions are presented on a common energy scale.

TABLE 6.6

Transition energies and intensities of the carbon Auger spectrum in formyl fluoride calculated using present approach.

Final state		Symmetry	Rel.En. (eV)	Rel.Int. Carbon	Rel.Int. Oxygen	Rel.Int. Fluorine
10a'	10a'	^{1}A'	-39.8	2.6	11.5	0.5
2a"	10a'	^{3}A"	-39.9	0.0	0.0	0.0
9a'	10a'	^{3}A'	-40.1	0.0	0.0	0.0
1a"	2a"	^{3}A'	-40.4	0.0	0.0	0.0
2a"	10a'	^{1}A"	-40.6	6.0	14.6	0.4
9a'	10a'	^{1}A'	-41.6	3.0	20.5	0.4
1a"	10a'	^{3}A"	-41.7	0.1	0.0	0.3
7a'	10a'	^{3}A'	-42.0	0.6	0.8	0.3
1a"	10a'	^{1}A"	-42.1	15.9	39.0	8.5
8a'	10a'	^{3}A'	-42.9	0.1	0.4	0.0
9a'	2a"	^{3}A"	-43.4	0.0	0.0	0.0
2a"	2a"	^{1}A'	-43.9	8.4	11.6	0.2
9a'	2a"	^{1}A"	-44.3	4.7	16.9	0.2
8a'	9a'	^{3}A'	-44.5	0.1	0.4	0.0
9a'	9a'	^{1}A'	-45.6	1.6	15.4	0.2
6a'	10a'	^{3}A'	-45.8	1.3	0.8	0.5
1a"	9a'	^{3}A"	-46.7	0.0	0.0	0.0
8a'	10a'	^{1}A'	-46.8	7.2	37.3	1.4
7a'	9a'	^{3}A'	-46.9	0.2	0.8	0.1
8a'	2a"	^{3}A"	-47.4	0.0	0.4	0.0
7a'	10a'	^{1}A'	-47.4	16.6	39.9	7.9
1a"	9a'	^{1}A"	-47.4	12.4	45.2	4.7
7a'	2a"	^{3}A"	-48.1	0.4	0.8	0.0
8a'	2a"	^{1}A"	-48.5	12.7	26.1	0.7
6a'	2a"	^{3}A"	-49.2	3.4	0.7	0.0
7a'	2a"	^{1}A"	-49.2	19.1	37.3	4.6
6a'	10a'	^{1}A'	-49.4	18.9	26.1	10.8
6a'	9a'	^{3}A'	-49.5	1.3	0.8	0.1
6a'	2a"	^{1}A"	-49.9	26.0	18.0	4.1
1a"	8a'	^{3}A"	-50.7	0.1	1.0	0.0
1a"	1a"	^{1}A'	-51.1	59.1	83.6	86.3
6a'	9a'	^{1}A'	-51.5	14.7	21.8	4.4
1a"	8a'	^{1}A"	-51.6	33.7	70.1	15.1
6a'	8a'	^{3}A'	-52.1	4.6	0.2	0.2
7a'	1a"	^{3}A"	-52.3	1.2	2.3	0.0
6a'	1a"	^{3}A"	-52.8	9.1	1.9	1.0
7a'	8a'	^{3}A'	-53.0	0.7	2.0	0.0
1a"	2a"	^{1}A'	-53.0	44.6	62.4	7.9
7a'	9a'	^{1}A'	-53.1	9.1	64.6	6.4
6a'	1a"	^{1}A"	-53.6	69.0	48.2	90.8
7a'	1a"	^{1}A"	-53.6	50.7	100.0 (487.4 eV)	100.0 (641.4 eV)
8a'	8a'	^{1}A'	-54.1	12.0	35.9	1.7
8a'	9a'	^{1}A'	-54.3	7.9	30.6	0.7
7a'	8a'	^{1}A'	-54.6	23.7	67.6	18.1
6a'	7a'	^{3}A'	-54.7	9.4	2.7	1.0
6a'	7a'	^{1}A'	-56.1	61.7	47.3	83.5
6a'	8a'	^{1}A'	-57.0	34.0	47.7	15.9
7a'	7a'	^{1}A'	-57.2	26.2	72.0	72.7

TABLE 6.6 Continuation

Transition energies and intensities of the carbon Auger spectrum in formyl fluoride calculated using present approach.

Final state		Symmetry	Rel.En. (eV)	Rel.Int. Carbon	Rel.Int. Oxygen	Rel.Int. Fluorine
6a'	6a'	^{1}A'	-60.4	55.9	16.4	58.5
5a'	10a'	^{3}A'	-61.3	0.1	0.9	0.1
5a'	2a"	^{3}A"	-63.3	0.2	0.9	0.0
4a'	10a'	^{3}A'	-63.7	3.1	7.6	1.1
5a'	9a'	^{3}A'	-63.8	0.1	1.1	0.0
5a'	10a'	^{1}A'	-64.2	8.8	3.5	0.4
4a'	10a'	^{1}A'	-65.7	11.1	26.3	6.5
5a'	1a"	^{3}A"	-65.8	0.5	2.5	0.4
5a'	2a"	^{1}A"	-66.1	15.0	3.3	0.2
5a'	9a'	^{1}A'	-66.3	8.6	4.0	0.2
5a'	8a'	^{3}A'	-67.5	0.1	1.8	0.1
4a'	2a"	^{3}A"	-67.6	5.1	7.7	0.8
5a'	7a'	^{3}A'	-67.7	1.3	2.0	0.4
5a'	1a"	^{1}A"	-67.8	39.8	8.9	3.9
4a'	9a'	^{3}A'	-68.6	2.3	9.0	0.7
5a'	8a'	^{1}A'	-70.2	27.8	6.9	0.5
4a'	2a"	^{1}A"	-70.4	17.1	26.3	2.8
5a'	6a'	^{3}A'	-70.6	5.7	1.2	0.3
5a'	7a'	^{1}A'	-70.9	29.7	10.5	4.5
4a'	9a'	^{1}A'	-71.4	8.1	30.8	2.9
4a'	1a"	^{3}A"	-71.9	13.6	20.7	18.1
5a'	6a'	^{1}A'	-72.0	40.4	5.8	3.7
4a'	8a'	^{3}A'	-72.5	5.9	14.5	2.5
4a'	7a'	^{3}A'	-74.1	7.3	20.6	16.7
4a'	6a'	^{3}A'	-75.1	12.6	9.5	15.4
4a'	1a"	^{1}A"	-75.3	45.4	70.6	60.5
4a'	8a'	^{1}A'	-75.4	21.4	55.0	8.5
4a'	6a'	^{1}A'	-76.9	100.0 (219.5 eV)	46.0	57.4
4a'	7a'	^{1}A'	-77.3	39.0	84.8	55.8
4a'	5a'	^{3}A'	-85.7	6.9	0.3	0.5
5a'	5a'	^{1}A'	-87.1	16.4	1.4	0.1
4a'	5a'	^{1}A'	-93.4	27.5	23.3	4.9
4a'	4a'	^{1}A'	-97.0	54.5	95.0	72.1
	Total rate		(mau)	**2.76**	**6.79**	**8.25**

In parentheses - absolute energy values (in eV) of the most intense transitions.

6.4.4.1. Carbon Spectrum. The calculated absolute total transition rate has a value of 2.76 mau. Among 81 possible double-hole final states 78% of them have relative intensities above 1%. The most intense transition is assigned as 100% to the [4a' 6a'] ^{1}A' final state at 219.5 eV (Table 6.6). In general, however, the Auger transitions in the C(KVV) spectrum with significant intensities involve 1a" and 6a' molecular orbitals. The maximum intensity of the simulated spectrum of carbon in FCHO appears in the region of higher kinetic energy (Fig.6.7), which is consistent with the experimental spectra of carbon in other compounds.

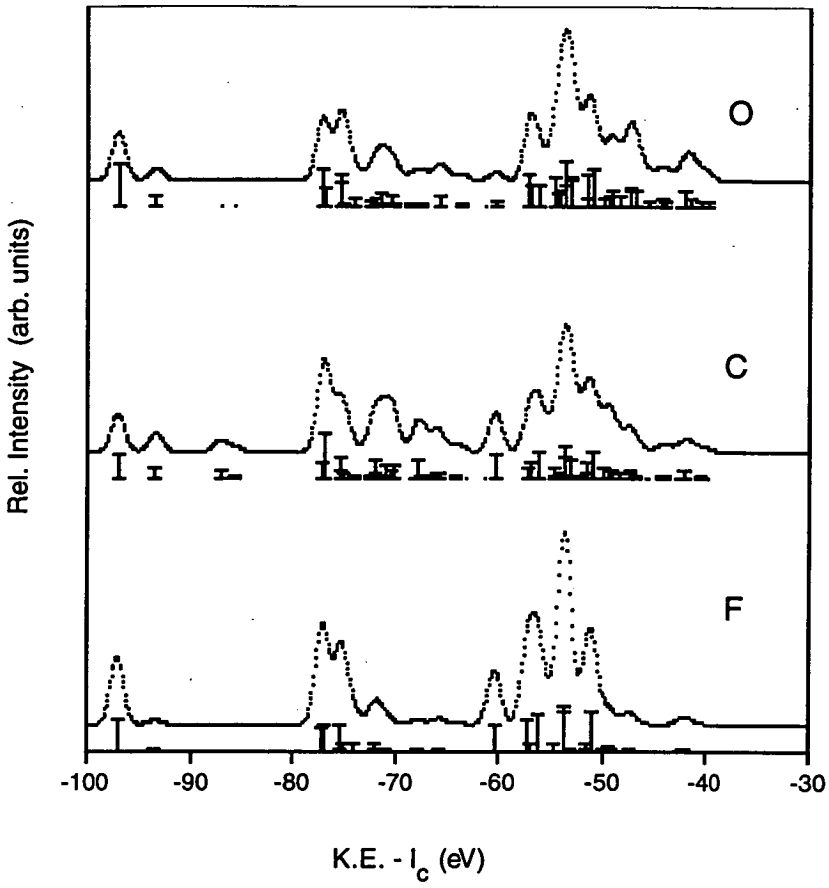

FIG. 6.7. The theoretical profiles of Auger spectra in FCHO (gaussian shape, FWHM = 1.5 eV).

6.4.4.1. Carbon Spectrum. The calculated absolute total transition rate has a value of 2.76 mau. Among 81 possible double-hole final states 78% of them have relative intensities above 1%. The most intense transition is assigned as 100% to the [4a' 6a'] ^{1}A' final state at 219.5 eV (Table 6.6). In general, however, the Auger transitions in the C(KVV) spectrum with significant intensities involve 1a" and 6a' molecular orbitals. The maximum intensity of the simulated spectrum of carbon in FCHO appears in the region of higher kinetic energy (Fig.6.7), which is consistent with the experimental spectra of carbon in other compounds.

6.4.4.2. Oxygen Spectrum. The most intense transition is associated with the [7a' 1a"] ^{1}A" final state at a kinetic energy of 487.4 eV (Table 6.6). There are several final states with relative intensities larger than 70%: [4a' 4a'] ^{1}A' , [4a' 7a'] ^{1}A' , [1a" 1a"] ^{1}A' , [7a' 7a'] ^{1}A' , [4a' 1a"] ^{1}A'. The total transition rate is 6.79 mau, only several percent lower than for the other compounds from the XCHO family. The theoretical profile of O(KVV) in FCHO does not differ significantly from C(KVV) (Fig.6.7) which suggests similar molecular orbital populations for carbon and for oxygen in the FCHO molecule. Since 77% of 81 transitions

have relative intensities larger than 1% any detailed assignment of the spectrum will be very difficult.

6.4.4.3. Fluorine Spectrum. The fluorine spectrum includes 52% of all possible final states with relative intensities smaller than 1%. The theoretical profile contains three distinguishable regions (Fig.6.7). This appearance can be associated with the presence of lone-pairs. The total transition rate is 8.25 mau and is almost identical to the rate calculated for fluorine in CH_3F (Table 5.2). The most intense transition corresponds to the [7a' 1a"] ^{1}A" final state, i.e. the same as for oxygen. In general, the significant intense transitions to final double-hole states in fluorine are associated with considerably intense transitions in oxygen and/or carbon in the FCHO molecule. Hence, the final states: [4a' 4a'] ^{1}A' , [4a' 7a'] ^{1}A' , [1a" 1a"] ^{1}A' , [7a' 7a'] ^{1}A' , [4a' 1a"] ^{1}A" significant in the oxygen spectrum and [6a' 1a"] ^{1}A" , [6a' 7a'] ^{1}A' , [6a' 6a']^{1}A' , [4a' 6a'] ^{1}A' significant in the carbon spectrum are also prominent (relative intensities are > 55%) in the fluorine spectrum (Table 6.6). An experimental Auger spectrum of the FCHO molecule is necessary to verify these findings.

6.4.5. HCHO

This is the smallest molecule in the XCHO family compounds. The number of possible final states is therefore reduced to 36. The presence of a hydrogen atom instead of an X atom in XCHO molecules affects Auger C(KVV) and O(KVV) spectra of formaldehyde. They are more structured than those of XCHO molecules.

The total width of the calculated Auger spectrum is 48.6 eV and is comparable with values obtained for other molecules considered in this chapter (except FCHO). Our results of Auger spectra calculations for carbon and oxygen in the HCHO molecule are presented in Table 6.7 while Figure 6.8 a and b shows experimental (Correia *et al.* 1991) and theoretical spectra, respectively. Figures 6.2 a,b and 6.3 a,b present experimental and simulated Auger spectra, respectively, in a wider energy range.

TABLE 6.7

Transition energies and intensities of the carbon Auger spectrum in formaldehyde calculated using various approaches.

Final	state	Symmetry	Rel.En.	Rel.Int.	Rel.Int.	Rel.En.	Expt.	Expt.
			(eV)	Carbon	Oxygen	Correia *et al.*	Correia *et al.*	present
$2b_2$	$2b_2$	$^1A_1$	-36.5	5.9	22.0	-33.8	1	1
$1b_2$	$2b_2$	$^3A_1$	-36.9	0.0	0.0			
$1b_1$	$2b_2$	$^3A_2$	-39.6	0.0	0.0			
$1b_1$	$2b_2$	$^1A_2$	-40.3	29.8	59.0	-37.0	2	2
$5a_1$	$2b_2$	$^3B_2$	-41.4	0.0	0.7			
$5a_1$	$2b_2$	$^1B_2$	-43.0	14.7	43.3	-39.3	3	3,4
$4a_1$	$2b_2$	$^3B_2$	-43.1	3.4	1.7			
$1b_2$	$1b_1$	$^3A_2$	-44.6	0.0	0.0			
$1b_2$	$2b_2$	$^1A_1$	-45.0	39.1	68.6			3,4
$1b_2$	$1b_1$	$^1A_2$	-45.1	98.3	92.1			)
$4a_1$	$2b_2$	$^1B_2$	-45.4	19.5	16.3			5,6
$1b_1$	$1b_1$	$^1A_1$	-45.6	94.6	100.0 (493.9 eV)	-42.5	5	)
$1b_2$	$5a_1$	$^3B_2$	-45.9	0.0	1.1			
$5a_1$	$1b_1$	$^3B_1$	-46.1	0.0	1.4			
$1b_2$	$5a_1$	$^1B_2$	-46.9	48.3	67.5			)
$1b_2$	$1b_2$	$^1A_1$	-47.0	64.5	53.5			7
$5a_1$	$1b_1$	$^1B_1$	-47.5	58.6	92.3			)
$4a_1$	$1b_1$	$^3B_1$	-47.8	13.7	3.6			
$4a_1$	$5a_1$	$^3A_1$	-47.9	7.1	1.1			
$4a_1$	$1b_1$	$^1B_1$	-49.3	77.8	34.8	-40.0	4	8
$4a_1$	$1b_2$	$^3B_2$	-49.7	11.3	2.7			
$5a_1$	$5a_1$	$^1A_1$	-51.2	22.9	51.9			)
$4a_1$	$1b_2$	$^1B_2$	-52.0	64.2	25.5			9
$4a_1$	$5a_1$	$^1A_1$	-52.4	49.1	36.2			)
$4a_1$	$4a_1$	$^1A_1$	-55.9	53.6	7.8			
$3a_1$	$2b_2$	$^3B_2$	-58.4	3.7	9.7			
$3a_1$	$2b_2$	$^1B_2$	-61.5	14.9	32.8			
$3a_1$	$1b_1$	$^3B_1$	-63.0	14.9	20.8			
$3a_1$	$1b_2$	$^3B_2$	-63.6	12.3	15.2			
$3a_1$	$5a_1$	$^3A_1$	-64.7	7.1	16.3			
$3a_1$	$1b_2$	$^1B_2$	-65.7	49.1	51.2			
$3a_1$	$1b_1$	$^1B_1$	-66.3	59.5	70.0			
$3a_1$	$4a_1$	$^3A_1$	-66.4	12.1	5.5			
$3a_1$	$5a_1$	$^1A_1$	-67.5	33.7	62.1			
$3a_1$	$4a_1$	$^1A_1$	-68.9	100.0 (225.6 eV)	41.2			
$3a_1$	$3a_1$	$^1A_1$	-85.1	45.6	79.4			
	Total	rate	(mau)	**3.09**	**6.72**			

In parentheses - absolute energy values (in eV) of the most intense transitions.

6.4.5.1. Carbon Spectrum. The present assignment of the theoretical spectrum to five experimental peaks is consistent with Correia *et al.* (1991) (Table 6.7) , except for a group marked as 4 (Fig.6.8) where we prefer to associate it with transitions involving the $2b_2$ orbital located on oxygen, rather than with $[4a_1\ 1b_1]^1B_1$ suggested by Correia *et al.* (1991). The calculated energies of transitions are about 3 eV too low when compared with Correia *et*

al. (1991). The authors do not analyse the experimental spectra above 42 eV. They claim that in this range of energy the C2s atomic orbital becomes more important as well as electron correlation effects becoming more evident and a simple quantitative discussion is less meaningful. In the present analysis, however, we have tried to assign theoretical transitions to the experimental groups of peaks marked as 6, 7, 8 and 9 (Table 6.7). The most intense transitions are associated with $[3a_1\ 4a_1]^1A_1$ (100%) , $[1b_2\ 1b_1]^1A_2$ (98%) and $[1b_1\ 1b_1]^1A_1$ (95%) final states. The absolute total transition rate has a value of 3.09 mau. The correspondence of theoretical and experimental Auger profiles for carbon is satisfactory. It seems however that theoretical intensities in the region of the 5th line are overestimated. Almost identical results were obtained by Correia *et al.* (1991) who applied a Green's function method. The authors associate these discrepancies with the initial state effect of orbital relaxation.

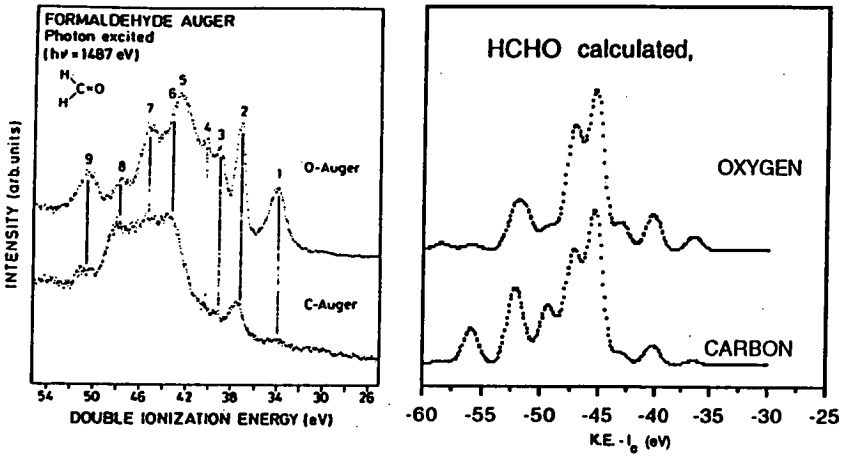

FIG. 6.8. An experimental (Correia *et al.* 1991) (a) and calculated (b) profiles of Auger spectra in formaldehyde (The theoretical shape is gaussian with FWHM = 1.5 eV).

6.4.5.2. Oxygen Spectrum. The presence of the hydrogen atom instead of an X element does not affect the oxygen spectrum of HCHO severely (Fig.6.2 a,b). The assignment of theoretical peaks to the experimental profile is the same as for carbon (see previous subchapter and Table 6.7). The measured Auger shape is satisfactorily approximated by the simulated spectrum except in the region of the 3rd and 4th experimental peaks (Fig.6.8) where intensity seems to be underestimated. Our calculations compare favourably with results obtained by Correia *et al.* (1991) who have used Hartree-Fock and Green's function calculations.

The calculated total transition rate is 6.72 mau and it is the lowest Auger transition rate for oxygen in the studied compounds from the XCHO family (Table 6.2). The most intense

transition is assigned to the $[1b_1\ 1b_1]^1A_1$ final state and line 5 in Fig.6.8. There are two more final states: $[1b_2\ 1b_1]^1A_2$ and $[5a_1\ 1b_1]^1B_1$ with relative intensities above 90% which are associated with peaks 5 and 7, respectively. Peak 9 in the experimental spectrum (Fig.6.8a) corresponds to several transitions involving orbitals $4a_1$, $5a_1$, and $1b_2$.

6.5. Comparison Between Molecules

6.5.1. Carbon Spectra

The Auger experimental spectra of the XCHO molecules lose their structures and become more band-like when proceeding from formaldehyde to formamide. The simulated spectra of C(KVV) in the XCHO molecules are good approximations to the experimental results. Better agreement with experiment has been achieved for acetaldehyde than for formamide carbon spectra. The transition rates for carbon in -CHO are 16% smaller than for carbon from $-CH_3$. However, there was no significant difference in the calculated profiles of both carbon atoms in CH_3CHO. The total transition rate decreases when $-CH_3$ is replaced by more X groups.

The presence of different X ligands in the XCHO molecules does not affect strongly the total transition rates for carbon atoms (see Fig.6.9 and Table 6.2). The calculated rates for carbon are found to be within 10% for all investigated XCHO compounds.

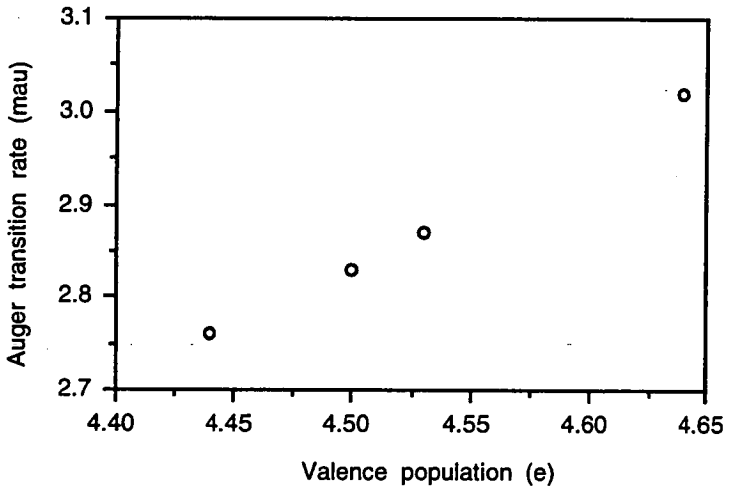

FIG. 6.9 Carbon Auger transition rates as a function of valence electron population on carbon atoms in XCHO molecules.

6.5.2. Oxygen Spectra

As for carbon the Auger experimental spectra of oxygen in the XCHO molecules become less structured when proceeding from formaldehyde to formamide. The total transition rate increases when proceeding from NH_2CHO to FCHO (Table 6.2). The rate for oxygen in CH_3CHO is between the values calculated for OHCHO and for FCHO which could be associated with the different charge distribution in the non-planar CH_3CHO molecule. There was no difference in the total transition rate calculated for oxygen from -OH and from -CHO suggesting that hydroxyl and carbonyl groups are very similar.

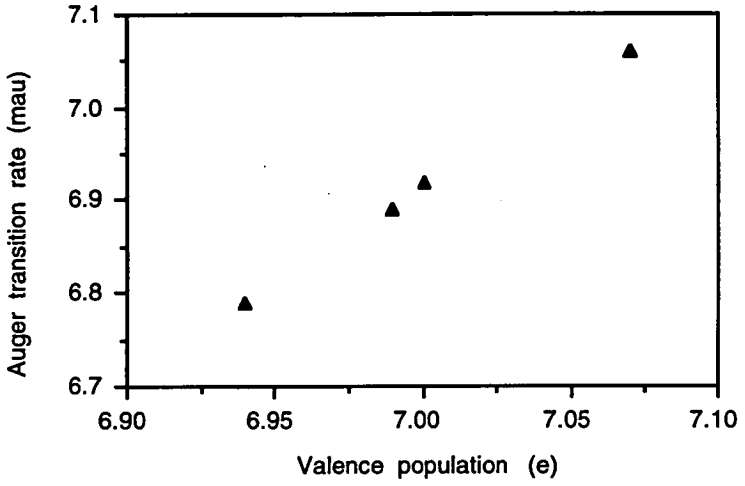

FIG. 6.10 Oxygen Auger transition rates as a function of valence electron population on oxygen atoms in XCHO molecules.

Figure 6.10 depicts calculated total rates for O(KVV) in XCHO molecules (presented in Table 6.2) as a function of valence population q expressed in *e*. Similar to carbon (Fig.6.9), there is not much variation in the total transition rates of oxygen.

6.5.3. X (X=C, N, O, F) Spectra

The calculated total transition rates for elements from X groups are almost identical for first row hydrides, CH_3X and XCHO compounds (Tables 4.2, 5.2 and 6.2, respectively). Figure 6.11 indicates that the rates of X(KVV) Auger transitions are rather insensitive to the presence of hydrogen atoms, carbonyl or methyl groups. However, they are proportional to the valence electron populations.

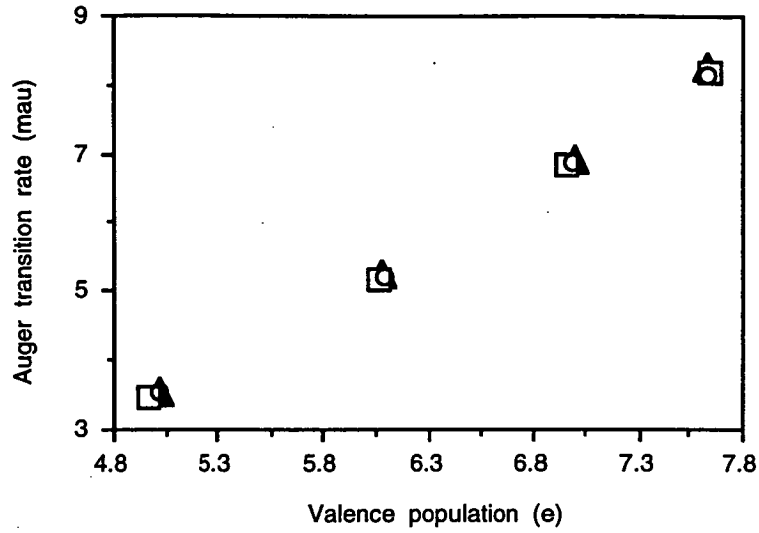

FIG. 6.11 Auger transition rates as a function of valence electron populations on X (X=C,N,O,F) atoms in first row hydrides (O), CH_3X (□) and XCHO (▲) molecules.

Any detailed analysis based on experimental and theoretical results is not possible since there are no experimental spectra available for X(KVV) groups for both (CH_3X and XCHO) sets of compounds.

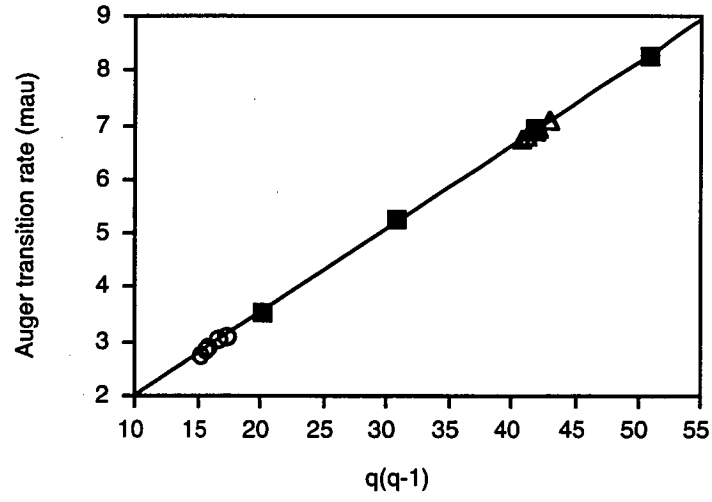

FIG. 6.12 Auger transition rates as a function of valence electron population q expressed as q*(q-1) relationship in XCHO molecules; (O) carbon from -CHO, (Δ) oxygen from -CHO, (■) X (X=C,N,O,F).

Figure 6.12 (similarly to Figure 5.9) displays the calculated total rates for KVV Auger transitions in XCHO molecules as a function of valence population q represented as q(q-1). The line represents the equation I = 0.38 + 0.16*q*(q-1) , where I symbolises the total Auger

transition rate. The relationship is linear and almost identical to the previously found for CH_3X molecules (see Section 5.5).

6.6. Conclusions

Auger spectra of carbon, oxygen and element in the X group (where X=F, OH, NH_2 and CH_3) have been calculated using the present method. The method compares favourably with other methods used for calculation of Auger spectra of XCHO molecules because it offers absolute intensity rates as well as reasonably good assignment of spectra for only a modest computational cost.

It has been established that the total transition rate for carbonyl carbon is smaller than for methyl carbon and decreases when proceeding from CH_3CHO to FCHO. In the case of oxygen there is an opposite trend: the absolute transition rate increases when proceeding from NH_2CHO to FCHO. However, the transition rate for oxygen in the CH_3CHO molecule is between the values calculated for OHCHO and for FCHO. This result could possibly be explained by hyperconjugation effects.

The intensities from the X group are almost identical for CH_3X and for XCHO compounds while transition rates of methyl carbon are 16% larger than of carbonyl carbon for the above two groups of compounds.

The total rates of KVV Auger transition can be estimated within 10% using a function of valence electron populations.

The presence of two different chemical sites for carbon in the CH_3CHO molecule seems to be more significant than for oxygen in OHCHO. Nevertheless, the overall effect is not substantial.

Chapter 7

SECOND ROW HYDRIDES

7.1. Introduction

The second row Auger spectra have not received as much attention as their first row counterparts mainly because of the complexity resulting from numerous possible double hole final states and difficulties in calculating $L_{23}VV$ transition rates. Comparisons of the spectra of molecules containing second row elements with KVV Auger molecular spectra for first row elements cannot be easily made because of the different symmetry of the initial core hole in the case of $L_{23}VV$ transitions. The second row hydride molecules are isoelectronic with the Ar atom and the number of possible double hole final states is larger than for KVV transitions since it increases with the higher angular momentum of the initial hole.

The second row hydrides present a good model for testing the methods of calculation. The Auger spectra of the second row hydrides appear in a low energy range and they exhibit some vibrational structure in the outer-outer region which, in general, makes the spectra more complicated than the spectra from long-lived states. Effects such as lifetime-vibrational interference (Cesar *et al.* 1989, Kaspar *et al.* 1979, Correia *et al.* 1985), continuum electron interaction (Carravetta *et al.* 1988) and also, in principle, lifetime variations with the geometry (Ågren *et al.* 1987), as well as the variations of the electronic transition moments with geometry (Cesar *et al.* 1989), may influence the spectrum. The effect of lifetime-vibrational interference can be constructive or destructive and may be revealed even when the intermediate core hole states are only moderately excited vibrationally. The discrete-continuum interaction effect is manifestation of the fact that core hole states are embedded in the electronic continua of lower lying valence core states and that they are metastable in character. For small Z elements this discrete-continuum interaction is strong enough to generate predominantly an Auger decay but small enough to only marginally perturb the core electron ionization potentials (Carravetta *et al.* 1988).

Additionally, there are dynamic correlation effects present in the low-kinetic energy parts of the spectra. For hydride spectra, only the inner-inner $2s^2$ states of the first row hydrides are subject to this breakdown of the molecular orbital picture (i.e. instead of

a single line appearing in a spectrum as expected from one-particle representation the relative intensity become distributed over many lines). This correlation in the low-kinetic energy region is substantially stronger than for the inner valence single hole states in the corresponding photoelectron spectra.

The second row hydrides represent systems which are simple enough to allow the study of molecular Auger spectra using our method of calculations to test if it can give reliable results for molecules where correlation, relaxation, polarization or other effects (which are common in larger and more complex molecules) do not compensate each other.

TABLE 7.1.

Symmetry and number of two-hole states for the second row hydrides isoelectronic with an argon atom.

Molecule	Symmetry	$[vv']\Gamma$	Valence orbitals
SiH_4	T_d	7	$3a_1,2t_2$
PH_3	C_{3v}	11	$4a_1,2e,5a_1$
SH_2	C_{2v}	16	$4a_1,2b_2,5a_1,2b_1$
ClH	$C_{\infty v}$	11	$4\sigma,5\sigma,2\pi$
(Ar)		(6)	(3s,3p)

The number of possible transitions is twice the number of final valence energy states $[vv']\Gamma$ due to the initial spin-orbit splitting.

7.2. Theoretical Considerations

The method of calculations used for the second row elements is analogous to the approach used for the first row elements. As in the previous chapters energies are calculated according to the relationship:

$$E(c\text{-}vv',^{2S+1}\Gamma) = I_c - I_v - I_{v'} - \Delta[vv']^{2S+1}\Gamma$$

where I_v , $I_{v'}$ represent experimental molecular ionization energies, while Ic represents the $2p_{1/2}$, $2p_{3/2}$ ionization energies. The two-hole correction term $\Delta[vv']^{2S+1}\Gamma$ is evaluated in terms of Coulomb- and exchange-type integrals calculated over one-electron molecular orbitals.

The intensities are calculated using an intra-atomic model discussed earlier (Chapter 3). The necessary expressions for the $I^{c\varepsilon}_{vv'}$ term for the 2p initial hole are presented elsewhere (Chelkowska and Larkins 1991a). In Appendix B the expressions for non-degenerate final states in the one centre approximation are given in an explicit form.

Experimental geometries and ionization potentials used in the present studies were obtained from various sources. Detailed information including geometries and ionization energies of the second row hydride molecules is provided in Appendix C.4. Fig.7.1 diagrammatically depicts ionization energy values for valence orbitals used in the current calculations. It is expected that the width of Auger spectra would be similar for phosphine and hydrogen sulphide, nonetheless, it should increase from silane to hydrogen chloride principally because of the greater spread of ionization potentials.

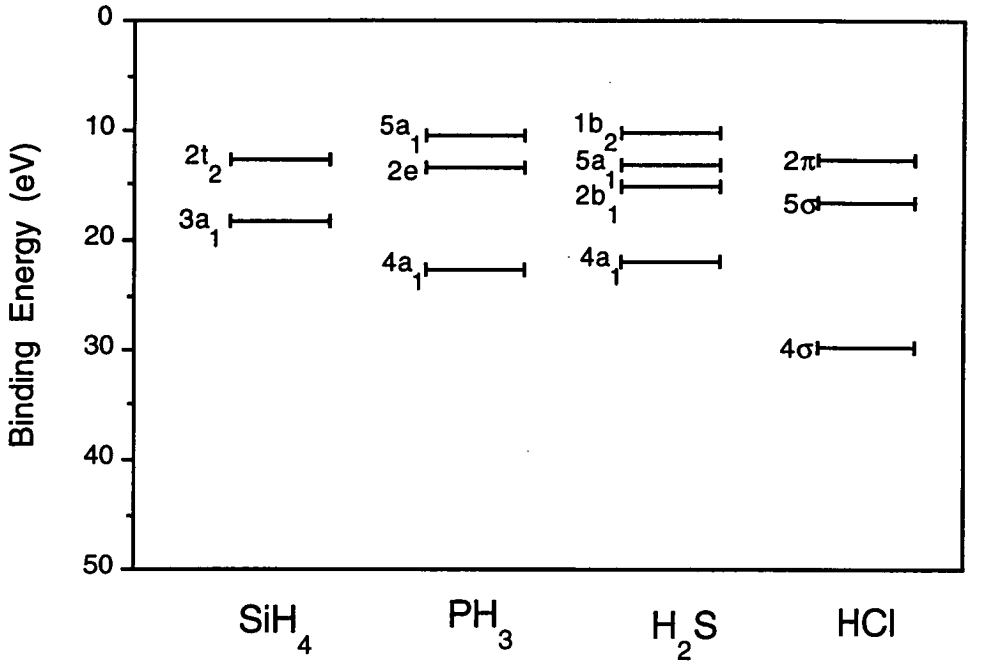

FIG.7.1. Experimental valence ionization energies of the second row hydride molecules.

TABLE 7.2.

Calculated valence electron population on the heavy atom and Auger rates for the second row hydrides using non-equivalent cores (NEC) and equivalent cores (EC) approaches.

Molecule	Atom	Valence -e⁻ population		Calc. Auger rate (mau)	
		NEC	EC	NEC	EC
SiH_4	Si	2.96	4.38	0.57	1.18
PH_3	P	4.50	5.08	1.21	1.66
H_2S	S	5.68	6.49	2.28	3.17
HCl	Cl	7.03	7.29	3.97	4.34

In Table 7.2 valence electron populations and total Auger transition rates obtained in the present studies for the second row hydrides using INDO semi-empirical parameters (Gordon *et al.*1978) and R^k atomic matrix elements (Chen *et al.* 1990, Chelkowska and Larkins 1991a) are given. All the above parameters used for the second row elements can be found in Appendix A.

7.3. Experimental Findings

Experimental Auger $L_{23}VV$ spectra of Ar and all Ar-like second row hydrides are available and they are displayed in Fig. 7.2 on a common scale representing negative values of double hole ionization potentials.

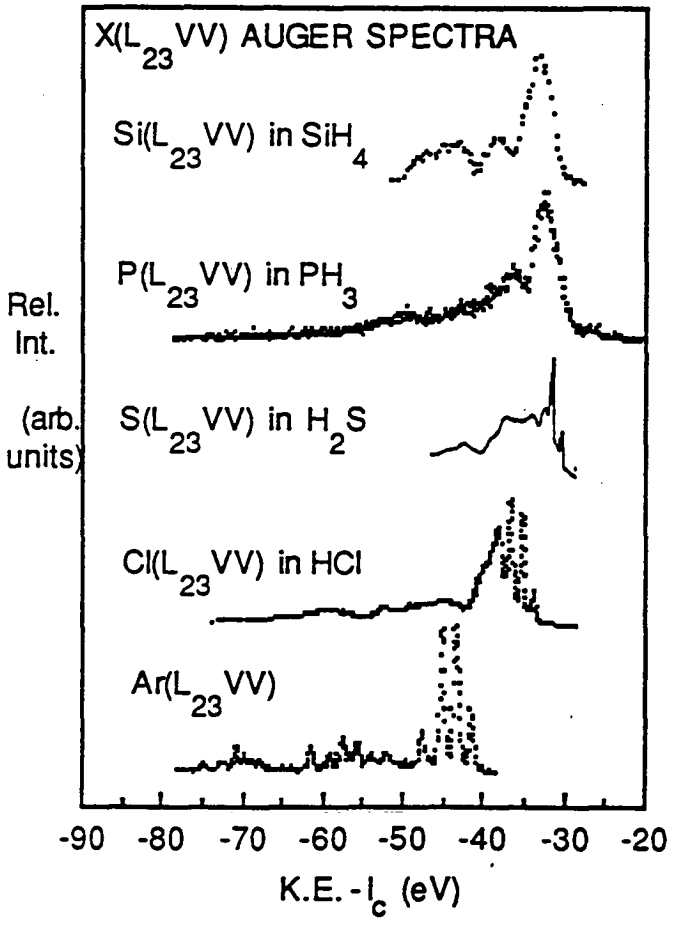

FIG. 7.2. Auger experimental spectra of second row hydrides.
SiH_4 spectrum measured by de Souza *et al.* (1986), PH_3 spectrum by Ueda *et al.*(1991), H_2S spectrum by Cesar *et al.* (1990), HCl and Ar spectra by Aksela *et al.*(1983).

Several LVV Auger spectra of silane have been reported up to date. They vary in absolute energy by up to 3 eV. The electron impact excited $L_{23}VV$ spectra of Si in SiH_4 molecule were measured by Moddeman (1970) and Maracci *et al.* (1980). Rye and

Houston (1983) also recorded an electron induced Auger spectrum of silane. In 1986 Yagishita *et al.*(1986) and de Souza *et al.* (1986) reported $L_{23}VV$ spectra of SiH_4 obtained by means of synchrotron radiation. The latest spectrum measured by de Souza *et al.* (1986) is presented in Figure 7.2.

Ariyasinghe *et al.* (1991) reported a PH_3 spectrum obtained with high energy alpha particles as the energy source. Hence, there were many satellites which are difficult to distinguish from normal Auger lines. Ueda *et al.* (1991) have recently measured the PH_3 Auger spectrum using synchrotron radiation. This spectrum contains far less satellites and therefore it is used in our analysis.

Auger spectra of H_2S were recorded by Thompson *et al.* (1976) and Cesar *et al.* (1990) using an electron beam. The latter spectrum covers a larger range of kinetic energy and it is given in Figure 7.2.

A $L_{23}VV$ Auger spectrum of HCl has been reported by Aksela *et al.*(1983) and Aksela *et al.* (1990) where electron beam and synchrotron radiation were used, respectively. The former Auger spectrum of HCl (Aksela *et al.*1983) covers a wider range of energy and it is used in the present analysis.

7.4. Results and Discussion

Theoretically predicted Auger $L_{23}VV$ spectra of X (where X=Si, P, S and Cl) in the second row hydrides are provided in Figure 7.3.

The theoretical profiles were generated using gaussians with FWHM=0.5eV, since the previously used FWHM=1.5 eV became too broad for the sharp experimental Auger lines occurring in the second row hydrides. As with the experimental spectra, the theoretical shapes for the X element are displayed on a common scale representing the difference between the kinetic energy of the Auger electrons and the energy required to create an initial core hole. Total areas under the peaks are set to be the same for each molecule. The generated profiles can be used as eye guides in spectra analysis. Detailed results of calculations can be found in Appendix D.4.

Recently Aksela *et al.* (1992) reported studies of decay channels of core-excited molecular states in HCl and H_2S. The authors performed multiconfiguration self-consistent-field (MCSCF) calculations for the excited states $[3\sigma\ 6\sigma]$ and $[3a_1\ 6a_1]$ in the HCl and H_2S molecules, respectively. The presence of atomic-like (sharp) and molecular lines in the ejected electron spectra was explained as a competition between neutral dissociation followed by Auger decay of atomic fragments and molecular Auger decay. The atomic contribution in the spectra was dominating (more than 60%) in the above molecules.

There have also been several calculations of energies reported for the second row hydrides. However, intensity calculations for the set of second row hydrides have been reported only by Sukhorukov *et al.*(1986) who used a one-centre method. Additionally, Kvalheim (1983) has used Ar rates to estimate intensities of $L_{23}VV$ transitions in the HCl molecule. To this date, there have been no reports of *ab initio* intensity calculations available for the second row hydrides.

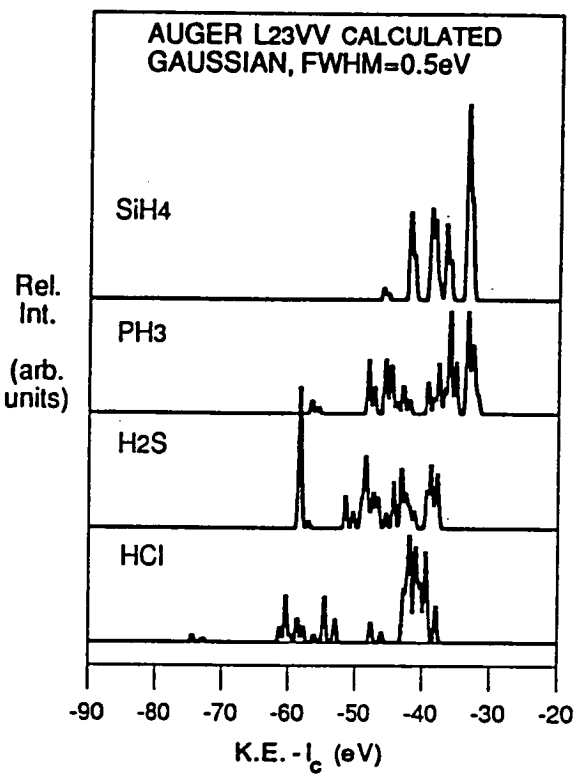

FIG. 7.3. Theoretical Auger spectra of the second row hydrides generated using gaussian shape with FWHM=0.5 eV.

7.4.1. SiH_4

Results of energy and intensity calculations for the $L_{23}VV$ spectrum of silane together with available experimental assignments are presented in Table 7.3, while in Figure 7.4 the spectrum measured by de Souza *et al.* (1986) together with results of our calculations represented as bars are shown.

There are 7 double hole final valence energy states. However, due to initial state spin-orbit splitting of the 2p orbital by 0.6 eV, a total of 14 Auger transitions is predicted. The calculated transitions are presented relative to the most intense transition set equal to 100% while the energy is presented relative to $[2t_2\ 2t_2]^1E$ state (Table 7.3).

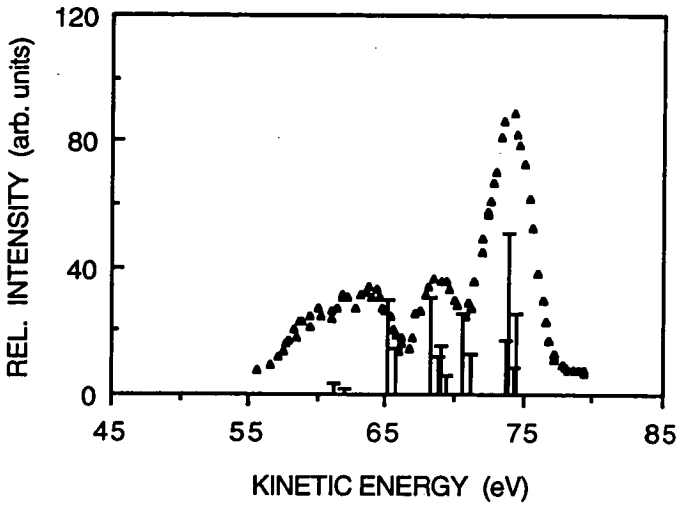

FIG.7.4 Experimental (de Souza *et al.* 1986) and calculated $L_{23}VV$ Auger spectra of silicon in silane.

TABLE 7.3

Silane transition energies and intensities; experimental and calculated by different authors.

Final state			Energy (eV)							Rel.Int. (%)		
			P	S	M	R&H	Md	DS	T	P	S	M
					Expt	Expt	Expt	Expt				
$2t_2$	$2t_2$	$^{*3}T_1$	-0.7	(-1.6)	-2.7*)					50.0		29*)
$2t_2$	$2t_2$	$^{*1}E$	-0.6							16.8		
$2t_2$	$2t_2$	$^3T_1$	-0.1	-1.2	-0.9				0.0	100.0	100.0	40.0
$2t_2$	$2t_2$	^1E	0.0	0.0	0.0	0.0	0.0	0.0	0.1	33.7	85.1	100.0
			(73.2)	(73.4)	(75.8)	(74.7)	(73.7)	(73.8)				
$2t_2$	$2t_2$	$^{*1}T_2$	2.5							25.3		
$2t_2$	$2t_2$	$^1T_2$	3.1		0.9		2.7	2.5	2.2	50.5		87.0
$2t_2$	$2t_2$	$^{*1}A_1$	4.2							11.3		
$2t_2$	$2t_2$	$^1A_1$	4.8	1.5	2.4	4.7	5.7	5.4	5.1	22.6	22.4	72.0
$3a_1$	$2t_2$	$^{*3}T_2$	4.8							30.0		
$3a_1$	$2t_2$	$^3T_2$	5.4	5.8	4.9				5.8	60.0	23.0	35.0
$3a_1$	$2t_2$	$^{*1}T_2$	8.0							29.1		
$3a_1$	$2t_2$	$^1T_2$	8.5	10.5	6.1	9.5	10.4	10.4	11.1	58.2	28.0	43.0
$3a_1$	$3a_1$	$^{*1}A_1$	11.8							3.7		
$3a_1$	$3a_1$	$^1A_1$	12.4	17.0	10.3		15.2	14.8	15.2	7.3	1.9	18.0
					64.3*)			33.3*)				11*)
						Total	rate	(mau)		**1.18**	**1.54**	

*) - not assigned.

The experimental spectrum was measured by de Souza *et al.*(1986) - DS;

Expt-experimental, P - present , S-Sukhorukov *et al.* (1986), M- Maracci *et al.* (1980), R&H - Rye and Houston (1983), Md - Moddeman (1970), T- Tarantelli *et al.* (1985c). An asterisk in the final state description means that the initial hole was in a $2p_{1/2}$ orbital.

The theoretically predicted spectrum is 13.1 eV wide. There is moderate agreement in the energy calculation results. Our method underestimates the total span of the spectrum while Sukhorukov's *et al.* (1986) method (where polarisation is included) overestimates this range. Results obtained by Tarantelli *et al.*(1985c) (who used the ADC(2) method) are in good agreement with the experimental data.

Nevertheless, there are major discrepancies in peak assignment. Intensity calculations using our and Sukhorukov's methods lead to consistent assignment of the most intense peak to the $^3T_1$ final state while Maracci (1980) and other authors (de Souza *et al.* 1986, Tarantelli *et al.*1985c) have assigned the most intense transition in the $L_{23}VV$ spectrum of SiH_4 to the ^1E final state (similarly as for KVV transitions in methane). Such assignment seems to be incorrect since the initial core hole in the case of the $L_{23}VV$ transitions has a different symmetry to the initial core hole in the KVV transitions (Chelkowska and Larkins 1991b). On the basis of results obtained in the present calculations the principal features of $L_{23}VV$ can be explained (Fig.7.4, Table 7.3). A more detailed analysis of the silane Auger spectrum will require incorporation of vibrational effects and satellite contribution due to correlation effects.

7.4.2. PH_3

The spectrum of Ueda *et al.* (1991) along with the calculated Auger spectrum of PH_3 represented as bars are displayed in Figure 7.5. The Roman numerals I-V represent regions fitted using Voight functions (Gaussian 0.8 and Lorentzian 0.2). This is the minimum number of peaks required to reasonably fit the experimental profile. A shift of 1 eV towards higher energy was applied to the calculated spectrum to align with the maximum experimental line.

Results of energy and intensity calculations for the $L_{23}VV$ spectrum of phosphine together with available experimental assignments are presented in Table 7.4.

There is a good agreement between the experimental and calculated spectra for the outer-outer region. However for the full width of the phosphine Auger spectrum the agreement of theory and experiment is at best semiquantitative. The direct comparison of theory and experiment is difficult because one cannot assume that linewidths for all these transitions will be equal (Larkins *et al.* 1993a).

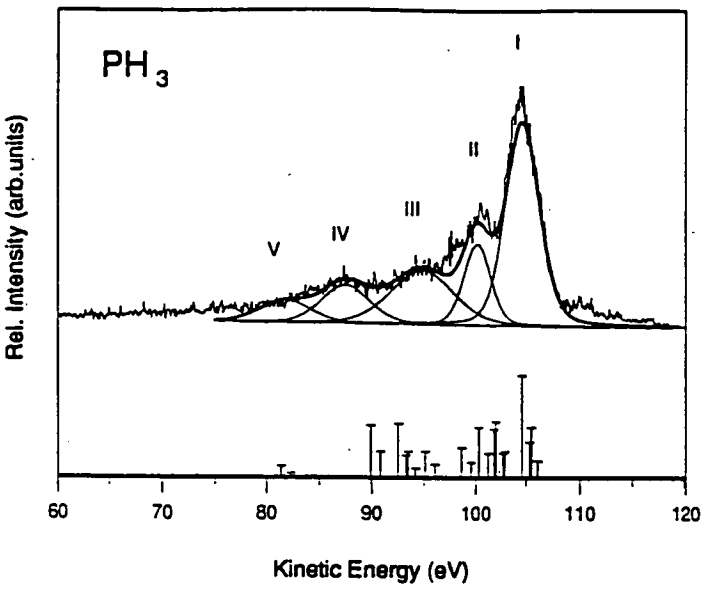

FIG.7.5 Experimental (Ueda *et al.* 1991) and calculated (shifted 1 eV toward higher energy) $L_{23}VV$ Auger spectra of phosphorus in phosphine. Regions I-V are fitted using Voight functions (Gaussian 0.8 and Lorentzian 0.2).

TABLE 7.4.

Phosphine experimental and calculated transition energies and intensities (by Sukhorukov's (1986) and present methods).

			Energy (eV)			Rel. Int. (%)		Region	Rel. Areas (%)	
Final	state		Present	Sukhorukov	Expt	Present	Sukhorukov	(Fig.7.5)	Expt	Present
$5a_1$	$5a_1$	$^{*1}A_1$	-1.6	(-0.5)	)	18.0			)	)
2e	$5a_1$	$^{*3}E$	-0.9			50.0				
$5a_1$	$5a_1$	$^1A_1$	-0.7	0.0 (108.2)		35.9	27.1			
2e	$5a_1$	^3E	0.0 (103.7)	3.9	0.0 (104.6)	100.0	100.0	I	43	39
2e	$5a_1$	$^{*1}E$	1.7			27.5				
2e	2e	$^{*3}A_2$	1.8			24.5				
2e	$5a_1$	^1E	2.6	5.3	)	55.0	51.1		)	)
2e	2e	$^3A_2$	2.7	9.7	)	49.0	49.6		)	)
2e	2e	$^{*1}E$	3.4			24.9				
2e	2e	^1E	4.3	11.1	4.4	49.7	51.1	II	15	27
2e	2e	$^{*1}A_1$	5.0			15.4				
2e	2e	$^1A_1$	5.9	12.2	)	30.8	29.3		)	)
$4a_1$	$5a_1$	$^{*3}A_1$	8.6		)	13.7			)	)
$4a_1$	$5a_1$	$^3A_1$	9.5	12.5	9.8	27.3	11.3	III	22	10
$4a_1$	$5a_1$	$^{*1}A_1$	10.5			11.3				
$4a_1$	$5a_1$	$^1A_1$	11.4	17.8	)	22.6	14.3		)	)

TABLE 7.4. Continuation

Phosphine experimental and calculated transition energies and intensities (by Sukhorukov's (1986) and present methods).

Final state			Energy (eV)			Rel. Int. (%)		Region	Rel. Areas (%)	
			Present	Sukhorukov	Expt	Present	Sukhorukov	(Fig.7.5)	Expt	Present
$4a_1$	2e	$^{*3}E$	11.2			26.9				
$4a_1$	2e	^3E	12.1	18.3	17.1	53.8	22.6	IV	12	22
$4a_1$	2e	$^{*1}E$	13.8			26.2				
$4a_1$	2e	^1E	14.7	23.6		52.4	28.6			
$4a_1$	$4a_1$	$^{*1}A_1$	22.3			6.0				
$4a_1$	$4a_1$	$^1A_1$	23.2	28.4	22.9	12.0	3.8	V	8	2
		Total rate	(mau)			**1.66**	**1.90**			

An asterisk in the final state description means that the initial hole was in a $2p_{1/2}$ orbital. Experimental spectrum is fitted with 5 Voightian (0.2) peaks.

There is also a possibility of satellite contributions to the experimental spectrum. Region I (106.0 eV, FWHM=3.9 eV) is dominated by transitions involving the outer valence $5a_1$, and 2e orbitals with predominantly 3p character. The $[2e\ 5a_1]^{1,3}E$ final double hole states are the most important. Region II (101.6 eV, FWHM=3.1 eV) originates from the [2e 2e] double hole multiplets while Region III (96.3 eV, FWHM=7.1 eV) is associated with the multiplets from the $[4a_1 5a_1]$ double hole states. Region IV (88.9 eV, FWHM=5.4 eV) results from transitions involving $[4a_1 1e]^{1,3}E$ double hole final states and region V (83.1 eV, FWHM=5.9 eV) arises from transitions to the $[4a_1\ 4a_1]^1A_1$state. The $4a_1$ orbital is predominantly of 3s character, hence electron correlation effects are expected to be manifested in the final states involving this orbital, i.e. regions III, IV and V.

There is reasonable agreement between the predicted total intensity in these regions (34%) when compared with experiment (42%), however the distribution in the inner-inner regions is affected by multielectron phenomena and we observe a break-down of the one-particle picture. This effect has not been adequately accounted for in the present calculations.

The theoretical results obtained by Sukhorukov *et al.*(1986) are generally similar to our results (Table 7.4). The width of the presently calculated spectrum is 24.8 eV while the width of the spectrum calculated by Sukhorukov *et al.*(1986) is larger than the experimental one. Hence, the polarisation effects introduced by Sukhorukov (1986) are overestimated.

Since both methods are using a one-centre approximation, there is very good agreement in the values of the total transition rates: 1.66 and 1.90 mau are rates calculated in the present work and by Sukhorukov *et al.*(1986), respectively.

7.4.3. H_2S

Significant electron correlation effects are present for the H_2S molecule. Additionally, the low symmetry of the molecule causes there to be a high number of possible final states and an accurate assignment of transitions is unachievable. Since the experimental spectrum is very broad any assignment of peaks in the inner-inner energy region is ambiguous. Results obtained by different authors together with experimental data are given in Table 7.5 while in Fig.7.6 the experimental spectrum measured by Cesar *et al.* (1990) together with a spectra calculated using the present method are shown.

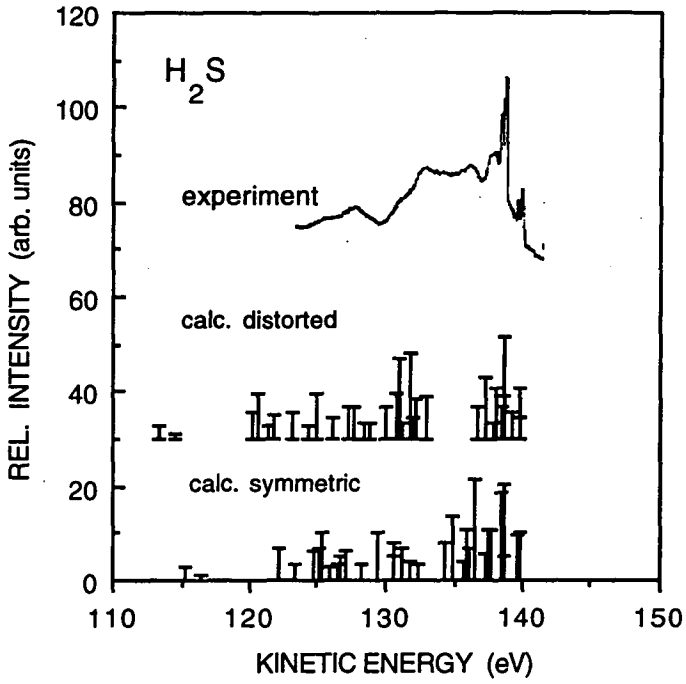

FIG.7.6 Experimental (Cesar *et al.* 1990) and calculated $L_{23}VV$ Auger spectra of sulphur in hydrogen sulphide. The lower bar spectrum is shifted 3.3 eV and represents theoretical predictions for symmetric molecule while the upper bar spectrum is shifted 1.3 eV and shows results of calculation for the distorted geometry (as in Aksela *et al.* 1992).

The lower bars are shifted 3.3 eV and represent theoretical predictions for symmetric molecule (for geometry see Appendix C.4.). The upper bar spectrum is shifted 1.6 eV for

better alignment with the experiment and shows results of calculation for the H_2S where one of the hydrogen atoms is at the distance of 3.9 au (from S), when the decay takes place (as in Aksela *et al.* 1992). The angle between hydrogen atoms and sulphur is 92.11° in both cases. The energy results in Table 7.5 are presented relatively to the $[2b_1\ 2b_1]^1A_1$ final state while intensity is given relatively to the most intense transition set to 100%. The theoretically predicted spectrum contains 32 transitions and is 24.5 eV or 26.4 eV wide for symmetric or distorted molecule, respectively. Spin-orbit splitting equal to 1.2 eV noticeable in the experimental spectrum is also included in the calculated profiles.

TABLE 7.5.

Hydrogen sulphide transition energies and intensities calculated by different authors.

Final	state		Energy (eV)								Rel.	Int. (%)		
			P sym	distort*	S	Th	E	C	Th Expt	C Expt	P sym	distort*	S	Th
$5a_1$	$2b_1$	$^{*3}B_1$	-1.5	-1.2	(-1.4)		-0.8	-0.4			47.2	50.0		
$2b_1$	$2b_1$	$^{*1}A_1$	-1.2	-1.2		-1.3	-1.3	-1.2	-1.2		43.3	20.8		46.7
$5a_1$	$2b_1$	$^3B_1$	-0.3	0.0	2.1		0.5	0.9			94.4	100.0	100.0	
$5a_1$	$2b_1$	$^{*1}B_1$	-0.2	-0.6		1.5	1.1	1.2	1.0		24.7	25.5		13.3
$2b_1$	$2b_1$	$^1A_1$	0.0	0.0	0.0	0.0	0.0	0.0	0.0	0.0	86.5	41.6	53.9	100.0
			(135.0)	(137.0)	(139.2)	(138.5)	(138.8)	(139.8)	(138.6)	(138.6)				
$2b_2$	$2b_1$	$^{*3}A_2$	0.7	0.2		3.6	1.9	2.0	3.3		50.0	30.8		
$5a_1$	$2b_1$	$^1B_1$	1.0	0.6	3.6	2.7	2.4	2.5	2.6	2.5	49.3	50.9	46.1	6.7?
$2b_2$	$2b_1$	$^{*1}A_2$	1.2	0.8			2.9	3.0		3.1	25.4	15.9		
$2b_2$	$2b_1$	$^3A_2$	1.9	1.4	3.4	4.8	3.2	4.3	4.7		100.0	61.5	100.0	
$2b_2$	$5a_1$	$^{*3}B_2$	2.2	5.6			4.5	4.9			31.2	42.4		
$2b_2$	$2b_1$	$^1A_2$	2.4	2.0	4.9		4.2	4.2		4.3	50.9	31.8	50.6	
$5a_1$	$5a_1$	$^{*1}A_1$	2.7	6.4			4.5	4.6			18.2	39.4		
$2b_2$	$5a_1$	$^3B_2$	3.4	6.8	7.6		5.8	6.1			62.4	84.7	100.0	
$5a_1$	$5a_1$	$^1A_1$	3.9	7.6	8.3	6.5	5.8	5.8	5.9	5.9	36.5	78.7	52.8	20.0
$2b_2$	$5a_1$	$^{*1}B_2$	5.9	6.7			6.2	6.6			16.3	21.9		
$2b_2$	$2b_2$	$^{*1}A_1$	6.6	10.1			9.7	9.8			18.9	15.6		
$2b_2$	$5a_1$	$^1B_2$	7.1	7.9	9.1	7.6	7.5	7.8	7.5		32.6	43.8	46.1	6.7
$4a_1$	$2b_1$	$^{*3}B_1$	7.7	7.4			11.8	12.4			23.6	16.0		
$2b_2$	$2b_2$	$^1A_1$	7.8	11.3	11.3		11.0	11.0		10.9	37.8	31.2	57.3	
$4a_1$	$2b_1$	$^3B_1$	8.9	8.6	12.3		13.3	13.7			47.2	32.1	21.3	
$4a_1$	$5a_1$	$^{*3}A_1$	10.0	12.5			14.8	15.3			14.7	22.1		
$4a_1$	$5a_1$	$^3A_1$	11.2	13.7	16.5		16.1	16.5			29.4	44.2	21.3	
$4a_1$	$2b_1$	$^{*1}B_1$	11.8	9.7			15.1	17.2			23.8	16.2		
$4a_1$	$2b_2$	$^{*3}B_2$	12.0	14.2			16.7	17.5			15.6	13.6		
$4a_1$	$5a_1$	$^{*1}A_1$	12.5	16.8		11.1	19.5	20.1	11.2		14.1	22.4		6.7
$4a_1$	$2b_1$	$^1B_1$	13.0	10.9	18.3		16.4	18.5		17.1	47.6	32.5	27.0	
$4a_1$	$2b_2$	$^3B_2$	13.2	15.4	17.8		18.0	18.7			31.2	27.2	21.3	

TABLE 7.5. Continuation

Hydrogen sulphide transition energies and intensities calculated by different authors.

Final	state		Energy (eV) P sym	P distort*	S	Th	E	C	Th Expt	C Expt	Rel. Int. (%) P sym	P distort*	S	Th
$4a_1$	$5a_1$	$^1A_1$	13.7	18.0	22.5	12.4	20.8	21.4	12.8	19.6	28.1	44.7	27.0	6.7
$4a_1$	$2b_2$	$^{*1}B_2$	15.0	17.3			22.9	23.5			15.7	13.4		
$4a_1$	$2b_2$	$^1B_2$	16.2	18.5	23.8		24.2	24.8		23.1	31.5	26.7	27.0	
$4a_1$	$4a_1$	$^{*1}A_1$	21.8	24.0			32.8	31.6			6.5	6.2		
$4a_1$	$4a_1$	$^1A_1$	23.0	25.2	32.3		34.1	32.8		26.6	12.9	12.3	13.5	
								Total	rate	(mau)	3.17	3.33	2.50	

The experimental spectra were measured by Thomson *et al.*(1976) - Th and by Cesar *et al.*(1990) - C;

P - present, sym - normal geometry, distort * - distorted geometry of the H_2S molecule (C_s symmetry; the symmetry of double hole states contains only A' and A" states and is not shown in the table) , S-Sukhorukov *et al.* (1986), Th - Thomson *et al.*(1976), E - Eade and Robb (1977), C - Cesar *et al.*(1990). An asterisk in the final state description means that the initial hole was in a $2p_{1/2}$ orbital.

The dominant transition in H_2S is assigned to the $[2b_2\,2b_1]^3A_2$ double hole final state for the symmetric molecule and to $[5a_1 2b_1]^3B_1$ for the distorted one (Table 7.5). Distortion of a H_2S molecule causes redistribution of relative intensities. Additionally, the total transition rate increases about 5% as hydrogen atom moves 1.5 au when decay takes place. The results obtained for the distorted molecule should be treated as preliminary, since the angle between hydrogen atoms will also change causing additional alteration of the previously calculated Auger spectrum. The problem of dissociative transitions requires further investigations and is beyond scope of this study (since one of its assumption - the Frank-Condon principle - is not obeyed).

There is a major disagreement between our and Cesar *et al.* (1990) (also Thompson *et al.* 1976 and Eade and Robb 1977) assignments of the most intense peaks. Cesar *et al.* (1990) say: "Although there are no strict selection rules controlling the Auger transitions a propensity rule based on simplifications of the Auger matrix elements tells that bands associated to the singlet final ionic states dominate over the triplet coupled counterparts". However, the present calculations where molecular orbitals are represented as LCAOs and atomic selection rules are imposed indicate that about 47% of the $L_{23}VV$ transitions in the second row hydrides are achieved via triplet states.

Calculated total transition rate for H_2S is 3.17 mau which gives 86 meV linewidth is in excellent agreement with measured (Thomas, private communication) S 2p linewidths (77±2 meV and 91±5 meV for $2p_{1/2}$ and $2p_{3/2}$, respectively).

Aksela's *et al.*(1992) findings about the dissociation of H_2S to an HS fragment followed by Auger decay is not incorporated in the spectra generated using Gaussians with FWHM=0.5 eV (Fig.7.3).

7.4.4. HCl

Results of Auger spectra calculations performed for the HCl molecule by different authors together with some assignments of an experimental spectrum by Aksela *et al.* (1983) are shown in Table 7.6. The experimental spectrum of Aksela *et al.*(1983) along with the calculated spectrum shifted towards higher energy by 3.6 eV are presented in Figure 7.7.

There are 22 possible transitions spread across 36.4 eV of energy. Detailed analysis of the whole spectrum is difficult because of the band-like character of the experimental spectrum in the energy region of inner-inner transitions which is affected by correlation phenomena. However, only in the experimental spectrum is the maximum transition assigned to the $^1\Delta$ final state while all other authors assign the maximum intensity peak to the $[5\sigma\ 2\pi]^3\Pi$ double hole state. The spin-orbit splitting equal 1.6 eV is incorporated in the calculated spectrum.

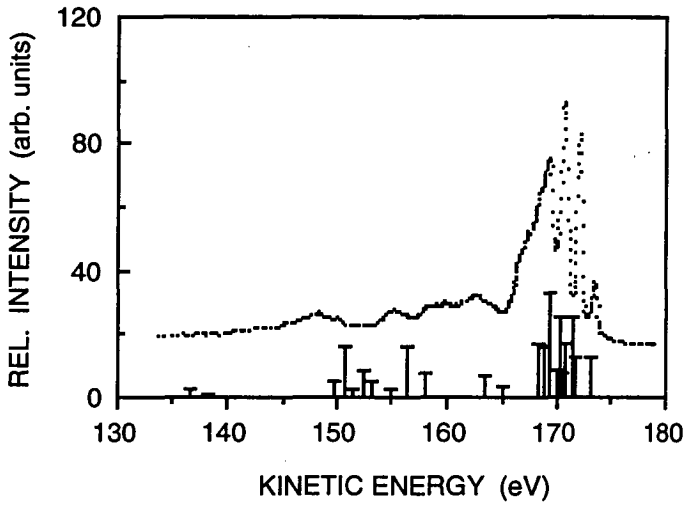

FIG.7.7 Experimental (Aksela *et al.* 1983) and calculated (shifted 3.6 eV) $L_{23}VV$ Auger spectra of chlorine in hydrogen chloride.

Sharp lines in the experimental spectrum indicate presence of species with long lifetime. It was suggested by Aksela *et al.* (1992) that molecular Auger decay of an HCl molecule is most probably followed by dissociation to atomic fragments. Only about 40% of the total intensity of the experimental spectrum is associated with a molecular Cl $L_{23}VV$ profile. It is conceivable that incorporation of the above findings in the present calculations will improve results obtained for HCl.

TABLE 7.6.

Hydrogen chloride transition energies and intensities calculated by different authors.

Final	state		Energy (eV) P	S	A	K	A Expt	Rel. Int. (%) P	S	K	A
2π	2π	$^{*3}\Sigma^-$	-3.9	(-5.2)	-5.7	-5.5	-5.1	37.4		25.3	31.3
2π	2π	$^{*1}\Delta$	-2.6		-4.0	-3.7	-3.6	38.1		35.7	81.3
2π	2π	$^3\Sigma^-$	-2.3	-4.2	-4.0	-3.9	-3.3	74.9	50.2	50.0	39.4
5σ	2π	$^{*3}\Pi$	-1.6		-1.7	-1.6	-1.6	50.0		50.0	56.9
2π	2π	$^{*1}\Sigma^+$	-1.3		-2.8	-2.5	-2.4	23.9		17.6	12.5
2π	2π	$^1\Delta$	-0.9	-2.4	-2.3	-2.1	-2.0	76.2	51.1	70.9	100.0
5σ	2π	$^{*1}\Pi$	-0.7		-0.2	0.0	-0.5	25.8		35.2	65.0
5σ	2π	$^3\Pi$	0.0 (165.6)	0.0 (168.7)	0.0 (167.6)	0.0	0.0 (168.2)	100.0	100.0	100.0	45.0
2π	2π	$^1\Sigma^+$	0.4	-1.1	-1.1	-0.9	-0.8	47.8	28.5	35.2	48.8
5σ	2π	$^1\Pi$	0.9	1.8	1.5	1.6	1.1	51.6	51.1	70.3	32.5
5σ	5σ	$^{*1}\Sigma^+$	4.1			5.1	0.5	10.0		19.8	68.1
5σ	5σ	$^1\Sigma^+$	5.8	6.9		6.7	1.5	20.0	28.1	39.6	43.8
4σ	2π	$^{*3}\Pi$	11.2					23.5		0.0	
4σ	2π	$^3\Pi$	12.8	12.7				46.9	20.4	0.0	
4σ	5σ	$^{*3}\Sigma^+$	14.3					7.8		0.0	
4σ	5σ	$^3\Sigma^+$	16.0	16.9		13.6		15.7	10.2	10.3	
4σ	2π	$^{*1}\Pi$	16.8					24.1		5.5	
4σ	5σ	$^{*1}\Sigma^+$	17.8					7.8		5.5	
4σ	2π	$^1\Pi$	18.5	19.6		13.2		48.2	26.4	24.0	
4σ	5σ	$^1\Sigma^+$	19.4	23.8		17.0		15.6	13.2	7.6	
4σ	4σ	$^{*1}\Sigma^+$	30.9					3.5		5.5	
4σ	4σ	$^1\Sigma^+$	32.5	35.9		23.9		7.0	5.5	2.4	
					Total	rate	(mau).	4.34	3.32		

The experimental spectrum was measured by Aksela *et al.*(1983) - A; P - present , S-Sukhorukov *et al.* (1986), A - Aksela *et al.*(1983), K - Kvalheim (1983). An asterisk in the final state description means that the initial hole was in a $2p_{1/2}$ orbital.

Absolute transition rate calculations give values of 4.34 mau and 3.32 mau using our and Sukhorukov's (1986) methods, respectively. The results obtained using present method can be overestimated since parameters for Ar were extrapolated (see section 3.2). Then Ar^+ may not be good approximation of a chlorine atom with a core hole.

7.5. Comparison Between Molecules

The experimental $L_{23}VV$ spectra of the second row hydrides change from broad profiles for silane and phosphine to the appearance of sharp features for hydrogen sulphide and hydrogen chloride spectra. The sharp atomic-like features are attributed to dissociated fragments of H_2S and HCl molecules.

The relationship between valence electron population and Auger transition rate is plotted in Fig. 7.8. The rate is proportional to the electron population for EC and NEC approaches. The most significant differences between EC and NEC methods are noted for silicon.

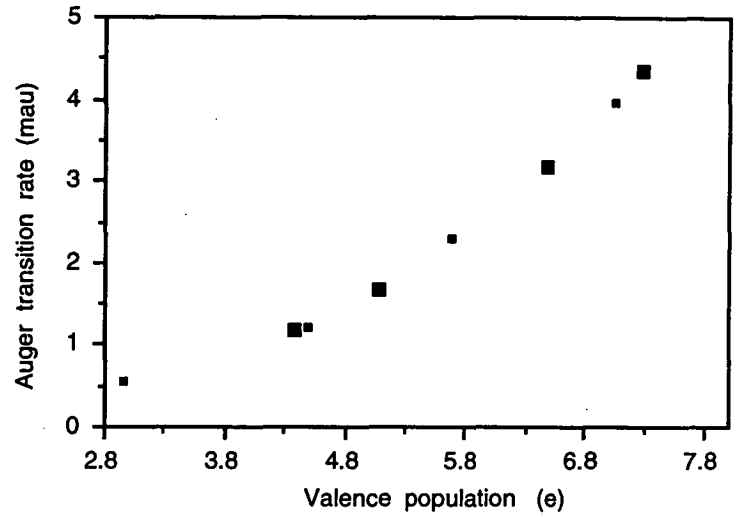

FIG.7.8 Theoretical transition rates as a function of valence electron population for the second row hydrides. (▪) non-equivalent cores approach (■) equivalent cores approach.

7.6. Conclusions

The present approach provides a reasonably simple method for intensity calculations of Auger transition probabilities for $L_{23}VV$ processes in molecules. Agreement between theory and experiment is encouraging. However, the detailed interpretation is very different to previous work and it requires further study. The interpretation of KVV Auger spectra for the first row hydrides cannot be automatically extended to the $L_{23}VV$ Auger spectra for the second row hydride molecules because of the different symmetry of the initial states for KVV and for $L_{23}VV$ transitions. In the $L_{23}VV$ Auger spectra for the second-row hydrides about 47% of the intensity arises from triplet states compared with typically less than 7% for KVV Auger spectra. The majority of intensity (about 2/3) of the $L_{23}VV$ Auger spectra of the second-row hydrides is gained via the p continuum channel.

There is an evidence that an equivalent cores technique offers good approximation of the total transition rates.

Aksela's *et al.* (1992) finding about neutral dissociation followed by Auger decay of atomic fragments as a dominating path in core decay in H_2S and HCl molecules

requires further studies. Yet, it is expected that incorporation of the findings in the present calculations will improve results obtained for the above molecules.

The semi-empirical method provides an efficient approach for the semiquantitative interpretation of an outer-outer region of complex Auger spectra.

Chapter 8

THE OCS MOLECULE

8.1. Introduction

Carbonyl sulphide is a polyatomic linear molecule containing first and second row elements and can be used as a test of our method of calculations since experimental Auger spectra of OCS in the gas phase are available (Carroll *et al.* 1990). The spectra of carbon and oxygen in OCS were measured and analysed by Carroll *et al.* (1990) using results of CNDO calculations obtained with the same programs as for the present work. The authors made a number of assignments for the double-hole final states on the basis of comparison of CNDO results with the experimental spectra. The $L_{23}VV$ experimental spectrum of S in OCS was also tentatively assigned without any Auger intensity calculations for sulphur. In this chapter we will compare existing assignments with results of our calculations. Significant localisation effects in OCS introduce an additional challenge in the calculations.

8.2. Theoretical Considerations

The electronic configuration for the molecule is $1\sigma^2 2\sigma^2 3\sigma^2 4\sigma^2 5\sigma^2 1\pi^4 6\sigma^2 7\sigma^2 8\sigma^2 9\sigma^2 2\pi^4 3\pi^4$ with the first six orbitals being core orbitals of S, C and O atoms. Carbonyl sulphide is a linear molecule and belongs to the $C_{\infty v}$ symmetry group with 44 final two-hole states possible for KVV Auger transitions and 88 states for $L_{23}VV$ transitions. In Table 8.1 Mulliken charges associated with each molecular orbital in the OCS are given.

TABLE 8.1.

Calculated (INDO) molecular orbital population in the OCS.

Mol. orbital / Atom	6σ	7σ	8σ	9σ	2π	2π	3π	3π	Total charge
S	0.01	1.22	0.35	1.03	0.08	0.08	1.65	1.65	**6.08**
C	0.65	0.66	0.27	0.66	0.68	0.68	0.07	0.07	**3.75**
O	1.34	0.12	1.38	0.31	1.23	1.23	0.28	0.28	**6.17**

The bond lengths between carbon-oxygen and between carbon-sulphur are equal to 1.15Å and 1.56Å, respectively. Detailed information about geometry and ionization energies of the OCS molecule is provided in Appendix C.5.

It has been previously established (Chapter 4) that the EC approach offers a better approximation of the experimental linewidths than NEC approach. However, in case of the OCS molecule energy convergence was not achieved for EC carbon calculations and hence for C(KVV) the NEC method was used.

In the following section comparison of experimental and theoretical Auger spectra of carbon, oxygen and sulphur in the OCS molecule will be given and the results obtained in the present studies will be analysed.

8.3. Experimental Findings

Auger spectra of gaseous OCS were measured by Carroll *et al.*(1990). The resolution of the spectra is assessed to be 0.5 eV for the sulphur $L_{23}VV$ spectrum and 1 eV for the KVV oxygen spectrum. The authors have used a 3 keV electron beam as an excitation source. Figure 8.1 a,b,c shows Auger spectra recorded for OCS together with bar spectra which represent the results of our calculations. A negative final-state energy scale is used. The calculated spectra are shifted 6 eV toward higher energy to align with the experiment.

In Figure 8.1a (depicting the sulphur $L_{23}VV$ spectra in OCS) only transitions coming from 2p3/2 initial hole can be shown on the final-energy axis. However, for sulphur $L_{23}VV$ spectra (Fig. 8.1a) the 6 eV shift seems to be too large for the theoretical spectrum. This phenomenon is caused by the fact that no relaxation correction is included in the calculated spectrum. However, from Chapter 7 it is known that the H_2S spectrum requires 3.3 eV shift to align with experiment. Hence, similar alignment may be required for the S($L_{23}VV$) spectrum in OCS.

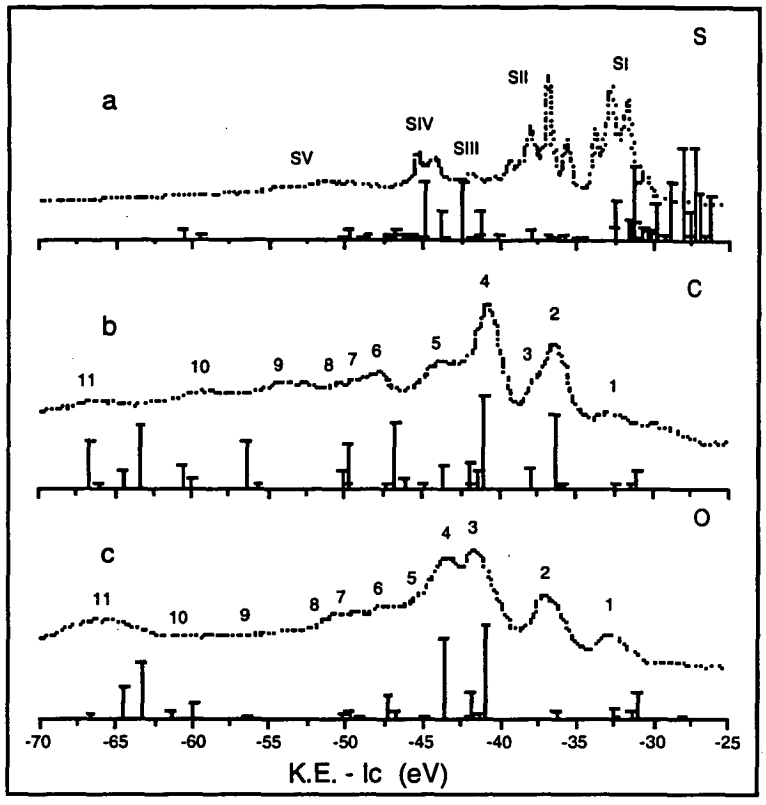

FIG.8.1 Experimental (Carroll *et al.* 1990) and calculated Auger spectra of (a) S($L_{23}VV$), (b) C(KVV) and (c) O(KVV) in the OCS molecule. The calculated spectra are shifted 6.0 eV toward higher energy.

8.4. Results and Discussion

The energies of double ionized OCS were calculated at the *ab initio* level by Millie *et al.* (1986). The multiplet splittings were not included in the calculations. Additionally, the calculations covered only a small fraction of a range of energy available for OCS^{+2}. Carroll *et al.*(1990) extrapolated the *ab initio* calculations and obtained energies of doubly ionized OCS for the higher-lying final states. The authors used energies predicted this way together with intensities calculated using a CNDO program. Detailed analysis of transitions was not performed since multiplets were not resolved in the calculations. There were no results of calculations available for sulphur at that time. Therefore the assignment of the peaks in the spectrum of sulphur in OCS was based on comparisons of three spectra (C, O and S).

All our calculations were performed using the EC approach for S and O and the NEC approach for C since convergence of energy in the EC method for carbon was not achievable. Relative energy is presented as the negative of the double hole ionization potential. Hence, for sulphur only one set of results (representing relative intensities

obtained for 2p3/2 initial hole) is given. It is assumed that relative intensities of the transitions arising as a result of the 2p1/2 initial hole are half of the intensities calculated for 2p3/2.

The results of energy and intensity calculations of Auger transitions in carbonyl sulphide together with experimental assignments by Carroll *et al.* (1990) are presented in Table 8.2. The absolute kinetic energy value is given for those transitions with relative intensities of 100%. For comparison purposes, the NEC results for S and O are presented in Table 8.2. Detailed results of calculations for OCS can be found in Appendix D.5.

TABLE 8.2

Carbonyl sulphide transition energies and intensities calculated in several studies.

Final state		Sym.	Rel. Energy (eV)			Rel. Int. S		R.Int. C	Rel. Int. O		Assign	
			present	CI	Expt	NEC	EC	NEC	NEC	EC	Carroll	present
3π	3π	$^3\Sigma^-$	-33.3	-31.4	-31.3	98.3	98.3	0.0	0.0	0.0	SI,C1,O1	SI
2π	3π	$^1\Sigma^-$	-33.7	-35.9	-36.7	4.7	6.6	0.0	0.0	0.0	)	
2π	3π	$^3\Delta$	-33.7	-35.9	-36.7	0.0	0.0	0.0	0.0	0.0	C1,O1	
2π	3π	$^3\Sigma^+$	-33.7	-35.9	-36.7	0.0	0.0	0.0	0.0	0.0	)	
3π	3π	$^1\Delta$	-34.1	-31.4	-31.3	100.0	100.0 (136.6eV)	1.0	5.2	2.1	SI,C1,O1	SI
3π	3π	$^1\Sigma^+$	-34.9	-31.4	-31.3	62.4	62.4	0.3	1.5	0.6	SI,C1,O1	SI
2π	3π	$^3\Sigma^-$	-36.6	-35.9	-36.7	10.1	14.3	0.0	0.0	0.0	C2,O2	
2π	3π	$^1\Delta$	-37.0	-35.9	-36.7	1.0	1.4	19.8	45.7	29.1	C2,O2	C1,O1
9σ	3π	$^3\Pi$	-37.1	-36.0	-35.9	84.1	76.3	0.8	0.1	0.0	SII	SII
2π	3π	$^1\Sigma^+$	-37.4	-35.9	-36.7	11.0	15.6	5.8	13.5	8.6	C2,O2	C1,O1
8σ	3π	$^3\Pi$	-37.5	-37.5	-37.9	15.8	22.8	0.6	1.4	0.4	C3,O2,SII	SII
9σ	3π	$^1\Pi$	-38.4	-36.0	-35.9	52.6	41.9	8.0	5.6	1.3	SII	SII
8σ	3π	$^1\Pi$	-38.6	-37.5	-37.9	14.5	15.1	2.6	22.6	12.4	C3,O2,SII	O2(1), SII
2π	9σ	$^3\Pi$	-41.8	-40.6	-41.0	4.3	5.5	7.6	0.2	0.0	C4	
8σ	9σ	$^3\Sigma^+$	-42.1	-43.1	-43.0	1.1	0.4	3.6	0.3	0.1	SIV	
2π	9σ	$^1\Pi$	-42.3	-40.6	-41.0	2.7	3.0	80.6	24.7	9.2	C4	C2,O2
9σ	9σ	$^1\Sigma^+$	-44.0	-41.1	-43.8	16.2	10.4	25.3	2.4	0.3	C5	C3, SIII-SIV

TABLE 8.2 Continuation

Carbonyl sulphide transition energies and intensities calculated in several studies.

Final state		Sym.	Rel. Energy (eV)			Rel. Int. S		R.Int. C	Rel. Int. O		Assign	
			present	CI	Expt	NEC	EC	NEC	NEC	EC	Carroll	present
2π	2π	$^3\Sigma^-$	-46.2	-40.7	-41.0	0.3	0.5	0.0	0.0	0.0		
2π	2π	$^1\Delta$	-47.0	-40.7	-41.0	0.3	0.5	100.0 (248.4eV)	100.0	100.0 (493.3eV)	C4,O3	C4,O3
8σ	9σ	$^1\Sigma^+$	-47.3	-43.1	-43.0	6.1	7.0	20.4	17.9	6.0	SIV	C4,O3
2π	2π	$^1\Sigma^+$	-47.8	-40.7	-41.0	0.2	0.3	29.4	29.4	29.4	C4,O3	C4,O3
8σ	2π	$^3\Pi$	-47.9	-42.6	-43.5	0.8	1.7	6.4	6.0	2.9	C5	C4,O3
7σ	3π	$^3\Pi$	-48.4	-47.9		55.9	62.9	1.2	0.3	0.1		SIV
8σ	2π	$^1\Pi$	-49.6	-42.6	-43.5	0.7	1.1	26.2	98.8	85.4	C5,O4	C5,O4
7σ	3π	$^1\Pi$	-50.9	-47.9		51.2	61.9	7.1	1.5	1.4		SIV
7σ	2π	$^3\Pi$	-52.1	-52.4		2.9	4.6	11.9	1.3	0.9		
7σ	2π	$^1\Pi$	-52.8	-52.4		2.6	4.5	71.4	6.6	9.7		
7σ	9σ	$^3\Sigma^+$	-52.8	-52.9		12.0	12.2	0.5	0.1	0.0		
8σ	8σ	$^1\Sigma^+$	-53.2	-45.2	-45.0	0.7	1.3	5.2	36.4	27.3	O5	C6,O6
7σ	8σ	$^3\Sigma^+$	-53.2	-55.0		1.4	3.3	3.0	0.2	0.1		
6σ	3π	$^3\Pi$	-55.1	-56.7		0.8	0.5	1.2	4.3	2.5		
7σ	9σ	$^1\Sigma^+$	-55.7	52.9		6.3	10.0	48.7	1.0	0.6		C6
6σ	3π	$^1\Pi$	-55.8	-56.7		0.5	0.3	6.9	15.3	8.5		
7σ	8σ	$^1\Sigma^+$	-56.2	-55.0		1.9	2.8	23.3	5.1	6.0		C6
6σ	9σ	$^3\Sigma^+$	-61.7	-61.6		0.1	0.1	9.1	2.5	0.8		
6σ	9σ	$^1\Sigma^+$	-62.4	-61.6		0.1	0.1	50.5	9.7	2.8		
6σ	2π	$^3\Pi$	-65.9	-61.1	-66-64	0.0	0.0	12.2	18.8	17.3	C11,O11	C10,O10
7σ	7σ	$^1\Sigma^+$	-66.6	-64.8		8.3	9.4	25.8	0.3	0.4	C11	
6σ	8σ	$^3\Sigma^+$	-67.5	-63.7	-66-64	0.0	0.0	0.1	10.5	7.9	O11	
6σ	2π	$^1\Pi$	-69.3	-61.1	-66-64	0.0	0.0	69.8	67.1	58.3	C11,O11	C11,O11
6σ	8σ	$^1\Sigma^+$	-70.5	-63.7	-66-64	0.0	0.0	22.4	55.6	34.9	O11	C11,O11
6σ	7σ	$^3\Sigma^+$	-72.0	-73.5		0.0	0.0	8.4	0.5	0.8		

TABLE 8.2 Continuation

Carbonyl sulphide transition energies and intensities calculated in several studies.

Final state		Sym.	Rel. Energy (eV)			Rel. Int. S		R.Int. C	Rel. Int. O		Assign	
			present	CI	Expt	NEC	EC	NEC	NEC	EC	Carroll	present
6σ	7σ	$^1\Sigma^+$	-72.6	-73.5		0.2	0.1	53.8	6.7	5.6		C11
6σ	6σ	$^1\Sigma^+$	-89.3	-82.2		0.0	0.0	25.5	42.0	34.5		
	Total	rate	(mau)			**2.70**	**3.27**	**1.96**	**5.34**	**6.71**		

In parentheses - absolute energy values (in eV) of the most intense transitions.

Relative energies CI - unweighted average of term energies from Millie *et al.* (1986) as found in Carroll *et al.* (1990), Expt - from Carroll *et al.* (1990),

The KVV spectrum is 56.0 eV wide. There are 44 KVV and 88 $L_{23}VV$ transitions possible in OCS. The variation between the NEC and EC approaches in relative intensity calculations seldom exceeds 10% of the intensities. The differences are more pronounced for final states involving heavily populated molecular orbitals. Hence, the 10.7% differences for relative intensities of transitions in sulphur calculated using the NEC and EC methods appear only for the $[7\sigma\ 3\pi]^1\Pi$ and $[9\sigma\ 3\pi]^1\Pi$ states because the 7σ, 9σ and 3π orbitals are dominated by sulphur (Table 8.1). In oxygen spectra the differences in EC and NEC calculated relative transition intensities would appear in lines involving 6σ, 8σ and 2π since these orbitals are localised mostly on oxygen (Table 8.1). In fact, relative intensities of six final states: $[7\sigma\ 8\sigma]^1\Sigma^+$, $[2\pi\ 3\pi]^1\Delta$, $[9\sigma\ 2\pi]^1\Pi$, $[8\sigma\ 9\sigma]^1\Sigma^+$, $[8\sigma\ 2\pi]^1\Pi$, $[8\sigma\ 3\pi]^1\Pi$ increase between 10 and 20% for the NEC approach when compared with EC results (Table 8.2). The differences between results obtained using the NEC and EC methods are smaller than 10% for all other transitions and can be considered insignificant. It is expected that disparities in relative carbon intensities calculated using EC and NEC approaches would not exceed 10% since there is no orbital solely localised on a carbon atom in OCS (Table 8.1).

8.4.1. Sulphur

The EC calculated Auger spectrum of sulphur contains 50 non-zero final states among 88 possible. The maximum intensity (100%) is assigned to the $[3\pi\ 3\pi]^1\Delta$ final state with the absolute transition rate 0.33 mau. There are additional strong transitions (over 75%) assigned to the triplets $[3\pi\ 3\pi]^3\Sigma^-$ and $[9\sigma\ 3\pi]^3\Pi$, respectively (Table 8.2). The total intensity of the sulphur spectrum is 3.27 and 2.70 mau for the equivalent and non-equivalent core approaches, respectively.

In Figure 8.2 the experimental spectrum of sulphur in OCS along with the theoretically predicted lines shown on a kinetic energy scale are presented. A shift of 1.7 eV was applied to the calculated spectrum.

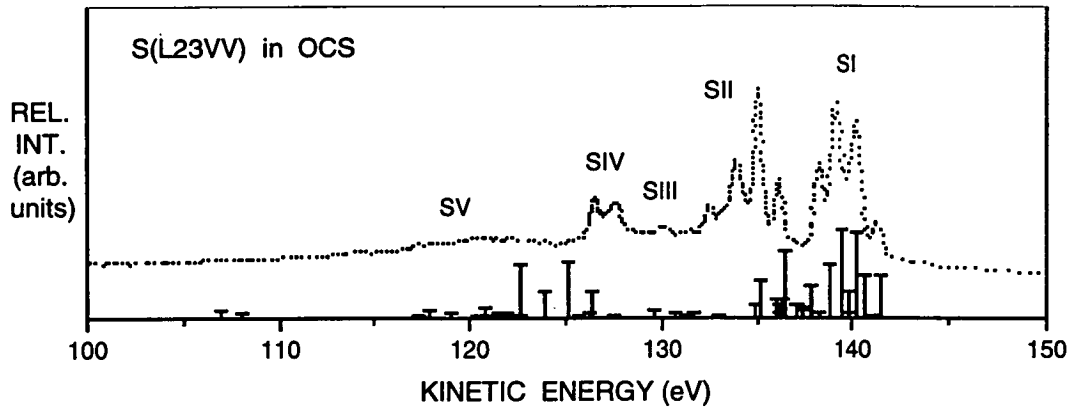

FIG.8.2 Experimental (Carroll *et al.* 1990) and calculated Auger spectra of S(L_{23}VV) in the OCS molecule. The calculated spectrum is shifted 1.7 eV toward higher energy.

The region marked as S I is assigned to final states generated with [3π 3π] double-hole states while S II is assigned to [9σ 3π] final double-hole states. The region S IV can be assigned to [7σ 3π] final hole states. The assignment of S III is not straightforward. S V can be associated with the final states involving 7σ and other orbitals. The orbitals 7σ, 9σ and 3π are localised on the sulphur atom. Hence, the intensity mostly comes from final states involving the above orbitals. The energy spacing of the final states requires adjustment within 2-3 eV.

The calculated spectrum satisfactorily approximates the outer-outer region of the experimental profile of sulphur in OCS (Figure 8.2). As for the transitions involving inner molecular orbitals a small energy refinement would be necessary to achieve better agreement with an experiment. In the inner-inner molecular orbital region some other effects (such as correlation etc.) start to play a significant role in the Auger transitions and our method of calculation cannot be applied there.

8.4.2. Carbon

There is a substantial agreement between our assignments of Auger transitions in carbon in OCS and the experimental assignments by Carroll *et al.* (1990) (Table 8.1). The only significant discrepancies appear for $[2\pi\ 9\sigma]^1\Pi$ and $[9\sigma\ 9\sigma]^1\Sigma^+$ where we prefer to assign the transitions to the regions C2 and C3, respectively (Figure 8.1b). On the basis of information available we can also assign $[7\sigma\ 9\sigma]^1\Sigma^+$ and $[7\sigma\ 8\sigma]^1\Sigma^+$ transitions to the region C6-7.

However, the detailed assignment of Auger transitions is difficult because of broad structures in the experimental spectrum. Additionally, the energy of the double-hole states is not accurate for some cases because additional effects such as correlation or localisation are not fully incorporated in the calculations.

The theory predicts 44 final hole states with 11 of them having negligible intensity. The maximum intensity is assigned to the $[2\pi\ 2\pi]^1\Pi$ final hole state with the absolute intensity rate 0.25 mau. There are two lines with relative intensities above 70%: $[9\sigma\ 2\pi]^1\Pi$ and $[7\sigma\ 2\pi]^1\Pi$.

The total transition rate for the KVV spectrum of carbon is calculated to be 1.99 mau , which is similar to the values obtained for KVV carbon intensity in the CH_3X molecules. On the basis of the results obtained in other calculations for carbon it is predicted that in the equivalent cores approach the absolute total transition rate for carbon in OCS should be about 3.3 mau.

We have compared charge distributions calculated for OCS using *ab initio* and INDO methods. The results of the present INDO calculations (Table 8.1) are very close to that obtained by CI methods (Carroll *et al.* 1990). The charge from the carbon atom is distributed between 6σ, 7σ, 9σ and 2π orbitals. As a result there is little intensity coming from $[3\pi\ 3\pi]$ or $[8\sigma\ 8\sigma]$ final states.

The total energy span of the calculated carbon spectrum is 56 eV while that of the experimental spectrum is about 40 eV. The calculated spectrum has to be shifted 6.0 eV to obtain better alignment with the experimental spectrum. The theoretical spectrum predicts the $[6\sigma 6\sigma]\ ^1\Sigma^+$ peak to have the lowest energy, while in the experimental spectrum there is no feature which can be assigned to this transition. Overall, however, there is good agreement between the calculated and the experimental spectra (Figure 8.1b).

8.4.3. Oxygen

The maximum intensity transition is assigned to the $[2\pi\ 2\pi]^1\Delta$ final state (Table 8.2). There is one more transition with relative intensity over 85%: $[8\sigma\ 2\pi]^1\Pi$. The total absolute rate calculated using the equivalent cores model is 6.71 mau, while the non-equivalent cores approach gives 5.34 mau which is within the range obtained for XCHO molecules. There are 24 non-zero intensities when the EC approach is used for the intensity calculations. The theoretical intensities are too low for the experimental O2 peak (Fig.8.1c).

Orbitals 6σ,8σ,2π are mostly localised on the oxygen atom (Table 8.1) and the majority of the intensity in the Auger O(KVV) spectrum comes from final states involving these orbitals. The peak assignments for the oxygen KVV spectrum by Carroll *et al.* (1990) are in agreement with our results. However, the singlet $[8\sigma\ 8\sigma]^1\Sigma^+$ can be assigned to O6 while triplet

$[6\sigma 2\pi]^3\Pi$ can be assigned to O10 (Table 8.2). Overall, the calculated spectrum fits the experiment very well (Fig.8.1c).

8.5. Conclusions

We have calculated Auger spectra of the OCS molecule. The agreement between the theoretical and experimental spectra is satisfactory and the method seems to be promising for semi-quantitative calculations of Auger spectra of polyatomic molecules even in the presence of localised orbitals.

Chapter 9

TETRAHEDRAL HYDRIDES AND FLUORIDES

9.1. Introduction

Tetrahedral molecules represent an interesting group of compounds from the spectroscopical point of view. The valence orbital structure is identical for hydrides (fluorides). Therefore effects of size and electronegativity can be studied. The high symmetry of the molecules invokes many double-hole states with zero intensity in the Auger spectra. Tetrahedral hydrides, CH_4 and SiH_4 , were studied in previous chapters (see Chapters 4&7). The Auger spectra of these molecules can be calculated and interpreted satisfactorily by the delocalized model. However, in the case of SiF_4 various researchers suggested that localisation method had to be used. (Lapiano-Smith *et al.*(1989), Rye and Houston (1983), also Ortiz (1984)). Rye and Houston (1983) interpreted the silicon $L_{23}VV$ spectrum as a composite of two profiles resulting from two versions (localised and delocalised) of the same final states while the fluorine spectrum is assumed to arise from two hole states both on the same fluorine atom. This is not consistent with assessment of the fluorine spectra in a CF_4 molecule by the same authors.

TABLE 9.1.

Number of two-hole states for the tetrahedral hydrides and fluorides containing first and second row atoms.

Molecule	Symmetry	[vv']Γ	Valence orbitals
CH_4	T_d	7	$2a_1,1t_2$
SiH_4	T_d	7(14)	$3a_1,2t_2$
CF_4	T_d	107	$3a_1,2t_2,4a_1,3t_2,1e,4t_2,1t_1$
SiF_4	T_d	107(214)	$4a_1,3t_2,5a_1,4t_2,1e,5t_2,1t_1$

9.2. Theoretical Considerations

Geometries and ionization energies used in the present studies were taken from various sources. Detailed information including experimental geometries and ionization energies of the tetrahedral molecules is provided in Appendix C.1, C.4 and C.5 for CH_4 , SiH_4 and CF_4 together with SiF_4, respectively. Fig.9.1 diagrammatically shows ionization energy values for valence orbitals used in the current calculations. The width of the Auger spectra is expected to be significantly larger for tetrahedral fluorides than for hydrides because of polarisation effects.

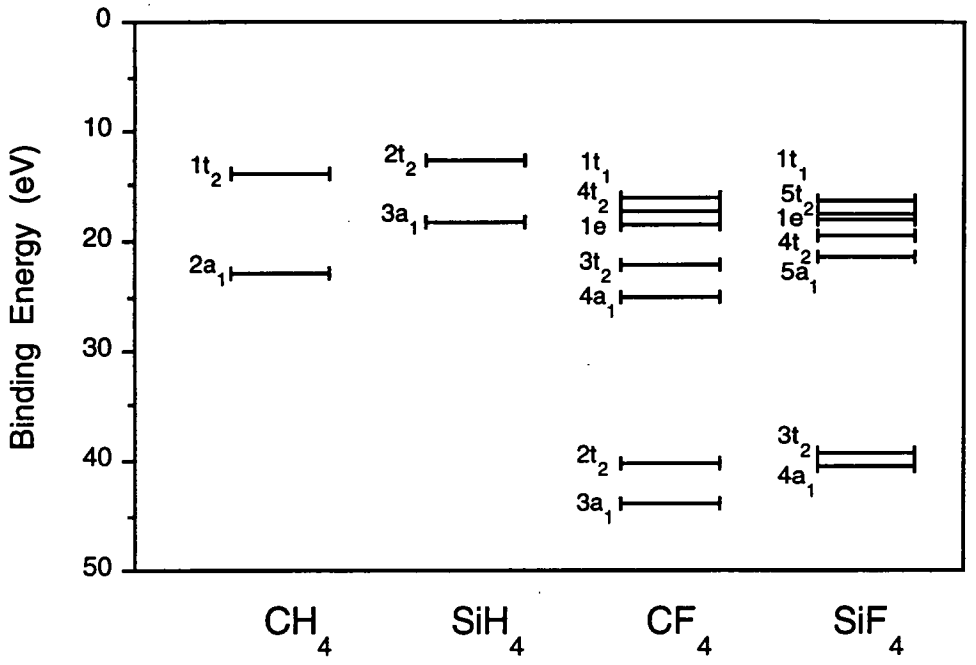

FIG.9.1. Experimental valence ionization energies of the tetrahedral hydride and fluoride molecules.

In Table 9.2 valence electron populations and total Auger transition rates obtained for the tetrahedral hydride and fluoride molecules containing first and second row elements are presented. R^k atomic matrix element values for the first row elements are taken from Walters and Bhalla (1971) while for the second row elements the values are adapted from Chen *et al.* (1990) (Chelkowska and Larkins 1991a).

TABLE 9.2.

Calculated valence electron populations and Auger rates for the tetrahedral molecules containing C and Si using non-equivalent cores (NEC) and equivalent cores (EC) approaches.

Molecule	Atom	Valence -e⁻ population		Calc. Auger rate (mau)	
		NEC	EC	NEC	EC
CH_4	C	3.96	5.02	2.20	3.54
CF_4	C	2.99	4.07	1.25	2.33
	F	7.25	-	6.89	-
SiH_4	Si	2.96	4.38	0.57	1.18
SiF_4	Si	1.88	3.04	0.23	0.52
	F	7.53	-	7.41	-

The EC approach offers a better approximation of the experimental linewidths than the NEC approach. However, for fluorine in the T_d symmetry molecules EC calculations were not achievable. Hence, only results obtained via the NEC method for fluorine are presented in Table 9.2.

9.3. Experimental Findings

All figures presented in this subchapter contain the experimental spectra together with the theoretical bar graphs representing calculated theoretical Auger transitions. Some of the theoretical spectra required shifts to align with experiments.

9.3.1. Carbon Spectra

All hydrides were considered earlier (Chapter 4 and 7). Hence, only brief reminders are shown in this chapter. The spectrum of methane was measured by many authors (see Chapter 4 for ref.). The experimental spectrum of Spohr *et al.*(1970) along with the calculated spectrum using the EC approach is presented in Fig.9.2a.

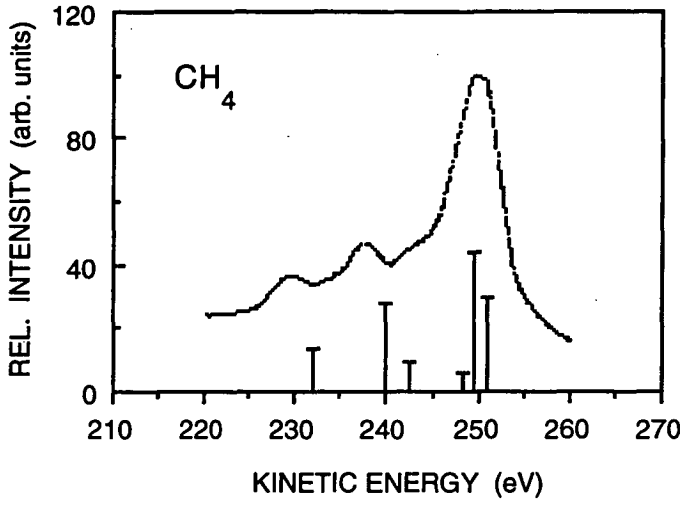

FIG.9.2.a Experimental (Spohr *et al.* 1970) and calculated Auger spectra of carbon in the CH_4 molecule. The calculated spectrum is shifted 0.1 eV toward higher energy.

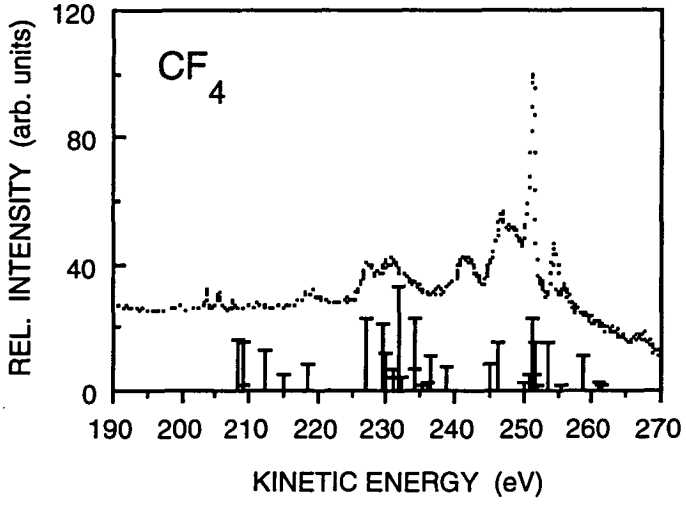

FIG.9.2.b Experimental (Aksela , unpublished) and calculated Auger spectra of carbon in the CF_4 molecule. The calculated spectrum is shifted 5.7 eV toward higher energy.

Carbon tetrafluoride Auger spectra were measured by Siegbahn *et al.* (1969), by Rye and Houston (1983) and by Aksela (unpublished) who has used synchrotron radiation as an

excitation medium. The latest spectrum of carbon is depicted in Fig.9.2b while the spectrum of fluorine is shown in Fig. 9.4a.

9.3.2. Silicon Spectra

An Auger spectrum of silane was measured by several researchers using different excitation sources (see Chapter 7 for ref.). The experimental spectrum by de Souza *et al.*(1986) is presented in Fig.9.3a along with the theoretically evaluated spectrum of SiH_4. The energy axis is 70 eV wide to match values used for SiF_4.

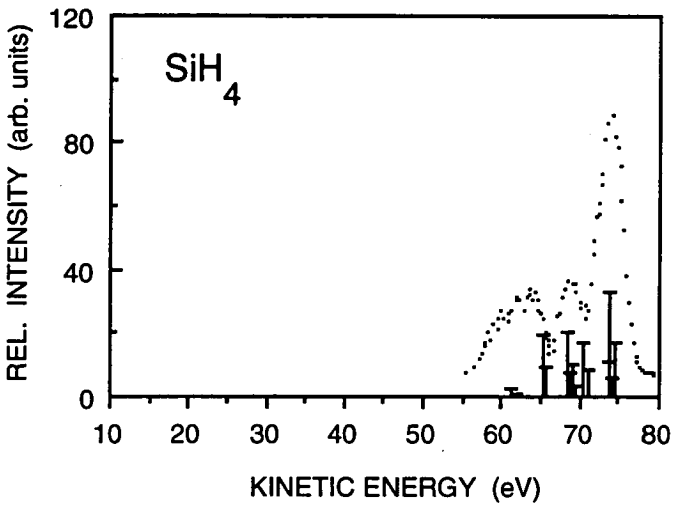

FIG.9.3.a Experimental (de Souza *et al.* 1986) and calculated Auger spectra of silicon in the SiH_4 molecule. No shift was applied.

Spectra of silicon and fluorine in the SiF_4 molecule were measured by Rye and Houston (1983) using an electron impact method. The fluorine spectrum obtained by the above authors together with our theoretical spectrum calculated using the NEC approach is shown in Fig.9.4b.

Synchrotron radiation induced spectra of silicon in SiF_4 are also available (Aksela *et al.*1986, Ferrett *et al.*1988). We present an experimental spectrum of Si(LVV) measured by Aksela *et al.* (1986) along with the spectrum representing results of our EC calculations in Fig.9.3b.

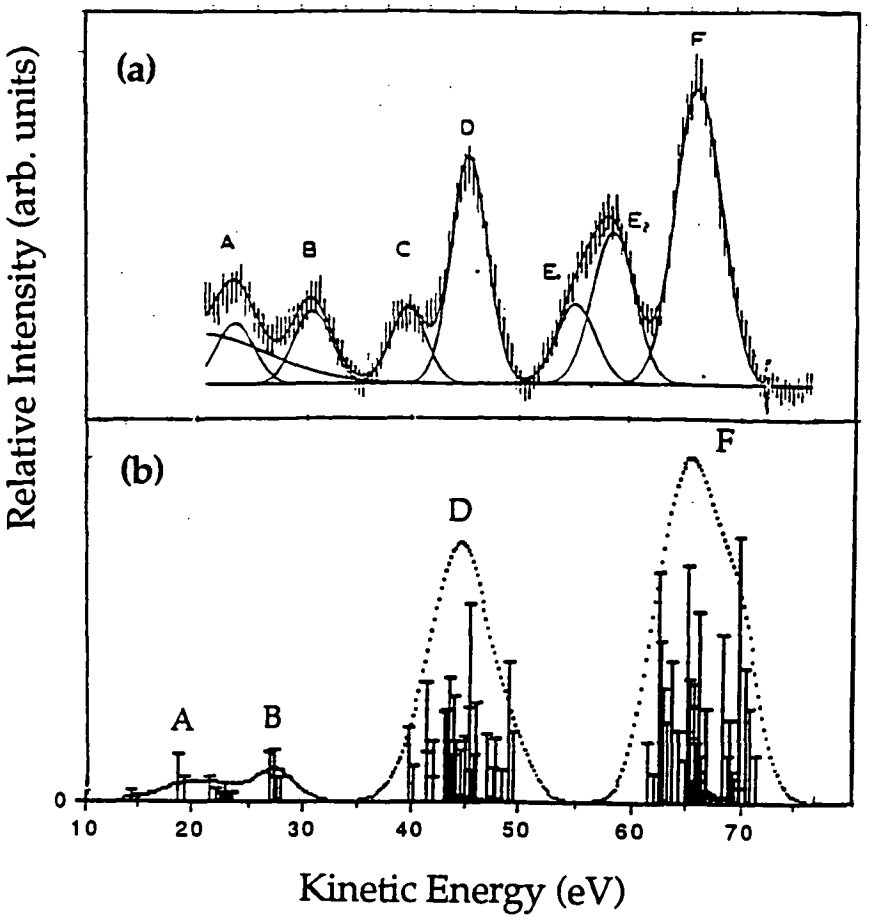

FIG.9.3.b Experimental (a) (Aksela *et al.*1986) and calculated (b) Auger spectra of silicon in the SiF_4 molecule. The calculated spectrum (generated using gaussians with FWHM=4.0 eV) is shifted 3.5 eV toward higher energy to align the leading edges in the high kinetic energy region with the experimental peaks.

9.3.3. Fluorine Spectra

Figures 9.4 a and b present fluorine spectra of CF_4 and SiF_4, respectively. The calculated spectra were obtained using the NEC method.

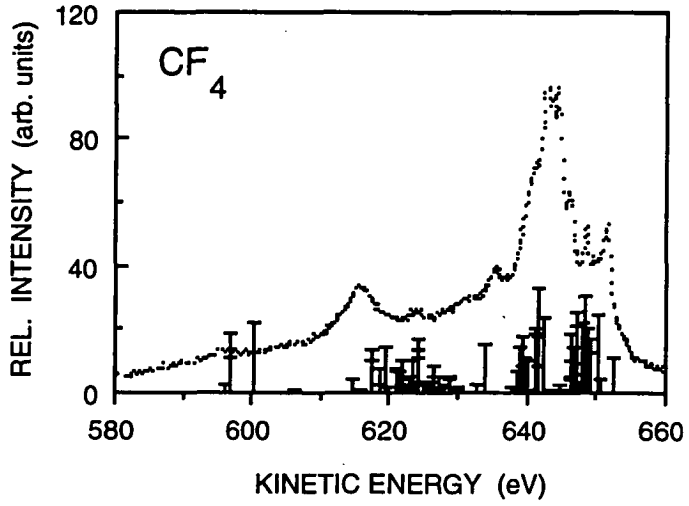

FIG.9.4.a Experimental (Aksela, unpublished) and calculated Auger spectra of fluorine in the CF_4 molecule. The calculated spectrum is not shifted.

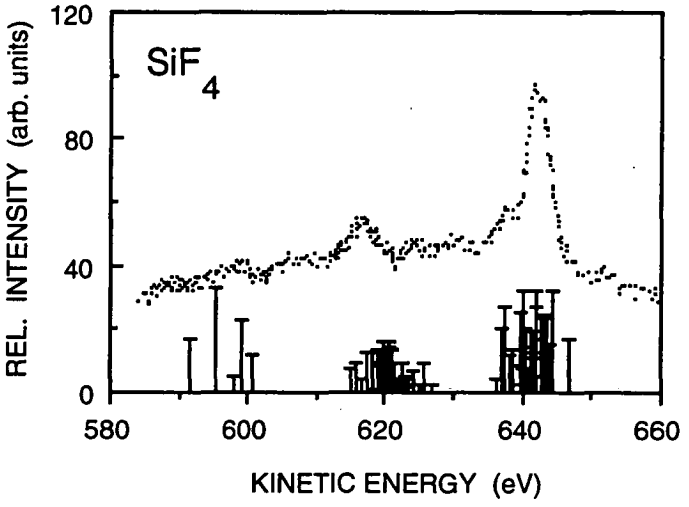

FIG.9.4.b Experimental (Rye and Houston (1983)) and calculated Auger spectra of fluorine in the SiF_4 molecule. The calculated spectrum is shifted 5.4 eV toward lower energy to align with the experiment.

9.4. Results and Discussion

Detailed results of our calculations are presented in Appendices D.1.1, D.4.1 and D.6 for CH_4, SiH_4 and the tetrahedral fluorides, respectively. In Fig. 9.5 theoretical profiles of C(KVV), Si(L_{23}VV) and F(KVV) in tetrahedral fluoride molecules are shown. The shapes (generated using gaussians with FWHM=0.5 eV) are displayed on a common scale representing the difference between the kinetic energy of the Auger electrons and the energy required to create an initial core hole. Total areas under the peaks are set to be the same for each element.

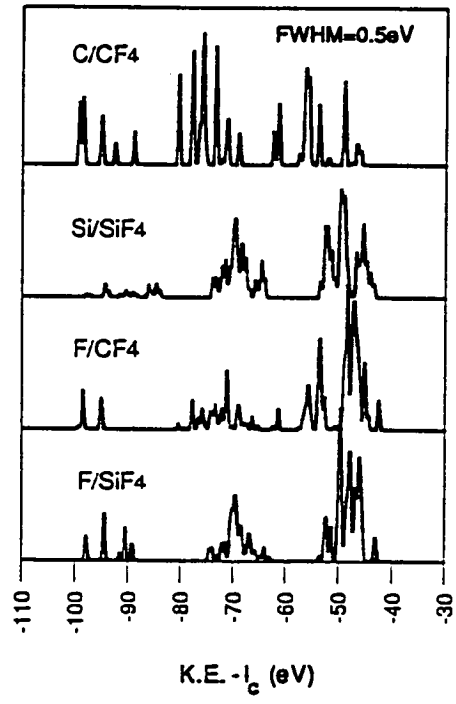

FIG.9.5 Theoretical Auger spectra of the tetrahedral hydrides and fluorides generated using gaussian shapes with FWHM=0.5 eV.

9.4.1. Tetrahedral Hydrides

The Auger spectra of tetrahedral hydrides were discussed in detail in the previous chapters (see Chapter 4 and 7). In general, there is a satisfactory agreement between the theoretical and experimental spectra of the central atoms (Fig.9.2.a and Fig.9.3.a). The positions of the $^1T_2$ [xa_1, yt_2] and [xa_1, xa_1] (where x=2 , y=1 and x=3, y=2, for CH_4 and SiH_4, respectively) require small corrections in both cases (Larkins *et al.* 1990, Chelkowska and Larkins 1991b). There is also some contribution of satellites in the normal Auger spectra. For CH_4 it has been estimated that ~16% of the intensity can be

attributed to initial state satellite lines (Larkins *et al.*1990), while no assessment has been made for the presence of satellite transitions in the Si(L_{23}VV) spectrum of silane.

9.4.2. Tetrahedral Fluorides

The spectra of the tetrahedral fluorides have been studied by several authors. Barber *et al.* (1977) assigned the Auger transition energies of CF_4 using the SCF X-alpha technique and stated that the results were moderately good. Rye and Houston (1983) postulated that in the silicon spectrum of SiF_4 two valence holes in a single configurational final state can appear spatially in the same Si-F bond or in different bonds. A very brief interpretation of an Auger Si(LVV) spectrum in agreement with that of Rye and Houston (1983) was presented by Akselaet *al.*(1986). Ferret *et al.*(1988) gave an alternative description of the doubly-ionized states of SiF_4^{+2} which could be an extension of a localization idea. In their interpretation each of the two-hole final states might be described by coupling two one-hole final states which in turn would be given by delocalized orbitals. In this model, energies of individual configurations would be shifted by different amounts depending on the hole-hole interactions, whereas Lapiano-Smith *et al.*(1989) suggested the presence of a "valence bond depopulation mechanism". The authors concluded that the fluorine KVV Auger mechanism involved the formation of a localized, two-hole final state that persists on the time scale of fragmentation of SiF_4. However, CF_4 fragmentation occured through a delocalized two-hole state because there was no evidence of F^{+2} ions.

The Auger spectra of the central atom in the tetrahedral fluorides are very different from that in the hydrides (Fig. 9.2b and 9.3b versus Fig.9.2a and 9.3a). The carbon spectrum contains several sharp lines on a band-like structure. The silicon spectrum is unusual and consists of 6 distinctive regions, where only 3 are expected (namely, equivalent to outer-outer, outer-inner and inner-inner regions). Fluorine spectra of CF_4 and SiF_4 diverge only in the outer-outer orbital region (Fig. 9.4a and b).

9.4.2.1. Carbon Tetrafluoride

Results of calculations of the KVV spectra in carbon tetrafluoride are given in Table 9.4, while in Figures 9.3a and 9.4a experimental spectra of CF_4 together with the theoretical results for carbon and fluorine, respectively, are shown. In Fig. 9.5 calculated profiles generated using gaussian FWHM=0.5 eV are presented.

The total width of the calculated spectra is 56.8 eV. The present theory predicts 107 final hole states, yet, many final double hole states lead to zero intensity transitions. Nevertheless, the detailed assignment of Auger transitions is not feasible.

TABLE 9.3

Transition energies and intensities of Auger spectra of carbon tetrafluoride calculated using present approach with equivalent cores for carbon and non-equivalent cores for fluorine.

Final state		Symmetry	Rel. Energy (eV)	Rel. Int.(%) Carbon (EC)	Fluorine (NEC)
$1t_1$	$1t_1$	^1E	-42.5	0.0	32.0
$1t_1$	$4t_2$	^1E	-44.4	0.0	13.8
$3t_2$	$1t_1$	$^3A_1$	-44.7	0.0	1.0
$1t_1$	$1t_1$	$^1T_2$	-45.1	0.0	73.3
$4t_2$	$4t_2$	^1E	-46.0	5.2	37.7
$1t_1$	$4t_2$	$^1A_1$	-46.3	0.0	50.2
$4t_2$	$4t_2$	$^1T_2$	-46.6	7.8	61.7
$3t_2$	$1t_1$	$^3T_2$	-46.8	0.0	2.1
$1t_1$	$1t_1$	$^1A_1$	-46.9	0.0	18.7
$1t_1$	$4t_2$	$^1T_1$	-47.0	0.0	90.3
1e	$1t_1$	$^1T_1$	-47.3	0.0	27.7
1e	$1t_1$	$^1T_2$	-47.4	0.0	65.8
$4t_2$	$4t_2$	$^1A_1$	-47.5	1.0	9.6
1e	$4t_2$	$^1T_2$	-48.2	0.0	64.6
$1t_1$	$4t_2$	$^1T_2$	-48.2	0.0	76.9
1e	1e	^1E	-48.5	0.0	42.6
1e	$4t_2$	$^1T_1$	-48.7	0.0	30.1
$3t_2$	$4t_2$	^1E	-49.0	31.9	15.1
1e	1e	$^1A_1$	-49.0	0.0	12.5
$1t_1$	$1t_1$	^1E	-42.5	0.0	32.0
$1t_1$	$4t_2$	^1E	-44.4	0.0	13.8
$3t_2$	$1t_1$	$^3A_1$	-44.7	0.0	1.0
$1t_1$	$1t_1$	$^1T_2$	-45.1	0.0	73.3
$4t_2$	$4t_2$	^1E	-46.0	5.2	37.7
$1t_1$	$4t_2$	$^1A_1$	-46.3	0.0	50.2
$4t_2$	$4t_2$	$^1T_2$	-46.6	7.8	61.7
$3t_2$	$1t_1$	$^3T_2$	-46.8	0.0	2.1
$1t_1$	$1t_1$	$^1A_1$	-46.9	0.0	18.7
$1t_1$	$4t_2$	$^1T_1$	-47.0	0.0	90.3
1e	$1t_1$	$^1T_1$	-47.3	0.0	27.7
1e	$1t_1$	$^1T_2$	-47.4	0.0	65.8
$4t_2$	$4t_2$	$^1A_1$	-47.5	1.0	9.6
1e	$4t_2$	$^1T_2$	-48.2	0.0	64.6
$1t_1$	$4t_2$	$^1T_2$	-48.2	0.0	76.9
1e	1e	^1E	-48.5	0.0	42.6
1e	$4t_2$	$^1T_1$	-48.7	0.0	30.1
$3t_2$	$4t_2$	^1E	-49.0	31.9	15.1
1e	1e	$^1A_1$	-49.0	0.0	12.5
$3t_2$	$1t_1$	^1E	-49.0	0.0	56.7
$3t_2$	$4t_2$	$^3T_2$	-49.0	0.0	1.5
$3t_2$	$1t_1$	$^1T_1$	-50.5	0.0	7.0
$3t_2$	1e	$^3T_2$	-50.6	0.0	1.4
$4a_1$	$1t_1$	$^3T_2$	-51.1	0.0	3.0
$4a_1$	$4t_2$	$^3T_2$	-52.0	5.3	2.6
$3t_2$	$4t_2$	$^1T_1$	-52.7	0.0	71.0
$3t_2$	1e	$^1T_1$	-53.4	0.0	25.2
$3t_2$	1e	$^1T_2$	-53.4	0.0	53.5
$3t_2$	$1t_1$	$^1T_2$	-53.5	0.0	100.0 (641.7eV)

TABLE 9.3 Continuation

Transition energies and intensities of Auger spectra of carbon tetrafluoride calculated using present approach with equivalent cores for carbon and non-equivalent cores for fluorine.

Final	state	Symmetry	Rel. Energy (eV)	Rel. Int.(%) Carbon (EC)	Fluorine (NEC)
$3t_2$	$4t_2$	$^1T_2$	-53.8	45.9	55.1
$4a_1$	$1t_1$	$^1T_2$	-53.9	0.0	60.1
$4a_1$	1e	^3E	-54.3	0.0	2.0
$4a_1$	1e	^1E	-55.2	0.0	30.6
$3t_2$	$4t_2$	$^1A_1$	-55.5	5.9	34.1
$4a_1$	$4t_2$	$^1T_2$	-55.8	15.8	54.5
$3t_2$	$3t_2$	^1E	-55.8	45.3	26.2
$3t_2$	$3t_2$	$^1T_2$	-56.3	67.9	42.2
$4a_1$	$3t_2$	$^3T_2$	-56.7	15.7	1.3
$3t_2$	$1t_1$	$^1A_1$	-56.8	0.0	19.5
$3t_2$	$3t_2$	$^1A_1$	-57.5	8.7	4.5
$4a_1$	$3t_2$	$^1T_2$	-61.3	46.6	45.1
$4a_1$	$4a_1$	$^1A_1$	-62.3	25.4	8.3
$2t_2$	$1t_1$	$^3T_1$	-65.2	0.0	4.7
$2t_2$	$1t_1$	^3E	-65.3	0.0	3.1
$2t_2$	$1t_1$	$^1T_1$	-66.3	0.0	15.5
$2t_2$	$1t_1$	^1E	-66.3	0.0	12.8
$2t_2$	$4t_2$	^3E	-67.4	0.0	4.5
$2t_2$	$4t_2$	$^3T_1$	-67.4	0.0	7.1
$2t_2$	$1t_1$	$^3T_2$	-68.0	0.0	14.0
$2t_2$	$4t_2$	$^3T_2$	-68.6	0.0	11.3
$2t_2$	$4t_2$	$^1T_1$	-68.8	0.0	25.1
$2t_2$	$4t_2$	^1E	-68.9	23.5	16.1
$2t_2$	1e	$^3T_1$	-69.1	0.0	3.1
$2t_2$	1e	$^3T_2$	-69.1	0.0	9.4
$2t_2$	$4t_2$	$^3A_1$	-69.2	0.0	4.5
$2t_2$	$1t_1$	$^3A_1$	-69.3	0.0	6.2
$3a_1$	$1t_1$	$^3T_2$	-70.2	0.0	7.7
$2t_2$	$4t_2$	$^1T_2$	-71.1	33.8	39.6
$2t_2$	1e	$^1T_2$	-71.1	0.0	32.8
$2t_2$	1e	$^1T_1$	-71.1	0.0	11.4
$2t_2$	$1t_1$	$^1T_2$	-71.2	0.0	49.9
$3a_1$	$4t_2$	$^3T_2$	-71.5	7.2	7.6
$3a_1$	$1t_1$	$^1T_2$	-72.0	0.0	30.5
$2t_2$	$4t_2$	$^1A_1$	-72.2	4.3	15.6
$2t_2$	$3t_2$	$^3T_1$	-72.2	0.0	5.0
$2t_2$	$3t_2$	^3E	-72.6	0.0	4.8
$3a_1$	1e	^3E	-72.7	0.0	5.1
$2t_2$	$3t_2$	$^3T_2$	-73.1	0.0	8.8
$2t_2$	$3t_2$	^1E	-73.3	69.4	12.9
$3a_1$	$4t_2$	$^1T_2$	-73.3	21.5	29.2
$2t_2$	$3t_2$	$^3A_1$	-73.4	0.0	3.2
$2t_2$	$1t_1$	$^1A_1$	-73.7	0.0	21.0
$2t_2$	$3t_2$	$^1T_1$	-74.1	0.0	23.2
$3a_1$	1e	^1E	-74.3	0.0	19.3
$2t_2$	$4a_1$	$^3T_2$	-75.3	11.6	6.3
$2t_2$	$3t_2$	$^1T_2$	-75.8	100.0 (226.0eV)	44.3
$3a_1$	$3t_2$	$^3T_2$	-76.4	21.4	6.5
$2t_2$	$3t_2$	$^1A_1$	-76.6	12.7	21.9

TABLE 9.3 Continuation

Transition energies and intensities of Auger spectra of carbon tetrafluoride calculated using present approach with equivalent cores for carbon and non-equivalent cores for fluorine.

Final	state	Symmetry	Rel. Energy (eV)	Rel. Int.(%) Carbon (EC)	Fluorine (NEC)
$2t_2$	$4a_1$	$^1T_2$	-77.7	34.3	40.0
$3a_1$	$3t_2$	$^1T_2$	-77.9	63.6	30.2
$3a_1$	$4a_1$	$^3A_1$	-79.3	0.0	2.1
$3a_1$	$4a_1$	$^1A_1$	-80.5	69.2	11.9
$2t_2$	$2t_2$	^1E	-88.9	24.5	1.4
$3a_1$	$2t_2$	$^3T_2$	-92.6	15.8	0.0
$2t_2$	$2t_2$	$^1T_2$	-95.1	36.8	66.9
$2t_2$	$2t_2$	$^1A_1$	-98.4	4.7	32.1
$3a_1$	$2t_2$	$^1T_2$	-98.5	46.8	55.8
$3a_1$	$3a_1$	$^1A_1$	-99.3	47.2	7.8
	Transition	rate	(mau)	2.33	6.89

In parentheses - absolute energy values (in eV) of the most intense transitions.

Our calculated spectrum of C(KVV) in CF_4 does not reflect the experimental intensities. There is not enough intensity appearing in the outer-outer region of the spectrum. Since fragmentation was suggested (manifested by presence of sharp lines in the experimental spectrum) some INDO calculation for the fragmented CF_4 molecule were performed (Chelkowska, unpublished) However, the results have not given a theoretical profile of C(KVV) which would satisfactorily match the experimental spectrum of carbon. When Gamess (Schmidt *et al.* 1991) package with a STO-3G basis was used to obtain wavefunctions, the calculated carbon spectrum represented better approximation of the experimental C(KVV) Auger profile. However, there were some problems with orthonormality of the wavefunctions .

An investigation (using some ab initio packages - GAUSSIAN 90, Gamess (Schmidt *et al.* 1991) of the carbon spectrum intensity problem suggests that the INDO representation of molecular orbitals may not adequately describe the bonding processes which are taking place in the CF_4 molecule. The parametrization works satisfactorily for many molecules containing carbon. Nevertheless, for the CF_4 molecule a more sophisticated molecular orbital basis is required.

In the case of a core-hole in an atom located in high symmetry position (as carbon in CF_4) one may assume that there is more pronounced departure from spherical symmetry for high symmetry core-holes because centroids (hybride charge location) are distorted away from nuclei and the density cannot be interpreted as a part of the atomic charge any more.

9.4.2.2. Silicon Tetrafluoride

Results of energy and intensity calculations for the KVV and $L_{23}VV$ spectra of silicon tetrafluoride are given in Table 9.4. The present theory predicts 107 final hole states for F(KVV) and 214 for Si($L_{23}VV$) since spin-orbit splitting effect is noticeable for silicon. Because of the high symmetry of the SiF_4 molecule only 44 double hole states lead to non-zero intensity transitions in the Si($L_{23}VV$) spectrum. However, the detailed interpretation of the spectra is not achievable and, in general, several transitions are attributed to a group of peaks. The total width of the calculated spectra is 54.7 eV.

In Figures 9.3b and 9.4b experimental spectra of SiF_4 along with the theoretical results for silicon and fluorine, respectively, are shown. Bars represent calculated single transitions. In Fig. 9.5 calculated profiles generated using gaussian FWHM=0.5 eV are presented.

TABLE 9.4

Transition energies and intensities of Auger spectra of silicon tetrafluoride calculated using present approach with equivalent cores for silicon and non-equivalent cores for fluorine.

Final	state	Symmetry	Rel. Energy (eV)	Rel. Int.(%) Silicon (EC)	Rel. Int.(%) Fluorine (NEC)	Assignment (Fig 9.3.b)
$1t_1$	$1t_1$	$^1T_2$	-43.1	0.0	50.9	
$5t_2$	$5t_2$	$^3T_1$	-44.1	35.6	0.0	Band F
$4t_2$	$5t_2$	$^3T_1$	-45.4	100.0 (66.3 eV)	0.0	
$1t_1$	$5t_2$	$^1T_1$	-45.5	0.0	97.6	
$5t_2$	$5t_2$	^1E	-45.7	12.0	45.8	
1e	$1t_1$	$^1T_1$	-45.9	0.0	25.4	
$1t_1$	$5t_2$	^1E	-46.0	0.0	43.7	
$5t_2$	$5t_2$	$^1T_2$	-46.1	18.0	73.1	
$1t_1$	$1t_1$	^1E	-46.1	0.0	74.2	
$5a_1$	$5t_2$	$^3T_2$	-46.6	63.0	0.0	
1e	$5t_2$	$^1T_2$	-46.6	0.0	71.8	
$1t_1$	$5t_2$	$^1T_2$	-46.7	0.0	72.6	
$4t_2$	$5t_2$	^3E	-47.0	2.8	0.0	
1e	1e	^1E	-47.0	0.0	50.9	
1e	1e	$^1A_1$	-47.5	0.0	14.9	
$4t_2$	$1t_1$	$^1T_2$	-47.6	0.0	97.3	
$4t_2$	$5t_2$	^1E	-47.7	3.0	38.7	
1e	$1t_1$	$^1T_2$	-47.8	0.0	81.3	
$1t_1$	$5t_2$	$^1A_1$	-48.0	0.0	59.2	
1e	$5t_2$	$^1T_1$	-48.1	0.0	32.1	
$4t_2$	$5t_2$	$^1T_2$	-48.4	4.8	57.2	
$4t_2$	$1t_1$	$^1T_1$	-48.5	0.0	42.6	
$5t_2$	$5t_2$	$^1A_1$	-48.7	8.1	20.4	
$4t_2$	$4t_2$	$^3T_1$	-48.9	70.2	0.0	Band F

TABLE 9.4 Continuation

Transition energies and intensities of Auger spectra of silicon tetrafluoride calculated using present approach with equivalent cores for silicon and non-equivalent cores for fluorine.

Final	state	Symmetry	Rel. Energy (eV)	Rel. Int.(%) Silicon (EC)	Fluorine (NEC)	Assignment (Fig 9.3.b)
$4t_2$	$4t_2$	^1E	-49.4	23.7	38.3	Band F
$4t_2$	$4t_2$	$^1T_2$	-49.4	35.5	57.5	
$4t_2$	1e	$^1T_2$	-49.4	0.0	61.8	
$4t_2$	$5t_2$	$^1T_1$	-49.6	45.7	95.4	
$4t_2$	$1t_1$	$^1A_1$	-49.6	0.0	22.6	
$4t_2$	$5a_1$	$^3T_2$	-49.8	88.4	0.0	
$5a_1$	$1t_1$	$^1T_2$	-49.8	0.0	75.1	
$4t_2$	$1t_1$	^1E	-49.8	0.0	77.0	
$1t_1$	$1t_1$	$^1A_1$	-50.0	0.0	26.6	
$5a_1$	1e	^1E	-50.0	0.0	40.0	
$4t_2$	$4t_2$	$^1A_1$	-50.1	15.9	6.8	
$4t_2$	$5t_2$	$^1A_1$	-51.3	53.1	39.6	
$4t_2$	1e	$^1T_1$	-51.4	0.0	36.4	
$5a_1$	$5t_2$	$^1T_2$	-52.2	61.1	80.0	
$4t_2$	$5a_1$	$^1T_2$	-52.6	85.8	60.2	
$5a_1$	$5a_1$	$^1A_1$	-53.5	22.7	12.2	Band F
$3t_2$	$1t_1$	$^3T_1$	-63.0	0.0	8.6	
$3t_2$	$1t_1$	$^1T_1$	-63.9	0.0	28.3	
$3t_2$	$5t_2$	$^3T_1$	-64.5	51.6	6.5	Band D
$3t_2$	$1t_1$	$^3T_2$	-64.9	0.0	8.6	
$3t_2$	$5t_2$	$^1T_1$	-65.7	23.6	21.4	
$3t_2$	$5t_2$	^3E	-66.2	1.4	8.4	
$4a_1$	$1t_1$	$^3T_2$	-66.4	0.0	12.4	
$3t_2$	$1t_1$	^3E	-66.5	0.0	14.4	
$3t_2$	$5t_2$	$^3T_2$	-66.8	0.0	14.6	
$3t_2$	1e	$^3T_1$	-66.8	0.0	4.3	
$3t_2$	1e	$^3T_2$	-66.8	0.0	12.9	
$3t_2$	$1t_1$	$^1T_2$	-67.0	0.0	28.6	
$4a_1$	$5t_2$	$^3T_2$	-67.5	24.9	12.1	
$3t_2$	$4t_2$	$^3A_1$	-67.6	0.0	3.1	
$3t_2$	$4t_2$	3E	-68.1	2.0	7.5	
$3t_2$	$4t_2$	$^3T_2$	-68.1	0.0	11.0	
$4a_1$	1e	3E	-68.1	0.0	8.3	
$3t_2$	$4t_2$	$^3T_1$	-68.3	72.4	11.7	
$3t_2$	$5t_2$	^1E	-68.4	1.6	27.7	
$4a_1$	$1t_1$	$^1T_2$	-68.6	0.0	41.1	
$3t_2$	1e	$^1T_2$	-69.1	0.0	42.4	
$3t_2$	1e	$^1T_1$	-69.1	0.0	15.0	
$3t_2$	$5t_2$	$^1T_2$	-69.3	2.5	48.2	
$4a_1$	$4t_2$	$^3T_2$	-69.4	35.0	10.8	
$3t_2$	$1t_1$	$^3A_1$	-69.4	0.0	7.2	
$4a_1$	$5t_2$	$^1T_2$	-69.6	24.2	40.1	Band D
$3t_2$	$5t_2$	$^3A_1$	-69.6	0.0	8.3	

TABLE 9.4 Continuation

Transition energies and intensities of Auger spectra of silicon tetrafluoride calculated using present approach with equivalent cores for silicon and non-equivalent cores for fluorine.

Final	state	Symmetry	Rel. Energy (eV)	Rel. Int.(%) Silicon (EC)	Fluorine (NEC)	Assignment (Fig 9.3.b)
$3t_2$	$4t_2$	$^1A_1$	-69.7	38.4	13.3	Band D
$3t_2$	$1t_1$	^1E	-69.7	0.0	47.2	
$3t_2$	$5a_1$	$^3T_2$	-70.0	45.6	10.0	
$3t_2$	$4t_2$	^1E	-70.1	2.2	25.5	
$3t_2$	$4t_2$	$^1T_2$	-70.1	3.5	38.1	
$4a_1$	1e	^1E	-70.3	0.0	27.3	
$3t_2$	$4t_2$	$^1T_1$	-70.5	33.1	39.8	
$4a_1$	$4t_2$	$^1T_2$	-71.4	33.9	37.6	
$4a_1$	$5a_1$	$^3A_1$	-71.4	0.0	3.3	
$3t_2$	$5a_1$	$^1T_2$	-72.1	44.3	37.8	
$4a_1$	$5a_1$	$^1A_1$	-73.1	18.0	12.2	
$3t_2$	$5t_2$	$^1A_1$	-73.9	27.4	27.1	Band D
$3t_2$	$1t_1$	$^1A_1$	-74.4	0.0	23.5	
$3t_2$	$3t_2$	$^3T_1$	-84.7	18.7	0.0	Band B, A
$4a_1$	$3t_2$	$^3T_2$	-86.1	18.0	0.0	
$3t_2$	$3t_2$	^1E	-89.1	6.3	34.8	
$3t_2$	$3t_2$	$^1T_2$	-90.5	9.4	69.5	
$4a_1$	$4a_1$	$^1A_1$	-91.6	3.6	16.0	
$4a_1$	$3t_2$	$^1T_2$	-94.5	17.5	100.0 (600.6 eV)	
$3t_2$	$3t_2$	$^1A_1$	-97.8	4.2	51.8	Band B, A
	Transition	rate	(mau)	**0.52**	**7.41**	

In parentheses - absolute energy values (in eV) of the most intense transitions.

There is a sharp contrast between the three- or four-peak structure which is calculated and the six-peak structure which is experimentally observed (Fig.9.3b). It has been shown (Larkins *et al.*1993b) that discrepancy cannot be attributed to localization effects in the silicon - fluorine bonds (as suggested by Rye and Houston 1983) or in fluorine pairs (as suggested by Lapiano-Smith *et al.* 1989) for the following reasons:

i) The present method incorporates hole-hole interaction energies for both, localized and delocalized cases and it has been used satisfactorily for to interpret LVV spectra of other molecules (Chelkowska and Larkins 1991b, Larkins *et al.* 1993). It has also been shown that hole-hole interaction values are within each broad band.

ii)The bond localization double-hole mechanism would be expected to be intrinsic to the molecule and therefore rather independent of photon excitation energy. However, analysis of results results obtained by Aksela *et al.* (1986) and Ferrett *et al.* (1988) do not support the above mechanism (see Larkins *et al.* 1993).

iii) If rearrangement of electrons is allowed as a consequence of the presence of the core hole the Auger decay is dominated by intra-atomic processes (McColl and Larkins 1992) then localization-delocalization of valence double holes on fluorine atoms (Lapiano-Smith *et al.* 1989) is not a significant factor influencing the $L_{23}VV$ Auger transition from silicon.

Another possible explanation would be distortion or pre-dissociation of the molecule prior to the Auger decay. Hence, the multipeak structure would result from daughter as well as the parent molecular species. However, work on other molecules with hydrogen atoms (Aksela *et al.* 1990) indicate that such effects are more probable for resonantly excited species. On this basis the ratio of bands C:D would be expected to be larger in the resonant Auger spectrum than in the normal Auger spectrum. Nevertheless, this is not the case for the Si $L_{23}VV$ spectrum of the SiF_4 molecule and molecular distortion or pre-dissociation is not considered to be the primary source of the multiple peak structure.

The most probable explanation is that the additional peaks are due to initial- and final-state correlation satellite contributions.In the photoabsorption spectrum near silicon 2p edge (Friedrich *et al.* 1980) there are strong absorptions to the $6a_1$ and $6t_2$ antibonding orbitals. Our semi-empirical calculations are consistent with the $6a_1$ orbital being predominantly of silicon 3s and the $6t_2$ orbitals are mainly silicon 3p character. The silicon atom in SiF_4 is electron defficient and therefore has the capacity to localize more electron density in its vicinity. Since the lowest unoccupied orbitals $6a_1$ and $6t_2$ are located on the silicon atom they are very suitable candidates to be occupied by shake-up type mechanisms associated with the ionization or filling of the silicon core hole.

The total shake probability for the SiF_4 molecule during Si 2p photoionization is about 10% (Larkins *et al. 1993b*). This indicates that a mechanism involving a shake process associated with the creation of the initial states during photoionization is plausible. Similar shake mechanism is likely when final states are created during the Auger process. In the Auger spectrum the observed effects are the manifestation of correlation phenomena involving valence electrons. In Table 9.5 the calculated relative intensities are compared with the experimental values obtained above the 2p ionization threshold by Aksela *et al.* (1986) and by Ferrett *et al.* (1988). There is about a 15% difference between the two sets of experimental values. The only direct comparison with theory is for the relative intensity of band D. Here the agreement is satisfactory. In the region of bands A and B there are other contributions to the experimental spectra. Detailed analysis (Larkins *et al. 1993b*) leads to the conclusion that the second set of peaks (A, C, E1,2) in the Si(LVV) spectrum of SiF_4 in Fig. 9.3 b has to be assigned to shake-up and shake-off satellites.

TABLE 9.5

Relative intensities of the bands in the silicon $L_{23}VV$ Auger spectrum of the SiF4 molecule

	Theory	Experi ment	
Peak label	P	A	F
A	5.6	17.8	16.8
B	5.4	26.8	20.6
C		23.1	21.5
D	65.3	76.9	64.0
E1		63.4	23.9
E2			48.1
F	100.0	100.0	100.0

P - present work, A - Aksela et al. (1986) with hv=130 eV, F - Ferrett et al. (1988) with hv=117.2 eV.

9.5. Comparison Between Molecules

The Auger spectra of the tetrahedral fluorides are far more complex than their hydride counterparts because of the larger number of electrons available (compare a and b in Fig.9.2 and 9.3). A very considerable change in the total width of the silicon spectra is noted for SiF_4 when compared with SiH_4, which just reflects the changes in the electronegativity (of F versus H) and the number of valence electron available. This effect is far less pronounced in the carbon spectra of CH_4 and CF_4. The total transition rates for central atoms diminish dramatically (over 50% for silicon) in presence of fluorine atoms (when hydrides and fluorides are compared). Fluorine transtion rates are almost identical (for the SiF_4 molecule) or lower (for the CF_4 molecule) than calculated for the HF molecule using NEC approach (Table 4.2 and 9.2).

A comparison of the fluorine spectra of CF_4 and SiF_4 (Fig.9.4a and b) supports a view of a considerable perturbation of the outer region F orbitals taking place in CF_4. The fluorine spectrum of SiF_4 is atom-like with some features which can be assigned to the shake-up and shake-off satellites. (The background of the F(KVV) spectrum in SiF_4 is probably very large and any unambiguous assignment is difficult to achieve.)

Figure 9.6 depicts calculated total rates for C(KVV) in all investigated molecules as a function of valence population q expressed in *e*. The linear relationship of the valence electron populations q and the calculated carbon Auger transition rates I(q) (Fig.9.6) is simply an approximation of a parabolic expression I(q) = a + b* q * (q-1) over small changes (less than 1e) in the valence population.

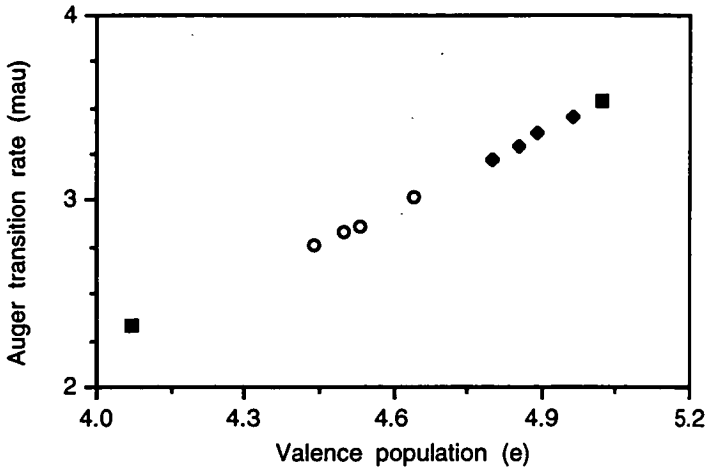

FIG. 9.6 Carbon Auger transition rates as a function of valence electron populations on carbon atoms in investigated molecules (■) CF_4 and CH_4, (◆) CH_3X, (○) XCHO.

Similar dependence of calculated rates was obtained by McColl and Larkins (1992) for silicon containing molecules.

9.6. Conclusions

We have investigated tetrahedral hydrides and fluorides containing first and second row central atoms. There are some discrepancies between the calculated and the experimental spectra. For the carbon spectrum in CF_4 this can be attributed to a non-adequate description of molecular orbitals when the INDO approximation is used with the high symmetry molecule.

The "additional" set of peaks in the Si (LVV) spectrum of SiF_4 is assigned to shake-up and shake-off satellites.

The fluorine spectra of CF_4 and SiF_4 are approximated reasonably well. However, calculations using an equivalent cores approach are needed to check if any improvement in the positions of peaks can be achieved.

Chapter 10

CONCLUSIONS

10.1. General Information

The semi-empirical model examined in this thesis based upon INDO-type wave functions provides a very good first estimate for absolute and relative transition rates in molecular Auger processes. It can be used as a first approximation to calculate larger polyatomic systems containing first and second row atoms. The method is very fast and can be applied in situations when the size of a molecule precludes any *ab initio* type calculations. It does incorporate relativistic effects implicitly, by using relativistic values for atomic Auger matrix elements. It also includes some correlation corrections through the use of the experimental ionization energies. The calculated width of the spectrum agrees well with the experimental ones. However, when electron correlation effects are very strong in a molecule (and the one-particle approximation breaks down) our model is unsuitable for energy prediction. It also fails for calculations of transitions localized on high symmetry cores such as carbon in CF_4. In this approximation satellite lines cannot be calculated, nevertheless the method may be extended to incorporate satellite lines. The absolute energy prediction is less accurate since an adiabatic relaxation correction term is difficult to assess in molecules. Because of the simplicity of the method there is no consideration of vibrational effects in molecular Auger spectra.

10.2. Conclusions and Future Directions

In particular our findings can be summarised as:

a) For the first row hydrides our method is able to compete with *ab initio* methods in cases where many electron effects are not too strong . The equivalent cores approach compensates some relaxation and correlation effects. The presence of dynamic and static correlation effects and satellite lines makes the interpretation of Auger spectra of some molecules very difficult.

If inner valence orbitals exhibit a breakdown of molecular orbital description, this cannot be corrected with the present method.

Establishing the effect of lone-pairs on the molecular Auger spectra presents difficulties since some other effects are usually influencing molecules containing atoms with lone-pairs.

Shifts of theoretical molecular spectra are required to achieve an alignment with experiments.

b) In the L_{23}-VV Auger spectra for the second-row hydrides about 47% of intensity is gained via triplet states compared with typically less than 7% for K-VV Auger spectra. The majority of intensity (about 2/3) of the L_{23}-VV Auger spectra of the second-row hydrides is gained via the p continuum channel.

c) The shift required to align calculated and experimental spectra of X atoms (where X=F, O, N and C) in the isoelectronic CH_3XHn molecules should be smaller than that which is required for the first row hydrides. The basic structure of the KVV Auger spectrum in the CH_3- environment stays similar to that of methane. More structures can be distinguished when moving from ethane to methyl fluoride.

d) The total transition rates are very similar for the carbon spectra of the whole CH_3XHn family of molecules.

However, the total transition rate for carbonyl carbon is about 16% smaller than for methyl carbon and also decreases when proceeding from CH_3CHO to FCHO.

The effect of total intensity change in carbon is far more pronounced in the carbon spectra of CH_4 and CF_4. There is dramatical decrease in rate in presence of fluorine atoms.

The above finding also applies to the T_d symmetry compounds containing second row atoms, i.e. SiH_4 and SiF_4.

In the case of oxygen the absolute transition rate increases when proceeding from NH_2CHO to FCHO. The rate for oxygen in CH_3CHO is between the values calculated for OHCHO and for FCHO. This result could possibly be explained by hyperconjugation effects.

The intensities from the X group are almost identical for the first row hydrides, CH_3X and XCHO compound.

e) The total theoretical rates of KVV Auger transition can be estimated within 10% using a function of valence electron populations.

f) The presence of two different chemical sites for carbon in the CH_3CHO molecule seems to be more significant than for oxygen in OHCHO. Nevertheless, the overall effect is not substantial.

g) The agreement between the theoretical and experimental spectra of OCS is satisfactory and the method seems to be promising for semiquantitative interpretation of an outer-outer region of complex Auger spectra of polyatomic molecules.

h) There are some discrepancies between the calculated and the experimental Auger spectra of tetrahedral hydrides and fluorides containing first and second row central atoms. For the carbon spectrum in CF_4 this can be attributed to in-adequate description of molecular orbitals when the INDO approximation is used with the high symmetry molecule. However in the Si (LVV) spectrum of SiF_4 the inconsistencies are accredited to the presence of satellite lines. The "additional" set of peaks in the spectrum can be assigned to initial and final state satellite lines. The fluorine spectra of CF_4 and SiF_4 are approximated reasonably well. Nevertheless, calculations using an equivalent core approach are needed to check if any improvement in the positions of peaks can be achieved.

i) An equivalent core technique gives better approximation of the total transition rates. However, for the $Z>8$ and $Z>16$ for the first and the second row elements, respectively, the equivalent cores approach may introduce too large polarisation effects and lead to overestimation of absolute intensity rates. This effect may originate from the values of parameters used for Ne and Ar. The parameters are extrapolated from the ones which have been calculated for other elements with $Z<10$ and $Z<18$ for Ne and Ar, respectively.

Our method compares favourably with other methods used for calculation of Auger spectra of molecules because it offers absolute transition rates as well as reasonably good assignment of spectra in a very short time (as a first approximation) and may be successful in some cases (even if it is the one-centre approximation with all drawbacks) simply because some empirical parameters are used which may cause compensation of dynamic and static correlation, relaxation or polarisation effects Justification of any method is very often done on a basis of *ab initio* calculation methods and effects influencing the Auger process. However, the usefulness of the approach is mainly for the interpretation of spectra for larger

systems where *ab initio* calculations are not readily accomplished. Further experimental measurements obtained using photoelectron-Auger electron coincidence studies are needed to remove uncertainties associated with the extent of satellite contributions present in many spectral profiles so far recorded.

Also moving towards usage of *ab initio* generated wavefunctions rather than their semi-empirical approximation in calculations of Auger molecular spectra would be desirable.

References

Åberg T and Howat G 1982 *Handbuch der Physik* Vol **31** (Berlin: Springer Verlag)

Ågren H 1991 *J. Quantum Chem.* **39** 455

Ågren H and Siegbahn H 1980 *Chem. Phys. Lett.* **69** 424

Ågren H, Cesar A and Carravetta 1987 *Chem. Phys. Lett.* **139** 145

Ågren H, Cesar A and Liegener C-M 1992 *Adv. Quantum Chem.* **23** 1

Ågren H, Svensson S and Wahlgren U I 1975 *Chem. Phys. Lett.* **35** 336

Aksela H, Aksela S, Ala-Korpela M, Sairanen O-P , Hotokka M , Bancroft G M , Tan K H and Tulkki J 1990 *Phys. Rev.* A **41** 6000

Aksela H, Aksela S, Hottoka M and Jaentti M 1983 *Phys. Rev.* A **28** 287

Aksela H, Aksela S, Naves de Brito A, Bancroft G M and Tan K H 1992 *Phys. Rev.* A **45** 7948

Aksela H, Aksela S, Sairanen O-P , Kivimäki A, Bancroft G M and Tan K H 1992x *Phys.Scr.* **T41** 122

Aksela S, *private communication*

Aksela S, Sairanen O P, Aksela H, Bancroft G M, Tan K H 1988 *Phys. Rev. A: Gen. Phys.* **37** 2934

Aksela S, Tan K H and Bancroft G M 1986 *Phys. Rev.* A **33** 258

Aksela H 1988 *NATO ASI Series B* **187** 15

Appel J and Horsley J A 1974 *J. Chem. Phys.* **60** 3445

Ariyasinghe W M, Powers D and Awuku (*Nucl.Instr. and Meth. in Phys.* 1991, in press)

Ariyasinghe W M, McElroy R D and Powers D 1987 *Nucl.Instr.Methods in Phys.Research* **B24/25** 162

Asplund L, Kelfve P, Blomster B, Siegbahn H and Siegbahn K 1977 *Phys.Scr.* **16** 268

Asplund L, Kelfve P, Siegbahn H, Goscinski O, Fellner-Feldegg H, Hamrin K, Blomster B and Siegbahn K 1976 *Chem. Phys. Lett.* **40** 453

Auger P 1923 *Compt. Rend. (Paris)* **177** 169

Auger P 1925 *Compt. Rend. (Paris)* **180** 65

Auger P 1926 *Ann. Phys. (Paris)* **6** 183

Bancroft G M, Aksela S, Aksela H, Tan K H, Yates B W, Coatsworth L L and Tse J S 1986 *J. Chem. Phys.* **84** 5

Bancroft G M, Tan K H, Sairanen O P, Aksela S and Aksela H 1990 *Phys. Rev.* A **41** 3716

Banna M S and Shirley D A 1975 *J. Chem. Phys.* **63** 4759

Barber M, Clark J D and Hincliffe 1977 *Chem. Phys. Lett.* **48** 593

Bergström I , in *Beta- and Gamma-Ray Spectroscopy* 1955 Siegbahn K *Ed.* (Amsterdam: North-Holland)

Briant C L and Messmer R P *Ed.* 1998 *Auger Electron Spectroscopy. Treatise on Materials Science and Technology* Vol 30 (Boston:Academic Press)

Briggs D and Seah M P *Ed.*1983 *Practical Surface Analysis by Auger and X-ray Photoelectron Spectroscopy* (Chichester: John Wiley and Sons)

Burhop E H S 1952 *The Auger Effect and Other Radiationless Transitions* (Cambridge: Cambridge University Press)

Camilloni R, Stefani G and Giardini-Guidoni A 1977 *Chem. Phys. Lett.* **50** 213

Carravetta V and Ågren H 1987 *Phys. Rev.* A **35** 1022

Carlson T A, Gerard P, Krause M O, Von Wald G, Taylor J W, Grimm F A and Pullen B P 1988 *J. Electron Spectrosc. Relat. Phenom.* **47** 227

Carlson T A 1975 *Photoelectron and Auger Spectroscopy* (New York: Plenum Press)

Carravetta V, Ågren H and Cesar A 1988 *Chem. Phys. Lett.* **148** 210

Carroll T X and Thomas T D 1990 *J. Chem. Phys.* **92** 7171

Carroll T X and Thomas T D 1991 *J. Chem. Phys.* **94** 11

Carroll T X and Thomas T D 1992 *J. Chem. Phys.* **97** 894

Carroll T X, De Ji and Thomas D T 1990 *J. Electron Spectrosc. Relat. Phenom.* **51** 471

Cesar A , Ågren H, Naves de Brito, Svensson S, Karlsson L, Keane M P, Wannberg B, Baltzer P, Fournier P G and Fournier J 1990 *J. Chem. Phys.* **93** 918

Cesar A, Ågren H and Carravetta V 1989 *Phys. Rev.* A **40** 187

Chattarji D 1976 *The theory of Auger Transitions* 1976 (London: Academic Press)

Chelkowska E Z and Larkins F P 1990, *unpublished*

Chelkowska E Z and Larkins F P 1991a *At.Data and Nuclear Data Tables* **49** 121

Chelkowska E Z and Larkins F P 1991b *J. Phys.B; At. Mol. Phys.* **24** 5083

Chen M H, Larkins F P and Crasemann B 1990 *At.Data and Nuclear Data Tables* **45** 1

Chong D P 1981 *Chem. Phys. Lett.* **82** 511

Cini M, Maracci F and Platania R 1986 *J. Electron Spectrosc. Relat. Phenom.* **41** 37

Cini M, Maracci F and Platania R 1987 *J. Phys. Coloq.* **C9** C9-781

Colle R and Simonucci S 1989 *Phys. Rev.* A **39** 6247

Connor J A, Hillier I H, Kendrick J, Barber M and Barrie A 1976 *J. Chem. Phys.* **64** 3325

Correia N, Flores-Reveros A, Ågren H, Helenelund K, Asplund L and Gelius U 1985 *J. Chem. Phys.* **83** 2035

Correira N, Naves de Brito A, Keane M P, Karlsson L,Svensson S, Liegener C-M, Cesar A and Ågren H 1991 *J. Chem. Phys.* **95** 5187

Coulman D, Puschmann A, Wurth W, Steinrueck H P and Menzel D 1988 *Chem. Phys. Lett.* **148** 371

Coville M and Thomas T D 1991 *Phys. Rev.* A **43** 6053

de Souza G G B, Morin P and Nenner I 1985 *J. Chem. Phys.* **83** 492

de Souza G G B, Morin P and Nenner I 1986 *Phys. Rev.* A **34** 4770

de Souza G G B, Morin P and Nenner I 1989 *J. Chem. Phys.* **90** 7071

Eade R H A and Robb M A 1977 *Chem. Phys. Lett.* **52** 526

Eberhardt W 1987 *Phys.Scr.* **T17** 28

Eberhardt W, Dudde R, Rocco M L M, Koch E E, Bernstorff S 1990 *J. Electron Spectrosc. Relat. Phenom.* **51** 373

Eberhardt W, Plummer E W, Lyo I W, Carr R and Ford W K 1987 *Phys. Rev. Lett.* **58** 207

Eberhardt W, Plummer E W, Lyo I W, Reininger R, Carr R, Ford W K and Sondericker D 1986 *Aust. J. Phys.* **39** 633

Eland J H D 1987 *Mol. Phys.* **61** 725

Faegri K 1977 *Chem. Phys. Lett.* **46** 541

Faegri K and Kelly H P 1979 *Phys. Rev.* A **19** 1649

Faegri K and Manne R 1976 *Mol. Phys.* **31** 1037

Ferrett T A, Lindle D W, Heimann P A, Piancastelli M N, Kobrin P H, Kerkhoff H G, Becker U, Brewer W D and Shirley D A 1988x *J. Chem. Phys.* **89** 4726

Ferrett T A, Piancastelli M N, Lindle D W, Heimann P A and Shirley D A 1988 *Phys. Rev. A: Gen. Phys.* **38** 701

Fournier P G, Mousselmal M, Peyerimhoff S D, Banichevich A, Adam M Y and Morgan T J 1987*Phys. Rev.* A **36** 2594

Fournier P G, Comtet G, Fournier J , Svensson S, Karlsson L, Keane M P and Naves de Brito A 1989 *Phys. Rev.* A **40** 163

Frasinski L J, Stankiewicz M, Randall K J, Hatherly P A and Codling K 1986 *J. Phys. B: At. Mol. Phys.* **19** L819

Fujimori A, Saeki M, Kimizuka N, Taniguchi M and Suga S 1986 *Phys. Rev. B: Condens. Matter* **34** 7318

GAMESS vesion 91 described by Schmidt M W, Baldridge K K, Boatz J A, Jensen J H, Koseki S, Gordon M S, Nguyen K A, Windus T L and Elbert S T in *QCPE Bulletin* 1990 **10** 52

GAUSSIAN 90 Revision F, Frisch M J, Head-Gordon M, Trucks G W, Foresman J B, Schlegel H B, Raghavachari K, Robb M, Binkley J S, Gonzalez C, Defrees D J, Fox D J, Whiteside R A, Seeger R, Melius C F, Baker J, Martin R L, Kahn L R, Stewart J J P, Topiol S and Pople J A, 1990 Gaussian, Inc., Pittsburgh PA, 1990

Gordon M S , Bjorke M D , Marsh F J and Korth M S 1978 *J.Am.Chem.Soc.* **100** 2670

Gordy W and Cook R L 1984 *Microwave molecular spectra* Vol.18 Techniques in Chemistry (New York: John Wiley and Sons)

Gutsev G L 1986 *Mol. Phys.* **57** 161

Habenicht W, Mueller-Dethlefs K and Schlag E W 1990 *J. Electron Spectrosc. Relat. Phenom.* **52** 697

Hanson D M, Ma C I, Lee K, Lapiano-Smith D and Kim D Y 1990 *J. Chem. Phys.* **93** 9200

Hatherly P A, Stankiewicz M, Frasinski L J, Codling K and Macdonald M A 1989 *Chem. Phys. Lett.* **159** 355

Hawkins D T 1977 *Auger Electron Spectroscopy. A Bibliography: 1925-1975* (New York: Plenum)

Hayes R G and Eberhardt W 1990 *Phys. Scr.* **41** 449

Hayes R G and Eberhardt W 1991 *J. Chem. Phys.* **94** 397

Hehre W J, Stewart R F and Pople J A 1969 *J. Chem. Phys.* **51** 2657

Higashi M, Hiroike E and Nakajima T 1982 *Chem. Phys.* **68** 377

Hillier I H and Kendrick J 1976 *Mol. Phys.* **31** 849

Hitchcock A P, Lablanquie P, Morin P, Lizon a Lugrin E, Simon M, Thiry P and Nenner I 1988 *Phys. Rev.* A **37** 2448

Hubin-Franskin M J and Delwiche J 1990 *Phys. Mag.* **12** 39

Hutson F L and Ramaker D E 1987 *J. Chem. Phys.* **87** 6824

Hutson F L and Ramaker D E 1987x *Phys. Rev. B: Condens. Matter* **35** 9799

Jennison D 1980 *Chem. Phys. Lett.* **69** 435

Jennison D 1981 *Phys. Rev.* A **23** 1215

Kaspar F, Domce W and Cederbaum L S 1979 *Chem. Phys.* **44** 33

Körber H and Mehlhorn W 1966 *Z.Phys.* **191** 217

Kvalheim O M 1982 *Chem. Phys. Lett.* **86** 159

Kvalheim O M 1983 *Chem. Phys. Lett.* **98** 457

Kvalheim O M and Faegri K 1979 *Chem. Phys. Lett.* **67** 127

Lablanquie P, Souza A C A, de Souza G G B, Morin P and Nenner I 1989 *J. Chem. Phys.* **90** 7078

Landolt-Börnstein 1976 Numerical data and functional relationships in science and technology, Group II: Atomic and molecular physics, Volume **7**: *Structure data of free polyatomic molecules* (Berlin: Springer Verlag)

Lapiano-Smith D A, Ma C I, Wu K T and Hanson D M 1989 *J. Chem. Phys.* **90** 2162

Lapiano-Smith D, Lee K, Ma C I, Wu K T and Hanson D M 1990 *J. Chem. Phys.* **93** 2169

Larkins F P 1971 *J. Phys.B; At. Mol. Phys.* **4** L29

Larkins F P 1976 *J. Phys.B; At. Mol. Phys.* **9** 47

Larkins F P 1977 *At.Data and Nuclear Data Tables* **20** 313

Larkins F P 1987 *J. Chem. Phys.* **86** 3239

Larkins F P 1990 *J. Electron Spectrosc. Relat. Phenom.* **51** 115

Larkins F P and Richards J A 1986 *Aus. J. Phys.* **39** 809

Larkins F P and Tulea L C 1987 *J. Phys.Colloq.* **C9** 725

Larkins F P, Chelkowska E Z, Sato Y, Ueda K, Shigemasa E and Yagishita A 1993a *J. Phys.B; At. Mol. Phys.* **26** 1479

Larkins F P, Eberhardt W, Whan Lyo In, Murphy R and Plummer E W 1988 *J. Chem. Phys.* **88** 2948

Larkins F P, McColl J and Chelkowska E Z 1993b *J. Electron Spectrosc. Relat. Phenom.* (in press)

Larkins F P, Tulea L C and Chelkowska E Z 1990 *Aus. J. Phys.* **43** 625

Liegener C-M 1982 *Chem. Phys. Lett.* **90** 188

Liegener C-M 1988 *Chem. Phys. Lett.* **151** 83

Liegener C-M, Abdel-Raouf M A and Ladik J 1991 *J. Mol. Struct.* **247** 253

Lindle D W, Truesdale C M, Kobrin P H, Ferrett T A, Heimann P A, Becker U, Kerkhoff H G and Shirley D A 1984 *J. Chem. Phys.* **81** 5375

Manne R and Ågren H 1985 *Chem. Phys.* **93** 201

Maracci F, Platania R and Salomone R 1980 *J. Electron Spectrosc. Relat. Phenom.* **19** 155

Maracci F, Platania R, de Azevedo e Souza A C and de Souza G G B 1989 *Chem. Phys.* **133** 291

Matthew J A D and Komninos Y 1975 *Surf. Sci.* **53** 716

McColl J and Larkins F P 1992 *Chem. Phys. Lett.* **196** 343

McGuire E J 1969 *Phys. Rev.* **185** 1

McGuire E J 1971 *Phys. Rev.* A **3** 1801

McGuire E J 1975 *Phys. Rev.* A **11** 1880

Mehlhorn W Z 1990 in *Inner-Shell Proc. (X-90 Conf)* July 9-13 1990 Knoxville (USA)

Mehlhorn W Z 1960 *Z.Phys.* **160** 247

Mehlhorn W Z 1978 lecture notes

Millie P, Nenner I, Archirel P, Lablanquie P, Fournier J and Eland J H D 1986 *J. Chem. Phys.* **84** 1259

Moddeman W E *PhD Thesis* 1970 University of Tennessee, USA

Moddeman W E, Carlson T A, Krause M O, Pullen B P, Bull W E and Schweitzer G K 1971 *J. Chem. Phys.* **55** 2317

Morin P, de Souza G G B, Nenner I and Lablanquie P 1986 *Phys. Rev. Lett.* **56** 131

Motte-Tollet F, Hubin-Franskin M J, Delwiche J and Morin P 1992 *AIP Conf. Proc.* **258** 348

Murphy R and Eberhardt W 1988 *J. Chem. Phys.* **89** 4054

Nagy A 1988 *J. Mol. Struct. (Theochem)* **165** 205

Novak I, Benson J M and Potts A W 1986 *Chem. Phys.* **104** 153

Ohrendorf E M-L, Tarantelli F and Cederbaum L S 1990 *J. Chem. Phys.***92** 2984

Økland M T, Faegri K and Manne R 1976 *Chem. Phys. Lett.* **40** 185

Ortenburger I B and Bagus P S 1975 *Phys. Rev.* A **11** 1501

Ortiz J V 1984 *J. Chem. Phys.* **81** 5873

Platania R, Maracci F , Souza A C A and de Souza G G B 1992 *Chem. Phys.* **163** 381

Pople J A and Beveridge P L 1970 *Approximate Molecular Orbital Theory* 1970 (New York: McGraw-Hill)

Ramaker D E 1991 *Solid State and Material Sciences* **17** 211

Ramaker D E, Murday J S, Turner N H, Moore G, Lagally M G and Houston J 1979 *Phys. Rev. B* **19** 5375

Rosenberg R A, Wen C R, Tan K, Chen J M 1990 *Springer Ser. Surf. Sci.* **19** 97

Rye R R and Houston J E 1983 *J. Chem. Phys.* **78** 4321

Rye R R, Jennison D R and Houston J E 1980 *J. Chem. Phys.* **73** 4867

Rye R R, Madey T E, Houston J E and Holloway P H 1978 *J. Chem. Phys.* **96** 1504

Sato Y, Ueda K, Chiba H, Shigemasa E and Yagishita A 1992 *Chem. Phys. Lett.* **196** 475

Schmidt M W, Baldridge K K, Boatz J A, Jensen J H, Koseki S, Gordon M S, Nguyen K A, Windus T L and Elbert S T 1991 *see* GAMESS version 91

Shaw R W and Thomas T D 1975 *Phys. Rev.* A **11** 1491

Shaw R W, Jen J S and Thomas T D 1977 *J. Electron Spectrosc. Relat. Phenom.* **11** 91

Shirley D A 1973 *Phys. Rev.* A **7** 1520

Siegbahn H, Asplund L and Kelfve P 1975 *Chem. Phys. Lett.* **35** 330

Siegbahn H 1978 in *Excited States in Quantum Chemistry* p.273-295 *Ed.* Nicolaides C A and Beck D R (Dordrecht: D Reidel Publishing Company)

Siegbahn K, Nordling C, Johansson G, Heden P F, Hamrin K, Gelius U, Bergmark T, Werme L O, Manne R and Baer Y 1969 *ESCA applied to free molecules* (Amsterdam:North-Holland)

Simon M, Thiry P and Nenner I 1988 *Phys. Rev.* A **37** 2448

Sinha D, Mukhopadhyay S K, Prasad M D and Mukherjee D 1986 *Chem. Phys. Lett.* **125** 213

Snyder L C and Basch H 1972 *Molecular wave functions and properties tabulated from SCF calculations in a gaussian basis set* (New York: J Willey and Sons)

Spohr R, Bergmark T, Magnusson N, Werme L O, Nordling C and Sieghban K 1970 *Phys.Scr.* **2** 31

Stankiewicz M, Hatherly P A, Frasinski L J, Codling K and Holland D M P 1989 *J. Phys. B: At. Mol. Opt. Phys.* **22** 21

Stolterfoht N, Schneider D and Harrison K G 1973 *Phys. Rev.* A **8** 2363

Stranges F, Adam M Y, Cauletti C, de Simone M, Furlani C, Piancastelli M N, Decleva P and Lisini A 1992 *J. Chem. Phys.* **97** 4764

Sukhorukov V L, Petrov I D, Sukhorukov B L and Demekhina I A 1986 *Khim.Fiz.***5** 175

Suoninen E J, Thomas T D, Anderson S E, Runyan M T and Ungier L 1985 *J. Electron Spectrosc. Relat. Phenom.* **35** 259

Tarantelli F, Tarantelli A, Sgamelotti A, Schirmer J, and Cederbaum L S 1985a *Chem. Phys. Lett.* **117** 577

Tarantelli F, Tarantelli A, Sgamelotti A, Schirmer J and Cederbaum L S 1985b *J. Chem. Phys.* **83** 4683

Tarantelli F, Schirmer J, Sgamelotti A and Cederbaum L S 1985c *Chem. Phys. Lett.* **122** 169

Tarantelli F, Sgamelotti A and Cederbaum L S 1992 *Appl. Many-Body Methods Spectrosc. Electron. Struct. [Proc. Symp.] Meeting Date 1990* 57 *Ed.* Mukherjee D (New York: Plenum)

Thomas T D, *personal communication*

Thompson M, Baker M D, Christie A and Tyson J F, 1985 *Auger Electron Spectroscopy* (New York: John Wiley&Sons)

Thompson M, Hewitt P A and Wooliscroft D S 1976 *Anal. Chem.* **48** 1336

Tiedje T, Colbow K M , Rogers D and Eberhardt W 1990 *Phys. Scr.* **41** 621

Truesdale C M, Lindle D W, Kobrin P H, Becker U E, Kerkhoff H G, Heimann P A, Ferrett T A and Shirley D A 1984 *J. Chem. Phys.* **80** 2319

Tulea L C 1987 *M.Sc. Thesis* University of Tasmania

Ueda K, Chiba B, Sato Y, and Hayaishi T, A Shigemasa E and Yagishita A 1992 *Phys. Rev.* A **46** R-5

Ueda K, Sato Y and Shigemasa E (1991) *personal communication*

Vayrynen I J, Kaurila T A, Cavell R G and Tan K H 1992 *J. Electron Spectrosc. Relat. Phenom.* **61** 55

Vayrynen J, Sodhi R N and Cavell R G 1983 *J. Chem. Phys.* **79** 5329

Walsh T R, Meehan T E and Larkins F P 1993 *J. Phys.B; At. Mol. Phys.* (submitted)

Walters D L and Bhalla C P 1971 *Atomic Data* **3** 301

Wandelt K, Almbladh C O and Nyholm R *Ed.* 1992 *Proceedings of the 2nd International Workshop on Auger Spectroscopy and Electronic Structure (IWASES-II), Malmoe, Sweden, September 4-6 1991* [in:*Phys. Scr. T 1992* **T41**]

Wentzel G 1927 *Z. Physik* **43** 524

Werme L O, Bergmark T and Siegbahn K 1973 *Phys.Scr.* **8** 149

White J M, Rye R R and Houston J E 1977 *Chem. Phys. Lett.* **46** 146

Yagishita A, Arai S, Brion C E, Hayaishi T, Murakami J, Sato Y and Ukai M 1986 *Chem. Phys. Lett.* **132** 437

Zähringer K, Meyer H-D and Cederbaum L S 1992 *Phys. Rev.* A **45** 318

List of Publications

A semiempirical approach to the prediction of molecular Auger spectra, F.P.Larkins, L.C.Tulea and E.Z.Chelkowska, The Australian Bicentenary Congress of Physicists, *Proc. 5th Australian Conference on Atom and Molecular Physics and Quantum Chemistry*, January 1988.

Auger Electron Spectra of Molecules: The First Row Hydrides, F.P.Larkins, L.C.Tulea and E.Z.Chelkowska, *Australian Journal of Physics*, **43** (1990) 625-639.

Analysis of Auger Spectra of Molecules Containing Second Row Atoms, E.Z.Chelkowska, F.P.Larkins *Proc.15th Int. Conf. on X-Ray and Inner Shell* , Knoxville, July 1990.

Auger Spectroscopy for Molecules. Tables of Matrix Elements for Transition-rate Calculations Corresponding to an s-, p-, or d-type Initial Hole, E.Z.Chelkowska and F.P.Larkins, *Atomic Data and.Nuclear Data Tables*, **49** (1991) 121-206.

Theoretical Interpretation of K and L Shell Auger Spectra for the SiH_4 Molecule, E.Z.Chelkowska and F.P.Larkins, *Journal of Physics B*, **24** (1991) 5083-5090.

Theoretical Studies of the L-Shell Auger Spectra of Second Row Hydride Molecules, F.P.Larkins and E.Z.Chelkowska, *17th Int. Conf. on the Physics of Electron and Atomic Collisions. Abstracts*, Brisbane, 10-16 July 1991, p.50.

Origin of the Double Peak Structure in the Auger Spectrum of the SiF_4 Molecule, E.Z.Chelkowska, J. McColl and F.P.Larkins, *VUV10 Conference*, Paris, July 1992, Th73.

The $L_{-23}VV$ Auger Spectra for the PX_3 Molecules: X=H, F, Cl, F.P.Larkins, E.Z.Chelkowska, Y.Sato, K.Ueda, E.Shigemasa and A.Yagishita, *Journal of Physics B* , **26** (1993) 1479-1490.

The Importance of Electron Correlation Satellites in the Silicon 2p Auger Spectrum for the SiF_4 Molecule, F.P.Larkins, J.McColl and E.Z.Chelkowska, *Journal of Electron Spectroscopy and Related Phenomena* (1993) accepted.

Appendix A

PARAMETERS USED FOR THE SECOND ROW ELEMENTS

INDO parameters: ζ (orbital exponent), F^2 and G^1 (Slater-Condon factors), β^0 (resonance parameter) and $1/2(I+A)\mu$ (Mulliken electronegativities for μ=s or p orbitals) were optimized for molecules containing Na-Cl atoms by Gordon *et al.*1978. Spin-orbit splitting values were calculated semiempirically (Larkins 1977).

Z	ζ a)	F^2 a) (a.u.)	G^1 a) (a.u.)	β^0 a) (eV)	1/2(I+A)a) (eV) *s*	*p*	Energies[b] (a.u.)	Splitting[c] (eV)
10[d]	2.925	0.3670	0.6400	-50.0	40.0	13.2	-40.489845	
11	1.21	0.071957	0.128648	-4.0	2.804	1.302	-0.206101	
12	1.28	0.090701	0.138735	-7.0	5.125	2.052	-1.037533	
13	1.39	0.108090	0.160025	-9.0	7.771	2.995	-2.211575	
14	1.55	0.12845	0.19179	-8.0	7.5	4.0	-3.834983	0.6
15	1.74	0.151521	0.231907	-13.0	16.2	4.1	-6.913990	0.9
16	1.93	0.175202	0.276683	-16.5	17.51	3.45	-10.192703	1.2
17	2.14	0.201492	0.329070	-18.0	25.11	6.34	-15.740044	1.6
18	2.25[e]	0.230000	0.393000	-22.0	28.00	6.40	-20.872346	

a) Gordon M S , Bjorke M D , Marsh F J and Korth M S 1978 *J.Am.Chem.Soc.* **100** 2670.

b) All energy values calculated using Gordon *et al.* parameters.

c) Larkins F P 1977 *Atomic Data and Nuclear Data Tables* **20** 311.

d) All parameters for neon were extrapolated from parameters available for the first row elements.

e) Calculated using Slater rules.

Atomic Auger matrix elements R^k for initial 2p hole and valence orbitals (Chen *et al.* 1990[a]) with the Walters and Bhalla normalisation[b] used in present calculations.

	R^0(3p3s,2pεs)	R^1(3s3p,2pεs)	R^0(3p3p,2pεp)	R^1(3s3s,2pεp)	R^2(3p3p,2pεp)
Z=14	0.0105911	0.0082840	0.0105363	0.0078213	0.0065599
Z=15	0.0108785	0.0087142	0.0110033	0.0086162	0.0070146
Z=16	0.0111023	0.0090509	0.0113812	0.0091598	0.0073736
Z=17	0.0112518	0.0092946	0.0116543	0.0095383	0.0076371
Z=18	0.0113704	0.0094858	0.0118873	0.0097939	0.0078515

	R^1(3s3p,2pεd)	R^2(3p3s,2pεd)	R^2(3p3p,2pεf)
Z=14	-0.0005342	-0.0022714	0.0119597
Z=15	-0.0003782	-0.0016512	0.0122739
Z=16	-0.0003579	-0.0012007	0.0124755
Z=17	-0.0004067	-0.0008553	0.0125477
Z=18	-0.0004910	-0.0005834	0.0126278

[a] Chen M H , Larkins F P and Crasemann B 1990 *Atomic Data and Nuclear Data Tables* **41** 1.

[b] The statistically weighted averages of the relevant *jj* values are multiplied by a factor of $(\sqrt{2\pi})^{-1}$.

Appendix B

INTENSITY EXPRESSIONS FOR 2P INITIAL HOLE

Molecular Auger intensity expressions for 2p initial hole and non-degenerate final states in one centre approximation.

Total singlet (+) (triplet (3)* and (-)) intensity via s channel

$$^{1,3}I^{\varepsilon s}_{vv'} = \pi * (3)*1/3* (R1\pm1/3*R2)^2 * [(C^{v'}_{ns} * C^{v}_{np_z} \pm C^{v'}_{np_z} * C^{v}_{ns})^2 + (C^{v'}_{ns} * C^{v}_{np_y} \pm C^{v'}_{np_y} * C^{v}_{ns})^2 + (C^{v'}_{ns} * C^{v}_{np_x} \pm C^{v'}_{np_x} * C^{v}_{ns})^2]$$

Total singlet intensity via p channel

$$\begin{aligned} ^{1}I^{\varepsilon p}_{vv'} = \pi * \{ & 2/3 * (R3+1/25*R5)^2 * [(C^{v'}_{np_x} * C^{v}_{np_y} + C^{v'}_{np_y} * C^{v}_{np_x})^2 + \\ & (C^{v'}_{np_x} * C^{v}_{np_x} - C^{v'}_{np_y} * C^{v}_{np_y})^2 + (C^{v'}_{np_z} * C^{v}_{np_y} + C^{v'}_{np_y} * C^{v}_{np_z})^2 + \\ & (C^{v'}_{np_z} * C^{v}_{np_x} + C^{v'}_{np_x} * C^{v}_{np_z})^2] \\ & + 2/3 * [2/3*R4 * C^{v'}_{ns} * C^{v}_{ns} + \\ & (R3+7/25*R5) * (C^{v'}_{np_x} * C^{v}_{np_x} + C^{v'}_{np_y} * C^{v}_{np_y}) + 6/25*R5 * C^{v'}_{np_z} * C^{v}_{np_z}]^2 \\ & + 4/3 * [1/3*R4 * C^{v'}_{ns} * C^{v}_{ns} + \\ & 3/25*R5 * (C^{v'}_{np_x} * C^{v}_{np_x} + C^{v'}_{np_y} * C^{v}_{np_y}) + (R3+4/25*R5) * C^{v'}_{np_z} * C^{v}_{np_z}]^2 \} \end{aligned}$$

Total triplet intensity via p channel

$$ {}^3I^{\varepsilon p}_{vv'} = \pi * 2 * (R3 - 1/5*R5)^2 * [(C^{v'}_{np_z} * C^{v}_{np_y} - C^{v'}_{np_y} * C^{v}_{np_z})^2 + C^{v'}_{np_z} * C^{v}_{np_x} - C^{v'}_{np_x} * C^{v}_{np_z})^2 + (C^{v'}_{np_y} * C^{v}_{np_x} - C^{v'}_{np_x} * C^{v}_{np_y})^2] $$

Total singlet intensity via d channel

$$ {}^1I^{\varepsilon d}_{vv'} = \pi * 1/3 * \{[(C^{v'}_{np_y} * C^{v}_{ns} + C^{v'}_{ns} * C^{v}_{np_y})^2 + (C^{v'}_{ns} * C^{v}_{np_x} + C^{v'}_{np_x} * C^{v}_{ns})^2] * (2/9*R6^2 + 2/25*R7^2 + 2*R6*R7*2/15) + (C^{v'}_{ns} * C^{v}_{np_z} + C^{v'}_{np_z} * C^{v}_{ns})^2 * (7/45*R6^2 + 7/125*R7^2 + 2*R6*R7*7/75)\} $$

Total triplet intensity via d channel

$$ {}^3I^{\varepsilon d}_{vv'} = \pi * [(C^{v'}_{np_y} * C^{v}_{ns} - C^{v'}_{ns} * C^{v}_{np_y})^2 + (C^{v'}_{ns} * C^{v}_{np_x} - C^{v'}_{np_x} * C^{v}_{ns})^2 + (C^{v'}_{ns} * C^{v}_{np_z} - C^{v'}_{np_z} * C^{v}_{ns})^2] * (2/9*R6^2 + 2/25*R7^2 - 2*R6*R7*2/15) $$

Total singlet intensity for transitions via f channel:

$$ {}^1I^{\varepsilon f}_{vv'} = \pi * R^2*(36/625)* [(C^{v'}_{np_y} * C^{v}_{np_x} + C^{v'}_{np_x} * C^{v}_{np_y})^2 + (C^{v'}_{np_y} * C^{v}_{np_y} - C^{v'}_{np_x} * C^{v}_{np_x})^2 + (C^{v'}_{np_y} * C^{v}_{np_z} + C^{v'}_{np_z} * C^{v}_{np_y})^2 + (C^{v'}_{np_z} * C^{v}_{np_x} + C^{v'}_{np_x} * C^{v}_{np_z})^2 + 1/3 * (C^{v'}_{np_x} * C^{v}_{np_x} + C^{v'}_{np_y} * C^{v}_{np_y} - 2 * C^{v'}_{np_z} * C^{v}_{np_z})^2] $$

where:

n - principal quantum number, v, v' - non-degenerate molecular orbitals and

R1= R^0(npns,2pεs)

R2= R^1(nsnp,2pεs)

R3= R^0(npnp,2pεp)

R4= R^1(nsns,2pεp)

R5= R^2(npnp,2pεp)

R6= R^1(nsnp,2pεd)

R7= R^2(npns,2pεd)

R=R^1(npnp,2pεf).

Appendix C

EXPERIMENTAL GEOMETRIES AND IONIZATION ENERGIES

C.1. First row hydrides

Molecule	Sym-metry	Geometry (bond)	Geometry (angle)	Geometry ref.	Orbital	Ioniz. energy (eV)	Ioniz. ref. (authors)	Ioniz. ref. (journal)
CH_4	T_d	C-H 1.094Å		Snyder and Basch	$1t_2$	14.0	Banna M S and Shirley D A	1975 *J. Chem. Phys.* 63 4359
					$2a_1$	23.0	"	"
					C1s	290.8	"	"
NH_3	C_{3v}	N-H 1.0141Å	∠H-N-H 106.76°	Snyder and Basch	$3a_1$	10.85	Banna M S and Shirley D A	1975 *J. Chem. Phys.* 63 4359
					1e	15.8	"	"
					$2a_1$	27.74	"	"
					N1s	405.6	"	"
H_2O	C_{2v}	O-H 0.959Å	∠H-O-H 104.7°	Snyder and Basch	$1b_1$	12.61	Banna M S and Shirley D A	1975 *J. Chem. Phys.* 63 4359
					$3a_1$	14.75	"	"
					$1b_1$	18.55	"	"
					$2a_1$	32.2	"	"
					O1s	539.7	"	"
HF	$C_{\infty v}$	F-H 0.917Å		Snyder and Basch	1π	16.04	Banna M S and Shirley D A	1975 *J. Chem. Phys.* 63 4359
					3σ	19.9	"	"
					2σ	39.65	"	"
					F1s	694.0	"	"

Snyder and Basch - Snyder L C and Basch H, *Molecular wave functions and properties tabulated from SCF calculations in a gaussian basis set,* J Willey and Sons, New York, 1972.

C.2. CH_3X molecules

Molecule	Symm.	Geom. (bond)	Geom. (angle)	Geom. ref.	Orbital	Ioniz. energy (eV)	Ioniz. ref. (authors)	Ioniz. ref. (journal)
C_2H_6	D_{3d}	C-C 1.5326Å	∠H-C-H 107.3°	LB II/7 p.196	$1e_g$	12.0	Bieri G and Åsbrink L	1980 *J. Electron Spectrosc. Relat. Phenom.* **20** 149
		C-H 1.1108Å			$3a_{1g}$	12.7	"	"
					$1e_u$	15.0	"	"
					$2a_{2u}$	20.4	"	"
					$2a_{1g}$	23.9	"	"
					C1s	290.6	Jolly W L , Bomben K D and Eyerman G J	1984 *At.Data. Nucl. Data Tabl.* **31** 433
CH_3NH_2	C_s	C-N 1.4714Å	∠H-C-N 110.3°	LB II/7 p.149	7a' (n N)	9.7	Bieri G, Åsbrink L and Niessen W	1982 *J. Electron Spectrosc. Relat. Phenom.* **27** 433
		C-H 1.0987Å	∠H-C-H 108.0°		2a"	13.3	"	"
		N-H 1.0096Å	∠H-N-H 107.1°		6a'	14.3	"	"
			∠CH_3 &C-N 2.9°		5a'	15.5	"	"
					1a"	17.0	"	"
					4a'	21.8	"	"
					3a'	27.92	"	"
					C1s	291.6	Jolly W L, Bomben K D and Eyerman G J	1984 *At.Data. Nucl. Data Tabl.*31 433
					N1s	405.15	"	"
CH_3OH	C_s	C-O 1.4246Å	∠C-O-H 108.5°	LB II/7 p.148	2a"	11.0	Niessen W, Bieri G and Åsbrink L	1980 *J. Electron Spectrosc. Relat. Phenom.* **21** 175
		C-H 1.0936Å	∠H-C-H 108.6°		7a'	12.7	"	"
			∠CH_3 &C-O 3.3°		6a'	15.1	"	"
		O-H 0.9451Å			1a"	15.6	"	"
					5a'	17.6	"	"
					4a	22.7	"	"
					3a'	32.2	"	"
					C1s	292.42	Jolly W L, Bomben K D and Eyerman G J	1984 *At.Data. Nucl. Data Tabl.*31 433
					O1s	539.13	"	"
CH_3F	C_{3v}	C-F 1.382Å	∠H-C-H 110.45°	LB II/7	2e	13.1	Bieri G, Åsbrink L and Niessen W	1981 *J. Electron Spectrosc. Relat. Phenom.* **23** 281
		C-H 1.095Å			$5a_1$	17.0	"	"
					1e (π F)	17.0	"	"
					$4a_1$	23.4	"	"
					$3a_1$	38.4	"	"
					C1s	293.6	Jolly W L, Bomben K D and Eyerman G J	1984 *At.Data. Nucl. Data Tabl.*31 433
					F1s	692.92	"	"

LBII/7 - Landolt-Börnstein, Numerical data and functional relationships in science and technology, Group II: Atomic and molecular physics, Volume 7: *Structure data of free polyatomic molecules*, Springer Verlag, Berlin 1976.

C.3. XCHO molecules

Molecule	Symm.	Geom. (bond)	Geom. (angle)	Geom. ref.	Orbital	Ioniz. energy (eV)	Ioniz. ref. (authors)	Ioniz. ref. (journal)
CH_3CHO	C_s	C1-C2 1.5005Å C2-H 1.114Å C1-H 1.086Å C2-O 1.2155Å	∠H-C1-H 108.3° ∠C1-C2-O 123.9° ∠C1-C2-H 117.5°	LB II/7 p.185	10a' 2a" 9a' 8a' 1a" 7a' 6a' 5a' 4a' C1s($C\text{-}H_3$) C1s O1s	10.3 13.2 14.2 15.4 15.4 16.5 19.4 24.2 33.39 291.19 293.83 538.43	Bieri G, Asbrink L and Niessen W " " " " " " " " Hitchcock A and P Brion C E " "	1982 *J. Electron Spectrosc. Relat. Phenom.* **27** 433 " " " " " " " " 1980 *J. Electron Spectrosc. Relat. Phenom.* **19** 231 " "
NH_2CHO	C_s planar	C-N 1.352Å C-H 1.098Å C-O 1.219Å N-H 1.0016Å	$\angle H_3\text{-}N\text{-}2H$ 121.6° $\angle H_3\text{-}N\text{-}C$ 118.5° ∠H2-N-C 120° ∠N-C-O 124.7° ∠N-C-H1 112.7° ∠O-C-H1 122.5°	Hirota E, Sugisaki R, Nielsen C J and Sørensen GO 1974 *J. Mol. Spec.* **49** 251	10a' (nO') 2a" (nN") 1a"(CO) 9a' 8a' 7a' 6a' 5a' 4a' C1s N1s O1s	10.4 10.7 14.1 14.8 16.3 18.8 20.7 28.5 33.1 294.45 406.41 537.9	Åsbrink L, Svensson A, Niessen W and Bieri G " " " " " " " " Jolly W L , Bomben K D and Eyerman G J " Siegbahn K	1981 *J. Electron Spectrosc. Relat. Phenom.* **24** 293 " " " " " " " " 1984 *At.Data. Nucl. Data Tabl.***31** 433 " 1974 *J. Electron Spectrosc. Relat. Phenom.* **5** 1059
OHCHO	C_s	C=O 1.194Å C-O 1.352Å C-H 1.105Å O-H 0.956Å	∠O-C=O 122.1° ∠O=C-H 123.2° ∠O-C-H 114.6° ∠C-O-H 109.7°	Bock C W, Trachtman M and George P 1980 *J. Mol. Spec.* **80** 131	10a' (nO') 2a" (nO") 9a' 1a"(CO) 8a' 7a' 6a' 5a' 4a' C1s O1s (CO) O1s (OH)	11.5 12.6 14.8 15.8 17.1 17.8 22.0 30.7 33.0 295.9 539.0 540.65	Niessen W, Bieri G and Åsbrink L " " " " " " " " Jolly W.L, Bomben K D and Eyerman G J " "	1980 *J. Electron Spectrosc. Relat. Phenom.* **21** 175 " " " " " " " " 1984 *At.Data. Nucl. Data Tabl.***31** 433 " "
FCHO	C_s	C=O 1.181Å C-F 1.338Å C-H 1.095Å	∠F-C=O 122.8° ∠O=C-H 123.7° ∠F-C-H 109.9°	LB II/7	7a' 2a" 6a' 1a" 5a' 4a' 3a' 2a' (CO) 1a'(OH)	12.55 14.54 15.45 17.74 19.2 20.17 23.61 36.29 40.62	Wittel K " " " " estimate from INDO calc. estimate from INDO calc. estimate from INDO calc. estimate from INDO calc.	1976 *J. Electron Spectrosc. Relat. Phenom.* **8** 246 " " " " ••• ••• ••• •••

LBII/7 - Landolt-Börnstein, Numerical data and functional relationships in science and technology, Group II: Atomic and molecular physics, Volume 7: *Structure data of free polyatomic molecules*, Springer Verlag, Berlin 1976.

Molecule	Symm.	Geom. (bond)	Geom. (angle)	Geom. ref.	Orbital	Ioniz. energy (eV)	Ioniz. ref. (authors)	Ioniz. ref. (journal)
FCHO					C1s	296.39* (dimer)	Jolly W L, Bomben K D and Eyerman G J	1984 *At.Data. Nucl. Data Tabl.*31 433
					O1s	540.99* (dimer)	"	"
					F1s	695.0	estimate from INDO calc.	"
HCHO	C_{2v}	C-O	∠H-C-H	LB II/7 p.132	$2b_2$	10.9	Niessen W, Bieri G and Åsbrink L	1980 *J. Electron Spectrosc. Relat. Phenom.* 21 175
		1.2078Å	116.5°		$1b_1$	14.5	"	"
		C-H			$5a_1$	16.1	"	"
		1.116Å			$1b_2$	17.0	"	"
					$4a_1$	21.4	"	"
					$3a_1$	34.2	"	"
					C1s	294.47	Hitchcock A and P Brion C E	1980 *J. Electron Spectrosc. Relat. Phenom.* 19 231
					O1s	539.44	"	"

C.4. Second row hydrides

Molecule	Symm.	Geom. (bond)	Geom. (angle)	Geom. ref.	Orbital	Ioniz. energy (eV)	Ioniz. ref. (authors)	Ioniz. ref. (journal)
SiH_4	T_d	Si-H 1.481Å		Radom and Hehre	$2t_2$	12.8	de Souza G G B, Morin P and Nenner I	1986 *Phys. Rev.* A **34** 4770
					$3a_1$	18.2	"	"
					Si $2p_{3/2}$	107.2	"	"
					Si $2p_{1/2}$	107.8	"	"
					Si 2s	155.0	Cooper G, Ibuki T and Brion C E	1990 *Chem. Phys.* **140** 147
					Si1s	1847.0	Cavell R G and Sodhi R	1979 *J. Electron Spectrosc. Relat. Phenom.* **15** 145
PH_3	C_{3v}	P-H 1.42Å	∠HPH 93.343°	LB II/15 p.118	$5a_1$	10.58	Domke W, Schirmer J, Cederbaum L S, Maier J P and Niessen W	1978 *J. Electron Spectrosc. Relat. Phenom.* **14** 59
					2e	13.5	"	"
					$4a_1$	20.0	Cauletti C, Piancastelli M N and Adam M Y	1988 *J.Mol.Struct.* **174** 135
					averaged (median)	(22.61)	(Hammet A, Hood S T and Brion C E)	(1977 *J. Electron Spectrosc. Relat. Phenom.* **11** 263)
					P $2p_{3/2}$	137.05	Sodhi R N S and Brion C E	1985 *J. Electron Spectrosc. Relat. Phenom.* **37** 97
					P $2p_{1/2}$			
					P 2s	194.88	"	"
					P1s	2150.87	Cavell R G and Sodhi R	1987 *J. Electron Spectrosc. Relat. Phenom.* **43** 215
SH_2	C_{2v}	S-H 1.3356Å	∠H-S-H 92.11°	LB II/15 p.114	$2b_1$	10.5	Bieri G, Åsbrink L and Niessen W	1982 *J. Electron Spectrosc. Relat. Phenom.* **27** 129
					$5a_1$	13.3	"	"
					$2b_2$	15.5	"	"
					$4a_1$	22.8	"	"
					averaged			
					S $2p_{3/2}$	170.36	Cesar A, Ågren H, Naves de Brito A, Svensson S, Karlsson L, Keane M P, Wannberg B, Baltzer P, Fournier P G and Fournier J	1990 *J.Chem.Phys.* **93** 918
					S $2p_{1/2}$	171.57	"	"
					S 2s	234.5	Dewar M J S, Komornicki A, Thiel W and Schweig A	1975 *Chem. Phys. Lett.* **31** 286
					S1s	2478.43	Cavell R G and Sodhi R	1987 *J. Electron Spectrosc. Relat. Phenom.* **43** 215
ClH	$C_{\infty v}$	Cl-H 1.2746Å		Gordy	$1\pi_{3/2}$	12.748	Niessen W, Åsbrink L and Bieri G	1982 *J. Electron Spectrosc. Relat. Phenom.* **26** 173
					$1\pi_{1/2}$	12.83	"	"
					2σ	16.6	Adam M Y	1986 *Chem. Phys. Lett.* **128** 280
					1σ	29.8 (weighted average of 25.8 32.8 37.8)	"	"
					Cl $2p_{3/2}$	207.4	Aitken E J, Bahl M K, Bomben K D, Gimzewski J K, Nolan G S and Thomas T D	1980 *J. Am. Chem. Soc.* **102** 4873
					Cl $2p_{1/2}$	209.0	"	"
					Cl 2s	278.22	Adams D B	1977 *J. Electron Spectrosc. Relat. Phenom.* **10** 247
					Cl 1s	2829.2	Cavell R G and Sodhi R	1979 *J. Electron Spectrosc. Relat. Phenom.* **15** 145
						(2841.7)	(Adams D B)	(1977 *J. Electron Spectrosc. Relat. Phenom.* **10** 247)

LBII/15 - Landolt-Börnstein, Numerical data and functional relationships in science and technology, Group II: Atomic and molecular physics, Volume 15 *Supplement to Volume II/7*, Springer Verlag, Berlin 1987.

Radom and Hehre - Hehre WJ, Radom L, Schleyer P v R and Pople JA, *Ab initio molecular orbital theory*, John Wiley and Sons, New York 1986.

Gordy - Gordy W, 1986 *TCH*, **18** 76.

C.5. OCS, CF_4 and SiF_4 molecules

Molecule	Symm.	Geom. (bond)	Geom. (angle)	Geom. ref.	Orbital	Ioniz. energy (eV)	Ioniz. ref. (authors)	Ioniz. ref. (journal)
COS	$C_{\infty v}$	C=O 1.1543Å C=S 1.5628Å	∠O-C-S 180.00°	LB II/15 p.214	3π	11.2	Perera R C C and LaVilla R E	1984 *J. Chem. Phys.* **81** 3375
					2π	15.5	"	"
					9σ	16.0	"	"
					8σ	18.0	"	"
					7σ	27.4	"	"
					6σ	35.8	"	"
					S $2p_{3/2}$	170.65	Carroll T X, De Ji and Thomas T D	1990 *J. Electron Spectrosc. Relat. Phenom.* **51** 471
					S $2p_{1/2}$	171.85	"	"
					S 2s	•••	•••	•••
					C 1s	295.43	Carroll T X, De Ji and Thomas T D	1990 *J. Electron Spectrosc. Relat. Phenom.* **51** 471
					O 1s	540.28	"	"
					S 1s	2478.7	Perera R C C and LaVilla R E	1984 *J. Chem. Phys.* **81** 3375
CF_4	T_d	C-F 1.317Å		Radom and Hehre	$1t_1$	16.2	Bieri G, Asbrink L and Niessen W	1981 *J. Electron Spectrosc. Relat. Phenom.* **23** 281
					$4t_2$	17.4	"	"
					1e	18.5	"	"
					$3t_2$	22.1	"	"
					$4a_1$	25.1	"	"
					$2t_2$	40.3	"	"
					$3a_1$	43.8	"	"
					C 1s	301.8	Lapiano-Smith D A, Ma C I, Wu K T and Hanson D M	1989 *J. Chem. Phys.* **90** 2162
					F 1s	695.2	"	"
SiF_4	T_d	Si-F 1.554Å		LB II/15 p.96	$1t_1$	16.4	Bieri G, Asbrink L and Niessen W	1982 *J. Electron Spectrosc. Relat. Phenom.* **27** 129
					$5t_2$	17.5	"	"
					1e	18.1	"	"
					$4t_2$	19.5	"	"
					$5a_1$	21.5	"	"
					$3t_2$	39.3	"	"
					$4a_1$	40.6	"	"
					Si $2p_{3/2}$	111.7	Bozek J D, Bancroft G M and Tan K H	1990 *Chem. Phys.* **145** 131
					Si $2p_{1/2}$	112.31	"	"
					Si 2s	163.3	"	"
					F 1s	695.1	Lapiano-Smith D A, Ma C I, Wu K T and Hanson D M	1989 *J. Chem. Phys.* **90** 2162
					Si 1s	1859.8	Hartmann E and Szargan R	1979 *Chem. Phys. Lett.* **68** 175

Appendix D

INPUT PARAMETERS AND COMPUTED MOLECULAR AUGER SPECTRA

D.0. Explanation of tables

Appendix D contains initial information necessary to calculate all presented molecular Auger spectra as well as the calculated spectra themselves.

For each molecule the first two lines of a table contain a description of the calculations. All Z numbers and x, y, z coordinates (in atomic units) of atoms forming a molecule are listed in the following lines.

Degeneracies of occupied orbitals are also specified.

Eigenvectors were calculated using the INDO approximation and an equivalent core approach (for the atom specified in the description of calculations). For some molecules equivalent core calculations were not achievable. Such cases are marked with an asterisk.

Molecular Coulomb and exchange integrals (and in some cases - special integrals) were calculated using a non-equivalent core approach. All values are in atomic units.

Molecular Auger spectra are calculated using an intra-atomic transition model. The atom of a molecule, for which the spectrum is calculated, is specified in a table. In the part of the table with an Auger spectrum, all values of energy as well as core (1s or 2p3/2) and valence ionization potentials are displayed in eV.

Abbreviations used in the tables:

PEAK NR.	Final state number
MO.INDEX, MO.NAME	Indexes and names of molecular orbitals partaking in a final state
SYM	Symmetry of a double hole final state
ABS.ENERGY	Energy of Auger transitions
REL.ENERGY	Energy of a final state relative to an initial core hole (1st column) or to the calculated highest energy Auger transition (2nd column)
ABS.RATE	Absolute Auger transition rate in atomic units
REL.INT.	Relative intensity in %; the most intense transition is set to be 100%.

Calculated total Auger transition rates (in atomic units) are presented in the last line of each table.

D.1.1. Methane - C(KVV)

```
      CALCULATIONS FOR CH4, GEOM. FROM SNYDER AND BASCH

   6      0.0000000      0.0000000      0.0000000
   1     -1.1930940      1.1930940     -1.1930940
   1      1.1930940     -1.1930940     -1.1930940
   1      1.1930940      1.1930940      1.1930940
   1     -1.1930940     -1.1930940      1.1930940
 DEGENERACY OF OCCUPIED ORBITALS
1 3 3 3


     EIGENVECTORS
  0.8128   0.0000   0.0000   0.0000
  0.0000   0.7852   0.0000   0.0000
  0.0000   0.0000   0.7852   0.0000
  0.0000   0.0000   0.0000   0.7852
  0.2913  -0.3097   0.3097  -0.3097
  0.2913   0.3097  -0.3097  -0.3097
  0.2913   0.3097   0.3097   0.3097
  0.2913  -0.3097  -0.3097   0.3097


     MOLECULAR J(PP,QQ) COULOMB INTEGRALS
  0.4737   0.4680   0.4680   0.4680
  0.4680   0.4691   0.4595   0.4595
  0.4680   0.4595   0.4691   0.4595
  0.4680   0.4595   0.4595   0.4691


     MOLECULAR K(PQ,PQ) EXCHANGE INTEGRALS
  0.4737   0.0504   0.0504   0.0504
  0.0504   0.4691   0.0356   0.0356
  0.0504   0.0356   0.4691   0.0356
  0.0504   0.0356   0.0356   0.4691


                    MOLECULE: CH4          ATOM: Carbon


                                AUGER SPECTRUM


                CORE AND VALENCE I.P.S USED

                  1s   290.800
                  2a1  23.000  1t2  14.000  1t2  14.000  1t2  14.000
```

PEAK NR.	MO.INDEX	MO.NAME		SYM	ABS.ENERGY	REL.ENERGY		ABS.RATE	REL.INT.
7	23	1t2	1t2	3T1	251.26	-39.5	0.0	0.0000000	0.0
6	22	1t2	1t2	1E	251.00	-39.8	0.3	0.0008008	66.7
5	23	1t2	1t2	1T2	249.33	-41.5	1.9	0.0012013	100.0
4	22	1t2	1t2	1A1	248.10	-42.7	3.2	0.0001532	12.7
3	12	2a1	1t2	3T2	242.44	-48.4	8.8	0.0002538	21.1
2	12	2a1	1t2	1T2	239.69	-51.1	11.6	0.0007532	62.7
1	11	2a1	2a1	1A1	231.91	-58.9	19.4	0.0003741	31.1

Total Transition Rate (in au) = 3.53640E-03

D.1.2. Ammonia - N(KVV)

```
      CALCULATIONS FOR NH3, GEOM. FROM SNYDER AND BASCH

   7      0.0000000      0.0000000      0.0000000
   1      1.7760000      0.0000000      0.7199600
   1     -0.8880000      1.5380000      0.7199600
   1     -0.8880000     -1.5380000      0.7199600
 DEGENERACY OF OCCUPIED ORBITALS
1 2 2 1


     EIGENVECTORS
 0.8559   0.0000   0.0000  -0.2529
 0.0000   0.8232   0.0000   0.0000
 0.0000   0.0000   0.8232   0.0000
 0.1054   0.0000   0.0000   0.9393
 0.2923   0.4636   0.0000   0.1339
 0.2923  -0.2318   0.4015   0.1339
 0.2923  -0.2318  -0.4015   0.1339


     MOLECULAR J(PP,QQ) COULOMB INTEGRALS
 0.5699   0.5483   0.5483   0.5968
 0.5483   0.5609   0.5142   0.5810
 0.5483   0.5142   0.5609   0.5810
 0.5968   0.5810   0.5810   0.7513


     MOLECULAR K(PQ,PQ) EXCHANGE INTEGRALS
 0.5699   0.0625   0.0625   0.0558
 0.0625   0.5609   0.0233   0.0226
 0.0625   0.0233   0.5609   0.0226
 0.0558   0.0226   0.0226   0.7513

                    MOLECULE: NH3          ATOM: Nitrogen

                                  AUGER SPECTRUM

                 CORE AND VALENCE I.P.S USED

                   1s   405.600
                   2a1  27.740  1e   15.800  1e   15.800  3a1  10.850

PEAK NR.  MO.INDEX   MO.NAME    SYM     ABS.ENERGY      REL.ENERGY      ABS.RATE     REL.INT.

   11        24      1e   3a1    3X       363.76         -41.8           0.0       0.0000180     1.4
   10        44      3a1  3a1    1A1      363.46         -42.1           0.3       0.0006906    52.4
    9        24      1e   3a1    1X       362.53         -43.1           1.2       0.0013175   100.0
    8        23      1e   1e     3A2      360.64         -45.0           3.1       0.0000000     0.0
    7        23      1e   1e     1E       359.37         -46.2           4.4       0.0009708    73.7
    6        22      1e   1e     1A1      358.10         -47.5           5.7       0.0002884    21.9
    5        14      2a1  3a1    3X       352.29         -53.3          11.5       0.0001432    10.9
    4        14      2a1  3a1    1X       349.25         -56.3          14.5       0.0004985    37.8
    3        12      2a1  1e     3E       348.84         -56.8          14.9       0.0002061    15.6
    2        12      2a1  1e     1E       345.44         -60.2          18.3       0.0006302    47.8
    1        11      2a1  2a1    1A1      334.61         -71.0          29.1       0.0004568    34.7

Total Transition Rate (in au)  =     5.21996E-03
```

D.1.3. Water - O(KVV)

```
      CALCULATIONS FOR H2O, GEOM FROM SNYDER AND BASCH

    8       0.0000000       0.0000000       0.0000000
    1       0.0000000       1.4345599       1.1071180
    1       0.0000000      -1.4345599       1.1071180
 DEGENERACY OF OCCUPIED ORBITALS
1 1 1 1


      EIGENVECTORS
 -0.9080    0.0000    0.2475    0.0000
  0.0000    0.0000    0.0000   -1.0000
  0.0000   -0.8660    0.0000    0.0000
 -0.1073    0.0000   -0.9173    0.0000
 -0.2863   -0.3536   -0.2206    0.0000
 -0.2863    0.3536   -0.2206    0.0000


      MOLECULAR J(PP,QQ) COULOMB INTEGRALS
  0.6922    0.6437    0.6861    0.7420
  0.6437    0.6294    0.6536    0.6748
  0.6861    0.6536    0.8177    0.7630
  0.7420    0.6748    0.7630    0.8691


      MOLECULAR K(PQ,PQ) EXCHANGE INTEGRALS
  0.6922    0.0827    0.0780    0.1050
  0.0827    0.6294    0.0377    0.0183
  0.0780    0.0377    0.8177    0.0432
  0.1050    0.0183    0.0432    0.8691


                    MOLECULE: H2O           ATOM: Oxygen


                                AUGER SPECTRUM


                CORE AND VALENCE I.P.S USED

                  1s   539.700
                  2a1  32.200  1b2  18.550  3a1  14.730  1b1  12.610
```

PEAK NR.	MO.INDEX	MO.NAME	SYM	ABS.ENERGY	REL.ENERGY		ABS.RATE	REL.INT.
16	34	3a1 1b1	3X	492.77	-46.9	0.0	0.0000122	1.3
15	44	1b1 1b1	1A1	490.83	-48.9	1.9	0.0008463	90.5
14	24	1b2 1b1	3X	490.68	-49.0	2.1	0.0000000	0.0
13	34	3a1 1b1	1X	490.42	-49.3	2.4	0.0009347	100.0
12	24	1b2 1b1	1X	489.68	-50.0	3.1	0.0007989	85.5
11	23	1b2 3a1	3X	489.66	-50.0	3.1	0.0000092	1.0
10	33	3a1 3a1	1A1	487.99	-51.7	4.8	0.0006320	67.6
9	23	1b2 3a1	1X	487.61	-52.1	5.2	0.0007010	75.0
8	22	1b2 1b2	1A1	485.47	-54.2	7.3	0.0004760	50.9
7	14	2a1 1b1	3X	477.56	-62.1	15.2	0.0001643	17.6
6	13	2a1 3a1	3X	476.22	-63.5	16.6	0.0001472	15.7
5	12	2a1 1b2	3X	473.68	-66.0	19.1	0.0001232	13.2
4	13	2a1 3a1	1X	471.98	-67.7	20.8	0.0005369	57.4
3	14	2a1 1b1	1X	471.84	-67.9	20.9	0.0005275	56.4
2	12	2a1 1b2	1X	469.18	-70.5	23.6	0.0003956	42.3
1	11	2a1 2a1	1A1	456.46	-83.2	36.3	0.0005734	61.3

```
Total Transition Rate (in au)  =     6.87824E-03
```

D.1.4. Hydrogen fluoride - F(KVV)

```
      CALCULATIONS FOR HF, GEOM. SNYDER AND BASCH, P.T-22

    9       0.0000000       0.0000000       0.0000000
    1       0.0000000       0.0000000       1.7330000
 DEGENERACY OF OCCUPIED ORBITALS
1 1 2 2


      EIGENVECTORS
  0.9585  -0.1748   0.0000   0.0000
  0.0000   0.0000   1.0000   0.0000
  0.0000   0.0000   0.0000   1.0000
  0.0840   0.9281   0.0000   0.0000
  0.2725   0.3287   0.0000   0.0000


      MOLECULAR J(PP,QQ) COULOMB INTEGRALS
  0.8540   0.7932   0.8891   0.8891
  0.7932   0.8501   0.8300   0.8300
  0.8891   0.8300   0.9951   0.9193
  0.8891   0.8300   0.9193   0.9951


      MOLECULAR K(PQ,PQ) EXCHANGE INTEGRALS
  0.8540   0.1142   0.1522   0.1522
  0.1142   0.8501   0.0412   0.0412
  0.1522   0.0412   0.9951   0.0379
  0.1522   0.0412   0.0379   0.9951


                    MOLECULE: HF            ATOM: Fluorine

                                AUGER SPECTRUM

                    CORE AND VALENCE I.P.S USED

                      1s   694.000
                      2si  39.650  3si  19.900  1pi  16.040  1pi  16.040
```

PEAK NR.	MO.INDEX	MO.NAME	SYM	ABS.ENERGY	REL.ENERGY		ABS.RATE	REL.INT.
11	34	1pi 1pi	3A2	637.94	-56.1	0.0	0.0000000	0.0
10	23	3si 1pi	3E	636.60	-57.4	1.3	0.0000117	0.6
9	34	1pi 1pi	1E	635.87	-58.1	2.1	0.0021068	100.0
8	23	3si 1pi	1E	634.35	-59.6	3.6	0.0018529	88.0
7	33	1pi 1pi	1A1	633.81	-60.2	4.1	0.0006159	29.2
6	22	3si 3si	1A1	631.07	-62.9	6.9	0.0006355	30.2
5	13	2si 1pi	3E	618.26	-75.7	19.7	0.0003528	16.7
4	12	2si 3si	3X	615.97	-78.0	22.0	0.0001570	7.5
3	13	2si 1pi	1E	609.97	-84.0	28.0	0.0011636	55.2
2	12	2si 3si	1X	609.76	-84.2	28.2	0.0005524	26.2
1	11	2si 2si	1A1	591.46	-102.5	46.5	0.0007016	33.3

Total Transition Rate (in au) = 8.15019E-03

D.2.1. Ethane - C(KVV)

```
        CALCULATIONS FOR C2H6, geom. LB7/II p.196

   6       0.0000000       0.0000000       0.0000000
   1       1.6906461       0.9760950       3.6676953
   1       0.0000000      -1.9521899       3.6676953
   1      -1.6906461       0.9760950       3.6676953
   6       0.0000000       0.0000000       2.8961954
   1       1.6906461      -0.9760950      -0.7714999
   1      -1.6906461      -0.9760950      -0.7714999
   1       0.0000000       1.9521899      -0.7714999
 DEGENERACY OF OCCUPIED ORBITALS
1 1 2 2 1 2 2


      EIGENVECTORS
  0.7277   0.3324   0.0000   0.0000   0.0797   0.0000   0.0000
  0.0000   0.0000   0.6837   0.0000   0.0000   0.3583   0.0000
  0.0000   0.0000   0.0000   0.6837   0.0000   0.0000   0.3583
  0.0850  -0.3439   0.0000   0.0000   0.7187   0.0000   0.0000
  0.1439  -0.3067   0.2192   0.1266  -0.1813  -0.4405  -0.2543
  0.1439  -0.3067   0.0000  -0.2531  -0.1813   0.0000   0.5087
  0.1439  -0.3067  -0.2192   0.1266  -0.1813   0.4405  -0.2543
  0.4219  -0.5966   0.0000   0.0000  -0.0663   0.0000   0.0000
  0.0000   0.0000   0.4073   0.0000   0.0000  -0.5924   0.0000
  0.0000   0.0000   0.0000   0.4073   0.0000   0.0000  -0.5924
 -0.1872  -0.1800   0.0000   0.0000  -0.5502   0.0000   0.0000
  0.2503   0.1833   0.3678  -0.2123  -0.1542   0.2575  -0.1487
  0.2503   0.1833  -0.3678  -0.2123  -0.1542  -0.2575  -0.1487
  0.2503   0.1833   0.0000   0.4247  -0.1542   0.0000   0.2973


      MOLECULAR J(PP,QQ) COULOMB INTEGRALS
  0.3999   0.3732   0.3822   0.3822   0.4075   0.3653   0.3653
  0.3732   0.3799   0.3698   0.3698   0.3883   0.3562   0.3562
  0.3822   0.3698   0.3830   0.3631   0.3880   0.3702   0.3468
  0.3822   0.3698   0.3631   0.3830   0.3880   0.3468   0.3702
  0.4075   0.3883   0.3880   0.3880   0.4269   0.3698   0.3698
  0.3653   0.3562   0.3702   0.3468   0.3698   0.3627   0.3329
  0.3653   0.3562   0.3468   0.3702   0.3698   0.3329   0.3627


      MOLECULAR K(PQ,PQ) EXCHANGE INTEGRALS
  0.3999   0.0717   0.0276   0.0276   0.0313   0.0244   0.0244
  0.0717   0.3799   0.0247   0.0247   0.0554   0.0305   0.0305
  0.0276   0.0247   0.3830   0.0100   0.0117   0.1213   0.0134
  0.0276   0.0247   0.0100   0.3830   0.0117   0.0134   0.1213
  0.0313   0.0554   0.0117   0.0117   0.4269   0.0115   0.0115
  0.0244   0.0305   0.1213   0.0134   0.0115   0.3627   0.0149
  0.0244   0.0305   0.0134   0.1213   0.0115   0.0149   0.3627


     SPECIAL J(PQ,RS) AND K(PS,RQ) INTEGRALS
        3    4    6    7   0.0117   0.0134
        3    4    7    6   0.0117   0.0946

                    MOLECULE: C2H6          ATOM: Carbon

                                  AUGER SPECTRUM

                  CORE AND VALENCE I.P.S USED

                    1s  290.600
                    2a1g 23.900  2a2u 20.400  1eu  15.000  1eu  15.000  3a1g 12.700
                    1eg  12.000  1eg  12.000

PEAK NR.  MO.INDEX  MO.NAME   SYM     ABS.ENERGY     REL.ENERGY        ABS.RATE   REL.INT.

  33        67      1eg  1eg   3A2      257.95      -32.7      0.0    0.0000000      0.0
  32        67      1eg  1eg    1E      257.14      -33.5      0.8    0.0000347      6.8
  31        36      1eu  1eg   3A1      256.87      -33.7      1.1    0.0000000      0.0
  30        36      1eu  1eg    3E      256.78      -33.8      1.2    0.0000000      0.0
  29        36      1eu  1eg   1A2      256.69      -33.9      1.3    0.0000000      0.0
  28        66      1eg  1eg   1A1      256.32      -34.3      1.6    0.0000102      2.0
  27        56      3a1g 1eg    3E      256.15      -34.4      1.8    0.0000003      0.1
```

26	56	3a1g	1eg	1E	255.52	-35.1	2.4	0.0001407	27.5
25	55	3a1g	3a1g	1A1	253.58	-37.0	4.4	0.0002251	43.9
24	35	1eu	3a1g	3X	252.66	-37.9	5.3	0.0000012	0.2
23	36	1eu	1eg	3A2	252.27	-38.3	5.7	0.0000000	0.0
22	35	1eu	3a1g	1X	252.02	-38.6	5.9	0.0005123	100.0
21	34	1eu	1eu	3A2	250.99	-39.6	7.0	0.0000000	0.0
20	36	1eu	1eg	1E	250.91	-39.7	7.0	0.0002529	49.4
19	34	1eu	1eu	1E	250.45	-40.2	7.5	0.0004604	89.9
18	33	1eu	1eu	1A1	249.91	-40.7	8.0	0.0001354	26.4
17	36	1eu	1eg	1A1	249.54	-41.1	8.4	0.0000744	14.5
16	26	2a2u	1eg	3E	249.34	-41.3	8.6	0.0000059	1.2
15	25	2a2u	3a1g	3X	248.44	-42.2	9.5	0.0000147	2.9
14	26	2a2u	1eg	1E	247.68	-42.9	10.3	0.0000495	9.7
13	23	2a2u	1eu	3E	245.81	-44.8	12.1	0.0000215	4.2
12	25	2a2u	3a1g	1X	245.43	-45.2	12.5	0.0001399	27.3
11	16	2a1g	1eg	3E	245.42	-45.2	12.5	0.0000282	5.5
10	23	2a2u	1eu	1E	244.47	-46.1	13.5	0.0001801	35.2
9	16	2a1g	1eg	1E	244.10	-46.5	13.9	0.0000858	16.7
8	15	2a1g	3a1g	3X	243.76	-46.8	14.2	0.0000553	10.8
7	15	2a1g	3a1g	1X	242.06	-48.5	15.9	0.0001802	35.2
6	13	2a1g	1eu	3E	242.05	-48.5	15.9	0.0001028	20.1
5	13	2a1g	1eu	1E	240.55	-50.1	17.4	0.0003123	61.0
4	22	2a2u	2a2u	1A1	239.46	-51.1	18.5	0.0000294	5.7
3	12	2a1g	2a2u	3X	238.10	-52.5	19.9	0.0000161	3.1
2	12	2a1g	2a2u	1X	234.19	-56.4	23.8	0.0001417	27.7
1	11	2a1g	2a1g	1A1	231.92	-58.7	26.0	0.0002425	47.3

Total Transition Rate (in au) = 3.45363E-03

D.2.2.1. Methylamine - C(KVV)

CALCULATIONS FOR CH3NH2, geom. Fink&Allen,JCP46(1967)2276

6	0.0000000	0.0000000	0.0000000
7	0.0000000	-0.1700000	2.7800000
1	1.6864001	-0.9746000	-0.6820000
1	-1.6864001	-0.9746000	-0.6820000
1	0.0000000	1.9492000	-0.6820000
1	1.5282000	0.7208000	3.5039999
1	-1.5282000	0.7208000	3.5039999

DEGENERACY OF OCCUPIED ORBITALS
1 1 1 1 1 1 1

EIGENVECTORS

-0.6706	-0.4416	0.0000	-0.0195	-0.0703	0.0000	-0.0519
0.0000	0.0000	0.6573	0.0000	0.0000	0.4068	0.0000
-0.0010	0.0396	0.0000	-0.7063	-0.2278	0.0000	0.2021
-0.1283	0.3224	0.0000	0.1934	-0.6588	0.0000	-0.1061
-0.5206	0.5812	0.0000	0.1049	0.0996	0.0000	0.3195
0.0000	0.0000	0.4548	0.0000	0.0000	-0.6029	0.0000
-0.0659	0.1292	0.0000	-0.3285	0.0298	0.0000	-0.8402
0.1608	0.1664	0.0000	-0.1551	0.5685	0.0000	0.1276
-0.2270	-0.2255	0.3509	0.1741	0.2110	0.2802	-0.0904
-0.2270	-0.2255	-0.3509	0.1741	0.2110	-0.2802	-0.0904
-0.2283	-0.1951	0.0000	-0.4936	-0.0327	0.0000	0.2478
-0.1968	0.2980	0.2396	-0.0897	0.2062	-0.3962	-0.1468
-0.1968	0.2980	-0.2396	-0.0897	0.2062	0.3962	-0.1468

MOLECULAR J(PP,QQ) COULOMB INTEGRALS

0.4536	0.4021	0.4202	0.4031	0.4453	0.3983	0.4667
0.4021	0.4132	0.3962	0.4028	0.4162	0.3844	0.4083
0.4202	0.3962	0.4109	0.3837	0.4191	0.3949	0.4313
0.4031	0.4028	0.3837	0.4532	0.4071	0.3700	0.4119
0.4453	0.4162	0.4191	0.4071	0.4577	0.4002	0.4622
0.3983	0.3844	0.3949	0.3700	0.4002	0.3853	0.4010
0.4667	0.4083	0.4313	0.4119	0.4622	0.4010	0.5830

MOLECULAR K(PQ,PQ) EXCHANGE INTEGRALS

0.4536	0.0789	0.0328	0.0275	0.0369	0.0277	0.0348
0.0789	0.4132	0.0279	0.0292	0.0597	0.0345	0.0230
0.0328	0.0279	0.4109	0.0083	0.0163	0.1291	0.0130
0.0275	0.0292	0.0083	0.4532	0.0176	0.0094	0.0976
0.0369	0.0597	0.0163	0.0176	0.4577	0.0167	0.0217
0.0277	0.0345	0.1291	0.0094	0.0167	0.3853	0.0110
0.0348	0.0230	0.0130	0.0976	0.0217	0.0110	0.5830

MOLECULE: CH3NH2 ATOM: Carbon

AUGER SPECTRUM

CORE AND VALENCE I.P.S USED

1s 291.600
3a' 27.920 4a' 21.800 1a" 17.000 5a' 15.500 6a' 14.300
2a" 13.300 7a' 9.700

PEAK NR.	MO.INDEX	MO.NAME	SYM	ABS.ENERGY	REL.ENERGY		ABS.RATE	REL.INT.
49	67	2a" 7a'	3X	257.99	-33.6	0.0	0.0000001	0.0
48	47	5a' 7a'	3X	257.85	-33.8	0.1	0.0000004	0.1
47	67	2a" 7a'	1X	257.39	-34.2	0.6	0.0000094	3.4
46	77	7a' 7a'	1A1	256.34	-35.3	1.7	0.0000024	0.9
45	57	6a' 7a'	3X	255.61	-36.0	2.4	0.0000003	0.1
44	66	2a" 2a"	1A1	254.52	-37.1	3.5	0.0000229	8.3
43	57	6a' 7a'	1X	254.43	-37.2	3.6	0.0000280	10.1
42	36	1a" 2a"	3X	254.07	-37.5	3.9	0.0000000	0.0
41	56	6a' 2a"	3X	253.56	-38.0	4.4	0.0000002	0.1
40	37	1a" 7a'	3X	253.52	-38.1	4.5	0.0000002	0.1
39	46	5a' 2a"	3X	252.99	-38.6	5.0	0.0000000	0.0
38	37	1a" 7a'	1X	252.81	-38.8	5.2	0.0000244	8.8
37	56	6a' 2a"	1X	252.66	-38.9	5.3	0.0000852	30.8
36	47	5a' 7a'	1X	252.54	-39.1	5.5	0.0000469	16.9

35	46	5a'	2a"	1X	252.48	-39.1	5.5	0.0000935	33.8
34	45	5a'	6a'	3X	251.20	-40.4	6.8	0.0000006	0.2
33	55	6a'	6a'	1A1	250.55	-41.1	7.4	0.0001989	71.8
32	45	5a'	6a'	1X	250.24	-41.4	7.7	0.0002769	100.0
31	27	4a'	7a'	3X	249.62	-42.0	8.4	0.0000024	0.9
30	35	1a"	6a'	3X	249.34	-42.3	8.6	0.0000004	0.2
29	34	1a"	5a'	3X	248.88	-42.7	9.1	0.0000000	0.0
28	35	1a"	6a'	1X	248.45	-43.1	9.5	0.0002225	80.3
27	34	1a"	5a'	1X	248.43	-43.2	9.6	0.0002442	88.2
26	27	4a'	7a'	1X	248.36	-43.2	9.6	0.0000136	4.9
25	44	5a'	5a'	1A1	248.27	-43.3	9.7	0.0002407	86.9
24	36	1a"	2a"	1X	247.04	-44.6	10.9	0.0001196	43.2
23	26	4a'	2a"	3X	246.98	-44.6	11.0	0.0000067	2.4
22	33	1a"	1a"	1A1	246.42	-45.2	11.6	0.0001562	56.4
21	25	4a'	6a'	3X	245.80	-45.8	12.2	0.0000226	8.2
20	26	4a'	2a"	1X	245.10	-46.5	12.9	0.0000383	13.8
19	24	4a'	5a'	3X	244.13	-47.5	13.9	0.0000216	7.8
18	23	4a'	1a"	3X	242.78	-48.8	15.2	0.0000175	6.3
17	25	4a'	6a'	1X	242.55	-49.0	15.4	0.0001456	52.6
16	24	4a'	5a'	1X	242.54	-49.1	15.4	0.0001249	45.1
15	17	3a'	7a'	3X	242.23	-49.4	15.8	0.0000047	1.7
14	23	4a'	1a"	1X	241.26	-50.3	16.7	0.0001000	36.1
13	17	3a'	7a'	1X	240.33	-51.3	17.7	0.0000175	6.3
12	16	3a'	2a"	3X	240.30	-51.3	17.7	0.0000155	5.6
11	16	3a'	2a"	1X	238.79	-52.8	19.2	0.0000487	17.6
10	15	3a'	6a'	3X	238.27	-53.3	19.7	0.0000437	15.8
9	14	3a'	5a'	3X	237.96	-53.6	20.0	0.0000502	18.1
8	22	4a'	4a'	1A1	236.76	-54.8	21.2	0.0000533	19.3
7	14	3a'	5a'	1X	236.46	-55.1	21.5	0.0001587	57.3
6	15	3a'	6a'	1X	236.26	-55.3	21.7	0.0001509	54.5
5	13	3a'	1a"	3X	236.14	-55.5	21.8	0.0000404	14.6
4	13	3a'	1a"	1X	234.35	-57.2	23.6	0.0001273	46.0
3	12	3a'	4a'	3X	233.09	-58.5	24.9	0.0000156	5.6
2	12	3a'	4a'	1X	228.79	-62.8	29.2	0.0001860	67.2
1	11	3a'	3a'	1A1	223.42	-68.2	34.6	0.0001777	64.2

Total Transition Rate (in au) = 3.35722E-03

D.2.2.2. Methylamine - N(KVV)

CALCULATIONS FOR CH3NH2, geom. Fink&Allen, JCP46(1967)2276

6	0.0000000	0.0000000	0.0000000
7	0.0000000	-0.1700000	2.7800000
1	1.6864001	-0.9746000	-0.6820000
1	-1.6864001	-0.9746000	-0.6820000
1	0.0000000	1.9492000	-0.6820000
1	1.5282000	0.7208000	3.5039999
1	-1.5282000	0.7208000	3.5039999

DEGENERACY OF OCCUPIED ORBITALS

1 1 1 1 1 1 1

EIGENVECTORS

-0.3477	0.6362	0.0000	0.0980	0.0837	0.0000	0.0025
0.0000	0.0000	-0.3562	0.0000	0.0000	0.6292	0.0000
-0.0024	-0.0311	0.0000	0.4107	-0.2239	0.0000	-0.5463
-0.2047	-0.1403	0.0000	-0.2429	-0.4411	0.0000	-0.0025
-0.7965	-0.2832	0.0000	-0.2017	0.0645	0.0000	-0.1456
0.0000	0.0000	-0.7364	0.0000	0.0000	-0.3322	0.0000
-0.0865	-0.0816	0.0000	0.6426	-0.3851	0.0000	0.5455
0.0729	-0.3644	0.0000	0.3166	0.6934	0.0000	-0.0493
-0.1118	0.3222	-0.1837	-0.0264	0.2260	0.4541	0.2392
-0.1118	0.3222	0.1837	-0.0264	0.2260	-0.4541	0.2392
-0.1146	0.3012	0.0000	0.3634	-0.0043	0.0000	-0.4850
-0.2757	-0.1684	-0.3628	0.1942	0.0801	-0.2016	0.1238
-0.2757	-0.1684	0.3628	0.1942	0.0801	0.2016	0.1238

MOLECULAR J(PP,QQ) COULOMB INTEGRALS

0.4536	0.4021	0.4202	0.4031	0.4453	0.3983	0.4667
0.4021	0.4132	0.3962	0.4028	0.4162	0.3844	0.4083
0.4202	0.3962	0.4109	0.3837	0.4191	0.3949	0.4313
0.4031	0.4028	0.3837	0.4532	0.4071	0.3700	0.4119
0.4453	0.4162	0.4191	0.4071	0.4577	0.4002	0.4622
0.3983	0.3844	0.3949	0.3700	0.4002	0.3853	0.4010
0.4667	0.4083	0.4313	0.4119	0.4622	0.4010	0.5830

MOLECULAR K(PQ,PQ) EXCHANGE INTEGRALS

0.4536	0.0789	0.0328	0.0275	0.0369	0.0277	0.0348
0.0789	0.4132	0.0279	0.0292	0.0597	0.0345	0.0230
0.0328	0.0279	0.4109	0.0083	0.0163	0.1291	0.0130
0.0275	0.0292	0.0083	0.4532	0.0176	0.0094	0.0976
0.0369	0.0597	0.0163	0.0176	0.4577	0.0167	0.0217
0.0277	0.0345	0.1291	0.0094	0.0167	0.3853	0.0110
0.0348	0.0230	0.0130	0.0976	0.0217	0.0110	0.5830

MOLECULE: CH3NH2 ATOM: Nitrogen

AUGER SPECTRUM

CORE AND VALENCE I.P.S USED

1s 405.150
3a' 27.920 4a' 21.800 1a" 17.000 5a' 15.500 6a' 14.300
2a" 13.300 7a' 9.700

PEAK NR.	MO.INDEX	MO.NAME	SYM	ABS.ENERGY	REL.ENERGY		ABS.RATE	REL.INT.
49	67	2a" 7a'	3X	371.54	-33.6	0.0	0.0000005	0.1
48	47	5a' 7a'	3X	371.40	-33.8	0.1	0.0000007	0.2
47	67	2a" 7a'	1X	370.94	-34.2	0.6	0.0000364	10.1
46	77	7a' 7a'	1A1	369.89	-35.3	1.7	0.0000797	22.0
45	57	6a' 7a'	3X	369.16	-36.0	2.4	0.0000021	0.6
44	66	2a" 2a"	1A1	368.07	-37.1	3.5	0.0000103	2.8
43	57	6a' 7a'	1X	367.98	-37.2	3.6	0.0002458	67.9
42	36	1a" 2a"	3X	367.62	-37.5	3.9	0.0000000	0.0
41	56	6a' 2a"	3X	367.11	-38.0	4.4	0.0000001	0.0
40	37	1a" 7a'	3X	367.07	-38.1	4.5	0.0000024	0.7
39	46	5a' 2a"	3X	366.54	-38.6	5.0	0.0000009	0.3
38	37	1a" 7a'	1X	366.36	-38.8	5.2	0.0001791	49.5
37	56	6a' 2a"	1X	366.21	-38.9	5.3	0.0000737	20.4
36	47	5a' 7a'	1X	366.09	-39.1	5.5	0.0002477	68.4

35	46	5a'	2a"	1X	366.03	-39.1	5.5	0.0000626	17.3
34	45	5a'	6a'	3X	364.75	-40.4	6.8	0.0000056	1.5
33	55	6a'	6a'	1A1	364.10	-41.1	7.4	0.0003349	92.5
32	45	5a'	6a'	1X	363.79	-41.4	7.7	0.0003591	99.2
31	27	4a'	7a'	3X	363.17	-42.0	8.4	0.0000061	1.7
30	35	1a"	6a'	3X	362.89	-42.3	8.6	0.0000005	0.1
29	34	1a"	5a'	3X	362.43	-42.7	9.1	0.0000046	1.3
28	35	1a"	6a'	1X	362.00	-43.1	9.5	0.0003620	100.0
27	34	1a"	5a'	1X	361.98	-43.2	9.6	0.0003078	85.0
26	27	4a'	7a'	1X	361.91	-43.2	9.6	0.0000644	17.8
25	44	5a'	5a'	1A1	361.82	-43.3	9.7	0.0002349	64.9
24	36	1a"	2a"	1X	360.59	-44.6	10.9	0.0001008	27.9
23	26	4a'	2a"	3X	360.53	-44.6	11.0	0.0000018	0.5
22	33	1a"	1a"	1A1	359.97	-45.2	11.6	0.0002477	68.4
21	25	4a'	6a'	3X	359.35	-45.8	12.2	0.0000089	2.5
20	26	4a'	2a"	1X	358.65	-46.5	12.9	0.0000217	6.0
19	24	4a'	5a'	3X	357.68	-47.5	13.9	0.0000137	3.8
18	23	4a'	1a"	3X	356.33	-48.8	15.2	0.0000090	2.5
17	25	4a'	6a'	1X	356.10	-49.0	15.4	0.0001551	42.8
16	24	4a'	5a'	1X	356.09	-49.1	15.4	0.0001290	35.6
15	17	3a'	7a'	3X	355.78	-49.4	15.8	0.0000420	11.6
14	23	4a'	1a"	1X	354.81	-50.3	16.7	0.0001068	29.5
13	17	3a'	7a'	1X	353.88	-51.3	17.7	0.0001470	40.6
12	16	3a'	2a"	3X	353.85	-51.3	17.7	0.0000145	4.0
11	16	3a'	2a"	1X	352.34	-52.8	19.2	0.0000448	12.4
10	15	3a'	6a'	3X	351.82	-53.3	19.7	0.0000846	23.4
9	14	3a'	5a'	3X	351.51	-53.6	20.0	0.0000699	19.3
8	22	4a'	4a'	1A1	350.31	-54.8	21.2	0.0000280	7.7
7	14	3a'	5a'	1X	350.01	-55.1	21.5	0.0002535	70.0
6	15	3a'	6a'	1X	349.81	-55.3	21.7	0.0002649	73.2
5	13	3a'	1a"	3X	349.69	-55.5	21.8	0.0000714	19.7
4	13	3a'	1a"	1X	347.90	-57.2	23.6	0.0002202	60.8
3	12	3a'	4a'	3X	346.64	-58.5	24.9	0.0000204	5.6
2	12	3a'	4a'	1X	342.34	-62.8	29.2	0.0001438	39.7
1	11	3a'	3a'	1A1	336.97	-68.2	34.6	0.0003438	95.0

Total Transition Rate (in au) = 5.16517E-03

D.2.3.1. Methanol - C(KVV)

```
       CALCULATIONS FOR CH3OH, geom. LB7/II p.148

   6      0.0000000      0.0000000      0.0000000
   1      1.9381039      0.0000000     -0.7179596
   1     -0.9689416     -1.6782560     -0.7179596
   1     -0.9689416      1.6782560     -0.7179596
   1     -1.5032893      0.0000000      3.3508968
   8      0.1549684      0.0000000      2.6876221
 DEGENERACY OF OCCUPIED ORBITALS
1 1 1 1 1 1 1


     EIGENVECTORS
 0.5948  -0.5445   0.0180   0.0000   0.0718   0.0562   0.0000
-0.0044  -0.0329  -0.6282   0.0000  -0.3233   0.3264   0.0000
 0.0000   0.0000   0.0000  -0.7243   0.0000   0.0000   0.2777
 0.1675   0.3022  -0.2188   0.0000   0.5970   0.1859   0.0000
 0.1881  -0.2647  -0.3209   0.0000  -0.3386   0.2357   0.0000
 0.1928  -0.2422   0.2426   0.3874  -0.0073  -0.1733  -0.2291
 0.1928  -0.2422   0.2426  -0.3874  -0.0073  -0.1733   0.2291
 0.2509   0.2759   0.2671   0.0000  -0.2275   0.3185   0.0000
 0.6452   0.5577  -0.1275   0.0000  -0.1631  -0.3212   0.0000
-0.0804  -0.1199  -0.4539   0.0000   0.0401  -0.7042   0.0000
 0.0000   0.0000   0.0000  -0.4187   0.0000   0.0000  -0.9044
-0.1509   0.1486   0.2071   0.0000  -0.5825  -0.1993   0.0000


   MOLECULAR J(PP,QQ) COULOMB INTEGRALS
 0.5502   0.4214   0.4682   0.4372   0.5034   0.5048   0.5519
 0.4214   0.4398   0.4191   0.4298   0.4380   0.4162   0.4251
 0.4682   0.4191   0.4530   0.4248   0.4553   0.4666   0.4682
 0.4372   0.4298   0.4248   0.4551   0.4297   0.4184   0.4518
 0.5034   0.4380   0.4553   0.4297   0.5118   0.4934   0.5050
 0.5048   0.4162   0.4666   0.4184   0.4934   0.5333   0.5226
 0.5519   0.4251   0.4682   0.4518   0.5050   0.5226   0.6020


   MOLECULAR K(PQ,PQ) EXCHANGE INTEGRALS
 0.5502   0.0793   0.0403   0.0329   0.0480   0.0429   0.0619
 0.0793   0.4398   0.0336   0.0343   0.0648   0.0325   0.0294
 0.0403   0.0336   0.4530   0.0173   0.0318   0.1244   0.0178
 0.0329   0.0343   0.0173   0.4551   0.0073   0.0161   0.1474
 0.0480   0.0648   0.0318   0.0073   0.5118   0.0521   0.0128
 0.0429   0.0325   0.1244   0.0161   0.0521   0.5333   0.0246
 0.0619   0.0294   0.0178   0.1474   0.0128   0.0246   0.6020


                MOLECULE: CH3OH          ATOM: Carbon

                                AUGER SPECTRUM


                CORE AND VALENCE I.P.S USED

                  1s   292.420
                  3a'  32.200  4a'  22.700  5a'  17.600  1a"  15.600  6a' 15.100
                  7a'  12.700  2a"  11.000

PEAK NR.  MO.INDEX  MO.NAME   SYM     ABS.ENERGY     REL.ENERGY        ABS.RATE    REL.INT.

  49        47      1a"  2a"    3X       257.54        -34.9        0.0   0.0000000     0.0
  48        67      7a'  2a"    3X       255.17        -37.3        2.4   0.0000001     0.0
  47        77      2a"  2a"   1A1       254.04        -38.4        3.5   0.0000050     1.9
  46        67      7a'  2a"    1X       253.83        -38.6        3.7   0.0000116     4.5
  45        46      1a"  7a'    3X       253.17        -39.2        4.4   0.0000003     0.1
  44        57      6a'  2a"    3X       252.93        -39.5        4.6   0.0000001     0.0
  43        36      5a'  7a'    3X       252.81        -39.6        4.7   0.0000004     0.2
  42        56      6a'  7a'    3X       252.61        -39.8        4.9   0.0000004     0.2
  41        66      7a'  7a'   1A1       252.51        -39.9        5.0   0.0000169     6.6
  40        46      1a"  7a'    1X       252.30        -40.1        5.2   0.0000790    30.8
  39        57      6a'  2a"    1X       252.23        -40.2        5.3   0.0000377    14.7
  38        37      5a'  2a"    3X       251.56        -40.9        6.0   0.0000000     0.0
  37        37      5a'  2a"    1X       250.60        -41.8        6.9   0.0000360    14.0
  36        45      1a"  6a'    3X       250.23        -42.2        7.3   0.0000006     0.2
  35        45      1a"  6a'    1X       249.83        -42.6        7.7   0.0002564   100.0
```

34	56	6a'	7a'	1X	249.78	-42.6	7.8	0.0000699	27.3
33	47	1a"	2a"	1X	249.51	-42.9	8.0	0.0000677	26.4
32	44	1a"	1a"	1A1	248.84	-43.6	8.7	0.0002302	89.8
31	55	6a'	6a'	1A1	248.29	-44.1	9.2	0.0001791	69.8
30	35	5a'	6a'	3X	248.20	-44.2	9.3	0.0000005	0.2
29	34	5a'	1a"	3X	248.13	-44.3	9.4	0.0000000	0.0
28	27	4a'	2a"	3X	247.95	-44.5	9.6	0.0000047	1.9
27	34	5a'	1a"	1X	247.19	-45.2	10.3	0.0002446	95.4
26	26	4a'	7a'	3X	246.58	-45.8	11.0	0.0000093	3.6
25	35	5a'	6a'	1X	246.47	-46.0	11.1	0.0002196	85.7
24	27	4a'	2a"	1X	246.35	-46.1	11.2	0.0000216	8.4
23	36	5a'	7a'	1X	246.04	-46.4	11.5	0.0001041	40.6
22	33	5a'	5a'	1A1	244.89	-47.5	12.6	0.0001639	63.9
21	26	4a'	7a'	1X	244.81	-47.6	12.7	0.0000428	16.7
20	25	4a'	6a'	3X	244.46	-48.0	13.1	0.0000316	12.3
19	24	4a'	1a"	3X	243.36	-49.1	14.2	0.0000323	12.6
18	23	4a'	5a'	3X	241.63	-50.8	15.9	0.0000271	10.6
17	24	4a'	1a"	1X	241.49	-50.9	16.0	0.0001469	57.3
16	25	4a'	6a'	1X	240.94	-51.5	16.6	0.0001556	60.7
15	23	4a'	5a'	1X	239.80	-52.6	17.7	0.0001254	48.9
14	17	3a'	2a"	3X	235.89	-56.5	21.7	0.0000057	2.2
13	22	4a'	4a'	1A1	235.05	-57.4	22.5	0.0000977	38.1
12	16	3a'	7a'	3X	234.95	-57.5	22.6	0.0000100	3.9
11	14	3a'	1a"	3X	233.62	-58.8	23.9	0.0000385	15.0
10	15	3a'	6a'	3X	232.73	-59.7	24.8	0.0000321	12.5
9	16	3a'	7a'	1X	232.62	-59.8	24.9	0.0000373	14.6
8	17	3a'	2a"	1X	232.52	-59.9	25.0	0.0000191	7.4
7	14	3a'	1a"	1X	231.83	-60.6	25.7	0.0001299	50.7
6	13	3a'	5a'	3X	230.98	-61.4	26.6	0.0000327	12.7
5	15	3a'	6a'	1X	230.12	-62.3	27.4	0.0001232	48.1
4	13	3a'	5a'	1X	228.78	-63.6	28.8	0.0001105	43.1
3	12	3a'	4a'	3X	228.21	-64.2	29.3	0.0000153	6.0
2	12	3a'	4a'	1X	223.90	-68.5	33.6	0.0002115	82.5
1	11	3a'	3a'	1A1	213.05	-79.4	44.5	0.0001135	44.2

Total Transition Rate (in au) = 3.29837E-03

D.2.3.2. Methanol - O(KVV)

```
       CALCULATIONS FOR CH3OH, geom. LB7/II p.148

   6      0.0000000      0.0000000      0.0000000
   1      1.9381039      0.0000000     -0.7179596
   1     -0.9689416     -1.6782560     -0.7179596
   1     -0.9689416      1.6782560     -0.7179596
   1     -1.5032893      0.0000000      3.3508968
   8      0.1549684      0.0000000      2.6876221
 DEGENERACY OF OCCUPIED ORBITALS
1 1 1 1 1 1 1

     EIGENVECTORS
-0.2849  -0.6440  -0.1363   0.0000  -0.1758   0.0024   0.0000
 0.0030  -0.0405   0.2961   0.0000  -0.0777   0.6633   0.0000
 0.0000   0.0000   0.0000  -0.3435   0.0000   0.0000  -0.6414
-0.2118   0.0905   0.1524   0.0000   0.4291  -0.0216   0.0000
-0.0803  -0.3209   0.0662   0.0000  -0.2301   0.5343   0.0000
-0.0835  -0.2959  -0.1775   0.1699  -0.1621  -0.2643   0.4569
-0.0835  -0.2959  -0.1775  -0.1699  -0.1621  -0.2643  -0.4569
-0.2902   0.1772  -0.3665   0.0000  -0.0307   0.1608   0.0000
-0.8690   0.2457   0.2201   0.0000  -0.0852  -0.0777   0.0000
 0.0877  -0.1105   0.7674   0.0000  -0.3062  -0.3201   0.0000
 0.0000   0.0000   0.0000  -0.9079   0.0000   0.0000   0.4137
 0.0802   0.4397  -0.1770   0.0000  -0.7560   0.0015   0.0000


   MOLECULAR J(PP,QQ) COULOMB INTEGRALS
0.5502  0.4214  0.4682  0.4372  0.5034  0.5048  0.5519
0.4214  0.4398  0.4191  0.4298  0.4380  0.4162  0.4251
0.4682  0.4191  0.4530  0.4248  0.4553  0.4666  0.4682
0.4372  0.4298  0.4248  0.4551  0.4297  0.4184  0.4518
0.5034  0.4380  0.4553  0.4297  0.5118  0.4934  0.5050
0.5048  0.4162  0.4666  0.4184  0.4934  0.5333  0.5226
0.5519  0.4251  0.4682  0.4518  0.5050  0.5226  0.6020


   MOLECULAR K(PQ,PQ) EXCHANGE INTEGRALS
0.5502  0.0793  0.0403  0.0329  0.0480  0.0429  0.0619
0.0793  0.4398  0.0336  0.0343  0.0648  0.0325  0.0294
0.0403  0.0336  0.4530  0.0173  0.0318  0.1244  0.0178
0.0329  0.0343  0.0173  0.4551  0.0073  0.0161  0.1474
0.0480  0.0648  0.0318  0.0073  0.5118  0.0521  0.0128
0.0429  0.0325  0.1244  0.0161  0.0521  0.5333  0.0246
0.0619  0.0294  0.0178  0.1474  0.0128  0.0246  0.6020

                MOLECULE: CH3OH          ATOM: Oxygen

                                AUGER SPECTRUM

                CORE AND VALENCE I.P.S USED

                 1s   539.130
                 3a'  32.200  4a'  22.700  5a'  17.600  1a"  15.600  6a' 15.100
                 7a'  12.700  2a"  11.000

PEAK NR.  MO.INDEX  MO.NAME   SYM     ABS.ENERGY    REL.ENERGY    ABS.RATE   REL.INT.

  49        47      1a"  2a"    3X      504.25       -34.9        0.0   0.0000000    0.0
  48        67      7a'  2a"    3X      501.88       -37.3        2.4   0.0000002    0.0
  47        77      2a"  2a"   1A1      500.75       -38.4        3.5   0.0000248    4.2
  46        67      7a'  2a"    1X      500.54       -38.6        3.7   0.0000193    3.3
  45        46      1a"  7a'    3X      499.88       -39.2        4.4   0.0000010    0.2
  44        57      6a'  2a"    3X      499.64       -39.5        4.6   0.0000002    0.0
  43        36      5a'  7a'    3X      499.52       -39.6        4.7   0.0000001    0.0
  42        56      6a'  7a'    3X      499.32       -39.8        4.9   0.0000007    0.1
  41        66      7a'  7a'   1A1      499.22       -39.9        5.0   0.0000093    1.6
  40        46      1a"  7a'    1X      499.01       -40.1        5.2   0.0000931   15.8
  39        57      6a'  2a"    1X      498.94       -40.2        5.3   0.0001221   20.8
  38        37      5a'  2a"    3X      498.27       -40.9        6.0   0.0000017    0.3
  37        37      5a'  2a"    1X      497.31       -41.8        6.9   0.0001183   20.1
  36        45      1a"  6a'    3X      496.94       -42.2        7.3   0.0000012    0.2
  35        45      1a"  6a'    1X      496.54       -42.6        7.7   0.0005880  100.0
```

34	56	6a'	7a'	1X	496.49	-42.6	7.8	0.0000815	13.9
33	47	1a"	2a"	1X	496.22	-42.9	8.0	0.0002388	40.6
32	44	1a"	1a"	1A1	495.55	-43.6	8.7	0.0005750	97.8
31	55	6a'	6a'	1A1	495.00	-44.1	9.2	0.0003774	64.2
30	35	5a'	6a'	3X	494.91	-44.2	9.3	0.0000066	1.1
29	34	5a'	1a"	3X	494.84	-44.3	9.4	0.0000080	1.4
28	27	4a'	2a"	3X	494.66	-44.5	9.6	0.0000021	0.4
27	34	5a'	1a"	1X	493.90	-45.2	10.3	0.0005696	96.9
26	26	4a'	7a'	3X	493.29	-45.8	11.0	0.0000018	0.3
25	35	5a'	6a'	1X	493.18	-46.0	11.1	0.0004694	79.8
24	27	4a'	2a"	1X	493.06	-46.1	11.2	0.0000439	7.5
23	36	5a'	7a'	1X	492.75	-46.4	11.5	0.0001111	18.9
22	33	5a'	5a'	1A1	491.60	-47.5	12.6	0.0003448	58.6
21	26	4a'	7a'	1X	491.52	-47.6	12.7	0.0000286	4.9
20	25	4a'	6a'	3X	491.17	-48.0	13.1	0.0000058	1.0
19	24	4a'	1a"	3X	490.07	-49.1	14.2	0.0000099	1.7
18	23	4a'	5a'	3X	488.34	-50.8	15.9	0.0000129	2.2
17	24	4a'	1a"	1X	488.20	-50.9	16.0	0.0002116	36.0
16	25	4a'	6a'	1X	487.65	-51.5	16.6	0.0002277	38.7
15	23	4a'	5a'	1X	486.51	-52.6	17.7	0.0001878	31.9
14	17	3a'	2a"	3X	482.60	-56.5	21.7	0.0000257	4.4
13	22	4a'	4a'	1A1	481.76	-57.4	22.5	0.0000459	7.8
12	16	3a'	7a'	3X	481.66	-57.5	22.6	0.0000162	2.8
11	14	3a'	1a"	3X	480.33	-58.8	23.9	0.0001240	21.1
10	15	3a'	6a'	3X	479.44	-59.7	24.8	0.0001027	17.5
9	16	3a'	7a'	1X	479.33	-59.8	24.9	0.0000582	9.9
8	17	3a'	2a"	1X	479.23	-59.9	25.0	0.0000833	14.2
7	14	3a'	1a"	1X	478.54	-60.6	25.7	0.0004014	68.3
6	13	3a'	5a'	3X	477.69	-61.4	26.6	0.0000975	16.6
5	15	3a'	6a'	1X	476.83	-62.3	27.4	0.0003387	57.6
4	13	3a'	5a'	1X	475.49	-63.6	28.8	0.0003664	62.3
3	12	3a'	4a'	3X	474.92	-64.2	29.3	0.0000333	5.7
2	12	3a'	4a'	1X	470.61	-68.5	33.6	0.0001777	30.2
1	11	3a'	3a'	1A1	459.76	-79.4	44.5	0.0004826	82.1

Total Transition Rate (in au) = 6.84778E-03

D.2.4.1. Methyl fluoride - C(KVV)

```
       CALCULATIONS FOR CH3F, geom. LB7/II

   9       0.0000000       0.0000000       2.6116025
   6       0.0000000       0.0000000       0.0000000
   1      -1.6996789      -0.9813106      -0.6556842
   1       1.6996789      -0.9813106      -0.6556842
   1       0.0000000       1.9626193      -0.6556842
 DEGENERACY OF OCCUPIED ORBITALS
1 1 2 2 1 2 2


      EIGENVECTORS
  0.7750  -0.5400   0.0000   0.0000  -0.2562   0.0000   0.0000
  0.0000   0.0000   0.5758   0.0000   0.0000   0.8152   0.0000
  0.0000   0.0000   0.0000   0.5758   0.0000   0.0000   0.8152
 -0.1615  -0.1498   0.0000   0.0000  -0.7057   0.0000   0.0000
  0.5090   0.6348   0.0000   0.0000   0.0307   0.0000   0.0000
  0.0000   0.0000   0.6641   0.0000   0.0000  -0.4214   0.0000
  0.0000   0.0000   0.0000   0.6641   0.0000   0.0000  -0.4214
  0.2046  -0.2613   0.0000   0.0000   0.6230   0.0000   0.0000
  0.1553   0.2676  -0.3373  -0.1947  -0.1256   0.2810   0.1622
  0.1553   0.2676   0.3373  -0.1947  -0.1256  -0.2810   0.1622
  0.1553   0.2676   0.0000   0.3894  -0.1256   0.0000  -0.3244


     MOLECULAR J(PP,QQ) COULOMB INTEGRALS
  0.6964   0.4469   0.5459   0.5459   0.6541   0.5956   0.5956
  0.4469   0.4635   0.4513   0.4513   0.4729   0.4441   0.4441
  0.5459   0.4513   0.5048   0.4770   0.5340   0.5228   0.4916
  0.5459   0.4513   0.4770   0.5048   0.5340   0.4916   0.5228
  0.6541   0.4729   0.5340   0.5340   0.7044   0.5780   0.5780
  0.5956   0.4441   0.5228   0.4916   0.5780   0.5601   0.5226
  0.5956   0.4441   0.4916   0.5228   0.5780   0.5226   0.5601


     MOLECULAR K(PQ,PQ) EXCHANGE INTEGRALS
  0.6964   0.0814   0.0603   0.0603   0.0826   0.0764   0.0764
  0.0814   0.4635   0.0384   0.0384   0.0874   0.0387   0.0387
  0.0603   0.0384   0.5048   0.0139   0.0180   0.2074   0.0156
  0.0603   0.0384   0.0139   0.5048   0.0180   0.0156   0.2074
  0.0826   0.0874   0.0180   0.0180   0.7044   0.0222   0.0222
  0.0764   0.0387   0.2074   0.0156   0.0222   0.5601   0.0188
  0.0764   0.0387   0.0156   0.2074   0.0222   0.0188   0.5601


    SPECIAL J(PQ,RS) AND K(PS,RQ) INTEGRALS
       3    4    6    7   0.0156   0.0156
       3    4    7    6   0.0156   0.1762

                    MOLECULE: CH3F          ATOM: Carbon

                                  AUGER SPECTRUM

                    CORE AND VALENCE I.P.S USED

                     1s   293.600
                     3a1  38.400  4a1  23.400  1e   17.000  1e   17.000  5a1 17.000
                     2e   13.100  2e   13.100
```

PEAK NR.	MO.INDEX	MO.NAME	SYM	ABS.ENERGY	REL.ENERGY		ABS.RATE	REL.INT.
33	36	1e 2e	3E	254.92	-38.7	0.0	0.0000000	0.0
32	36	1e 2e	3A1	254.92	-38.7	0.0	0.0000000	0.0
31	36	1e 2e	1A2	254.92	-38.7	0.0	0.0000000	0.0
30	67	2e 2e	3A2	253.69	-39.9	1.2	0.0000000	0.0
29	67	2e 2e	1E	252.67	-40.9	2.2	0.0000664	16.2
28	66	2e 2e	1A1	251.65	-42.0	3.3	0.0000195	4.8
27	56	5a1 2e	3E	248.38	-45.2	6.5	0.0000001	0.0
26	56	5a1 2e	1E	247.17	-46.4	7.7	0.0001454	35.5
25	34	1e 1e	3A2	247.00	-46.6	7.9	0.0000000	0.0
24	34	1e 1e	1E	246.24	-47.4	8.7	0.0004098	100.0
23	36	1e 2e	3A2	246.18	-47.4	8.7	0.0000000	0.0
22	26	4a1 2e	3E	246.07	-47.5	8.8	0.0000297	7.3
21	35	1e 5a1	3X	245.56	-48.0	9.4	0.0000002	0.0

20	33	1e	1e	1A1	245.49	-48.1	9.4	0.0001205	29.4
19	35	1e	5a1	1X	244.58	-49.0	10.3	0.0003611	88.1
18	36	1e	2e	1E	244.48	-49.1	10.4	0.0003300	80.5
17	26	4a1	2e	1E	243.96	-49.6	11.0	0.0001138	27.8
16	36	1e	2e	1A1	242.78	-50.8	12.1	0.0000971	23.7
15	25	4a1	5a1	3X	242.71	-50.9	12.2	0.0000338	8.3
14	23	4a1	1e	3E	241.96	-51.6	13.0	0.0000738	18.0
13	55	5a1	5a1	1A1	240.43	-53.2	14.5	0.0001262	30.8
12	23	4a1	1e	1E	239.87	-53.7	15.0	0.0002825	68.9
11	25	4a1	5a1	1X	237.95	-55.6	17.0	0.0001418	34.6
10	22	4a1	4a1	1A1	234.19	-59.4	20.7	0.0001583	38.6
9	16	3a1	2e	3E	227.97	-65.6	26.9	0.0000191	4.7
8	13	3a1	1e	3E	224.99	-68.6	29.9	0.0000475	11.6
7	16	3a1	2e	1E	223.81	-69.8	31.1	0.0000724	17.7
6	15	3a1	5a1	3X	222.65	-71.0	32.3	0.0000201	4.9
5	12	3a1	4a1	3X	221.85	-71.7	33.1	0.0000144	3.5
4	13	3a1	1e	1E	221.70	-71.9	33.2	0.0001798	43.9
3	15	3a1	5a1	1X	218.15	-75.4	36.8	0.0000894	21.8
2	12	3a1	4a1	1X	217.42	-76.2	37.5	0.0002072	50.6
1	11	3a1	3a1	1A1	197.85	-95.8	57.1	0.0000650	15.9

Total Transition Rate (in au) = 3.22499E-03

D.2.4.2. Methyl fluoride - F(KVV)

```
      CALCULATIONS FOR CH3F, geom. LB7/II

   9       0.0000000       0.0000000       2.6116025
   6       0.0000000       0.0000000       0.0000000
   1      -1.6996789      -0.9813106      -0.6556842
   1       1.6996789      -0.9813106      -0.6556842
   1       0.0000000       1.9626193      -0.6556842
 DEGENERACY OF OCCUPIED ORBITALS
1 1 2 2 1 2 2


      EIGENVECTORS
  0.9383  -0.2605   0.0000   0.0000   0.0246   0.0000   0.0000
  0.0000   0.0000   0.9684   0.0000   0.0000   0.2436   0.0000
  0.0000   0.0000   0.0000   0.9684   0.0000   0.0000   0.2436
 -0.1002  -0.7138   0.0000   0.0000  -0.6035   0.0000   0.0000
  0.2318   0.5274   0.0000   0.0000  -0.4764   0.0000   0.0000
  0.0000   0.0000   0.2149   0.0000   0.0000  -0.7087   0.0000
  0.0000   0.0000   0.0000   0.2149   0.0000   0.0000  -0.7087
  0.2104   0.0479   0.0000   0.0000   0.3872   0.0000   0.0000
  0.0621   0.2177  -0.0893  -0.0516  -0.2934   0.4682   0.2703
  0.0621   0.2177   0.0893  -0.0516  -0.2934  -0.4682   0.2703
  0.0621   0.2177   0.0000   0.1032  -0.2934   0.0000  -0.5406


    MOLECULAR J(PP,QQ) COULOMB INTEGRALS
  0.6964   0.4469   0.5459   0.5459   0.6541   0.5956   0.5956
  0.4469   0.4635   0.4513   0.4513   0.4729   0.4441   0.4441
  0.5459   0.4513   0.5048   0.4770   0.5340   0.5228   0.4916
  0.5459   0.4513   0.4770   0.5048   0.5340   0.4916   0.5228
  0.6541   0.4729   0.5340   0.5340   0.7044   0.5780   0.5780
  0.5956   0.4441   0.5228   0.4916   0.5780   0.5601   0.5226
  0.5956   0.4441   0.4916   0.5228   0.5780   0.5226   0.5601


    MOLECULAR K(PQ,PQ) EXCHANGE INTEGRALS
  0.6964   0.0814   0.0603   0.0603   0.0826   0.0764   0.0764
  0.0814   0.4635   0.0384   0.0384   0.0874   0.0387   0.0387
  0.0603   0.0384   0.5048   0.0139   0.0180   0.2074   0.0156
  0.0603   0.0384   0.0139   0.5048   0.0180   0.0156   0.2074
  0.0826   0.0874   0.0180   0.0180   0.7044   0.0222   0.0222
  0.0764   0.0387   0.2074   0.0156   0.0222   0.5601   0.0188
  0.0764   0.0387   0.0156   0.2074   0.0222   0.0188   0.5601


   SPECIAL J(PQ,RS) AND K(PS,RQ) INTEGRALS
     3    4    6    7   0.0156   0.0156
     3    4    7    6   0.0156   0.1762

                    MOLECULE: CH3F          ATOM: Fluorine

                                    AUGER SPECTRUM

                    CORE AND VALENCE I.P.S USED

                     1s   692.920
                     3a1  38.400  4a1  23.400  1e   17.000  1e   17.000  5a1 17.000
                     2e   13.100  2e   13.100

PEAK NR.  MO.INDEX   MO.NAME    SYM     ABS.ENERGY     REL.ENERGY          ABS.RATE    REL.INT.

  33        36       1e   2e     3E       654.24        -38.7       0.0     0.0000000     0.0
  32        36       1e   2e     3A1      654.24        -38.7       0.0     0.0000000     0.0
  31        36       1e   2e     1A2      654.24        -38.7       0.0     0.0000000     0.0
  30        67       2e   2e     3A2      653.01        -39.9       1.2     0.0000000     0.0
  29        67       2e   2e      1E      651.99        -40.9       2.2     0.0000074     0.4
  28        66       2e   2e     1A1      650.97        -42.0       3.3     0.0000022     0.1
  27        56       5a1  2e      3E      647.70        -45.2       6.5     0.0000000     0.0
  26        56       5a1  2e      1E      646.49        -46.4       7.7     0.0000456     2.5
  25        34       1e   1e     3A2      646.32        -46.6       7.9     0.0000000     0.0
  24        34       1e   1e      1E      645.56        -47.4       8.7     0.0018529   100.0
  23        36       1e   2e     3A2      645.50        -47.4       8.7     0.0000000     0.0
  22        26       4a1  2e      3E      645.39        -47.5       8.8     0.0000015     0.1
  21        35       1e   5a1     3X      644.88        -48.0       9.4     0.0000002     0.0
```

20	33	1e	1e	1A1	644.81	-48.1	9.4	0.0005417	29.2
19	35	1e	5a1	1X	643.90	-49.0	10.3	0.0007203	38.9
18	36	1e	2e	1E	643.80	-49.1	10.4	0.0002345	12.7
17	26	4a1	2e	1E	643.28	-49.6	11.0	0.0000687	3.7
16	36	1e	2e	1A1	642.10	-50.8	12.1	0.0000685	3.7
15	25	4a1	5a1	3X	642.03	-50.9	12.2	0.0000059	0.3
14	23	4a1	1e	3E	641.28	-51.6	13.0	0.0000244	1.3
13	55	5a1	5a1	1A1	639.75	-53.2	14.5	0.0001108	6.0
12	23	4a1	1e	1E	639.19	-53.7	15.0	0.0010862	58.6
11	25	4a1	5a1	1X	637.27	-55.6	17.0	0.0003257	17.6
10	22	4a1	4a1	1A1	633.51	-59.4	20.7	0.0002408	13.0
9	16	3a1	2e	3E	627.29	-65.6	26.9	0.0000201	1.1
8	13	3a1	1e	3E	624.31	-68.6	29.9	0.0003170	17.1
7	16	3a1	2e	1E	623.13	-69.8	31.1	0.0000666	3.6
6	15	3a1	5a1	3X	621.97	-71.0	32.3	0.0000610	3.3
5	12	3a1	4a1	3X	621.17	-71.7	33.1	0.0000930	5.0
4	13	3a1	1e	1E	621.02	-71.9	33.2	0.0010522	56.8
3	15	3a1	5a1	1X	617.47	-75.4	36.8	0.0002074	11.2
2	12	3a1	4a1	1X	616.74	-76.2	37.5	0.0003894	21.0
1	11	3a1	3a1	1A1	597.17	-95.8	57.1	0.0006460	34.9

Total Transition Rate (in au) = 8.19009E-03

D.3.1.1. Acetaldehyde - C(KVV) in CHO

CALCULATIONS FOR CH3CHO, geom. LB II/7 p.185

1	0.0000000	-1.9207902	-0.7226844
1	1.6634529	0.9603951	-0.7226844
1	-1.6634529	0.9603951	-0.7226844
1	0.0000000	1.8672960	3.8151309
6	0.0000000	0.0000000	0.0000000
6	0.0000000	0.0000000	2.8355353
8	0.0000000	-1.9065075	4.1166549

DEGENERACY OF OCCUPIED ORBITALS

1 1 1 1 1 1 1 1 1

EIGENVECTORS

-0.0894	-0.2042	0.2667	-0.0701	0.0000	-0.2644	-0.4891	0.0000	0.1481
-0.0675	-0.2474	0.1335	-0.2513	-0.2699	-0.0491	0.2754	0.3939	0.0134
-0.0675	-0.2474	0.1335	-0.2513	0.2699	-0.0491	0.2754	-0.3939	0.0134
-0.1673	-0.1097	-0.4029	-0.1842	0.0000	0.0660	-0.1410	0.0000	0.3597
-0.2322	-0.5721	0.3108	-0.2226	0.0000	-0.0926	-0.0054	0.0000	-0.0508
0.0000	0.0000	0.0000	0.0000	-0.4802	0.0000	0.0000	0.5420	0.0000
0.0342	-0.0579	-0.1638	-0.1970	0.0000	0.2211	0.6351	0.0000	-0.0902
-0.1396	-0.0833	-0.1704	0.3666	0.0000	0.3122	-0.0755	0.0000	-0.2774
-0.6248	-0.2499	-0.4041	0.2084	0.0000	0.0131	-0.0390	0.0000	-0.0254
0.0000	0.0000	0.0000	0.0000	-0.6318	0.0000	0.0000	-0.3629	0.0000
0.1969	-0.2324	-0.4157	-0.3182	0.0000	0.2839	-0.2058	0.0000	0.2164
-0.0831	0.3848	-0.2295	-0.3305	0.0000	-0.4059	0.0664	0.0000	0.3262
-0.6176	0.4639	0.3128	-0.2885	0.0000	0.3680	-0.0494	0.0000	-0.0034
0.0000	0.0000	0.0000	0.0000	-0.4739	0.0000	0.0000	-0.5141	0.0000
-0.2005	0.0615	-0.2669	-0.0079	0.0000	-0.6069	0.1017	0.0000	-0.4501
0.1509	0.0525	-0.1433	-0.5244	0.0000	0.1291	-0.3450	0.0000	-0.6357

MOLECULAR J(PP,QQ) COULOMB INTEGRALS

0.5052	0.3744	0.3920	0.3980	0.3477	0.3964	0.4339	0.4593	0.4876
0.3744	0.3940	0.3524	0.3907	0.3895	0.3780	0.3679	0.3730	0.3581
0.3920	0.3524	0.4256	0.3560	0.3417	0.3649	0.3709	0.3685	0.3915
0.3980	0.3907	0.3560	0.4147	0.3805	0.3807	0.3973	0.3965	0.3970
0.3477	0.3895	0.3417	0.3805	0.4055	0.3602	0.3448	0.3595	0.3240
0.3964	0.3780	0.3649	0.3807	0.3602	0.4224	0.4063	0.3919	0.4005
0.4339	0.3679	0.3709	0.3973	0.3448	0.4063	0.4426	0.4251	0.4452
0.4593	0.3730	0.3685	0.3965	0.3595	0.3919	0.4251	0.4593	0.4562
0.4876	0.3581	0.3915	0.3970	0.3240	0.4005	0.4452	0.4562	0.5267

MOLECULAR K(PQ,PQ) EXCHANGE INTEGRALS

0.5052	0.0829	0.0270	0.0280	0.0176	0.0274	0.0293	0.0393	0.0466
0.0829	0.3940	0.0253	0.0591	0.0289	0.0286	0.0279	0.0255	0.0252
0.0270	0.0253	0.4256	0.0088	0.0068	0.0769	0.0351	0.0095	0.0589
0.0280	0.0591	0.0088	0.4147	0.0189	0.0132	0.0843	0.0185	0.0780
0.0176	0.0289	0.0068	0.0189	0.4055	0.0069	0.0107	0.1214	0.0041
0.0274	0.0286	0.0769	0.0132	0.0069	0.4224	0.0996	0.0125	0.0580
0.0293	0.0279	0.0351	0.0843	0.0107	0.0996	0.4426	0.0152	0.0232
0.0393	0.0255	0.0095	0.0185	0.1214	0.0125	0.0152	0.4593	0.0106
0.0466	0.0252	0.0589	0.0780	0.0041	0.0580	0.0232	0.0106	0.5267

MOLECULE: CH3CHO ATOM: Carbon in CHO

AUGER SPECTRUM

CORE AND VALENCE I.P.S USED

1s 293.830
4a' 33.390 5a' 24.200 6a' 19.400 7a' 16.500 1a" 15.400
8a' 15.400 9a' 14.200 2a" 13.200 10a' 10.300

PEAK NR.	MO.INDEX	MO.NAME	SYM	ABS.ENERGY	REL.ENERGY		ABS.RATE	REL.INT.
81	59	1a" 10a'	3X	259.43	-34.4	0.0	0.0000001	0.0
80	59	1a" 10a'	1X	259.20	-34.6	0.2	0.0000646	35.2
79	99	10a' 10a'	1A1	258.90	-34.9	0.5	0.0000197	10.7
78	69	8a' 10a'	3X	258.81	-35.0	0.6	0.0000000	0.0
77	58	1a" 2a"	3X	258.75	-35.1	0.7	0.0000000	0.0
76	49	7a' 10a'	3X	258.35	-35.5	1.1	0.0000010	0.6
75	89	2a" 10a'	3X	258.20	-35.6	1.2	0.0000000	0.0
74	79	9a' 10a'	3X	257.85	-36.0	1.6	0.0000001	0.0
73	89	2a" 10a'	1X	257.63	-36.2	1.8	0.0000213	11.6

72	79	9a'	10a'	1X	256.58	-37.2	2.8	0.0000080	4.4
71	67	8a'	9a'	3X	255.88	-37.9	3.5	0.0000001	0.0
70	69	8a'	10a'	1X	255.65	-38.2	3.8	0.0000428	23.4
69	78	9a'	2a"	3X	255.28	-38.6	4.1	0.0000000	0.0
68	57	1a"	9a'	3X	255.14	-38.7	4.3	0.0000001	0.1
67	39	6a'	10a'	3X	255.08	-38.8	4.3	0.0000059	3.2
66	88	2a"	2a"	1A1	254.93	-38.9	4.5	0.0000145	7.9
65	68	8a'	2a"	3X	254.91	-38.9	4.5	0.0000000	0.0
64	47	7a'	9a'	3X	254.61	-39.2	4.8	0.0000006	0.3
63	57	1a"	9a'	1X	254.56	-39.3	4.9	0.0000200	10.9
62	78	9a'	2a"	1X	254.45	-39.4	5.0	0.0000066	3.6
61	68	8a'	2a"	1X	254.23	-39.6	5.2	0.0000340	18.6
60	49	7a'	10a'	1X	254.10	-39.7	5.3	0.0000574	31.3
59	48	7a'	2a"	3X	253.84	-40.0	5.6	0.0000012	0.6
58	56	1a"	8a'	3X	253.42	-40.4	6.0	0.0000000	0.0
57	77	9a'	9a'	1A1	253.39	-40.4	6.0	0.0000019	1.0
56	56	1a"	8a'	1X	253.04	-40.8	6.4	0.0001032	56.3
55	48	7a'	2a"	1X	252.84	-41.0	6.6	0.0000327	17.8
54	58	1a"	2a"	1X	252.14	-41.7	7.3	0.0000879	47.9
53	45	7a'	1a"	3X	252.09	-41.7	7.3	0.0000036	2.0
52	55	1a"	1a"	1A1	252.00	-41.8	7.4	0.0001333	72.7
51	46	7a'	8a'	3X	251.93	-41.9	7.5	0.0000022	1.2
50	39	6a'	10a'	1X	251.87	-42.0	7.6	0.0000691	37.7
49	66	8a'	8a'	1A1	251.54	-42.3	7.9	0.0000504	27.5
48	38	6a'	2a"	3X	251.46	-42.4	8.0	0.0000045	2.4
47	46	7a'	8a'	1X	251.21	-42.6	8.2	0.0000622	33.9
46	36	6a'	8a'	3X	251.19	-42.6	8.2	0.0000083	4.5
45	37	6a'	9a'	3X	251.09	-42.7	8.3	0.0000012	0.7
44	45	7a'	1a"	1X	251.06	-42.8	8.4	0.0000992	54.1
43	38	6a'	2a"	1X	250.94	-42.9	8.5	0.0000445	24.3
42	67	8a'	9a'	1X	250.46	-43.4	9.0	0.0000168	9.2
41	29	5a'	10a'	3X	250.27	-43.6	9.2	0.0000018	1.0
40	47	7a'	9a'	1X	250.02	-43.8	9.4	0.0000131	7.2
39	35	6a'	1a"	3X	249.92	-43.9	9.5	0.0000135	7.4
38	35	6a'	1a"	1X	249.55	-44.3	9.9	0.0001350	73.6
37	44	7a'	7a'	1A1	249.55	-44.3	9.9	0.0000437	23.9
36	37	6a'	9a'	1X	249.18	-44.6	10.2	0.0000194	10.6
35	29	5a'	10a'	1X	248.90	-44.9	10.5	0.0000421	23.0
34	34	6a'	7a'	3X	248.48	-45.3	10.9	0.0000165	9.0
33	34	6a'	7a'	1X	248.00	-45.8	11.4	0.0001184	64.6
32	36	6a'	8a'	1X	247.01	-46.8	12.4	0.0000834	45.5
31	28	5a'	2a"	3X	246.97	-46.9	12.5	0.0000017	0.9
30	27	5a'	9a'	3X	246.18	-47.7	13.2	0.0000004	0.2
29	28	5a'	2a"	1X	245.59	-48.2	13.8	0.0000331	18.0
28	26	5a'	8a'	3X	244.72	-49.1	14.7	0.0000029	1.6
27	27	5a'	9a'	1X	244.66	-49.2	14.8	0.0000154	8.4
26	25	5a'	1a"	3X	244.42	-49.4	15.0	0.0000052	2.8
25	24	5a'	7a'	3X	244.11	-49.7	15.3	0.0000034	1.9
24	33	6a'	6a'	1A1	243.45	-50.4	16.0	0.0000858	46.8
23	26	5a'	8a'	1X	243.17	-50.7	16.3	0.0000922	50.3
22	25	5a'	1a"	1X	242.84	-51.0	16.6	0.0001003	54.7
21	23	5a'	6a'	3X	241.33	-52.5	18.1	0.0000094	5.1
20	24	5a'	7a'	1X	240.89	-52.9	18.5	0.0000644	35.1
19	23	5a'	6a'	1X	239.95	-53.9	19.5	0.0000944	51.5
18	19	4a'	10a'	3X	238.14	-55.7	21.3	0.0000123	6.7
17	15	4a'	1a"	3X	236.06	-57.8	23.4	0.0000324	17.6
16	18	4a'	2a"	3X	235.81	-58.0	23.6	0.0000107	5.8
15	19	4a'	10a'	1X	235.60	-58.2	23.8	0.0000448	24.4
14	17	4a'	9a'	3X	235.23	-58.6	24.2	0.0000043	2.3
13	15	4a'	1a"	1X	235.10	-58.7	24.3	0.0001152	62.8
12	16	4a'	8a'	3X	235.00	-58.8	24.4	0.0000202	11.0
11	22	5a'	5a'	1A1	234.71	-59.1	24.7	0.0000445	24.3
10	14	4a'	7a'	3X	233.87	-60.0	25.6	0.0000156	8.5
9	18	4a'	2a"	1X	233.67	-60.2	25.8	0.0000380	20.7
8	17	4a'	9a'	1X	233.64	-60.2	25.8	0.0000160	8.7
7	16	4a'	8a'	1X	233.51	-60.3	25.9	0.0000760	41.5
6	14	4a'	7a'	1X	232.35	-61.5	27.1	0.0000912	49.8
5	13	4a'	6a'	3X	231.11	-62.7	28.3	0.0000264	14.4
4	13	4a'	6a'	1X	229.64	-64.2	29.8	0.0001834	100.0
3	12	4a'	5a'	3X	228.31	-65.5	31.1	0.0000220	12.0
2	12	4a'	5a'	1X	223.80	-70.0	35.6	0.0001071	58.4
1	11	4a'	4a'	1A1	213.30	-80.5	46.1	0.0001422	77.5

Total Transition Rate (in au) = 3.01700E-03

D.3.1.2. Acetaldehyde - O(KVV)

```
      CALCULATIONS FOR CH3CHO, geom. LBII/7 p.185

   1      0.0000000     -1.9207902     -0.7226844
   1      1.6634529      0.9603951     -0.7226844
   1     -1.6634529      0.9603951     -0.7226844
   1      0.0000000      1.8672960      3.8151309
   6      0.0000000      0.0000000      0.0000000
   6      0.0000000      0.0000000      2.8355353
   8      0.0000000     -1.9065075      4.1166549
 DEGENERACY OF OCCUPIED ORBITALS
1 1 1 1 1 1 1 1 1

     EIGENVECTORS
 0.0572   0.2396  -0.2062   0.0171   0.0000  -0.3008   0.3299   0.0000  -0.3859
 0.0293   0.2658  -0.0711   0.1976  -0.1641  -0.1156  -0.3035   0.4220   0.0622
 0.0293   0.2658  -0.0711   0.1976   0.1641  -0.1156  -0.3035  -0.4220   0.0622
 0.0973   0.1442   0.4362   0.0982   0.0000   0.1954  -0.0268   0.0000  -0.4408
 0.1210   0.6408  -0.1922   0.1837   0.0000  -0.1796  -0.0053   0.0000   0.0302
 0.0000   0.0000   0.0000   0.0000  -0.3063   0.0000   0.0000   0.6483   0.0000
-0.0434   0.0324   0.1620   0.2000   0.0000   0.1977  -0.5491   0.0000   0.3480
 0.0795   0.1081   0.1379  -0.2270   0.0000   0.3881   0.3168   0.0000   0.3577
 0.4034   0.3808   0.4008  -0.1880   0.0000   0.1875   0.1214   0.0000   0.0000
 0.0000   0.0000   0.0000   0.0000  -0.4625   0.0000   0.0000   0.0773   0.0000
-0.2484   0.1186   0.3303   0.3222   0.0000   0.2601   0.0099   0.0000  -0.2560
 0.1399  -0.3350   0.2942   0.0690   0.0000  -0.2704  -0.2466   0.0000  -0.3699
 0.8286  -0.2652  -0.2112   0.2881   0.0000   0.1292  -0.0095   0.0000   0.0207
 0.0000   0.0000   0.0000   0.0000  -0.7991   0.0000   0.0000  -0.4665   0.0000
 0.1446   0.0088   0.4794  -0.2429   0.0000  -0.6375  -0.0025   0.0000   0.3259
-0.1060  -0.1242   0.2104   0.7078   0.0000  -0.1536   0.4781   0.0000   0.3002

     MOLECULAR J(PP,QQ) COULOMB INTEGRALS
 0.5052   0.3744   0.3920   0.3980   0.3477   0.3964   0.4339   0.4593   0.4876
 0.3744   0.3940   0.3524   0.3907   0.3895   0.3780   0.3679   0.3730   0.3581
 0.3920   0.3524   0.4256   0.3560   0.3417   0.3649   0.3709   0.3685   0.3915
 0.3980   0.3907   0.3560   0.4147   0.3805   0.3807   0.3973   0.3965   0.3970
 0.3477   0.3895   0.3417   0.3805   0.4055   0.3602   0.3448   0.3595   0.3240
 0.3964   0.3780   0.3649   0.3807   0.3602   0.4224   0.4063   0.3919   0.4005
 0.4339   0.3679   0.3709   0.3973   0.3448   0.4063   0.4426   0.4251   0.4452
 0.4593   0.3730   0.3685   0.3965   0.3595   0.3919   0.4251   0.4593   0.4562
 0.4876   0.3581   0.3915   0.3970   0.3240   0.4005   0.4452   0.4562   0.5267

     MOLECULAR K(PQ,PQ) EXCHANGE INTEGRALS
 0.5052   0.0829   0.0270   0.0280   0.0176   0.0274   0.0293   0.0393   0.0466
 0.0829   0.3940   0.0253   0.0591   0.0289   0.0286   0.0279   0.0255   0.0252
 0.0270   0.0253   0.4256   0.0088   0.0068   0.0769   0.0351   0.0095   0.0589
 0.0280   0.0591   0.0088   0.4147   0.0189   0.0132   0.0843   0.0185   0.0780
 0.0176   0.0289   0.0068   0.0189   0.4055   0.0069   0.0107   0.1214   0.0041
 0.0274   0.0286   0.0769   0.0132   0.0069   0.4224   0.0996   0.0125   0.0580
 0.0293   0.0279   0.0351   0.0843   0.0107   0.0996   0.4426   0.0152   0.0232
 0.0393   0.0255   0.0095   0.0185   0.1214   0.0125   0.0152   0.4593   0.0106
 0.0466   0.0252   0.0589   0.0780   0.0041   0.0580   0.0232   0.0106   0.5267

                MOLECULE: CH3CHO          ATOM: Oxygen

                                AUGER SPECTRUM

                CORE AND VALENCE I.P.S USED

                1s   538.430
                4a'  33.390  5a'  24.200  6a'  19.400  7a'  16.500  1a" 15.400
                8a'  15.400  9a'  14.200  2a"  13.200  10a' 10.300

PEAK NR.  MO.INDEX  MO.NAME   SYM    ABS.ENERGY   REL.ENERGY    ABS.RATE    REL.INT.

  81        59      1a"  10a'   3X      504.02      -34.4        0.0      0.0000001    0.0
  80        59      1a"  10a'   1X      503.80      -34.6        0.2      0.0001337   32.3
  79        99      10a' 10a'   1A1     503.50      -34.9        0.5      0.0000327    7.9
  78        69      8a'  10a'   3X      503.41      -35.0        0.6      0.0000010    0.2
  77        58      1a"  2a"    3X      503.35      -35.1        0.7      0.0000000    0.0
  76        49      7a'  10a'   3X      502.95      -35.5        1.1      0.0000030    0.7
  75        89      2a"  10a'   3X      502.80      -35.6        1.2      0.0000000    0.0
  74        79      9a'  10a'   3X      502.45      -36.0        1.6      0.0000000    0.0
  73        89      2a"  10a'   1X      502.23      -36.2        1.8      0.0000456   11.0
```

72	79	9a'	10a'	1X	501.18	-37.2	2.8	0.0000607	14.6
71	67	8a'	9a'	3X	500.48	-37.9	3.5	0.0000007	0.2
70	69	8a'	10a'	1X	500.25	-38.2	3.8	0.0001326	32.0
69	78	9a'	2a"	3X	499.88	-38.6	4.1	0.0000000	0.0
68	57	1a"	9a'	3X	499.74	-38.7	4.3	0.0000000	0.0
67	39	6a'	10a'	3X	499.68	-38.8	4.3	0.0000022	0.5
66	88	2a"	2a"	1A1	499.53	-38.9	4.5	0.0000401	9.7
65	68	8a'	2a"	3X	499.51	-38.9	4.5	0.0000007	0.2
64	47	7a'	9a'	3X	499.21	-39.2	4.8	0.0000042	1.0
63	57	1a"	9a'	1X	499.16	-39.3	4.9	0.0001555	37.6
62	78	9a'	2a"	1X	499.05	-39.4	5.0	0.0000530	12.8
61	68	8a'	2a"	1X	498.83	-39.6	5.2	0.0001020	24.6
60	49	7a'	10a'	1X	498.70	-39.7	5.3	0.0001386	33.5
59	48	7a'	2a"	3X	498.44	-40.0	5.6	0.0000036	0.9
58	56	1a"	8a'	3X	498.02	-40.4	6.0	0.0000021	0.5
57	77	9a'	9a'	1A1	497.99	-40.4	6.0	0.0000442	10.7
56	56	1a"	8a'	1X	497.64	-40.8	6.4	0.0002992	72.3
55	48	7a'	2a"	1X	497.44	-41.0	6.6	0.0001411	34.1
54	58	1a"	2a"	1X	496.74	-41.7	7.3	0.0002352	56.8
53	45	7a'	1a"	3X	496.69	-41.7	7.3	0.0000106	2.6
52	55	1a"	1a"	1A1	496.60	-41.8	7.4	0.0003451	83.3
51	46	7a'	8a'	3X	496.53	-41.9	7.5	0.0000083	2.0
50	39	6a'	10a'	1X	496.47	-42.0	7.6	0.0000932	22.5
49	66	8a'	8a'	1A1	496.14	-42.3	7.9	0.0001608	38.8
48	38	6a'	2a"	3X	496.06	-42.4	8.0	0.0000019	0.5
47	46	7a'	8a'	1X	495.81	-42.6	8.2	0.0002881	69.6
46	36	6a'	8a'	3X	495.79	-42.6	8.2	0.0000011	0.3
45	37	6a'	9a'	3X	495.69	-42.7	8.3	0.0000020	0.5
44	45	7a'	1a"	1X	495.66	-42.8	8.4	0.0004141	100.0
43	38	6a'	2a"	1X	495.54	-42.9	8.5	0.0000696	16.8
42	67	8a'	9a'	1X	495.06	-43.4	9.0	0.0001104	26.7
41	29	5a'	10a'	3X	494.87	-43.6	9.2	0.0000027	0.6
40	47	7a'	9a'	1X	494.62	-43.8	9.4	0.0002204	53.2
39	35	6a'	1a"	3X	494.52	-43.9	9.5	0.0000057	1.4
38	35	6a'	1a"	1X	494.15	-44.3	9.9	0.0002043	49.3
37	44	7a'	7a'	1A1	494.15	-44.3	9.9	0.0002979	71.9
36	37	6a'	9a'	1X	493.78	-44.6	10.2	0.0000793	19.2
35	29	5a'	10a'	1X	493.50	-44.9	10.5	0.0000127	3.1
34	34	6a'	7a'	3X	493.08	-45.3	10.9	0.0000103	2.5
33	34	6a'	7a'	1X	492.60	-45.8	11.4	0.0002004	48.4
32	36	6a'	8a'	1X	491.61	-46.8	12.4	0.0002124	51.3
31	28	5a'	2a"	3X	491.57	-46.9	12.5	0.0000030	0.7
30	27	5a'	9a'	3X	490.78	-47.7	13.2	0.0000033	0.8
29	28	5a'	2a"	1X	490.19	-48.2	13.8	0.0000132	3.2
28	26	5a'	8a'	3X	489.32	-49.1	14.7	0.0000063	1.5
27	27	5a'	9a'	1X	489.26	-49.2	14.8	0.0000161	3.9
26	25	5a'	1a"	3X	489.02	-49.4	15.0	0.0000089	2.2
25	24	5a'	7a'	3X	488.71	-49.7	15.3	0.0000054	1.3
24	33	6a'	6a'	1A1	488.05	-50.4	16.0	0.0000723	17.5
23	26	5a'	8a'	1X	487.77	-50.7	16.3	0.0000283	6.8
22	25	5a'	1a"	1X	487.44	-51.0	16.6	0.0000386	9.3
21	23	5a'	6a'	3X	485.93	-52.5	18.1	0.0000045	1.1
20	24	5a'	7a'	1X	485.49	-52.9	18.5	0.0000488	11.8
19	23	5a'	6a'	1X	484.55	-53.9	19.5	0.0000227	5.5
18	19	4a'	10a'	3X	482.74	-55.7	21.3	0.0000268	6.5
17	15	4a'	1a"	3X	480.66	-57.8	23.4	0.0000873	21.1
16	18	4a'	2a"	3X	480.41	-58.0	23.6	0.0000298	7.2
15	19	4a'	10a'	1X	480.20	-58.2	23.8	0.0000916	22.1
14	17	4a'	9a'	3X	479.83	-58.6	24.2	0.0000311	7.5
13	15	4a'	1a"	1X	479.70	-58.7	24.3	0.0002959	71.5
12	16	4a'	8a'	3X	479.60	-58.8	24.4	0.0000622	15.0
11	22	5a'	5a'	1A1	479.31	-59.1	24.7	0.0000050	1.2
10	14	4a'	7a'	3X	478.47	-60.0	25.6	0.0000876	21.2
9	18	4a'	2a"	1X	478.27	-60.2	25.8	0.0001008	24.4
8	17	4a'	9a'	1X	478.24	-60.2	25.8	0.0001076	26.0
7	16	4a'	8a'	1X	478.11	-60.3	25.9	0.0002231	53.9
6	14	4a'	7a'	1X	476.95	-61.5	27.1	0.0003665	88.5
5	13	4a'	6a'	3X	475.71	-62.7	28.3	0.0000411	9.9
4	13	4a'	6a'	1X	474.24	-64.2	29.8	0.0001813	43.8
3	12	4a'	5a'	3X	472.91	-65.5	31.1	0.0000038	0.9
2	12	4a'	5a'	1X	468.40	-70.0	35.6	0.0000897	21.7
1	11	4a'	4a'	1A1	457.90	-80.5	46.1	0.0004073	98.4

Total Transition Rate (in au) = 6.89239E-03

D.3.1.3. Acetaldehyde - C(KVV) in CH_3

```
      CALCULATIONS FOR CH3CHO, geom. LBII/7 p.185

   1       0.0000000      -1.9207902      -0.7226844
   1       1.6634529       0.9603951      -0.7226844
   1      -1.6634529       0.9603951      -0.7226844
   1       0.0000000       1.8672960       3.8151309
   6       0.0000000       0.0000000       0.0000000
   6       0.0000000       0.0000000       2.8355353
   8       0.0000000      -1.9065075       4.1166549
 DEGENERACY OF OCCUPIED ORBITALS
1 1 1 1 1 1 1 1 1

      EIGENVECTORS
 0.1984   0.1794  -0.3111  -0.0747   0.0000  -0.4168   0.1580   0.0000   0.0942
 0.1755   0.2215  -0.0136   0.2698  -0.3940   0.1264  -0.1274  -0.1986   0.0340
 0.1755   0.2215  -0.0136   0.2698   0.3940   0.1264  -0.1274   0.1986   0.0340
 0.1435  -0.0336   0.4419   0.1161   0.0000  -0.2576   0.2083   0.0000   0.3675
 0.5334   0.5629  -0.1264   0.0756   0.0000   0.0108   0.0448   0.0000  -0.1608
 0.0000   0.0000   0.0000   0.0000  -0.7245   0.0000   0.0000  -0.2701   0.0000
-0.0323   0.0545   0.3407   0.3694   0.0000   0.5406  -0.2335   0.0000  -0.0250
 0.0997  -0.0331   0.3398  -0.5733   0.0000   0.2469   0.1772   0.0000  -0.3335
 0.5126  -0.1238   0.4361  -0.1661   0.0000  -0.1470  -0.0790   0.0000   0.1024
 0.0000   0.0000   0.0000   0.0000  -0.3419   0.0000   0.0000   0.5656   0.0000
-0.1622   0.2215   0.4074   0.1813   0.0000  -0.1227   0.3824   0.0000   0.1718
-0.0418  -0.3459   0.0378   0.3719   0.0000  -0.2970  -0.1276   0.0000   0.0713
 0.5076  -0.5860  -0.2436   0.1915   0.0000   0.2800   0.3291   0.0000  -0.0024
 0.0000   0.0000   0.0000   0.0000  -0.2186   0.0000   0.0000   0.7268   0.0000
 0.1293  -0.1400   0.1943   0.0876   0.0000  -0.3988  -0.4978   0.0000  -0.5303
-0.1329   0.0244   0.0730   0.3484   0.0000  -0.1112   0.5351   0.0000  -0.6243

   MOLECULAR J(PP,QQ) COULOMB INTEGRALS
 0.5052   0.3744   0.3920   0.3980   0.3477   0.3964   0.4339   0.4593   0.4876
 0.3744   0.3940   0.3524   0.3907   0.3895   0.3780   0.3679   0.3730   0.3581
 0.3920   0.3524   0.4256   0.3560   0.3417   0.3649   0.3709   0.3685   0.3915
 0.3980   0.3907   0.3560   0.4147   0.3805   0.3807   0.3973   0.3965   0.3970
 0.3477   0.3895   0.3417   0.3805   0.4055   0.3602   0.3448   0.3595   0.3240
 0.3964   0.3780   0.3649   0.3807   0.3602   0.4224   0.4063   0.3919   0.4005
 0.4339   0.3679   0.3709   0.3973   0.3448   0.4063   0.4426   0.4251   0.4452
 0.4593   0.3730   0.3685   0.3965   0.3595   0.3919   0.4251   0.4593   0.4562
 0.4876   0.3581   0.3915   0.3970   0.3240   0.4005   0.4452   0.4562   0.5267

   MOLECULAR K(PQ,PQ) EXCHANGE INTEGRALS
 0.5052   0.0829   0.0270   0.0280   0.0176   0.0274   0.0293   0.0393   0.0466
 0.0829   0.3940   0.0253   0.0591   0.0289   0.0286   0.0279   0.0255   0.0252
 0.0270   0.0253   0.4256   0.0088   0.0068   0.0769   0.0351   0.0095   0.0589
 0.0280   0.0591   0.0088   0.4147   0.0189   0.0132   0.0843   0.0185   0.0780
 0.0176   0.0289   0.0068   0.0189   0.4055   0.0069   0.0107   0.1214   0.0041
 0.0274   0.0286   0.0769   0.0132   0.0069   0.4224   0.0996   0.0125   0.0580
 0.0293   0.0279   0.0351   0.0843   0.0107   0.0996   0.4426   0.0152   0.0232
 0.0393   0.0255   0.0095   0.0185   0.1214   0.0125   0.0152   0.4593   0.0106
 0.0466   0.0252   0.0589   0.0780   0.0041   0.0580   0.0232   0.0106   0.5267

                MOLECULE: CH3CHO          ATOM: Carbon in CH3

                                AUGER SPECTRUM

                CORE AND VALENCE I.P.S USED

                  1s   291.190
                  4a'  33.390  5a'  24.200  6a'  19.400  7a'  16.500  1a" 15.400
                  8a'  15.400  9a'  14.200  2a"  13.200  10a' 10.300

PEAK NR.  MO.INDEX  MO.NAME    SYM    ABS.ENERGY    REL.ENERGY    ABS.RATE    REL.INT.

  81        59      1a"  10a'    3X      256.79       -34.4         0.0      0.0000028     1.1
  80        59      1a"  10a'    1X      256.56       -34.6         0.2      0.0000702    27.1
  79        99      10a' 10a'    1A1     256.26       -34.9         0.5      0.0000126     4.9
  78        69      8a'  10a'    3X      256.17       -35.0         0.6      0.0000018     0.7
  77        58      1a"  2a"     3X      256.11       -35.1         0.7      0.0000000     0.0
  76        49      7a'  10a'    3X      255.71       -35.5         1.1      0.0000036     1.4
  75        89      2a"  10a'    3X      255.56       -35.6         1.2      0.0000004     0.2
  74        79      9a'  10a'    3X      255.21       -36.0         1.6      0.0000003     0.1
  73        89      2a"  10a'    1X      254.99       -36.2         1.8      0.0000098     3.8
```

72	79	9a'	10a'	1X	253.94	-37.2	2.8	0.0000134	5.2
71	67	8a'	9a'	3X	253.24	-37.9	3.5	0.0000002	0.1
70	69	8a'	10a'	1X	253.01	-38.2	3.8	0.0000529	20.4
69	78	9a'	2a"	3X	252.64	-38.6	4.1	0.0000000	0.0
68	57	1a"	9a'	3X	252.50	-38.7	4.3	0.0000002	0.1
67	39	6a'	10a'	3X	252.44	-38.8	4.3	0.0000026	1.0
66	88	2a"	2a"	1A1	252.29	-38.9	4.5	0.0000045	1.7
65	68	8a'	2a"	3X	252.27	-38.9	4.5	0.0000000	0.0
64	47	7a'	9a'	3X	251.97	-39.2	4.8	0.0000006	0.2
63	57	1a"	9a'	1X	251.92	-39.3	4.9	0.0000481	18.6
62	78	9a'	2a"	1X	251.81	-39.4	5.0	0.0000067	2.6
61	68	8a'	2a"	1X	251.59	-39.6	5.2	0.0000271	10.5
60	49	7a'	10a'	1X	251.46	-39.7	5.3	0.0000837	32.3
59	48	7a'	2a"	3X	251.20	-40.0	5.6	0.0000001	0.0
58	56	1a"	8a'	3X	250.78	-40.4	6.0	0.0000000	0.0
57	77	9a'	9a'	1A1	250.75	-40.4	6.0	0.0000063	2.4
56	56	1a"	8a'	1X	250.40	-40.8	6.4	0.0001953	75.4
55	48	7a'	2a"	1X	250.20	-41.0	6.6	0.0000360	13.9
54	58	1a"	2a"	1X	249.50	-41.7	7.3	0.0000640	24.7
53	45	7a'	1a"	3X	249.45	-41.7	7.3	0.0000006	0.2
52	55	1a"	1a"	1A1	249.36	-41.8	7.4	0.0002304	89.0
51	46	7a'	8a'	3X	249.29	-41.9	7.5	0.0000004	0.2
50	39	6a'	10a'	1X	249.23	-42.0	7.6	0.0000423	16.3
49	66	8a'	8a'	1A1	248.90	-42.3	7.9	0.0001044	40.3
48	38	6a'	2a"	3X	248.82	-42.4	8.0	0.0000002	0.1
47	46	7a'	8a'	1X	248.57	-42.6	8.2	0.0001765	68.1
46	36	6a'	8a'	3X	248.55	-42.6	8.2	0.0000013	0.5
45	37	6a'	9a'	3X	248.45	-42.7	8.3	0.0000003	0.1
44	45	7a'	1a"	1X	248.42	-42.8	8.4	0.0002590	100.0
43	38	6a'	2a"	1X	248.30	-42.9	8.5	0.0000185	7.1
42	67	8a'	9a'	1X	247.82	-43.4	9.0	0.0000366	14.1
41	29	5a'	10a'	3X	247.63	-43.6	9.2	0.0000077	3.0
40	47	7a'	9a'	1X	247.38	-43.8	9.4	0.0000649	25.1
39	35	6a'	1a"	3X	247.28	-43.9	9.5	0.0000017	0.7
38	35	6a'	1a"	1X	246.91	-44.3	9.9	0.0001332	51.4
37	44	7a'	7a'	1A1	246.91	-44.3	9.9	0.0001825	70.5
36	37	6a'	9a'	1X	246.54	-44.6	10.2	0.0000224	8.6
35	29	5a'	10a'	1X	246.26	-44.9	10.5	0.0000366	14.1
34	34	6a'	7a'	3X	245.84	-45.3	10.9	0.0000015	0.6
33	34	6a'	7a'	1X	245.36	-45.8	11.4	0.0001219	47.0
32	36	6a'	8a'	1X	244.37	-46.8	12.4	0.0001342	51.8
31	28	5a'	2a"	3X	244.33	-46.9	12.5	0.0000048	1.9
30	27	5a'	9a'	3X	243.54	-47.7	13.2	0.0000059	2.3
29	28	5a'	2a"	1X	242.95	-48.2	13.8	0.0000146	5.6
28	26	5a'	8a'	3X	242.08	-49.1	14.7	0.0000232	9.0
27	27	5a'	9a'	1X	242.02	-49.2	14.8	0.0000185	7.1
26	25	5a'	1a"	3X	241.78	-49.4	15.0	0.0000345	13.3
25	24	5a'	7a'	3X	241.47	-49.7	15.3	0.0000299	11.6
24	33	6a'	6a'	1A1	240.81	-50.4	16.0	0.0000471	18.2
23	26	5a'	8a'	1X	240.53	-50.7	16.3	0.0000708	27.3
22	25	5a'	1a"	1X	240.20	-51.0	16.6	0.0001048	40.4
21	23	5a'	6a'	3X	238.69	-52.5	18.1	0.0000155	6.0
20	24	5a'	7a'	1X	238.25	-52.9	18.5	0.0000967	37.3
19	23	5a'	6a'	1X	237.31	-53.9	19.5	0.0000550	21.2
18	19	4a'	10a'	3X	235.50	-55.7	21.3	0.0000055	2.1
17	15	4a'	1a"	3X	233.42	-57.8	23.4	0.0000310	12.0
16	18	4a'	2a"	3X	233.17	-58.0	23.6	0.0000043	1.7
15	19	4a'	10a'	1X	232.96	-58.2	23.8	0.0000340	13.1
14	17	4a'	9a'	3X	232.59	-58.6	24.2	0.0000048	1.9
13	15	4a'	1a"	1X	232.46	-58.7	24.3	0.0000981	37.9
12	16	4a'	8a'	3X	232.36	-58.8	24.4	0.0000209	8.1
11	22	5a'	5a'	1A1	232.07	-59.1	24.7	0.0000868	33.5
10	14	4a'	7a'	3X	231.23	-60.0	25.6	0.0000287	11.1
9	18	4a'	2a"	1X	231.03	-60.2	25.8	0.0000136	5.3
8	17	4a'	9a'	1X	231.00	-60.2	25.8	0.0000174	6.7
7	16	4a'	8a'	1X	230.87	-60.3	25.9	0.0000661	25.5
6	14	4a'	7a'	1X	229.71	-61.5	27.1	0.0000931	35.9
5	13	4a'	6a'	3X	228.47	-62.7	28.3	0.0000144	5.5
4	13	4a'	6a'	1X	227.00	-64.2	29.8	0.0000517	20.0
3	12	4a'	5a'	3X	225.67	-65.5	31.1	0.0000016	0.6
2	12	4a'	5a'	1X	221.16	-70.0	35.6	0.0001577	60.9
1	11	4a'	4a'	1A1	210.66	-80.5	46.1	0.0000712	27.5

Total Transition Rate (in au) = 3.54299E-03

D.3.2.1. Formamide - C(KVV)

CALCULATIONS FOR NH2CHO, geom. J.MOL.SPECTR.49(1974)251

7	0.0000000	-2.1671388	0.3118049
6	0.0000000	0.0604713	-0.7812131
8	0.0000000	2.1418164	0.3798351
1	0.0000000	-2.2680502	2.2037995
1	0.0000000	-3.7153921	-0.7744101
1	0.0000000	0.0944863	-2.8555663

DEGENERACY OF OCCUPIED ORBITALS

1 1 1 1 1 1 1 1 1

EIGENVECTORS

0.4345	-0.5592	-0.2941	0.2006	-0.0441	0.0000	0.0100	0.0000	-0.0849
0.0000	0.0000	0.0000	0.0000	0.0000	-0.5357	0.0000	-0.7535	0.0000
0.1692	0.0069	0.1036	-0.5755	0.0876	0.0000	0.2887	0.0000	-0.1840
-0.0513	0.0835	-0.3490	-0.0790	-0.5164	0.0000	0.3704	0.0000	0.1361
0.6566	0.0118	0.4094	-0.1794	-0.1271	0.0000	-0.0490	0.0000	0.0283
0.0000	0.0000	0.0000	0.0000	0.0000	-0.7055	0.0000	0.1513	0.0000
0.0147	0.4866	-0.0763	0.2120	-0.3933	0.0000	-0.2810	0.0000	0.0737
0.1403	0.0393	-0.4663	-0.4069	0.1012	0.0000	-0.3166	0.0000	-0.2288
0.4616	0.5723	-0.2997	0.2674	0.4109	0.0000	0.2433	0.0000	0.0012
0.0000	0.0000	0.0000	0.0000	0.0000	-0.4640	0.0000	0.6398	0.0000
-0.1921	-0.0790	0.0235	0.2784	0.2478	0.0000	0.5230	0.0000	-0.3882
-0.0763	-0.1118	-0.1875	-0.1791	0.3851	0.0000	0.0783	0.0000	0.7939
0.1510	-0.1818	-0.3138	0.0580	-0.3625	0.0000	0.2820	0.0000	0.1034
0.1307	-0.2497	-0.0584	0.4033	0.1326	0.0000	-0.3493	0.0000	0.0203
0.1824	-0.0116	0.4034	0.1803	-0.1229	0.0000	0.2395	0.0000	0.2997

MOLECULAR J(PP,QQ) COULOMB INTEGRALS

0.4417	0.4272	0.4021	0.4226	0.4050	0.4474	0.4012	0.4365	0.4031
0.4272	0.4613	0.3777	0.4043	0.3994	0.4354	0.4589	0.4675	0.4786
0.4021	0.3777	0.4315	0.3892	0.3974	0.4159	0.3582	0.3796	0.3511
0.4226	0.4043	0.3892	0.4761	0.3969	0.4377	0.3738	0.4203	0.3463
0.4050	0.3994	0.3974	0.3969	0.4105	0.4150	0.3985	0.4141	0.3942
0.4474	0.4354	0.4159	0.4377	0.4150	0.4785	0.4117	0.4632	0.4019
0.4012	0.4589	0.3582	0.3738	0.3985	0.4117	0.5640	0.4733	0.5417
0.4365	0.4675	0.3796	0.4203	0.4141	0.4632	0.4733	0.5156	0.4857
0.4031	0.4786	0.3511	0.3463	0.3942	0.4019	0.5417	0.4857	0.6194

MOLECULAR K(PQ,PQ) EXCHANGE INTEGRALS

0.4417	0.1155	0.0303	0.0335	0.0279	0.0321	0.0204	0.0322	0.0305
0.1155	0.4613	0.0195	0.0615	0.0321	0.0266	0.0421	0.0439	0.0500
0.0303	0.0195	0.4315	0.0072	0.1050	0.0104	0.0229	0.0071	0.0397
0.0335	0.0615	0.0072	0.4761	0.0135	0.0113	0.0778	0.0136	0.0409
0.0279	0.0321	0.1050	0.0135	0.4105	0.0083	0.0577	0.0121	0.0747
0.0321	0.0266	0.0104	0.0113	0.0083	0.4785	0.0089	0.1705	0.0067
0.0204	0.0421	0.0229	0.0778	0.0577	0.0089	0.5640	0.0175	0.0317
0.0322	0.0439	0.0071	0.0136	0.0121	0.1705	0.0175	0.5156	0.0141
0.0305	0.0500	0.0397	0.0409	0.0747	0.0067	0.0317	0.0141	0.6194

MOLECULE: NH2CHO ATOM: Carbon

AUGER SPECTRUM

CORE AND VALENCE I.P.S USED

1s 294.450
4a' 33.100 5a' 28.500 6a' 20.700 7a' 18.800 8a' 16.300
1a" 14.100 9a' 14.800 2a" 10.700 10a' 10.400

PEAK NR.	MO.INDEX	MO.NAME	SYM	ABS.ENERGY	REL.ENERGY		ABS.RATE	REL.INT.
81	68	1a" 2a"	3X	261.69	-32.8	0.0	0.0000000	0.0
80	89	2a" 10a'	3X	260.52	-33.9	1.2	0.0000000	0.0
79	89	2a" 10a'	1X	259.75	-34.7	1.9	0.0000014	0.7
78	69	1a" 10a'	3X	259.20	-35.3	2.5	0.0000001	0.0
77	59	8a' 10a'	3X	259.06	-35.4	2.6	0.0000001	0.1
76	88	2a" 2a"	1A1	259.02	-35.4	2.7	0.0000004	0.2
75	69	1a" 10a'	1X	258.83	-35.6	2.9	0.0000305	14.7
74	49	7a' 10a'	3X	256.94	-37.5	4.7	0.0000007	0.3
73	99	10a' 10a'	1A1	256.80	-37.7	4.9	0.0000028	1.4
72	78	9a' 2a"	3X	256.55	-37.9	5.1	0.0000000	0.0

71	58	8a'	2a"	3X	256.51	-37.9	5.2	0.0000001	0.0
70	58	8a'	2a"	1X	255.85	-38.6	5.8	0.0000042	2.0
69	78	9a'	2a"	1X	255.59	-38.9	6.1	0.0000044	2.1
68	79	9a'	10a'	3X	255.37	-39.1	6.3	0.0000001	0.0
67	59	8a'	10a'	1X	254.99	-39.5	6.7	0.0000124	6.0
66	39	6a'	10a'	3X	254.88	-39.6	6.8	0.0000016	0.8
65	49	7a'	10a'	1X	254.71	-39.7	7.0	0.0000215	10.4
64	67	1a"	9a'	3X	254.59	-39.9	7.1	0.0000002	0.1
63	67	1a"	9a'	1X	254.10	-40.3	7.6	0.0000947	45.7
62	57	8a'	9a'	3X	254.08	-40.4	7.6	0.0000005	0.2
61	48	7a'	2a"	3X	253.88	-40.6	7.8	0.0000002	0.1
60	79	9a'	10a'	1X	253.65	-40.8	8.0	0.0000128	6.2
59	66	1a"	1a"	1A1	253.23	-41.2	8.5	0.0002072	100.0
58	48	7a'	2a"	1X	253.14	-41.3	8.5	0.0000055	2.7
57	56	8a'	1a"	3X	252.98	-41.5	8.7	0.0000017	0.8
56	38	6a'	2a"	3X	252.91	-41.5	8.8	0.0000008	0.4
55	47	7a'	9a'	3X	252.80	-41.7	8.9	0.0000010	0.5
54	39	6a'	10a'	1X	252.72	-41.7	9.0	0.0000261	12.6
53	56	8a'	1a"	1X	252.53	-41.9	9.2	0.0000914	44.1
52	38	6a'	2a"	1X	252.53	-41.9	9.2	0.0000077	3.7
51	68	1a"	2a"	1X	252.41	-42.0	9.3	0.0000191	9.2
50	57	8a'	9a'	1X	250.94	-43.5	10.7	0.0000370	17.8
49	55	8a'	8a'	1A1	250.68	-43.8	11.0	0.0000245	11.8
48	46	7a'	1a"	3X	249.95	-44.5	11.7	0.0000033	1.6
47	37	6a'	9a'	3X	249.83	-44.6	11.9	0.0000078	3.7
46	77	9a'	9a'	1A1	249.50	-44.9	12.2	0.0000271	13.1
45	35	6a'	8a'	3X	249.49	-45.0	12.2	0.0000061	3.0
44	46	7a'	1a"	1X	249.33	-45.1	12.4	0.0001202	58.0
43	45	7a'	8a'	3X	248.92	-45.5	12.8	0.0000030	1.4
42	36	6a'	1a"	3X	248.62	-45.8	13.1	0.0000173	8.4
41	37	6a'	9a'	1X	248.58	-45.9	13.1	0.0000798	38.5
40	47	7a'	9a'	1X	248.56	-45.9	13.1	0.0000466	22.5
39	45	7a'	8a'	1X	248.18	-46.3	13.5	0.0000528	25.5
38	36	6a'	1a"	1X	248.05	-46.4	13.6	0.0001685	81.3
37	34	6a'	7a'	3X	244.56	-49.9	17.1	0.0000141	6.8
36	34	6a'	7a'	1X	244.16	-50.3	17.5	0.0001052	50.8
35	44	7a'	7a'	1A1	243.89	-50.6	17.8	0.0000417	20.1
34	29	5a'	10a'	3X	243.89	-50.6	17.8	0.0000000	0.0
33	35	6a'	8a'	1X	243.78	-50.7	17.9	0.0000628	30.3
32	28	5a'	2a"	3X	243.72	-50.7	18.0	0.0000000	0.0
31	28	5a'	2a"	1X	241.33	-53.1	20.4	0.0000057	2.8
30	33	6a'	6a'	1A1	241.31	-53.1	20.4	0.0000865	41.7
29	29	5a'	10a'	1X	241.17	-53.3	20.5	0.0000151	7.3
28	19	4a'	10a'	3X	240.81	-53.6	20.9	0.0000054	2.6
27	26	5a'	1a"	3X	240.73	-53.7	21.0	0.0000000	0.0
26	27	5a'	9a'	3X	239.81	-54.6	21.9	0.0000001	0.0
25	25	5a'	8a'	3X	239.66	-54.8	22.0	0.0000007	0.3
24	18	4a'	2a"	3X	239.65	-54.8	22.0	0.0000020	1.0
23	26	5a'	1a"	1X	239.28	-55.2	22.4	0.0001250	60.3
22	19	4a'	10a'	1X	239.15	-55.3	22.5	0.0000178	8.6
21	25	5a'	8a'	1X	237.91	-56.5	23.8	0.0000655	31.6
20	18	4a'	2a"	1X	237.90	-56.6	23.8	0.0000066	3.2
19	24	5a'	7a'	3X	237.82	-56.6	23.9	0.0000017	0.8
18	27	5a'	9a'	1X	237.52	-56.9	24.2	0.0000591	28.5
17	17	4a'	9a'	3X	236.19	-58.3	25.5	0.0000154	7.4
16	16	4a'	1a"	3X	235.95	-58.5	25.7	0.0000446	21.5
15	23	5a'	6a'	3X	235.50	-58.9	26.2	0.0000084	4.1
14	17	4a'	9a'	1X	235.08	-59.4	26.6	0.0000544	26.3
13	15	4a'	8a'	3X	234.79	-59.7	26.9	0.0000151	7.3
12	24	5a'	7a'	1X	234.47	-60.0	27.2	0.0000623	30.1
11	23	5a'	6a'	1X	234.44	-60.0	27.2	0.0000827	39.9
10	16	4a'	1a"	1X	234.20	-60.2	27.5	0.0001427	68.9
9	15	4a'	8a'	1X	233.27	-61.2	28.4	0.0000596	28.7
8	14	4a'	7a'	3X	231.96	-62.5	29.7	0.0000163	7.9
7	13	4a'	6a'	3X	230.53	-63.9	31.2	0.0000281	13.6
6	14	4a'	7a'	1X	230.14	-64.3	31.5	0.0000856	41.3
5	13	4a'	6a'	1X	228.88	-65.6	32.8	0.0001949	94.0
4	22	5a'	5a'	1A1	224.90	-69.6	36.8	0.0000475	22.9
3	12	4a'	5a'	3X	224.37	-70.1	37.3	0.0000213	10.3
2	12	4a'	5a'	1X	218.08	-76.4	43.6	0.0000685	33.1
1	11	4a'	4a'	1A1	216.23	-78.2	45.5	0.0001644	79.3

Total Transition Rate (in au) = 2.87034E-03

D.3.2.2. Formamide - O(KVV)

CALCULATIONS FOR NH2CHO, geom. J.MOL.SPECTR.49(1974)251

7	0.0000000	-2.1671388	0.3118049
6	0.0000000	0.0604713	-0.7812131
8	0.0000000	2.1418164	0.3798351
1	0.0000000	-2.2680502	2.2037995
1	0.0000000	-3.7153921	-0.7744101
1	0.0000000	0.0944863	-2.8555663

DEGENERACY OF OCCUPIED ORBITALS
1 1 1 1 1 1 1 1 1

EIGENVECTORS

-0.2469	0.6970	0.2005	-0.1643	-0.0890	0.0000	-0.0204	0.0000	0.0861
0.0000	0.0000	0.0000	0.0000	0.0000	0.3845	0.0000	-0.7758	0.0000
-0.1114	0.0596	-0.0916	0.5359	0.2555	0.0000	-0.4135	0.0000	0.1806
-0.0045	-0.0794	0.4035	0.1627	-0.4376	0.0000	-0.2954	0.0000	-0.3312
-0.4462	0.2593	-0.4280	0.2515	-0.0215	0.0000	-0.0326	0.0000	-0.0878
0.0000	0.0000	0.0000	0.0000	0.0000	0.4989	0.0000	-0.2814	0.0000
-0.1699	-0.3930	-0.0078	-0.0078	-0.3764	0.0000	0.2264	0.0000	-0.0897
-0.1701	0.0367	0.4209	0.2943	0.0898	0.0000	0.1328	0.0000	0.3803
-0.7828	-0.3664	0.1570	-0.2925	0.2116	0.0000	-0.0961	0.0000	0.0040
0.0000	0.0000	0.0000	0.0000	0.0000	0.7767	0.0000	0.5648	0.0000
0.1572	-0.0329	0.0060	-0.5128	0.1602	0.0000	-0.6661	0.0000	0.1393
0.0694	0.0587	0.3211	0.0574	0.6333	0.0000	0.1593	0.0000	-0.6188
-0.1030	0.2377	0.3109	0.0135	-0.3290	0.0000	-0.2088	0.0000	-0.2513
-0.0617	0.2784	-0.0111	-0.3938	-0.0109	0.0000	0.3673	0.0000	0.0778
-0.1140	0.0922	-0.4512	-0.0489	-0.0721	0.0000	-0.1204	0.0000	-0.4673

MOLECULAR J(PP,QQ) COULOMB INTEGRALS

0.4417	0.4272	0.4021	0.4226	0.4050	0.4474	0.4012	0.4365	0.4031
0.4272	0.4613	0.3777	0.4043	0.3994	0.4354	0.4589	0.4675	0.4786
0.4021	0.3777	0.4315	0.3892	0.3974	0.4159	0.3582	0.3796	0.3511
0.4226	0.4043	0.3892	0.4761	0.3969	0.4377	0.3738	0.4203	0.3463
0.4050	0.3994	0.3974	0.3969	0.4105	0.4150	0.3985	0.4141	0.3942
0.4474	0.4354	0.4159	0.4377	0.4150	0.4785	0.4117	0.4632	0.4019
0.4012	0.4589	0.3582	0.3738	0.3985	0.4117	0.5640	0.4733	0.5417
0.4365	0.4675	0.3796	0.4203	0.4141	0.4632	0.4733	0.5156	0.4857
0.4031	0.4786	0.3511	0.3463	0.3942	0.4019	0.5417	0.4857	0.6194

MOLECULAR K(PQ,PQ) EXCHANGE INTEGRALS

0.4417	0.1155	0.0303	0.0335	0.0279	0.0321	0.0204	0.0322	0.0305
0.1155	0.4613	0.0195	0.0615	0.0321	0.0266	0.0421	0.0439	0.0500
0.0303	0.0195	0.4315	0.0072	0.1050	0.0104	0.0229	0.0071	0.0397
0.0335	0.0615	0.0072	0.4761	0.0135	0.0113	0.0778	0.0136	0.0409
0.0279	0.0321	0.1050	0.0135	0.4105	0.0083	0.0577	0.0121	0.0747
0.0321	0.0266	0.0104	0.0113	0.0083	0.4785	0.0089	0.1705	0.0067
0.0204	0.0421	0.0229	0.0778	0.0577	0.0089	0.5640	0.0175	0.0317
0.0322	0.0439	0.0071	0.0136	0.0121	0.1705	0.0175	0.5156	0.0141
0.0305	0.0500	0.0397	0.0409	0.0747	0.0067	0.0317	0.0141	0.6194

MOLECULE: NH2CHO ATOM: Oxygen

AUGER SPECTRUM

CORE AND VALENCE I.P.S USED

1s 537.900
4a' 33.100 5a' 28.500 6a' 20.700 7a' 18.800 8a' 16.300
1a" 14.100 9a' 14.800 2a" 10.700 10a' 10.400

PEAK NR.	MO.INDEX	MO.NAME	SYM	ABS.ENERGY	REL.ENERGY		ABS.RATE	REL.INT.
81	68	1a" 2a"	3X	505.14	-32.8	0.0	0.0000000	0.0
80	89	2a" 10a'	3X	503.97	-33.9	1.2	0.0000000	0.0
79	89	2a" 10a'	1X	503.20	-34.7	1.9	0.0001367	42.0
78	69	1a" 10a'	3X	502.65	-35.3	2.5	0.0000000	0.0
77	59	8a' 10a'	3X	502.51	-35.4	2.6	0.0000037	1.1
76	88	2a" 2a"	1A1	502.47	-35.4	2.7	0.0000861	26.4
75	69	1a" 10a'	1X	502.28	-35.6	2.9	0.0002586	79.4
74	49	7a' 10a'	3X	500.39	-37.5	4.7	0.0000068	2.1
73	99	10a' 10a'	1A1	500.25	-37.7	4.9	0.0001370	42.1
72	78	9a' 2a"	3X	500.00	-37.9	5.1	0.0000006	0.2

71	58	8a'	2a"	3X	499.96	-37.9	5.2	0.0000028	0.9
70	58	8a'	2a"	1X	499.30	-38.6	5.8	0.0001539	47.3
69	78	9a'	2a"	1X	499.04	-38.9	6.1	0.0001612	49.5
68	79	9a'	10a'	3X	498.82	-39.1	6.3	0.0000007	0.2
67	59	8a'	10a'	1X	498.44	-39.5	6.7	0.0002799	85.9
66	39	6a'	10a'	3X	498.33	-39.6	6.8	0.0000020	0.6
65	49	7a'	10a'	1X	498.16	-39.7	7.0	0.0001428	43.8
64	67	1a"	9a'	3X	498.04	-39.9	7.1	0.0000011	0.3
63	67	1a"	9a'	1X	497.55	-40.3	7.6	0.0003049	93.6
62	57	8a'	9a'	3X	497.53	-40.4	7.6	0.0000049	1.5
61	48	7a'	2a"	3X	497.33	-40.6	7.8	0.0000054	1.7
60	79	9a'	10a'	1X	497.10	-40.8	8.0	0.0002263	69.5
59	66	1a"	1a"	1A1	496.68	-41.2	8.5	0.0003080	94.6
58	48	7a'	2a"	1X	496.59	-41.3	8.5	0.0001075	33.0
57	56	8a'	1a"	3X	496.43	-41.5	8.7	0.0000054	1.7
56	38	6a'	2a"	3X	496.36	-41.5	8.8	0.0000016	0.5
55	47	7a'	9a'	3X	496.25	-41.7	8.9	0.0000046	1.4
54	39	6a'	10a'	1X	496.17	-41.7	9.0	0.0000750	23.0
53	56	8a'	1a"	1X	495.98	-41.9	9.2	0.0002911	89.4
52	38	6a'	2a"	1X	495.98	-41.9	9.2	0.0000400	12.3
51	68	1a"	2a"	1X	495.86	-42.0	9.3	0.0003257	100.0
50	57	8a'	9a'	1X	494.39	-43.5	10.7	0.0002295	70.5
49	55	8a'	8a'	1A1	494.13	-43.8	11.0	0.0001668	51.2
48	46	7a'	1a"	3X	493.40	-44.5	11.7	0.0000103	3.2
47	37	6a'	9a'	3X	493.28	-44.6	11.9	0.0000028	0.9
46	77	9a'	9a'	1A1	492.95	-44.9	12.2	0.0001888	58.0
45	35	6a'	8a'	3X	492.94	-45.0	12.2	0.0000003	0.1
44	46	7a'	1a"	1X	492.78	-45.1	12.4	0.0002034	62.4
43	45	7a'	8a'	3X	492.37	-45.5	12.8	0.0000085	2.6
42	36	6a'	1a"	3X	492.07	-45.8	13.1	0.0000030	0.9
41	37	6a'	9a'	1X	492.03	-45.9	13.1	0.0000612	18.8
40	47	7a'	9a'	1X	492.01	-45.9	13.1	0.0002372	72.8
39	45	7a'	8a'	1X	491.63	-46.3	13.5	0.0001587	48.7
38	36	6a'	1a"	1X	491.50	-46.4	13.6	0.0000756	23.2
37	34	6a'	7a'	3X	488.01	-49.9	17.1	0.0000033	1.0
36	34	6a'	7a'	1X	487.61	-50.3	17.5	0.0000426	13.1
35	44	7a'	7a'	1A1	487.34	-50.6	17.8	0.0000792	24.3
34	29	5a'	10a'	3X	487.34	-50.6	17.8	0.0000107	3.3
33	35	6a'	8a'	1X	487.23	-50.7	17.9	0.0000837	25.7
32	28	5a'	2a"	3X	487.17	-50.7	18.0	0.0000085	2.6
31	28	5a'	2a"	1X	484.78	-53.1	20.4	0.0000283	8.7
30	33	6a'	6a'	1A1	484.76	-53.1	20.4	0.0000110	3.4
29	29	5a'	10a'	1X	484.62	-53.3	20.5	0.0000367	11.3
28	19	4a'	10a'	3X	484.26	-53.6	20.9	0.0000491	15.1
27	26	5a'	1a"	3X	484.18	-53.7	21.0	0.0000161	5.0
26	27	5a'	9a'	3X	483.26	-54.6	21.9	0.0000121	3.7
25	25	5a'	8a'	3X	483.11	-54.8	22.0	0.0000124	3.8
24	18	4a'	2a"	3X	483.10	-54.8	22.0	0.0000389	12.0
23	26	5a'	1a"	1X	482.73	-55.2	22.4	0.0000535	16.4
22	19	4a'	10a'	1X	482.60	-55.3	22.5	0.0001670	51.3
21	25	5a'	8a'	1X	481.36	-56.5	23.8	0.0000489	15.0
20	18	4a'	2a"	1X	481.35	-56.6	23.8	0.0001322	40.6
19	24	5a'	7a'	3X	481.27	-56.6	23.9	0.0000063	1.9
18	27	5a'	9a'	1X	480.97	-56.9	24.2	0.0000442	13.6
17	17	4a'	9a'	3X	479.64	-58.3	25.5	0.0000601	18.5
16	16	4a'	1a"	3X	479.40	-58.5	25.7	0.0000736	22.6
15	23	5a'	6a'	3X	478.95	-58.9	26.2	0.0000032	1.0
14	17	4a'	9a'	1X	478.53	-59.4	26.6	0.0002102	64.5
13	15	4a'	8a'	3X	478.24	-59.7	26.9	0.0000569	17.5
12	24	5a'	7a'	1X	477.92	-60.0	27.2	0.0000431	13.2
11	23	5a'	6a'	1X	477.89	-60.0	27.2	0.0000151	4.6
10	16	4a'	1a"	1X	477.65	-60.2	27.5	0.0002500	76.8
9	15	4a'	8a'	1X	476.72	-61.2	28.4	0.0002276	69.9
8	14	4a'	7a'	3X	475.41	-62.5	29.7	0.0000400	12.3
7	13	4a'	6a'	3X	473.98	-63.9	31.2	0.0000139	4.3
6	14	4a'	7a'	1X	473.59	-64.3	31.5	0.0002049	62.9
5	13	4a'	6a'	1X	472.33	-65.6	32.8	0.0000691	21.2
4	22	5a'	5a'	1A1	468.35	-69.6	36.8	0.0000154	4.7
3	12	4a'	5a'	3X	467.82	-70.1	37.3	0.0000015	0.5
2	12	4a'	5a'	1X	461.53	-76.4	43.6	0.0001418	43.5
1	11	4a'	4a'	1A1	459.68	-78.2	45.5	0.0003248	99.7

Total Transition Rate (in au) = 7.05685E-03

D.3.2.3. Formamide - N(KVV)

CALCULATIONS FOR NH2CHO, geom. J.MOL.SPECTR.49(1974)251

7	0.0000000	-2.1671388	0.3118049
6	0.0000000	0.0604713	-0.7812131
8	0.0000000	2.1418164	0.3798351
1	0.0000000	-2.2680502	2.2037995
1	0.0000000	-3.7153921	-0.7744101
1	0.0000000	0.0944863	-2.8555663

DEGENERACY OF OCCUPIED ORBITALS

1 1 1 1 1 1 1 1 1

EIGENVECTORS

0.7814	0.2676	-0.1286	0.0823	0.0355	0.0000	0.0528	0.0000	0.1552
0.0000	0.0000	0.0000	0.0000	0.0000	-0.8799	0.0000	-0.4349	0.0000
0.0883	-0.1243	0.1329	-0.7547	0.0486	0.0000	0.1960	0.0000	0.1881
-0.0329	-0.0475	-0.6294	-0.1113	-0.4644	0.0000	0.1112	0.0000	-0.1265
0.3932	-0.3518	0.3591	-0.1500	-0.2591	0.0000	-0.1358	0.0000	-0.1202
0.0000	0.0000	0.0000	0.0000	0.0000	-0.4148	0.0000	0.5058	0.0000
-0.1756	-0.3778	-0.1627	0.2357	-0.1737	0.0000	-0.2656	0.0000	0.0806
0.1361	-0.1143	-0.3188	-0.2416	0.3754	0.0000	-0.3154	0.0000	0.1483
0.1794	-0.7464	-0.1402	0.2336	0.3252	0.0000	0.3555	0.0000	-0.0102
0.0000	0.0000	0.0000	0.0000	0.0000	-0.2320	0.0000	0.7451	0.0000
-0.0993	0.1619	0.0080	0.1588	0.0544	0.0000	0.7300	0.0000	0.2953
-0.0020	0.1195	-0.1151	-0.1268	0.3958	0.0000	0.1458	0.0000	-0.8181
0.2510	0.0568	-0.3813	-0.0155	-0.2888	0.0000	0.0948	0.0000	-0.1098
0.2458	0.1408	0.1063	0.4177	0.1500	0.0000	-0.1676	0.0000	-0.0348
0.1052	-0.1028	0.3505	0.0645	-0.4139	0.0000	0.2009	0.0000	-0.3344

MOLECULAR J(PP,QQ) COULOMB INTEGRALS

0.4417	0.4272	0.4021	0.4226	0.4050	0.4474	0.4012	0.4365	0.4031
0.4272	0.4613	0.3777	0.4043	0.3994	0.4354	0.4589	0.4675	0.4786
0.4021	0.3777	0.4315	0.3892	0.3974	0.4159	0.3582	0.3796	0.3511
0.4226	0.4043	0.3892	0.4761	0.3969	0.4377	0.3738	0.4203	0.3463
0.4050	0.3994	0.3974	0.3969	0.4105	0.4150	0.3985	0.4141	0.3942
0.4474	0.4354	0.4159	0.4377	0.4150	0.4785	0.4117	0.4632	0.4019
0.4012	0.4589	0.3582	0.3738	0.3985	0.4117	0.5640	0.4733	0.5417
0.4365	0.4675	0.3796	0.4203	0.4141	0.4632	0.4733	0.5156	0.4857
0.4031	0.4786	0.3511	0.3463	0.3942	0.4019	0.5417	0.4857	0.6194

MOLECULAR K(PQ,PQ) EXCHANGE INTEGRALS

0.4417	0.1155	0.0303	0.0335	0.0279	0.0321	0.0204	0.0322	0.0305
0.1155	0.4613	0.0195	0.0615	0.0321	0.0266	0.0421	0.0439	0.0500
0.0303	0.0195	0.4315	0.0072	0.1050	0.0104	0.0229	0.0071	0.0397
0.0335	0.0615	0.0072	0.4761	0.0135	0.0113	0.0778	0.0136	0.0409
0.0279	0.0321	0.1050	0.0135	0.4105	0.0083	0.0577	0.0121	0.0747
0.0321	0.0266	0.0104	0.0113	0.0083	0.4785	0.0089	0.1705	0.0067
0.0204	0.0421	0.0229	0.0778	0.0577	0.0089	0.5640	0.0175	0.0317
0.0322	0.0439	0.0071	0.0136	0.0121	0.1705	0.0175	0.5156	0.0141
0.0305	0.0500	0.0397	0.0409	0.0747	0.0067	0.0317	0.0141	0.6194

MOLECULE: NH2CHO ATOM: Nitrogen

AUGER SPECTRUM

CORE AND VALENCE I.P.S USED

1s 406.410
4a' 33.100 5a' 28.500 6a' 20.700 7a' 18.800 8a' 16.300
1a" 14.100 9a' 14.800 2a" 10.700 10a' 10.400

PEAK NR.	MO.INDEX	MO.NAME	SYM	ABS.ENERGY	REL.ENERGY		ABS.RATE	REL.INT.
81	68	1a" 2a"	3X	373.65	-32.8	0.0	0.0000000	0.0
80	89	2a" 10a'	3X	372.48	-33.9	1.2	0.0000009	0.2
79	89	2a" 10a'	1X	371.71	-34.7	1.9	0.0000131	2.6
78	69	1a" 10a'	3X	371.16	-35.3	2.5	0.0000039	0.8
77	59	8a' 10a'	3X	371.02	-35.4	2.6	0.0000009	0.2
76	88	2a" 2a"	1A1	370.98	-35.4	2.7	0.0000301	6.0
75	69	1a" 10a'	1X	370.79	-35.6	2.9	0.0000536	10.6
74	49	7a' 10a'	3X	368.90	-37.5	4.7	0.0000037	0.7
73	99	10a' 10a'	1A1	368.76	-37.7	4.9	0.0000034	0.7
72	78	9a' 2a"	3X	368.51	-37.9	5.1	0.0000001	0.0

71	58	8a'	2a"	3X	368.47	-37.9	5.2	0.0000000	0.0
70	58	8a'	2a"	1X	367.81	-38.6	5.8	0.0000437	8.7
69	78	9a'	2a"	1X	367.55	-38.9	6.1	0.0000105	2.1
68	79	9a'	10a'	3X	367.33	-39.1	6.3	0.0000002	0.0
67	59	8a'	10a'	1X	366.95	-39.5	6.7	0.0000180	3.6
66	39	6a'	10a'	3X	366.84	-39.6	6.8	0.0000031	0.6
65	49	7a'	10a'	1X	366.67	-39.7	7.0	0.0000512	10.1
64	67	1a"	9a'	3X	366.55	-39.9	7.1	0.0000004	0.1
63	67	1a"	9a'	1X	366.06	-40.3	7.6	0.0000429	8.5
62	57	8a'	9a'	3X	366.04	-40.4	7.6	0.0000002	0.0
61	48	7a'	2a"	3X	365.84	-40.6	7.8	0.0000003	0.1
60	79	9a'	10a'	1X	365.61	-40.8	8.0	0.0000040	0.8
59	66	1a"	1a"	1A1	365.19	-41.2	8.5	0.0005050	100.0
58	48	7a'	2a"	1X	365.10	-41.3	8.5	0.0001171	23.2
57	56	8a'	1a"	3X	364.94	-41.5	8.7	0.0000002	0.0
56	38	6a'	2a"	3X	364.87	-41.5	8.8	0.0000006	0.1
55	47	7a'	9a'	3X	364.76	-41.7	8.9	0.0000007	0.1
54	39	6a'	10a'	1X	364.68	-41.7	9.0	0.0000370	7.3
53	56	8a'	1a"	1X	364.49	-41.9	9.2	0.0001790	35.5
52	38	6a'	2a"	1X	364.49	-41.9	9.2	0.0000847	16.8
51	68	1a"	2a"	1X	364.37	-42.0	9.3	0.0002467	48.9
50	57	8a'	9a'	1X	362.90	-43.5	10.7	0.0000132	2.6
49	55	8a'	8a'	1A1	362.64	-43.8	11.0	0.0000402	8.0
48	46	7a'	1a"	3X	361.91	-44.5	11.7	0.0000011	0.2
47	37	6a'	9a'	3X	361.79	-44.6	11.9	0.0000003	0.1
46	77	9a'	9a'	1A1	361.46	-44.9	12.2	0.0000023	0.4
45	35	6a'	8a'	3X	361.45	-45.0	12.2	0.0000014	0.3
44	46	7a'	1a"	1X	361.29	-45.1	12.4	0.0004795	94.9
43	45	7a'	8a'	3X	360.88	-45.5	12.8	0.0000004	0.1
42	36	6a'	1a"	3X	360.58	-45.8	13.1	0.0000027	0.5
41	37	6a'	9a'	1X	360.54	-45.9	13.1	0.0000247	4.9
40	47	7a'	9a'	1X	360.52	-45.9	13.1	0.0000487	9.6
39	45	7a'	8a'	1X	360.14	-46.3	13.5	0.0001356	26.9
38	36	6a'	1a"	1X	360.01	-46.4	13.6	0.0003466	68.6
37	34	6a'	7a'	3X	356.52	-49.9	17.1	0.0000024	0.5
36	34	6a'	7a'	1X	356.12	-50.3	17.5	0.0002630	52.1
35	44	7a'	7a'	1A1	355.85	-50.6	17.8	0.0002876	56.9
34	29	5a'	10a'	3X	355.85	-50.6	17.8	0.0000012	0.2
33	35	6a'	8a'	1X	355.74	-50.7	17.9	0.0001542	30.5
32	28	5a'	2a"	3X	355.68	-50.7	18.0	0.0000028	0.6
31	28	5a'	2a"	1X	353.29	-53.1	20.4	0.0000119	2.4
30	33	6a'	6a'	1A1	353.27	-53.1	20.4	0.0001483	29.4
29	29	5a'	10a'	1X	353.13	-53.3	20.5	0.0000067	1.3
28	19	4a'	10a'	3X	352.77	-53.6	20.9	0.0000055	1.1
27	26	5a'	1a"	3X	352.69	-53.7	21.0	0.0000115	2.3
26	27	5a'	9a'	3X	351.77	-54.6	21.9	0.0000009	0.2
25	25	5a'	8a'	3X	351.62	-54.8	22.0	0.0000032	0.6
24	18	4a'	2a"	3X	351.61	-54.8	22.0	0.0000240	4.7
23	26	5a'	1a"	1X	351.24	-55.2	22.4	0.0000488	9.7
22	19	4a'	10a'	1X	351.11	-55.3	22.5	0.0000448	8.9
21	25	5a'	8a'	1X	349.87	-56.5	23.8	0.0000140	2.8
20	18	4a'	2a"	1X	349.86	-56.6	23.8	0.0000732	14.5
19	24	5a'	7a'	3X	349.78	-56.6	23.9	0.0000078	1.5
18	27	5a'	9a'	1X	349.48	-56.9	24.2	0.0000042	0.8
17	17	4a'	9a'	3X	348.15	-58.3	25.5	0.0000062	1.2
16	16	4a'	1a"	3X	347.91	-58.5	25.7	0.0000981	19.4
15	23	5a'	6a'	3X	347.46	-58.9	26.2	0.0000064	1.3
14	17	4a'	9a'	1X	347.04	-59.4	26.6	0.0000226	4.5
13	15	4a'	8a'	3X	346.75	-59.7	26.9	0.0000274	5.4
12	24	5a'	7a'	1X	346.43	-60.0	27.2	0.0000435	8.6
11	23	5a'	6a'	1X	346.40	-60.0	27.2	0.0000284	5.6
10	16	4a'	1a"	1X	346.16	-60.2	27.5	0.0002997	59.4
9	15	4a'	8a'	1X	345.23	-61.2	28.4	0.0000859	17.0
8	14	4a'	7a'	3X	343.92	-62.5	29.7	0.0000755	14.9
7	13	4a'	6a'	3X	342.49	-63.9	31.2	0.0000538	10.7
6	14	4a'	7a'	1X	342.10	-64.3	31.5	0.0002353	46.6
5	13	4a'	6a'	1X	340.84	-65.6	32.8	0.0001784	35.3
4	22	5a'	5a'	1A1	336.86	-69.6	36.8	0.0000053	1.0
3	12	4a'	5a'	3X	336.33	-70.1	37.3	0.0000032	0.6
2	12	4a'	5a'	1X	330.04	-76.4	43.6	0.0000812	16.1
1	11	4a'	4a'	1A1	328.19	-78.2	45.5	0.0003172	62.8

Total Transition Rate (in au) = 5.23609E-03

D.3.3.1. Formic acid - C(KVV)

CALCULATIONS FOR HNOOH, geom. J.MOL.SPECTR.80(1980)131

1	0.0000000	1.8986199	-0.8692555
1	0.0000000	-1.7008411	3.1638999
6	0.0000000	0.0000000	0.0000000
8	0.0000000	0.0000000	2.5549107
8	0.0000000	-1.9113907	-1.1990128

DEGENERACY OF OCCUPIED ORBITALS
1 1 1 1 1 1 1 1 1

EIGENVECTORS

-0.1519	-0.0027	-0.4105	0.2124	0.0000	-0.0354	-0.2357	0.0000	-0.2756
-0.1703	0.2290	0.2443	0.1916	0.0000	0.2440	-0.3282	0.0000	-0.0421
-0.6183	-0.0142	-0.4842	-0.1536	0.0000	0.1147	-0.0808	0.0000	-0.0118
0.0000	0.0000	0.0000	0.0000	-0.6882	0.0000	0.0000	-0.2314	0.0000
0.1853	0.1948	-0.4551	0.3077	0.0000	-0.2624	-0.2810	0.0000	-0.1501
-0.0183	0.4217	0.0911	-0.4189	0.0000	-0.2976	-0.0858	0.0000	0.2432
-0.4181	0.6647	0.2068	0.3212	0.0000	-0.0718	0.3082	0.0000	-0.0351
0.0000	0.0000	0.0000	0.0000	-0.5082	0.0000	0.0000	0.8302	0.0000
0.0709	-0.0365	-0.2653	0.0150	0.0000	-0.3968	0.6983	0.0000	-0.1401
0.1421	-0.0749	0.2111	0.4723	0.0000	0.2025	0.1507	0.0000	-0.3858
-0.5266	-0.5127	0.3401	0.1602	0.0000	-0.4731	-0.0841	0.0000	0.0108
0.0000	0.0000	0.0000	0.0000	-0.5178	0.0000	0.0000	-0.5072	0.0000
-0.1772	-0.1408	-0.1972	0.1138	0.0000	0.5367	0.3457	0.0000	0.4152
-0.1491	0.0160	0.0982	-0.5092	0.0000	0.2307	0.1089	0.0000	-0.7059

MOLECULAR J(PP,QQ) COULOMB INTEGRALS

0.4740	0.4675	0.4110	0.4560	0.4698	0.4448	0.4440	0.4773	0.4401
0.4675	0.4854	0.4043	0.4576	0.4715	0.4695	0.4571	0.4888	0.4775
0.4110	0.4043	0.4512	0.4169	0.4227	0.3953	0.4050	0.4030	0.3917
0.4560	0.4576	0.4169	0.4907	0.4662	0.4530	0.4609	0.4774	0.4286
0.4698	0.4715	0.4227	0.4662	0.4958	0.4634	0.4589	0.5044	0.4394
0.4448	0.4695	0.3953	0.4530	0.4634	0.5378	0.4955	0.4891	0.4817
0.4440	0.4571	0.4050	0.4609	0.4589	0.4955	0.4855	0.4779	0.4407
0.4773	0.4888	0.4030	0.4774	0.5044	0.4891	0.4779	0.5412	0.4595
0.4401	0.4775	0.3917	0.4286	0.4394	0.4817	0.4407	0.4595	0.5649

MOLECULAR K(PQ,PQ) EXCHANGE INTEGRALS

0.4740	0.1492	0.0287	0.0376	0.0365	0.0278	0.0277	0.0410	0.0385
0.1492	0.4854	0.0252	0.0487	0.0360	0.0570	0.0391	0.0489	0.0500
0.0287	0.0252	0.4512	0.0535	0.0118	0.0507	0.0388	0.0082	0.0447
0.0376	0.0487	0.0535	0.4907	0.0121	0.0221	0.0397	0.0143	0.1289
0.0365	0.0360	0.0118	0.0121	0.4958	0.0181	0.0124	0.2094	0.0081
0.0278	0.0570	0.0507	0.0221	0.0181	0.5378	0.2094	0.0244	0.0286
0.0277	0.0391	0.0388	0.0397	0.0124	0.2094	0.4855	0.0164	0.0264
0.0410	0.0489	0.0082	0.0143	0.2094	0.0244	0.0164	0.5412	0.0118
0.0385	0.0500	0.0447	0.1289	0.0081	0.0286	0.0264	0.0118	0.5649

MOLECULE: OHCHO ATOM: Carbon

AUGER SPECTRUM

CORE AND VALENCE I.P.S USED

1s 295.900
4a' 33.000 5a' 30.700 6a' 22.000 7a' 17.800 1a" 15.800
8a' 17.100 9a' 14.800 2a" 12.600 10a' 11.500

PEAK NR.	MO.INDEX	MO.NAME	SYM	ABS.ENERGY	REL.ENERGY		ABS.RATE	REL.INT.
81	89	2a" 10a'	3X	259.62	-36.3	0.0	0.0000000	0.0
80	58	1a" 2a"	3X	259.47	-36.4	0.1	0.0000000	0.0
79	89	2a" 10a'	1X	258.98	-36.9	0.6	0.0000046	2.0
78	49	7a' 10a'	3X	258.44	-37.5	1.2	0.0000005	0.2
77	79	9a' 10a'	3X	258.33	-37.6	1.3	0.0000001	0.0
76	99	10a' 10a'	1A1	257.53	-38.4	2.1	0.0000056	2.5
75	79	9a' 10a'	1X	256.89	-39.0	2.7	0.0000080	3.6
74	59	1a" 10a'	3X	256.86	-39.0	2.8	0.0000000	0.0
73	59	1a" 10a'	1X	256.42	-39.5	3.2	0.0000408	18.1
72	67	8a' 9a'	3X	256.21	-39.7	3.4	0.0000008	0.4
71	88	2a" 2a"	1A1	255.97	-39.9	3.6	0.0000024	1.1
70	78	9a' 2a"	3X	255.94	-40.0	3.7	0.0000001	0.0
69	78	9a' 2a"	1X	255.05	-40.9	4.6	0.0000051	2.3

68	69	8a'	10a'	3X	254.97	-40.9	4.6	0.0000002	0.1
67	68	8a'	2a"	3X	253.55	-42.3	6.1	0.0000001	0.1
66	69	8a'	10a'	1X	253.41	-42.5	6.2	0.0000149	6.6
65	57	1a"	9a'	3X	253.15	-42.7	6.5	0.0000006	0.3
64	77	9a'	9a'	1A1	253.09	-42.8	6.5	0.0000066	2.9
63	39	6a'	10a'	3X	252.96	-42.9	6.7	0.0000038	1.7
62	48	7a'	2a"	3X	252.90	-43.0	6.7	0.0000003	0.1
61	57	1a"	9a'	1X	252.48	-43.4	7.1	0.0000450	20.0
60	68	8a'	2a"	1X	252.23	-43.7	7.4	0.0000093	4.1
59	48	7a'	2a"	1X	252.12	-43.8	7.5	0.0000160	7.1
58	47	7a'	9a'	3X	251.84	-44.1	7.8	0.0000010	0.5
57	49	7a'	10a'	1X	251.43	-44.5	8.2	0.0000381	16.9
56	56	1a"	8a'	3X	250.88	-45.0	8.7	0.0000013	0.6
55	55	1a"	1a"	1A1	250.81	-45.1	8.8	0.0001877	83.4
54	38	6a'	2a"	3X	250.56	-45.3	9.1	0.0000026	1.2
53	39	6a'	10a'	1X	250.52	-45.4	9.1	0.0000354	15.7
52	38	6a'	2a"	1X	250.11	-45.8	9.5	0.0000199	8.8
51	45	7a'	1a"	3X	249.94	-46.0	9.7	0.0000023	1.0
50	56	1a"	8a'	1X	249.90	-46.0	9.7	0.0000824	36.6
49	47	7a'	9a'	1X	249.68	-46.2	9.9	0.0000288	12.8
48	45	7a'	1a"	1X	249.28	-46.6	10.3	0.0001417	62.9
47	46	7a'	8a'	3X	249.27	-46.6	10.3	0.0000018	0.8
46	37	6a'	9a'	3X	249.14	-46.8	10.5	0.0000025	1.1
45	58	1a"	2a"	1X	248.08	-47.8	11.5	0.0000424	18.9
44	46	7a'	8a'	1X	248.07	-47.8	11.5	0.0000511	22.7
43	36	6a'	8a'	3X	247.42	-48.5	12.2	0.0000104	4.6
42	66	8a'	8a'	1A1	247.07	-48.8	12.6	0.0000220	9.8
41	37	6a'	9a'	1X	247.02	-48.9	12.6	0.0000439	19.5
40	44	7a'	7a'	1A1	246.95	-49.0	12.7	0.0000651	28.9
39	35	6a'	1a"	3X	246.92	-49.0	12.7	0.0000231	10.2
38	35	6a'	1a"	1X	246.28	-49.6	13.3	0.0001759	78.2
37	34	6a'	7a'	3X	246.21	-49.7	13.4	0.0000197	8.8
36	67	8a'	9a'	1X	244.82	-51.1	14.8	0.0000220	9.8
35	36	6a'	8a'	1X	244.66	-51.2	15.0	0.0000714	31.7
34	34	6a'	7a'	1X	243.30	-52.6	16.3	0.0001343	59.7
33	29	5a'	10a'	3X	242.07	-53.8	17.6	0.0000000	0.0
32	28	5a'	2a"	3X	240.63	-55.3	19.0	0.0000000	0.0
31	19	4a'	10a'	3X	240.47	-55.4	19.1	0.0000066	2.9
30	33	6a'	6a'	1A1	239.62	-56.3	20.0	0.0001139	50.6
29	29	5a'	10a'	1X	239.35	-56.6	20.3	0.0000219	9.7
28	27	5a'	9a'	3X	239.03	-56.9	20.6	0.0000003	0.2
27	18	4a'	2a"	3X	238.43	-57.5	21.2	0.0000043	1.9
26	19	4a'	10a'	1X	238.38	-57.5	21.2	0.0000230	10.2
25	28	5a'	2a"	1X	237.97	-57.9	21.6	0.0000122	5.4
24	25	5a'	1a"	3X	237.55	-58.4	22.1	0.0000000	0.0
23	27	5a'	9a'	1X	236.90	-59.0	22.7	0.0000256	11.4
22	26	5a'	8a'	3X	236.88	-59.0	22.7	0.0000005	0.2
21	17	4a'	9a'	3X	236.77	-59.1	22.8	0.0000079	3.5
20	24	5a'	7a'	3X	236.27	-59.6	23.3	0.0000012	0.5
19	18	4a'	2a"	1X	236.20	-59.7	23.4	0.0000146	6.5
18	25	5a'	1a"	1X	235.59	-60.3	24.0	0.0001077	47.9
17	15	4a'	1a"	3X	235.31	-60.6	24.3	0.0000376	16.7
16	17	4a'	9a'	1X	235.26	-60.6	24.4	0.0000298	13.2
15	16	4a'	8a'	3X	234.45	-61.4	25.2	0.0000113	5.0
14	26	5a'	8a'	1X	233.77	-62.1	25.8	0.0000569	25.3
13	14	4a'	7a'	3X	233.71	-62.2	25.9	0.0000191	8.5
12	24	5a'	7a'	1X	233.62	-62.3	26.0	0.0000731	32.5
11	15	4a'	1a"	1X	233.32	-62.6	26.3	0.0001289	57.3
10	16	4a'	8a'	1X	232.94	-63.0	26.7	0.0000525	23.3
9	23	5a'	6a'	3X	232.88	-63.0	26.7	0.0000107	4.7
8	14	4a'	7a'	1X	231.67	-64.2	27.9	0.0000913	40.6
7	23	5a'	6a'	1X	231.51	-64.4	28.1	0.0000819	36.4
6	13	4a'	6a'	3X	230.50	-65.4	29.1	0.0000295	13.1
5	13	4a'	6a'	1X	228.94	-67.0	30.7	0.0002251	100.0
4	12	4a'	5a'	3X	223.54	-72.4	36.1	0.0000170	7.6
3	22	5a'	5a'	1A1	221.29	-74.6	38.3	0.0000390	17.3
2	11	4a'	4a'	1A1	217.00	-78.9	42.6	0.0001336	59.4
1	12	4a'	5a'	1X	215.42	-80.5	44.2	0.0000593	26.4

Total Transition Rate (in au) = 2.82808E-03

D.3.3.2. Formic acid - O(KVV) in CHO

CALCULATIONS FOR HCFOH, geom. J.MOL.SPECTR.80(1980)131-144

1	0.0000000	1.8986199	-0.8692555
1	0.0000000	-1.7008411	3.1638999
6	0.0000000	0.0000000	0.0000000
8	0.0000000	0.0000000	2.5549107
8	0.0000000	-1.9113907	-1.1990128

DEGENERACY OF OCCUPIED ORBITALS
1 1 1 1 1 1 1 1 1

EIGENVECTORS

-0.0926	-0.0641	0.4547	-0.1164	0.0000	0.0441	0.0155	0.0000	0.4604
-0.1084	-0.2773	-0.2140	-0.0175	0.0000	-0.3122	0.1943	0.0000	0.2760
-0.4229	-0.2263	0.4928	0.1658	0.0000	0.0884	0.1064	0.0000	0.1174
0.0000	0.0000	0.0000	0.0000	-0.4805	0.0000	0.0000	0.2046	0.0000
0.2565	-0.0944	0.3521	-0.3405	0.0000	0.1334	0.0282	0.0000	0.2986
0.0899	-0.3764	-0.1794	0.0650	0.0000	0.3411	0.1969	0.0000	-0.2498
-0.2163	-0.7663	-0.1215	-0.2592	0.0000	-0.1294	-0.2900	0.0000	-0.1322
0.0000	0.0000	0.0000	0.0000	-0.3162	0.0000	0.0000	0.8665	0.0000
0.0659	0.0630	0.2608	-0.1921	0.0000	0.3297	-0.6369	0.0000	-0.3327
0.0751	0.1198	-0.2084	-0.2214	0.0000	-0.4333	-0.4886	0.0000	0.3321
-0.7984	0.3201	-0.2096	-0.2900	0.0000	0.1716	-0.0046	0.0000	-0.0148
0.0000	0.0000	0.0000	0.0000	-0.8180	0.0000	0.0000	-0.4553	0.0000
-0.1434	0.0442	0.3989	0.2782	0.0000	-0.6056	-0.0579	0.0000	-0.4353
-0.1098	-0.0855	-0.1385	0.7238	0.0000	0.2216	-0.4235	0.0000	0.3441

MOLECULAR J(PP,QQ) COULOMB INTEGRALS

0.4740	0.4675	0.4110	0.4560	0.4698	0.4448	0.4440	0.4773	0.4401
0.4675	0.4854	0.4043	0.4576	0.4715	0.4695	0.4571	0.4888	0.4775
0.4110	0.4043	0.4512	0.4169	0.4227	0.3953	0.4050	0.4030	0.3917
0.4560	0.4576	0.4169	0.4907	0.4662	0.4530	0.4609	0.4774	0.4286
0.4698	0.4715	0.4227	0.4662	0.4958	0.4634	0.4589	0.5044	0.4394
0.4448	0.4695	0.3953	0.4530	0.4634	0.5378	0.4955	0.4891	0.4817
0.4440	0.4571	0.4050	0.4609	0.4589	0.4955	0.4855	0.4779	0.4407
0.4773	0.4888	0.4030	0.4774	0.5044	0.4891	0.4779	0.5412	0.4595
0.4401	0.4775	0.3917	0.4286	0.4394	0.4817	0.4407	0.4595	0.5649

MOLECULAR K(PQ,PQ) EXCHANGE INTEGRALS

0.4740	0.1492	0.0287	0.0376	0.0365	0.0278	0.0277	0.0410	0.0385
0.1492	0.4854	0.0252	0.0487	0.0360	0.0570	0.0391	0.0489	0.0500
0.0287	0.0252	0.4512	0.0535	0.0118	0.0507	0.0388	0.0082	0.0447
0.0376	0.0487	0.0535	0.4907	0.0121	0.0221	0.0397	0.0143	0.1289
0.0365	0.0360	0.0118	0.0121	0.4958	0.0181	0.0124	0.2094	0.0081
0.0278	0.0570	0.0507	0.0221	0.0181	0.5378	0.2094	0.0244	0.0286
0.0277	0.0391	0.0388	0.0397	0.0124	0.2094	0.4855	0.0164	0.0264
0.0410	0.0489	0.0082	0.0143	0.2094	0.0244	0.0164	0.5412	0.0118
0.0385	0.0500	0.0447	0.1289	0.0081	0.0286	0.0264	0.0118	0.5649

MOLECULE: OHCHO ATOM: Oxygen in CHO

AUGER SPECTRUM

CORE AND VALENCE I.P.S USED

1s 539.000
4a' 33.000 5a' 30.700 6a' 22.000 7a' 17.800 1a" 15.800
8a' 17.100 9a' 14.800 2a" 12.600 10a' 11.500

PEAK NR.	MO.INDEX	MO.NAME	SYM	ABS.ENERGY	REL.ENERGY		ABS.RATE	REL.INT.
81	89	2a" 10a'	3X	502.72	-36.3	0.0	0.0000000	0.0
80	58	1a" 2a"	3X	502.57	-36.4	0.1	0.0000000	0.0
79	89	2a" 10a'	1X	502.08	-36.9	0.6	0.0000680	14.7
78	49	7a' 10a'	3X	501.54	-37.5	1.2	0.0000050	1.1
77	79	9a' 10a'	3X	501.43	-37.6	1.3	0.0000000	0.0
76	99	10a' 10a'	1A1	500.63	-38.4	2.1	0.0000803	17.3
75	79	9a' 10a'	1X	499.99	-39.0	2.7	0.0000691	14.9
74	59	1a" 10a'	3X	499.96	-39.0	2.8	0.0000000	0.0
73	59	1a" 10a'	1X	499.52	-39.5	3.2	0.0002196	47.3
72	67	8a' 9a'	3X	499.31	-39.7	3.4	0.0000011	0.2
71	88	2a" 2a"	1A1	499.07	-39.9	3.6	0.0000364	7.8
70	78	9a' 2a"	3X	499.04	-40.0	3.7	0.0000000	0.0

69	78	9a'	2a"	1X	498.15	-40.9	4.6	0.0000404	8.7
68	69	8a'	10a'	3X	498.07	-40.9	4.6	0.0000022	0.5
67	68	8a'	2a"	3X	496.65	-42.3	6.1	0.0000012	0.3
66	69	8a'	10a'	1X	496.51	-42.5	6.2	0.0002147	46.3
65	57	1a"	9a'	3X	496.25	-42.7	6.5	0.0000000	0.0
64	77	9a'	9a'	1A1	496.19	-42.8	6.5	0.0000283	6.1
63	39	6a'	10a'	3X	496.06	-42.9	6.7	0.0000030	0.6
62	48	7a'	2a"	3X	496.00	-43.0	6.7	0.0000035	0.7
61	57	1a"	9a'	1X	495.58	-43.4	7.1	0.0001302	28.1
60	68	8a'	2a"	1X	495.33	-43.7	7.4	0.0000957	20.6
59	48	7a'	2a"	1X	495.22	-43.8	7.5	0.0001437	31.0
58	47	7a'	9a'	3X	494.94	-44.1	7.8	0.0000032	0.7
57	49	7a'	10a'	1X	494.53	-44.5	8.2	0.0002237	48.2
56	56	1a"	8a'	3X	493.98	-45.0	8.7	0.0000039	0.8
55	55	1a"	1a"	1A1	493.91	-45.1	8.8	0.0003789	81.7
54	38	6a'	2a"	3X	493.66	-45.3	9.1	0.0000018	0.4
53	39	6a'	10a'	1X	493.62	-45.4	9.1	0.0000978	21.1
52	38	6a'	2a"	1X	493.21	-45.8	9.5	0.0000451	9.7
51	45	7a'	1a"	3X	493.04	-46.0	9.7	0.0000112	2.4
50	56	1a"	8a'	1X	493.00	-46.0	9.7	0.0003088	66.6
49	47	7a'	9a'	1X	492.78	-46.2	9.9	0.0001920	41.4
48	45	7a'	1a"	1X	492.38	-46.6	10.3	0.0004638	100.0
47	46	7a'	8a'	3X	492.37	-46.6	10.3	0.0000103	2.2
46	37	6a'	9a'	3X	492.24	-46.8	10.5	0.0000016	0.3
45	58	1a"	2a"	1X	491.18	-47.8	11.5	0.0002348	50.6
44	46	7a'	8a'	1X	491.17	-47.8	11.5	0.0003034	65.4
43	36	6a'	8a'	3X	490.52	-48.5	12.2	0.0000008	0.2
42	66	8a'	8a'	1A1	490.17	-48.8	12.6	0.0001541	33.2
41	37	6a'	9a'	1X	490.12	-48.9	12.6	0.0000405	8.7
40	44	7a'	7a'	1A1	490.05	-49.0	12.7	0.0003410	73.5
39	35	6a'	1a"	3X	490.02	-49.0	12.7	0.0000059	1.3
38	35	6a'	1a"	1X	489.38	-49.6	13.3	0.0001455	31.4
37	34	6a'	7a'	3X	489.31	-49.7	13.4	0.0000080	1.7
36	67	8a'	9a'	1X	487.92	-51.1	14.8	0.0000865	18.6
35	36	6a'	8a'	1X	487.76	-51.2	15.0	0.0001414	30.5
34	34	6a'	7a'	1X	486.40	-52.6	16.3	0.0001463	31.5
33	29	5a'	10a'	3X	485.17	-53.8	17.6	0.0000062	1.3
32	28	5a'	2a"	3X	483.73	-55.3	19.0	0.0000042	0.9
31	19	4a'	10a'	3X	483.57	-55.4	19.1	0.0000390	8.4
30	33	6a'	6a'	1A1	482.72	-56.3	20.0	0.0000330	7.1
29	29	5a'	10a'	1X	482.45	-56.6	20.3	0.0000243	5.2
28	27	5a'	9a'	3X	482.13	-56.9	20.6	0.0000037	0.8
27	18	4a'	2a"	3X	481.53	-57.5	21.2	0.0000263	5.7
26	19	4a'	10a'	1X	481.48	-57.5	21.2	0.0001339	28.9
25	28	5a'	2a"	1X	481.07	-57.9	21.6	0.0000153	3.3
24	25	5a'	1a"	3X	480.65	-58.4	22.1	0.0000137	2.9
23	27	5a'	9a'	1X	480.00	-59.0	22.7	0.0000142	3.1
22	26	5a'	8a'	3X	479.98	-59.0	22.7	0.0000095	2.1
21	17	4a'	9a'	3X	479.87	-59.1	22.8	0.0000231	5.0
20	24	5a'	7a'	3X	479.37	-59.6	23.3	0.0000106	2.3
19	18	4a'	2a"	1X	479.30	-59.7	23.4	0.0000898	19.4
18	25	5a'	1a"	1X	478.69	-60.3	24.0	0.0000495	10.7
17	15	4a'	1a"	3X	478.41	-60.6	24.3	0.0000850	18.3
16	17	4a'	9a'	1X	478.36	-60.6	24.4	0.0000810	17.5
15	16	4a'	8a'	3X	477.55	-61.4	25.2	0.0000564	12.2
14	26	5a'	8a'	1X	476.87	-62.1	25.8	0.0000375	8.1
13	14	4a'	7a'	3X	476.81	-62.2	25.9	0.0000879	19.0
12	24	5a'	7a'	1X	476.72	-62.3	26.0	0.0000604	13.0
11	15	4a'	1a"	1X	476.42	-62.6	26.3	0.0002898	62.5
10	16	4a'	8a'	1X	476.04	-63.0	26.7	0.0002154	46.4
9	23	5a'	6a'	3X	475.98	-63.0	26.7	0.0000045	1.0
8	14	4a'	7a'	1X	474.77	-64.2	27.9	0.0003634	78.3
7	23	5a'	6a'	1X	474.61	-64.4	28.1	0.0000217	4.7
6	13	4a'	6a'	3X	473.60	-65.4	29.1	0.0000257	5.5
5	13	4a'	6a'	1X	472.04	-67.0	30.7	0.0001267	27.3
4	12	4a'	5a'	3X	466.64	-72.4	36.1	0.0000022	0.5
3	22	5a'	5a'	1A1	464.39	-74.6	38.3	0.0000094	2.0
2	11	4a'	4a'	1A1	460.10	-78.9	42.6	0.0003523	76.0
1	12	4a'	5a'	1X	458.52	-80.5	44.2	0.0001153	24.9

Total Transition Rate (in au) = 6.92317E-03

D.3.3.3. Formic acid - O(KVV) in OH

CALCULATIONS FOR OHCHO, geom. J.MOL.SPECTR.80(1980)131-144

1	0.0000000	1.8986199	-0.8692555
1	0.0000000	-1.7008411	3.1638999
6	0.0000000	0.0000000	0.0000000
8	0.0000000	0.0000000	2.5549107
8	0.0000000	-1.9113907	-1.1990128

DEGENERACY OF OCCUPIED ORBITALS
1 1 1 1 1 1 1 1 1

EIGENVECTORS

-0.0751	-0.1010	-0.2950	0.1822	0.0000	0.3960	0.1977	0.0000	-0.3366
-0.2752	0.0394	0.3317	-0.0924	0.0000	0.2441	0.0812	0.0000	-0.0974
-0.3285	-0.3820	-0.3774	-0.0080	0.0000	0.3124	-0.1220	0.0000	-0.1743
0.0000	0.0000	0.0000	0.0000	0.3257	0.0000	0.0000	0.5645	0.0000
0.0611	0.2745	-0.2953	0.2217	0.0000	0.2675	0.3823	0.0000	-0.1900
-0.2151	0.2705	-0.1151	-0.3149	0.0000	-0.2568	0.0527	0.0000	-0.0766
-0.8420	0.2669	0.0684	0.2429	0.0000	-0.1272	-0.0088	0.0000	0.1414
0.0000	0.0000	0.0000	0.0000	0.9261	0.0000	0.0000	-0.3520	0.0000
0.0840	0.0532	-0.4743	0.5314	0.0000	-0.4862	-0.2362	0.0000	-0.0029
0.1037	0.0601	0.5478	0.6150	0.0000	0.1208	-0.1819	0.0000	-0.2893
-0.1563	-0.7559	0.1539	0.1166	0.0000	-0.3486	0.3520	0.0000	-0.0202
0.0000	0.0000	0.0000	0.0000	0.1903	0.0000	0.0000	0.7466	0.0000
-0.0380	-0.1925	-0.0811	0.1083	0.0000	0.3860	-0.4715	0.0000	0.5814
-0.0897	-0.0874	-0.0001	-0.2548	0.0000	-0.1041	-0.5962	0.0000	-0.6022

MOLECULAR J(PP,QQ) COULOMB INTEGRALS

0.4740	0.4675	0.4110	0.4560	0.4698	0.4448	0.4440	0.4773	0.4401
0.4675	0.4854	0.4043	0.4576	0.4715	0.4695	0.4571	0.4888	0.4775
0.4110	0.4043	0.4512	0.4169	0.4227	0.3953	0.4050	0.4030	0.3917
0.4560	0.4576	0.4169	0.4907	0.4662	0.4530	0.4609	0.4774	0.4286
0.4698	0.4715	0.4227	0.4662	0.4958	0.4634	0.4589	0.5044	0.4394
0.4448	0.4695	0.3953	0.4530	0.4634	0.5378	0.4955	0.4891	0.4817
0.4440	0.4571	0.4050	0.4609	0.4589	0.4955	0.4855	0.4779	0.4407
0.4773	0.4888	0.4030	0.4774	0.5044	0.4891	0.4779	0.5412	0.4595
0.4401	0.4775	0.3917	0.4286	0.4394	0.4817	0.4407	0.4595	0.5649

MOLECULAR K(PQ,PQ) EXCHANGE INTEGRALS

0.4740	0.1492	0.0287	0.0376	0.0365	0.0278	0.0277	0.0410	0.0385
0.1492	0.4854	0.0252	0.0487	0.0360	0.0570	0.0391	0.0489	0.0500
0.0287	0.0252	0.4512	0.0535	0.0118	0.0507	0.0388	0.0082	0.0447
0.0376	0.0487	0.0535	0.4907	0.0121	0.0221	0.0397	0.0143	0.1289
0.0365	0.0360	0.0118	0.0121	0.4958	0.0181	0.0124	0.2094	0.0081
0.0278	0.0570	0.0507	0.0221	0.0181	0.5378	0.2094	0.0244	0.0286
0.0277	0.0391	0.0388	0.0397	0.0124	0.2094	0.4855	0.0164	0.0264
0.0410	0.0489	0.0082	0.0143	0.2094	0.0244	0.0164	0.5412	0.0118
0.0385	0.0500	0.0447	0.1289	0.0081	0.0286	0.0264	0.0118	0.5649

MOLECULE: OHCHO ATOM: Oxygen in OH

AUGER SPECTRUM

CORE AND VALENCE I.P.S USED

1s 540.650
4a' 33.000 5a' 30.700 6a' 22.000 7a' 17.800 1a" 15.800
8a' 17.100 9a' 14.800 2a" 12.600 10a' 11.500

PEAK NR.	MO.INDEX	MO.NAME	SYM	ABS.ENERGY	REL.ENERGY		ABS.RATE	REL.INT.
81	89	2a" 10a'	3X	504.37	-36.3	0.0	0.0000005	0.1
80	58	1a" 2a"	3X	504.22	-36.4	0.1	0.0000000	0.0
79	89	2a" 10a'	1X	503.73	-36.9	0.6	0.0000126	2.0
78	49	7a' 10a'	3X	503.19	-37.5	1.2	0.0000061	1.0
77	79	9a' 10a'	3X	503.08	-37.6	1.3	0.0000004	0.1
76	99	10a' 10a'	1A1	502.28	-38.4	2.1	0.0000072	1.1
75	79	9a' 10a'	1X	501.64	-39.0	2.7	0.0000108	1.7
74	59	1a" 10a'	3X	501.61	-39.0	2.8	0.0000034	0.5
73	59	1a" 10a'	1X	501.17	-39.5	3.2	0.0000872	13.7
72	67	8a' 9a'	3X	500.96	-39.7	3.4	0.0000002	0.0
71	88	2a" 2a"	1A1	500.72	-39.9	3.6	0.0000130	2.0
70	78	9a' 2a"	3X	500.69	-40.0	3.7	0.0000000	0.0
69	78	9a' 2a"	1X	499.80	-40.9	4.6	0.0000117	1.8

68	69	8a'	10a'	3X	499.72	-40.9	4.6	0.0000010	0.2
67	68	8a'	2a"	3X	498.30	-42.3	6.1	0.0000004	0.1
66	69	8a'	10a'	1X	498.16	-42.5	6.2	0.0000276	4.3
65	57	1a"	9a'	3X	497.90	-42.7	6.5	0.0000000	0.0
64	77	9a'	9a'	1A1	497.84	-42.8	6.5	0.0000067	1.1
63	39	6a'	10a'	3X	497.71	-42.9	6.7	0.0000028	0.4
62	48	7a'	2a"	3X	497.65	-43.0	6.7	0.0000015	0.2
61	57	1a"	9a'	1X	497.23	-43.4	7.1	0.0000812	12.8
60	68	8a'	2a"	1X	496.98	-43.7	7.4	0.0000344	5.4
59	48	7a'	2a"	1X	496.87	-43.8	7.5	0.0000917	14.4
58	47	7a'	9a'	3X	496.59	-44.1	7.8	0.0000009	0.1
57	49	7a'	10a'	1X	496.18	-44.5	8.2	0.0000930	14.6
56	56	1a"	8a'	3X	495.63	-45.0	8.7	0.0000028	0.4
55	55	1a"	1a"	1A1	495.56	-45.1	8.8	0.0006225	98.0
54	38	6a'	2a"	3X	495.31	-45.3	9.1	0.0000001	0.0
53	39	6a'	10a'	1X	495.27	-45.4	9.1	0.0000694	10.9
52	38	6a'	2a"	1X	494.86	-45.8	9.5	0.0000697	11.0
51	45	7a'	1a"	3X	494.69	-46.0	9.7	0.0000101	1.6
50	56	1a"	8a'	1X	494.65	-46.0	9.7	0.0002380	37.5
49	47	7a'	9a'	1X	494.43	-46.2	9.9	0.0001012	15.9
48	45	7a'	1a"	1X	494.03	-46.6	10.3	0.0006352	100.0
47	46	7a'	8a'	3X	494.02	-46.6	10.3	0.0000028	0.4
46	37	6a'	9a'	3X	493.89	-46.8	10.5	0.0000001	0.0
45	58	1a"	2a"	1X	492.83	-47.8	11.5	0.0001798	28.3
44	46	7a'	8a'	1X	492.82	-47.8	11.5	0.0002149	33.8
43	36	6a'	8a'	3X	492.17	-48.5	12.2	0.0000030	0.5
42	66	8a'	8a'	1A1	491.82	-48.8	12.6	0.0000559	8.8
41	37	6a'	9a'	1X	491.77	-48.9	12.6	0.0000501	7.9
40	44	7a'	7a'	1A1	491.70	-49.0	12.7	0.0003947	62.1
39	35	6a'	1a"	3X	491.67	-49.0	12.7	0.0000008	0.1
38	35	6a'	1a"	1X	491.03	-49.6	13.3	0.0004823	75.9
37	34	6a'	7a'	3X	490.96	-49.7	13.4	0.0000062	1.0
36	67	8a'	9a'	1X	489.57	-51.1	14.8	0.0000301	4.7
35	36	6a'	8a'	1X	489.41	-51.2	15.0	0.0002021	31.8
34	34	6a'	7a'	1X	488.05	-52.6	16.3	0.0003957	62.3
33	29	5a'	10a'	3X	486.82	-53.8	17.6	0.0000015	0.2
32	28	5a'	2a"	3X	485.38	-55.3	19.0	0.0000018	0.3
31	19	4a'	10a'	3X	485.22	-55.4	19.1	0.0000105	1.6
30	33	6a'	6a'	1A1	484.37	-56.3	20.0	0.0002348	37.0
29	29	5a'	10a'	1X	484.10	-56.6	20.3	0.0000070	1.1
28	27	5a'	9a'	3X	483.78	-56.9	20.6	0.0000012	0.2
27	18	4a'	2a"	3X	483.18	-57.5	21.2	0.0000175	2.8
26	19	4a'	10a'	1X	483.13	-57.5	21.2	0.0000628	9.9
25	28	5a'	2a"	1X	482.72	-57.9	21.6	0.0000064	1.0
24	25	5a'	1a"	3X	482.30	-58.4	22.1	0.0000122	1.9
23	27	5a'	9a'	1X	481.65	-59.0	22.7	0.0000049	0.8
22	26	5a'	8a'	3X	481.63	-59.0	22.7	0.0000033	0.5
21	17	4a'	9a'	3X	481.52	-59.1	22.8	0.0000127	2.0
20	24	5a'	7a'	3X	481.02	-59.6	23.3	0.0000078	1.2
19	18	4a'	2a"	1X	480.95	-59.7	23.4	0.0000572	9.0
18	25	5a'	1a"	1X	480.34	-60.3	24.0	0.0000441	6.9
17	15	4a'	1a"	3X	480.06	-60.6	24.3	0.0001212	19.1
16	17	4a'	9a'	1X	480.01	-60.6	24.4	0.0000421	6.6
15	16	4a'	8a'	3X	479.20	-61.4	25.2	0.0000367	5.8
14	26	5a'	8a'	1X	478.52	-62.1	25.8	0.0000150	2.4
13	14	4a'	7a'	3X	478.46	-62.2	25.9	0.0001024	16.1
12	24	5a'	7a'	1X	478.37	-62.3	26.0	0.0000434	6.8
11	15	4a'	1a"	1X	478.07	-62.6	26.3	0.0003963	62.4
10	16	4a'	8a'	1X	477.69	-63.0	26.7	0.0001361	21.4
9	23	5a'	6a'	3X	477.63	-63.0	26.7	0.0000074	1.2
8	14	4a'	7a'	1X	476.42	-64.2	27.9	0.0003853	60.7
7	23	5a'	6a'	1X	476.26	-64.4	28.1	0.0000276	4.3
6	13	4a'	6a'	3X	475.25	-65.4	29.1	0.0000746	11.7
5	13	4a'	6a'	1X	473.69	-67.0	30.7	0.0002485	39.1
4	12	4a'	5a'	3X	468.29	-72.4	36.1	0.0000021	0.3
3	22	5a'	5a'	1A1	466.04	-74.6	38.3	0.0000045	0.7
2	11	4a'	4a'	1A1	461.75	-78.9	42.6	0.0004275	67.3
1	12	4a'	5a'	1X	460.17	-80.5	44.2	0.0000885	13.9

Total Transition Rate (in au) = 6.90644E-03

D.3.4.1. Formyl fluoride - C(KVV)

CALCULATIONS FOR FCHO, geom. LBII/7

1	0.0000000	0.0000000	-2.0692508
6	0.0000000	0.0000000	0.0000000
8	0.0000000	1.7753193	1.3524252
9	0.0000000	-2.3774757	0.8606342

DEGENERACY OF OCCUPIED ORBITALS
1 1 1 1 1 1 1 1 1

EIGENVECTORS

-0.1523	-0.0120	0.4189	0.1716	0.0000	0.0692	0.1639	0.0000	0.3122
-0.6019	-0.1193	0.4937	-0.1763	0.0000	-0.0584	0.0242	0.0000	0.0591
0.0000	0.0000	0.0000	0.0000	-0.6262	0.0000	0.0000	0.3847	0.0000
0.0041	-0.4426	-0.0615	0.2701	0.0000	-0.3961	-0.1532	0.0000	0.1137
-0.1656	-0.0747	-0.4660	-0.4197	0.0000	-0.1357	-0.2043	0.0000	-0.2623
-0.4729	-0.5481	-0.3768	0.2346	0.0000	0.4169	0.1189	0.0000	-0.0034
0.0000	0.0000	0.0000	0.0000	-0.4467	0.0000	0.0000	0.5359	0.0000
0.1883	0.0815	0.0022	0.4425	0.0000	0.3304	0.4148	0.0000	-0.4234
0.1023	0.1413	-0.2407	-0.2414	0.0000	0.4904	0.0292	0.0000	0.6675
-0.5422	0.6716	-0.2860	0.3223	0.0000	-0.1455	-0.0355	0.0000	0.0197
0.0000	0.0000	0.0000	0.0000	-0.6390	0.0000	0.0000	-0.7516	0.0000
-0.1505	0.0476	0.1142	-0.5221	0.0000	0.1621	0.4030	0.0000	-0.3406
0.0307	-0.0621	-0.2552	-0.0681	0.0000	-0.4956	0.7461	0.0000	0.2757

MOLECULAR J(PP,QQ) COULOMB INTEGRALS

0.5805	0.4649	0.4311	0.5475	0.5602	0.5203	0.5108	0.5087	0.4239
0.4649	0.5342	0.4186	0.4717	0.4697	0.4907	0.4898	0.5090	0.5110
0.4311	0.4186	0.4836	0.4283	0.4344	0.4305	0.4211	0.4182	0.4199
0.5475	0.4717	0.4283	0.6201	0.5523	0.5295	0.5299	0.5125	0.4405
0.5602	0.4697	0.4344	0.5523	0.5754	0.5210	0.5088	0.5293	0.4276
0.5203	0.4907	0.4305	0.5295	0.5210	0.5781	0.5414	0.5220	0.4819
0.5108	0.4898	0.4211	0.5299	0.5088	0.5414	0.5403	0.5100	0.4720
0.5087	0.5090	0.4182	0.5125	0.5293	0.5220	0.5100	0.5438	0.4842
0.4239	0.5110	0.4199	0.4405	0.4276	0.4819	0.4720	0.4842	0.5408

MOLECULAR K(PQ,PQ) EXCHANGE INTEGRALS

0.5805	0.1427	0.0334	0.0601	0.0627	0.0538	0.0521	0.0516	0.0380
0.1427	0.5342	0.0266	0.0600	0.0380	0.0495	0.0465	0.0509	0.0549
0.0334	0.0266	0.4836	0.0262	0.0141	0.0892	0.0376	0.0125	0.0667
0.0601	0.0600	0.0262	0.6201	0.0240	0.0302	0.1141	0.0211	0.0980
0.0627	0.0380	0.0141	0.0240	0.5754	0.0165	0.0132	0.2321	0.0079
0.0538	0.0495	0.0892	0.0302	0.0165	0.5781	0.1797	0.0214	0.0717
0.0521	0.0465	0.0376	0.1141	0.0132	0.1797	0.5403	0.0156	0.0281
0.0516	0.0509	0.0125	0.0211	0.2321	0.0214	0.0156	0.5438	0.0123
0.0380	0.0549	0.0667	0.0980	0.0079	0.0717	0.0281	0.0123	0.5408

MOLECULE: FCHO ATOM: Carbon

AUGER SPECTRUM

CORE AND VALENCE I.P.S USED

1s 296.390
4a' 40.620 5a' 36.290 6a' 23.610 7a' 20.170 1a" 17.740
8a' 19.200 9a' 15.450 2a" 14.540 10a' 12.550

PEAK NR.	MO.INDEX	MO.NAME	SYM	ABS.ENERGY	REL.ENERGY		ABS.RATE	REL.INT.
81	99	10a' 10a'	1A1	256.57	-39.8	0.0	0.0000058	2.6
80	89	2a" 10a'	3X	256.46	-39.9	0.1	0.0000001	0.0
79	79	9a' 10a'	3X	256.31	-40.1	0.3	0.0000000	0.0
78	58	1a" 2a"	3X	256.02	-40.4	0.6	0.0000000	0.0
77	89	2a" 10a'	1X	255.79	-40.6	0.8	0.0000131	6.0
76	79	9a' 10a'	1X	254.78	-41.6	1.8	0.0000066	3.0
75	59	1a" 10a'	3X	254.68	-41.7	1.9	0.0000003	0.1
74	49	7a' 10a'	3X	254.35	-42.0	2.2	0.0000013	0.6
73	59	1a" 10a'	1X	254.25	-42.1	2.3	0.0000346	15.9
72	69	8a' 10a'	3X	253.48	-42.9	3.1	0.0000002	0.1
71	78	9a' 2a"	3X	252.95	-43.4	3.6	0.0000000	0.0
70	88	2a" 2a"	1A1	252.51	-43.9	4.1	0.0000183	8.4
69	78	9a' 2a"	1X	252.10	-44.3	4.5	0.0000102	4.7
68	67	8a' 9a'	3X	251.90	-44.5	4.7	0.0000001	0.1
67	77	9a' 9a'	1A1	250.79	-45.6	5.8	0.0000036	1.6

66	39	6a'	10a'	3X	250.62	-45.8	6.0	0.0000029	1.3
65	57	1a"	9a'	3X	249.71	-46.7	6.9	0.0000000	0.0
64	69	8a'	10a'	1X	249.58	-46.8	7.0	0.0000157	7.2
63	47	7a'	9a'	3X	249.46	-46.9	7.1	0.0000005	0.2
62	68	8a'	2a"	3X	249.03	-47.4	7.5	0.0000001	0.0
61	49	7a'	10a'	1X	249.02	-47.4	7.6	0.0000362	16.6
60	57	1a"	9a'	1X	249.00	-47.4	7.6	0.0000271	12.4
59	48	7a'	2a"	3X	248.31	-48.1	8.3	0.0000010	0.4
58	68	8a'	2a"	1X	247.86	-48.5	8.7	0.0000276	12.7
57	38	6a'	2a"	3X	247.20	-49.2	9.4	0.0000075	3.4
56	48	7a'	2a"	1X	247.16	-49.2	9.4	0.0000417	19.1
55	39	6a'	10a'	1X	246.99	-49.4	9.6	0.0000410	18.9
54	37	6a'	9a'	3X	246.89	-49.5	9.7	0.0000028	1.3
53	38	6a'	2a"	1X	246.52	-49.9	10.1	0.0000567	26.0
52	56	1a"	8a'	3X	245.72	-50.7	10.9	0.0000003	0.1
51	55	1a"	1a"	1A1	245.25	-51.1	11.3	0.0001286	59.1
50	37	6a'	9a'	1X	244.85	-51.5	11.7	0.0000319	14.7
49	56	1a"	8a'	1X	244.82	-51.6	11.8	0.0000733	33.7
48	36	6a'	8a'	3X	244.29	-52.1	12.3	0.0000101	4.6
47	45	7a'	1a"	3X	244.10	-52.3	12.5	0.0000025	1.2
46	35	6a'	1a"	3X	243.60	-52.8	13.0	0.0000198	9.1
45	46	7a'	8a'	3X	243.43	-53.0	13.1	0.0000015	0.7
44	58	1a"	2a"	1X	243.39	-53.0	13.2	0.0000971	44.6
43	47	7a'	9a'	1X	243.25	-53.1	13.3	0.0000197	9.1
42	35	6a'	1a"	1X	242.84	-53.6	13.7	0.0001502	69.0
41	45	7a'	1a"	1X	242.80	-53.6	13.8	0.0001104	50.7
40	66	8a'	8a'	1A1	242.26	-54.1	14.3	0.0000261	12.0
39	67	8a'	9a'	1X	242.12	-54.3	14.5	0.0000171	7.9
38	46	7a'	8a'	1X	241.79	-54.6	14.8	0.0000517	23.7
37	34	6a'	7a'	3X	241.67	-54.7	14.9	0.0000205	9.4
36	34	6a'	7a'	1X	240.24	-56.1	16.3	0.0001344	61.7
35	36	6a'	8a'	1X	239.44	-57.0	17.1	0.0000741	34.0
34	44	7a'	7a'	1A1	239.18	-57.2	17.4	0.0000570	26.2
33	33	6a'	6a'	1A1	236.01	-60.4	20.6	0.0001216	55.9
32	29	5a'	10a'	3X	235.14	-61.3	21.4	0.0000003	0.1
31	28	5a'	2a"	3X	233.09	-63.3	23.5	0.0000004	0.2
30	19	4a'	10a'	3X	232.72	-63.7	23.9	0.0000068	3.1
29	27	5a'	9a'	3X	232.59	-63.8	24.0	0.0000003	0.1
28	29	5a'	10a'	1X	232.15	-64.2	24.4	0.0000191	8.8
27	19	4a'	10a'	1X	230.65	-65.7	25.9	0.0000242	11.1
26	25	5a'	1a"	3X	230.61	-65.8	26.0	0.0000012	0.5
25	28	5a'	2a"	1X	230.32	-66.1	26.2	0.0000327	15.0
24	27	5a'	9a'	1X	230.06	-66.3	26.5	0.0000188	8.6
23	26	5a'	8a'	3X	228.89	-67.5	27.7	0.0000001	0.1
22	18	4a'	2a"	3X	228.79	-67.6	27.8	0.0000111	5.1
21	24	5a'	7a'	3X	228.73	-67.7	27.8	0.0000028	1.3
20	25	5a'	1a"	1X	228.54	-67.8	28.0	0.0000867	39.8
19	17	4a'	9a'	3X	227.84	-68.6	28.7	0.0000051	2.3
18	26	5a'	8a'	1X	226.20	-70.2	30.4	0.0000604	27.8
17	18	4a'	2a"	1X	225.98	-70.4	30.6	0.0000373	17.1
16	23	5a'	6a'	3X	225.82	-70.6	30.8	0.0000124	5.7
15	24	5a'	7a'	1X	225.46	-70.9	31.1	0.0000647	29.7
14	17	4a'	9a'	1X	225.00	-71.4	31.6	0.0000176	8.1
13	15	4a'	1a"	3X	224.49	-71.9	32.1	0.0000295	13.6
12	23	5a'	6a'	1X	224.38	-72.0	32.2	0.0000879	40.4
11	16	4a'	8a'	3X	223.88	-72.5	32.7	0.0000129	5.9
10	14	4a'	7a'	3X	222.34	-74.1	34.2	0.0000158	7.3
9	13	4a'	6a'	3X	221.34	-75.1	35.2	0.0000275	12.6
8	15	4a'	1a"	1X	221.08	-75.3	35.5	0.0000989	45.4
7	16	4a'	8a'	1X	220.95	-75.4	35.6	0.0000466	21.4
6	13	4a'	6a'	1X	219.52	-76.9	37.1	0.0002177	100.0
5	14	4a'	7a'	1X	219.07	-77.3	37.5	0.0000848	39.0
4	12	4a'	5a'	3X	210.71	-85.7	45.9	0.0000149	6.9
3	22	5a'	5a'	1A1	209.27	-87.1	47.3	0.0000357	16.4
2	12	4a'	5a'	1X	202.95	-93.4	53.6	0.0000599	27.5
1	11	4a'	4a'	1A1	199.35	-97.0	57.2	0.0001186	54.5

Total Transition Rate (in au) = 2.75571E-03

D.3.4.2. Formyl fluoride - O(KVV)

```
      CALCULATIONS FOR FCHO,  geom. LBII/7

   1       0.0000000       0.0000000      -2.0692508
   6       0.0000000       0.0000000       0.0000000
   8       0.0000000       1.7753193       1.3524252
   9       0.0000000      -2.3774757       0.8606342
 DEGENERACY OF OCCUPIED ORBITALS
1 1 1 1 1 1 1 1 1

      EIGENVECTORS
  0.0907   0.0746   0.4485  -0.0999   0.0000   0.1743   0.0307   0.0000   0.4289
  0.4205   0.2110   0.4834   0.1939   0.0000   0.1334  -0.0546   0.0000   0.1285
  0.0000   0.0000   0.0000   0.0000   0.4799   0.0000   0.0000  -0.0853   0.0000
  0.1782  -0.3770   0.0892  -0.0371   0.0000  -0.3502   0.1735   0.0000   0.1130
  0.2049   0.0251  -0.3891   0.3467   0.0000  -0.1437  -0.0631   0.0000  -0.3324
  0.8081  -0.2819  -0.2437  -0.2673   0.0000   0.1742  -0.0151   0.0000  -0.0174
  0.0000   0.0000   0.0000   0.0000   0.7874   0.0000   0.0000   0.4808   0.0000
 -0.1505  -0.0398  -0.0361  -0.7334   0.0000   0.1500  -0.4738   0.0000  -0.1209
 -0.0985   0.0634  -0.4974   0.0954   0.0000   0.6102   0.2040   0.0000   0.4638
  0.2214   0.8384  -0.1868  -0.2418   0.0000  -0.2663   0.0978   0.0000   0.0245
  0.0000   0.0000   0.0000   0.0000   0.3869   0.0000   0.0000  -0.8727   0.0000
  0.0810   0.1210   0.0832   0.3701   0.0000   0.3283  -0.6388   0.0000  -0.2085
  0.0127  -0.0672  -0.2364   0.1307   0.0000  -0.4524  -0.5273   0.0000   0.6342

      MOLECULAR J(PP,QQ) COULOMB INTEGRALS
  0.5805   0.4649   0.4311   0.5475   0.5602   0.5203   0.5108   0.5087   0.4239
  0.4649   0.5342   0.4186   0.4717   0.4697   0.4907   0.4898   0.5090   0.5110
  0.4311   0.4186   0.4836   0.4283   0.4344   0.4305   0.4211   0.4182   0.4199
  0.5475   0.4717   0.4283   0.6201   0.5523   0.5295   0.5299   0.5125   0.4405
  0.5602   0.4697   0.4344   0.5523   0.5754   0.5210   0.5088   0.5293   0.4276
  0.5203   0.4907   0.4305   0.5295   0.5210   0.5781   0.5414   0.5220   0.4819
  0.5108   0.4898   0.4211   0.5299   0.5088   0.5414   0.5403   0.5100   0.4720
  0.5087   0.5090   0.4182   0.5125   0.5293   0.5220   0.5100   0.5438   0.4842
  0.4239   0.5110   0.4199   0.4405   0.4276   0.4819   0.4720   0.4842   0.5408

      MOLECULAR K(PQ,PQ) EXCHANGE INTEGRALS
  0.5805   0.1427   0.0334   0.0601   0.0627   0.0538   0.0521   0.0516   0.0380
  0.1427   0.5342   0.0266   0.0600   0.0380   0.0495   0.0465   0.0509   0.0549
  0.0334   0.0266   0.4836   0.0262   0.0141   0.0892   0.0376   0.0125   0.0667
  0.0601   0.0600   0.0262   0.6201   0.0240   0.0302   0.1141   0.0211   0.0980
  0.0627   0.0380   0.0141   0.0240   0.5754   0.0165   0.0132   0.2321   0.0079
  0.0538   0.0495   0.0892   0.0302   0.0165   0.5781   0.1797   0.0214   0.0717
  0.0521   0.0465   0.0376   0.1141   0.0132   0.1797   0.5403   0.0156   0.0281
  0.0516   0.0509   0.0125   0.0211   0.2321   0.0214   0.0156   0.5438   0.0123
  0.0380   0.0549   0.0667   0.0980   0.0079   0.0717   0.0281   0.0123   0.5408

                    MOLECULE: FCHO          ATOM: Oxygen

                                AUGER SPECTRUM

                    CORE AND VALENCE I.P.S USED

                    1s   540.990
                    4a'  40.620  5a'  36.290  6a'  23.610  7a'  20.170  1a"  17.740
                    8a'  19.200  9a'  15.450  2a"  14.540  10a' 12.550

PEAK NR.  MO.INDEX  MO.NAME    SYM     ABS.ENERGY     REL.ENERGY      ABS.RATE   REL.INT.

  81        99      10a' 10a'   1A1      501.17        -39.8          0.0      0.0000447   11.5
  80        89      2a"  10a'   3X       501.06        -39.9          0.1      0.0000000    0.0
  79        79      9a'  10a'   3X       500.91        -40.1          0.3      0.0000000    0.0
  78        58      1a"  2a"    3X       500.62        -40.4          0.6      0.0000000    0.0
  77        89      2a"  10a'   1X       500.39        -40.6          0.8      0.0000566   14.6
  76        79      9a'  10a'   1X       499.38        -41.6          1.8      0.0000796   20.5
  75        59      1a"  10a'   3X       499.28        -41.7          1.9      0.0000000    0.0
  74        49      7a'  10a'   3X       498.95        -42.0          2.2      0.0000031    0.8
  73        59      1a"  10a'   1X       498.85        -42.1          2.3      0.0001518   39.0
  72        69      8a'  10a'   3X       498.08        -42.9          3.1      0.0000017    0.4
  71        78      9a'  2a"    3X       497.55        -43.4          3.6      0.0000000    0.0
  70        88      2a"  2a"    1A1      497.11        -43.9          4.1      0.0000452   11.6
  69        78      9a'  2a"    1X       496.70        -44.3          4.5      0.0000655   16.9
  68        67      8a'  9a'    3X       496.50        -44.5          4.7      0.0000017    0.4
```

67	77	9a'	9a'	1A1	495.39	-45.6	5.8	0.0000599	15.4
66	39	6a'	10a'	3X	495.22	-45.8	6.0	0.0000031	0.8
65	57	1a"	9a'	3X	494.31	-46.7	6.9	0.0000000	0.0
64	69	8a'	10a'	1X	494.18	-46.8	7.0	0.0001451	37.3
63	47	7a'	9a'	3X	494.06	-46.9	7.1	0.0000032	0.8
62	68	8a'	2a"	3X	493.63	-47.4	7.5	0.0000014	0.4
61	49	7a'	10a'	1X	493.62	-47.4	7.6	0.0001552	39.9
60	57	1a"	9a'	1X	493.60	-47.4	7.6	0.0001758	45.2
59	48	7a'	2a"	3X	492.91	-48.1	8.3	0.0000033	0.8
58	68	8a'	2a"	1X	492.46	-48.5	8.7	0.0001016	26.1
57	38	6a'	2a"	3X	491.80	-49.2	9.4	0.0000027	0.7
56	48	7a'	2a"	1X	491.76	-49.2	9.4	0.0001450	37.3
55	39	6a'	10a'	1X	491.59	-49.4	9.6	0.0001017	26.1
54	37	6a'	9a'	3X	491.49	-49.5	9.7	0.0000033	0.8
53	38	6a'	2a"	1X	491.12	-49.9	10.1	0.0000698	18.0
52	56	1a"	8a'	3X	490.32	-50.7	10.9	0.0000037	1.0
51	55	1a"	1a"	1A1	489.85	-51.1	11.3	0.0003253	83.6
50	37	6a'	9a'	1X	489.45	-51.5	11.7	0.0000849	21.8
49	56	1a"	8a'	1X	489.42	-51.6	11.8	0.0002725	70.1
48	36	6a'	8a'	3X	488.89	-52.1	12.3	0.0000009	0.2
47	45	7a'	1a"	3X	488.70	-52.3	12.5	0.0000088	2.3
46	35	6a'	1a"	3X	488.20	-52.8	13.0	0.0000073	1.9
45	46	7a'	8a'	3X	488.03	-53.0	13.1	0.0000080	2.0
44	58	1a"	2a"	1X	487.99	-53.0	13.2	0.0002425	62.4
43	47	7a'	9a'	1X	487.85	-53.1	13.3	0.0002513	64.6
42	35	6a'	1a"	1X	487.44	-53.6	13.7	0.0001873	48.2
41	45	7a'	1a"	1X	487.40	-53.6	13.8	0.0003889	100.0
40	66	8a'	8a'	1A1	486.86	-54.1	14.3	0.0001396	35.9
39	67	8a'	9a'	1X	486.72	-54.3	14.5	0.0001188	30.6
38	46	7a'	8a'	1X	486.39	-54.6	14.8	0.0002631	67.6
37	34	6a'	7a'	3X	486.27	-54.7	14.9	0.0000106	2.7
36	34	6a'	7a'	1X	484.84	-56.1	16.3	0.0001838	47.3
35	36	6a'	8a'	1X	484.04	-57.0	17.1	0.0001855	47.7
34	44	7a'	7a'	1A1	483.78	-57.2	17.4	0.0002799	72.0
33	33	6a'	6a'	1A1	480.61	-60.4	20.6	0.0000638	16.4
32	29	5a'	10a'	3X	479.74	-61.3	21.4	0.0000036	0.9
31	28	5a'	2a"	3X	477.69	-63.3	23.5	0.0000037	0.9
30	19	4a'	10a'	3X	477.32	-63.7	23.9	0.0000297	7.6
29	27	5a'	9a'	3X	477.19	-63.8	24.0	0.0000042	1.1
28	29	5a'	10a'	1X	476.75	-64.2	24.4	0.0000135	3.5
27	19	4a'	10a'	1X	475.25	-65.7	25.9	0.0001024	26.3
26	25	5a'	1a"	3X	475.21	-65.8	26.0	0.0000098	2.5
25	28	5a'	2a"	1X	474.92	-66.1	26.2	0.0000129	3.3
24	27	5a'	9a'	1X	474.66	-66.3	26.5	0.0000155	4.0
23	26	5a'	8a'	3X	473.49	-67.5	27.7	0.0000069	1.8
22	18	4a'	2a"	3X	473.39	-67.6	27.8	0.0000301	7.7
21	24	5a'	7a'	3X	473.33	-67.7	27.8	0.0000077	2.0
20	25	5a'	1a"	1X	473.14	-67.8	28.0	0.0000345	8.9
19	17	4a'	9a'	3X	472.44	-68.6	28.7	0.0000349	9.0
18	26	5a'	8a'	1X	470.80	-70.2	30.4	0.0000269	6.9
17	18	4a'	2a"	1X	470.58	-70.4	30.6	0.0001023	26.3
16	23	5a'	6a'	3X	470.42	-70.6	30.8	0.0000048	1.2
15	24	5a'	7a'	1X	470.06	-70.9	31.1	0.0000407	10.5
14	17	4a'	9a'	1X	469.60	-71.4	31.6	0.0001197	30.8
13	15	4a'	1a"	3X	469.09	-71.9	32.1	0.0000807	20.7
12	23	5a'	6a'	1X	468.98	-72.0	32.2	0.0000227	5.8
11	16	4a'	8a'	3X	468.48	-72.5	32.7	0.0000562	14.5
10	14	4a'	7a'	3X	466.94	-74.1	34.2	0.0000803	20.6
9	13	4a'	6a'	3X	465.94	-75.1	35.2	0.0000370	9.5
8	15	4a'	1a"	1X	465.68	-75.3	35.5	0.0002744	70.6
7	16	4a'	8a'	1X	465.55	-75.4	35.6	0.0002139	55.0
6	13	4a'	6a'	1X	464.12	-76.9	37.1	0.0001790	46.0
5	14	4a'	7a'	1X	463.67	-77.3	37.5	0.0003300	84.8
4	12	4a'	5a'	3X	455.31	-85.7	45.9	0.0000012	0.3
3	22	5a'	5a'	1A1	453.87	-87.1	47.3	0.0000056	1.4
2	12	4a'	5a'	1X	447.55	-93.4	53.6	0.0000908	23.3
1	11	4a'	4a'	1A1	443.95	-97.0	57.2	0.0003693	95.0

Total Transition Rate (in au) = 6.79286E-03

D.3.4.3 Formyl fluoride - F(KVV)

CALCULATIONS FOR FCHO, geom. LBII/7

1	0.0000000	0.0000000	-2.0692508
6	0.0000000	0.0000000	0.0000000
8	0.0000000	1.7753193	1.3524252
9	0.0000000	-2.3774757	0.8606342

DEGENERACY OF OCCUPIED ORBITALS
1 1 1 1 1 1 1 1 1

EIGENVECTORS

-0.0627	-0.1063	-0.1413	-0.1635	0.0000	0.4803	0.1740	0.0000	-0.3311
-0.2460	-0.4420	-0.2414	-0.0962	0.0000	0.3923	-0.1684	0.0000	-0.2116
0.0000	0.0000	0.0000	0.0000	-0.2114	0.0000	0.0000	0.6210	0.0000
0.2084	-0.2991	0.2697	-0.0933	0.0000	0.1020	-0.1248	0.0000	0.2317
-0.0890	-0.1889	0.0663	0.2401	0.0000	-0.4503	-0.3570	0.0000	0.1265
-0.0589	-0.7592	0.1767	-0.1001	0.0000	-0.3213	0.3863	0.0000	-0.0429
0.0000	0.0000	0.0000	0.0000	-0.0936	0.0000	0.0000	0.7558	0.0000
0.0584	0.1701	0.0579	-0.0799	0.0000	0.0103	0.7579	0.0000	0.2930
-0.0080	0.1439	-0.0260	0.1054	0.0000	-0.4091	0.1808	0.0000	-0.7800
-0.9300	0.1458	0.2193	-0.0406	0.0000	-0.0269	0.0443	0.0000	0.1160
0.0000	0.0000	0.0000	0.0000	-0.9729	0.0000	0.0000	-0.2077	0.0000
-0.1047	-0.1349	-0.7011	0.5577	0.0000	-0.0424	0.1772	0.0000	0.2201
0.0363	-0.0521	0.5194	0.7467	0.0000	0.3592	0.0931	0.0000	-0.1339

MOLECULAR J(PP,QQ) COULOMB INTEGRALS

0.5805	0.4649	0.4311	0.5475	0.5602	0.5203	0.5108	0.5087	0.4239
0.4649	0.5342	0.4186	0.4717	0.4697	0.4907	0.4898	0.5090	0.5110
0.4311	0.4186	0.4836	0.4283	0.4344	0.4305	0.4211	0.4182	0.4199
0.5475	0.4717	0.4283	0.6201	0.5523	0.5295	0.5299	0.5125	0.4405
0.5602	0.4697	0.4344	0.5523	0.5754	0.5210	0.5088	0.5293	0.4276
0.5203	0.4907	0.4305	0.5295	0.5210	0.5781	0.5414	0.5220	0.4819
0.5108	0.4898	0.4211	0.5299	0.5088	0.5414	0.5403	0.5100	0.4720
0.5087	0.5090	0.4182	0.5125	0.5293	0.5220	0.5100	0.5438	0.4842
0.4239	0.5110	0.4199	0.4405	0.4276	0.4819	0.4720	0.4842	0.5408

MOLECULAR K(PQ,PQ) EXCHANGE INTEGRALS

0.5805	0.1427	0.0334	0.0601	0.0627	0.0538	0.0521	0.0516	0.0380
0.1427	0.5342	0.0266	0.0600	0.0380	0.0495	0.0465	0.0509	0.0549
0.0334	0.0266	0.4836	0.0262	0.0141	0.0892	0.0376	0.0125	0.0667
0.0601	0.0600	0.0262	0.6201	0.0240	0.0302	0.1141	0.0211	0.0980
0.0627	0.0380	0.0141	0.0240	0.5754	0.0165	0.0132	0.2321	0.0079
0.0538	0.0495	0.0892	0.0302	0.0165	0.5781	0.1797	0.0214	0.0717
0.0521	0.0465	0.0376	0.1141	0.0132	0.1797	0.5403	0.0156	0.0281
0.0516	0.0509	0.0125	0.0211	0.2321	0.0214	0.0156	0.5438	0.0123
0.0380	0.0549	0.0667	0.0980	0.0079	0.0717	0.0281	0.0123	0.5408

MOLECULE: FCHO ATOM: Fluorine

AUGER SPECTRUM

CORE AND VALENCE I.P.S USED

1s 695.000
4a' 40.620 5a' 36.290 6a' 23.610 7a' 20.170 1a" 17.740
8a' 19.200 9a' 15.450 2a" 14.540 10a' 12.550

PEAK NR.	MO.INDEX	MO.NAME	SYM	ABS.ENERGY	REL.ENERGY		ABS.RATE	REL.INT.
81	99	10a' 10a'	1A1	655.18	-39.8	0.0	0.0000043	0.5
80	89	2a" 10a'	3X	655.07	-39.9	0.1	0.0000001	0.0
79	79	9a' 10a'	3X	654.92	-40.1	0.3	0.0000001	0.0
78	58	1a" 2a"	3X	654.63	-40.4	0.6	0.0000000	0.0
77	89	2a" 10a'	1X	654.40	-40.6	0.8	0.0000034	0.4
76	79	9a' 10a'	1X	653.39	-41.6	1.8	0.0000037	0.4
75	59	1a" 10a'	3X	653.29	-41.7	1.9	0.0000024	0.3
74	49	7a' 10a'	3X	652.96	-42.0	2.2	0.0000023	0.3
73	59	1a" 10a'	1X	652.86	-42.1	2.3	0.0000741	8.5
72	69	8a' 10a'	3X	652.09	-42.9	3.1	0.0000003	0.0
71	78	9a' 2a"	3X	651.56	-43.4	3.6	0.0000000	0.0
70	88	2a" 2a"	1A1	651.12	-43.9	4.1	0.0000016	0.2
69	78	9a' 2a"	1X	650.71	-44.3	4.5	0.0000019	0.2
68	67	8a' 9a'	3X	650.51	-44.5	4.7	0.0000001	0.0

67	77	9a'	9a'	1A1	649.40	-45.6	5.8	0.0000014	0.2
66	39	6a'	10a'	3X	649.23	-45.8	6.0	0.0000048	0.5
65	57	1a"	9a'	3X	648.32	-46.7	6.9	0.0000004	0.0
64	69	8a'	10a'	1X	648.19	-46.8	7.0	0.0000123	1.4
63	47	7a'	9a'	3X	648.07	-46.9	7.1	0.0000005	0.1
62	68	8a'	2a"	3X	647.64	-47.4	7.5	0.0000000	0.0
61	49	7a'	10a'	1X	647.63	-47.4	7.6	0.0000684	7.9
60	57	1a"	9a'	1X	647.61	-47.4	7.6	0.0000411	4.7
59	48	7a'	2a"	3X	646.92	-48.1	8.3	0.0000000	0.0
58	68	8a'	2a"	1X	646.47	-48.5	8.7	0.0000060	0.7
57	38	6a'	2a"	3X	645.81	-49.2	9.4	0.0000004	0.0
56	48	7a'	2a"	1X	645.77	-49.2	9.4	0.0000395	4.6
55	39	6a'	10a'	1X	645.60	-49.4	9.6	0.0000940	10.8
54	37	6a'	9a'	3X	645.50	-49.5	9.7	0.0000009	0.1
53	38	6a'	2a"	1X	645.13	-49.9	10.1	0.0000359	4.1
52	56	1a"	8a'	3X	644.33	-50.7	10.9	0.0000001	0.0
51	55	1a"	1a"	1A1	643.86	-51.1	11.3	0.0007478	86.3
50	37	6a'	9a'	1X	643.46	-51.5	11.7	0.0000380	4.4
49	56	1a"	8a'	1X	643.43	-51.6	11.8	0.0001309	15.1
48	36	6a'	8a'	3X	642.90	-52.1	12.3	0.0000018	0.2
47	45	7a'	1a"	3X	642.71	-52.3	12.5	0.0000003	0.0
46	35	6a'	1a"	3X	642.21	-52.8	13.0	0.0000087	1.0
45	46	7a'	8a'	3X	642.04	-53.0	13.1	0.0000001	0.0
44	58	1a"	2a"	1X	642.00	-53.0	13.2	0.0000681	7.9
43	47	7a'	9a'	1X	641.86	-53.1	13.3	0.0000552	6.4
42	35	6a'	1a"	1X	641.45	-53.6	13.7	0.0007876	90.8
41	45	7a'	1a"	1X	641.41	-53.6	13.8	0.0008669	100.0
40	66	8a'	8a'	1A1	640.87	-54.1	14.3	0.0000143	1.7
39	67	8a'	9a'	1X	640.73	-54.3	14.5	0.0000061	0.7
38	46	7a'	8a'	1X	640.40	-54.6	14.8	0.0001571	18.1
37	34	6a'	7a'	3X	640.28	-54.7	14.9	0.0000083	1.0
36	34	6a'	7a'	1X	638.85	-56.1	16.3	0.0007235	83.5
35	36	6a'	8a'	1X	638.05	-57.0	17.1	0.0001382	15.9
34	44	7a'	7a'	1A1	637.79	-57.2	17.4	0.0006304	72.7
33	33	6a'	6a'	1A1	634.62	-60.4	20.6	0.0005072	58.5
32	29	5a'	10a'	3X	633.75	-61.3	21.4	0.0000005	0.1
31	28	5a'	2a"	3X	631.70	-63.3	23.5	0.0000002	0.0
30	19	4a'	10a'	3X	631.33	-63.7	23.9	0.0000099	1.1
29	27	5a'	9a'	3X	631.20	-63.8	24.0	0.0000002	0.0
28	29	5a'	10a'	1X	630.76	-64.2	24.4	0.0000033	0.4
27	19	4a'	10a'	1X	629.26	-65.7	25.9	0.0000563	6.5
26	25	5a'	1a"	3X	629.22	-65.8	26.0	0.0000039	0.4
25	28	5a'	2a"	1X	628.93	-66.1	26.2	0.0000015	0.2
24	27	5a'	9a'	1X	628.67	-66.3	26.5	0.0000020	0.2
23	26	5a'	8a'	3X	627.50	-67.5	27.7	0.0000005	0.1
22	18	4a'	2a"	3X	627.40	-67.6	27.8	0.0000072	0.8
21	24	5a'	7a'	3X	627.34	-67.7	27.8	0.0000033	0.4
20	25	5a'	1a"	1X	627.15	-67.8	28.0	0.0000334	3.9
19	17	4a'	9a'	3X	626.45	-68.6	28.7	0.0000064	0.7
18	26	5a'	8a'	1X	624.81	-70.2	30.4	0.0000048	0.5
17	18	4a'	2a"	1X	624.59	-70.4	30.6	0.0000239	2.8
16	23	5a'	6a'	3X	624.43	-70.6	30.8	0.0000025	0.3
15	24	5a'	7a'	1X	624.07	-70.9	31.1	0.0000387	4.5
14	17	4a'	9a'	1X	623.61	-71.4	31.6	0.0000251	2.9
13	15	4a'	1a"	3X	623.10	-71.9	32.1	0.0001572	18.1
12	23	5a'	6a'	1X	622.99	-72.0	32.2	0.0000319	3.7
11	16	4a'	8a'	3X	622.49	-72.5	32.7	0.0000216	2.5
10	14	4a'	7a'	3X	620.95	-74.1	34.2	0.0001447	16.7
9	13	4a'	6a'	3X	619.95	-75.1	35.2	0.0001338	15.4
8	15	4a'	1a"	1X	619.69	-75.3	35.5	0.0005241	60.5
7	16	4a'	8a'	1X	619.56	-75.4	35.6	0.0000736	8.5
6	13	4a'	6a'	1X	618.13	-76.9	37.1	0.0004973	57.4
5	14	4a'	7a'	1X	617.68	-77.3	37.5	0.0004839	55.8
4	12	4a'	5a'	3X	609.32	-85.7	45.9	0.0000042	0.5
3	22	5a'	5a'	1A1	607.88	-87.1	47.3	0.0000010	0.1
2	12	4a'	5a'	1X	601.56	-93.4	53.6	0.0000424	4.9
1	11	4a'	4a'	1A1	597.96	-97.0	57.2	0.0006248	72.1

Total Transition Rate (in au) = 8.25434E-03

D.3.5.1. Formaldehyde - C(KVV)

CALCULATIONS FOR HCHO, geom. LBII/7 p.132

6	0.0000000	0.0000000	0.0000000
8	0.0000000	0.0000000	-2.2824121
1	0.0000000	-1.7934984	1.1098505
1	0.0000000	1.7934984	1.1098505

DEGENERACY OF OCCUPIED ORBITALS
1 1 1 1 1 1

EIGENVECTORS

-0.5941	0.5700	0.0000	-0.0195	0.0000	0.0000
0.0000	0.0000	0.0000	0.0000	0.7461	0.0000
0.0000	0.0000	0.6779	0.0000	0.0000	-0.3732
0.2674	0.4162	0.0000	0.5229	0.0000	0.0000
-0.6797	-0.5309	0.0000	0.4108	0.0000	0.0000
0.0000	0.0000	0.0000	0.0000	0.6659	0.0000
0.0000	0.0000	0.5781	0.0000	0.0000	0.8029
-0.2603	0.1462	0.0000	-0.7014	0.0000	0.0000
-0.1514	0.3152	-0.3212	0.1810	0.0000	0.3287
-0.1514	0.3152	0.3212	0.1810	0.0000	-0.3287

MOLECULAR J(PP,QQ) COULOMB INTEGRALS

0.6128	0.4426	0.4941	0.5805	0.5871	0.5451
0.4426	0.4822	0.4583	0.4644	0.4641	0.4396
0.4941	0.4583	0.4764	0.4896	0.4916	0.4791
0.5805	0.4644	0.4896	0.6980	0.5958	0.5580
0.5871	0.4641	0.4916	0.5958	0.6094	0.5354
0.5451	0.4396	0.4791	0.5580	0.5354	0.5399

MOLECULAR K(PQ,PQ) EXCHANGE INTEGRALS

0.6128	0.0467	0.0398	0.0508	0.0603	0.0572
0.0467	0.4822	0.0429	0.0824	0.0271	0.0436
0.0398	0.0429	0.4764	0.0190	0.0095	0.1495
0.0508	0.0824	0.0190	0.6980	0.0252	0.0297
0.0603	0.0271	0.0095	0.0252	0.6094	0.0124
0.0572	0.0436	0.1495	0.0297	0.0124	0.5399

MOLECULE: HCHO ATOM: Carbon

AUGER SPECTRUM

CORE AND VALENCE I.P.S USED

1s 294.470
3a1 34.200 4a1 21.400 1b2 17.000 5a1 16.100 1b1 14.500
2b2 10.900

PEAK NR.	MO.INDEX	MO.NAME		SYM	ABS.ENERGY	REL.ENERGY		ABS.RATE	REL.INT.
36	66	2b2	2b2	1A1	257.98	-36.5	0.0	0.0000162	5.9
35	36	1b2	2b2	3X	257.60	-36.9	0.4	0.0000000	0.0
34	56	1b1	2b2	3X	254.84	-39.6	3.1	0.0000000	0.0
33	56	1b1	2b2	1X	254.16	-40.3	3.8	0.0000816	29.8
32	46	5a1	2b2	3X	253.09	-41.4	4.9	0.0000000	0.0
31	46	5a1	2b2	1X	251.48	-43.0	6.5	0.0000401	14.7
30	26	4a1	2b2	3X	251.39	-43.1	6.6	0.0000094	3.4
29	35	1b2	1b1	3X	249.85	-44.6	8.1	0.0000000	0.0
28	36	1b2	2b2	1X	249.46	-45.0	8.5	0.0001071	39.1
27	35	1b2	1b1	1X	249.33	-45.1	8.6	0.0002694	98.3
26	26	4a1	2b2	1X	249.02	-45.4	9.0	0.0000533	19.5
25	55	1b1	1b1	1A1	248.89	-45.6	9.1	0.0002592	94.6
24	34	1b2	5a1	3X	248.56	-45.9	9.4	0.0000000	0.0
23	45	5a1	1b1	3X	248.34	-46.1	9.6	0.0000000	0.0
22	34	1b2	5a1	1X	247.53	-46.9	10.4	0.0001325	48.3
21	33	1b2	1b2	1A1	247.51	-47.0	10.5	0.0001766	64.5
20	45	5a1	1b1	1X	246.97	-47.5	11.0	0.0001605	58.6
19	25	4a1	1b1	3X	246.68	-47.8	11.3	0.0000376	13.7
18	24	4a1	5a1	3X	246.58	-47.9	11.4	0.0000195	7.1
17	25	4a1	1b1	1X	245.20	-49.3	12.8	0.0002131	77.8
16	23	4a1	1b2	3X	244.77	-49.7	13.2	0.0000310	11.3
15	44	5a1	5a1	1A1	243.28	-51.2	14.7	0.0000626	22.9
14	23	4a1	1b2	1X	242.43	-52.0	15.5	0.0001759	64.2
13	24	4a1	5a1	1X	242.09	-52.4	15.9	0.0001346	49.1

12	22	4a1	4a1	1A1	238.55	-55.9	19.4	0.0001468	53.6
11	16	3a1	2b2	3X	236.09	-58.4	21.9	0.0000102	3.7
10	16	3a1	2b2	1X	232.98	-61.5	25.0	0.0000408	14.9
9	15	3a1	1b1	3X	231.43	-63.0	26.5	0.0000408	14.9
8	13	3a1	1b2	3X	230.91	-63.6	27.1	0.0000337	12.3
7	14	3a1	5a1	3X	229.76	-64.7	28.2	0.0000194	7.1
6	13	3a1	1b2	1X	228.74	-65.7	29.2	0.0001346	49.1
5	15	3a1	1b1	1X	228.15	-66.3	29.8	0.0001630	59.5
4	12	3a1	4a1	3X	228.10	-66.4	29.9	0.0000332	12.1
3	14	3a1	5a1	1X	226.99	-67.5	31.0	0.0000923	33.7
2	12	3a1	4a1	1X	225.56	-68.9	32.4	0.0002740	100.0
1	11	3a1	3a1	1A1	209.39	-85.1	48.6	0.0001250	45.6

Total Transition Rate (in au) = 3.09379E-03

D.3.5.2 Formaldehyde - O(KVV)

```
        CALCULATIONS FOR HCHO geom 1bII/7 p.132

   6       0.0000000       0.0000000       0.0000000
   8       0.0000000       0.0000000      -2.2824121
   1       0.0000000      -1.7934984       1.1098505
   1       0.0000000       1.7934984       1.1098505
 DEGENERACY OF OCCUPIED ORBITALS
1 1 1 1 1 1

      EIGENVECTORS
 0.3744  -0.6440   0.0000   0.1395   0.0000   0.0000
 0.0000   0.0000   0.0000   0.0000  -0.4269   0.0000
 0.0000   0.0000  -0.5255   0.0000   0.0000  -0.5069
-0.3045  -0.2234   0.0000   0.4916   0.0000   0.0000
 0.8498   0.3549   0.0000   0.2238   0.0000   0.0000
 0.0000   0.0000   0.0000   0.0000  -0.9043   0.0000
 0.0000   0.0000  -0.7734   0.0000   0.0000   0.6193
 0.1764  -0.3904   0.0000  -0.7551   0.0000   0.0000
 0.0832  -0.3584   0.2507   0.2435   0.0000   0.4240
 0.0832  -0.3584  -0.2507   0.2435   0.0000  -0.4240

     MOLECULAR J(PP,QQ) COULOMB INTEGRALS
 0.6128   0.4426   0.4941   0.5805   0.5871   0.5451
 0.4426   0.4822   0.4583   0.4644   0.4641   0.4396
 0.4941   0.4583   0.4764   0.4896   0.4916   0.4791
 0.5805   0.4644   0.4896   0.6980   0.5958   0.5580
 0.5871   0.4641   0.4916   0.5958   0.6094   0.5354
 0.5451   0.4396   0.4791   0.5580   0.5354   0.5399

     MOLECULAR K(PQ,PQ) EXCHANGE INTEGRALS
 0.6128   0.0467   0.0398   0.0508   0.0603   0.0572
 0.0467   0.4822   0.0429   0.0824   0.0271   0.0436
 0.0398   0.0429   0.4764   0.0190   0.0095   0.1495
 0.0508   0.0824   0.0190   0.6980   0.0252   0.0297
 0.0603   0.0271   0.0095   0.0252   0.6094   0.0124
 0.0572   0.0436   0.1495   0.0297   0.0124   0.5399

                MOLECULE: HCHO          ATOM: Oxygen

                                AUGER SPECTRUM

                CORE AND VALENCE I.P.S USED

                1s   539.440
                3a1   34.200  4a1   21.400  1b2  17.000  5a1   16.100  1b1 14.500
                2b2  10.900

PEAK NR.  MO.INDEX  MO.NAME   SYM      ABS.ENERGY    REL.ENERGY        ABS.RATE   REL.INT.

  36        66      2b2  2b2     1A1     502.95       -36.5       0.0     0.0001245   22.0
  35        36      1b2  2b2     3X      502.57       -36.9       0.4     0.0000000    0.0
  34        56      1b1  2b2     3X      499.81       -39.6       3.1     0.0000000    0.0
  33        56      1b1  2b2     1X      499.13       -40.3       3.8     0.0003342   59.0
  32        46      5a1  2b2     3X      498.06       -41.4       4.9     0.0000038    0.7
  31        46      5a1  2b2     1X      496.45       -43.0       6.5     0.0002450   43.3
  30        26      4a1  2b2     3X      496.36       -43.1       6.6     0.0000096    1.7
  29        35      1b2  1b1     3X      494.82       -44.6       8.1     0.0000000    0.0
  28        36      1b2  2b2     1X      494.43       -45.0       8.5     0.0003883   68.6
  27        35      1b2  1b1     1X      494.30       -45.1       8.6     0.0005211   92.1
  26        26      4a1  2b2     1X      493.99       -45.4       9.0     0.0000925   16.3
  25        55      1b1  1b1     1A1     493.86       -45.6       9.1     0.0005660  100.0
  24        34      1b2  5a1     3X      493.53       -45.9       9.4     0.0000060    1.1
  23        45      5a1  1b1     3X      493.31       -46.1       9.6     0.0000082    1.4
  22        34      1b2  5a1     1X      492.50       -46.9      10.4     0.0003821   67.5
  21        33      1b2  1b2     1A1     492.48       -47.0      10.5     0.0003028   53.5
  20        45      5a1  1b1     1X      491.94       -47.5      11.0     0.0005224   92.3
  19        25      4a1  1b1     3X      491.65       -47.8      11.3     0.0000205    3.6
  18        24      4a1  5a1     3X      491.55       -47.9      11.4     0.0000065    1.1
  17        25      4a1  1b1     1X      490.17       -49.3      12.8     0.0001972   34.8
  16        23      4a1  1b2     3X      489.74       -49.7      13.2     0.0000150    2.7
  15        44      5a1  5a1     1A1     488.25       -51.2      14.7     0.0002937   51.9
  14        23      4a1  1b2     1X      487.40       -52.0      15.5     0.0001442   25.5
  13        24      4a1  5a1     1X      487.06       -52.4      15.9     0.0002050   36.2
```

12	22	4a1	4a1	1A1	483.52	-55.9	19.4	0.0000440	7.8
11	16	3a1	2b2	3X	481.06	-58.4	21.9	0.0000552	9.7
10	16	3a1	2b2	1X	477.95	-61.5	25.0	0.0001858	32.8
9	15	3a1	1b1	3X	476.40	-63.0	26.5	0.0001177	20.8
8	13	3a1	1b2	3X	475.88	-63.6	27.1	0.0000860	15.2
7	14	3a1	5a1	3X	474.73	-64.7	28.2	0.0000924	16.3
6	13	3a1	1b2	1X	473.71	-65.7	29.2	0.0002898	51.2
5	15	3a1	1b1	1X	473.12	-66.3	29.8	0.0003962	70.0
4	12	3a1	4a1	3X	473.07	-66.4	29.9	0.0000310	5.5
3	14	3a1	5a1	1X	471.96	-67.5	31.0	0.0003513	62.1
2	12	3a1	4a1	1X	470.53	-68.9	32.4	0.0002333	41.2
1	11	3a1	3a1	1A1	454.36	-85.1	48.6	0.0004493	79.4

Total Transition Rate (in au) = 6.72036E-03

D.4.1. Silane - Si($L_{23}VV$)

```
         CALCULATIONS FOR SiH4, geom. LBII/15 p.119

  14      0.0000000      0.0000000      0.0000000
   1     -1.6160237      1.6160237      1.6160237
   1      1.6160237      1.6160237     -1.6160237
   1     -1.6160237     -1.6160237     -1.6160237
   1      1.6160237     -1.6160237      1.6160237
 DEGENERACY OF OCCUPIED ORBITALS
1 3 3 3


     EIGENVECTORS
 0.8834   0.0000   0.0000   0.0000
 0.0000   0.6853   0.0000   0.0000
 0.0000   0.0000   0.6853   0.0000
 0.0000   0.0000   0.0000   0.6853
 0.2343  -0.3641   0.3641   0.3641
 0.2343   0.3641   0.3641  -0.3641
 0.2343  -0.3641  -0.3641  -0.3641
 0.2343   0.3641  -0.3641   0.3641


    MOLECULAR J(PP,QQ) COULOMB INTEGRALS
 0.3498   0.3476   0.3476   0.3476
 0.3476   0.3490   0.3453   0.3453
 0.3476   0.3453   0.3490   0.3453
 0.3476   0.3453   0.3453   0.3490


    MOLECULAR K(PQ,PQ) EXCHANGE INTEGRALS
 0.3498   0.0578   0.0578   0.0578
 0.0578   0.3490   0.0593   0.0593
 0.0578   0.0593   0.3490   0.0593
 0.0578   0.0593   0.0593   0.3490

                              MOLECULE: SiH4          ATOM: Silicon 2p

                                      AUGER SPECTRUM

                          CORE AND VALENCE I.P.S USED

                           2p3/2   107.200
                           3a1 18.200   2t2 12.800   2t2 12.800   2t2 12.800

 SPIN - ORBIT  SPLITTING =    0.60 eV

  CONTRIBUTIONS FROM 2p1/2 INITIAL HOLE ARE MARKED WITH *

 PEAK NR.  MO.INDEX   MO.NAME    SYM      ABS.ENERGY     REL.ENERGY       ABS.RATE   REL.INT.

   14        23       2t2  2t2   *3T1      74.42       -32.8       0.0     0.0001179    50.0
   13        22       2t2  2t2   * 1E      74.32       -32.9       0.1     0.0000397    16.8
   12        23       2t2  2t2    3T1      73.82       -33.4       0.6     0.0002359   100.0
   11        22       2t2  2t2     1E      73.72       -33.5       0.7     0.0000795    33.7
   10        23       2t2  2t2   *1T2      71.19       -36.0       3.2     0.0000596    25.3
    9        23       2t2  2t2    1T2      70.59       -36.6       3.8     0.0001192    50.5
    8        22       2t2  2t2   *1A1      69.48       -37.7       4.9     0.0000267    11.3
    7        12       3a1  2t2   *3T2      68.91       -38.3       5.5     0.0000708    30.0
    6        22       2t2  2t2    1A1      68.88       -38.3       5.5     0.0000534    22.6
    5        12       3a1  2t2    3T2      68.31       -38.9       6.1     0.0001415    60.0
    4        12       3a1  2t2   *1T2      65.77       -41.4       8.6     0.0000687    29.1
    3        12       3a1  2t2    1T2      65.17       -42.0       9.2     0.0001374    58.3
    2        11       3a1  3a1   *1A1      61.88       -45.3      12.5     0.0000087     3.7
    1        11       3a1  3a1    1A1      61.28       -45.9      13.1     0.0000173     7.3

Total Transition Rate(au) =     1.17626E-03
```

D.4.2. Phosphine - P($L_{23}VV$)

```
      CALCULATIONS FOR PH3 coord from LB II/15 page 118

    1       1.9519986      -1.1269870       1.4561260
    1      -1.9519986      -1.1269870       1.4561260
    1       0.0000000       2.2539740       1.4561260
   15       0.0000000       0.0000000       0.0000000
 DEGENERACY OF OCCUPIED ORBITALS
1 2 2 1


      EIGENVECTORS
-0.2407   0.4813  -0.2779  -0.3471
-0.2407  -0.4813  -0.2779  -0.3471
-0.2407   0.0000   0.5557  -0.3471
-0.9010   0.0000   0.0000   0.3726
 0.0000   0.7326   0.0000   0.0000
 0.0000   0.0000   0.7326   0.0000
-0.1203   0.0000   0.0000  -0.7069


      MOLECULAR J(PP,QQ) COULOMB INTEGRALS
 0.4164   0.3907   0.3907   0.3899
 0.3907   0.4198   0.3613   0.3879
 0.3907   0.3613   0.4198   0.3879
 0.3899   0.3879   0.3879   0.4223


      MOLECULAR K(PQ,PQ) EXCHANGE INTEGRALS
 0.4164   0.0467   0.0467   0.0343
 0.0467   0.4198   0.0292   0.0477
 0.0467   0.0292   0.4198   0.0477
 0.0343   0.0477   0.0477   0.4223

                              MOLECULE: PH3 2p          ATOM: Phosphor

                                      AUGER SPECTRUM

                          CORE AND VALENCE I.P.S USED

                          2p3/2   137.050
                          4a1 22.610    2e 13.500    2e 13.500    5a1 10.580

SPIN - ORBIT  SPLITTING =     0.90 eV

 CONTRIBUTIONS FROM 2p1/2 INITIAL HOLE ARE MARKED WITH *
```

PEAK NR.	MO.INDEX	MO.NAME		SYM	ABS.ENERGY	REL.ENERGY		ABS.RATE	REL.INT.
22	44	5a1	5a1	*1A1	105.30	-31.8	0.0	0.0000408	18.0
21	24	2e	5a1	* 3X	104.61	-32.4	0.7	0.0001135	50.0
20	44	5a1	5a1	1A1	104.40	-32.7	0.9	0.0000815	35.9
19	24	2e	5a1	3X	103.71	-33.3	1.6	0.0002270	100.0
18	24	2e	5a1	* 1X	102.02	-35.0	3.3	0.0000625	27.5
17	23	2e	2e	*3A2	101.91	-35.1	3.4	0.0000556	24.5
16	24	2e	5a1	1X	101.12	-35.9	4.2	0.0001249	55.0
15	23	2e	2e	3A2	101.01	-36.0	4.3	0.0001112	49.0
14	23	2e	2e	* 1E	100.32	-36.7	5.0	0.0000564	24.9
13	23	2e	2e	1E	99.42	-37.6	5.9	0.0001129	49.7
12	22	2e	2e	*1A1	98.73	-38.3	6.6	0.0000350	15.4
11	22	2e	2e	1A1	97.83	-39.2	7.5	0.0000700	30.8
10	14	4a1	5a1	* 3X	95.08	-42.0	10.2	0.0000310	13.7
9	14	4a1	5a1	3X	94.18	-42.9	11.1	0.0000620	27.3
8	14	4a1	5a1	* 1X	93.22	-43.8	12.1	0.0000256	11.3
7	12	4a1	2e	* 3E	92.48	-44.6	12.8	0.0000611	26.9
6	14	4a1	5a1	1X	92.32	-44.7	13.0	0.0000512	22.6
5	12	4a1	2e	3E	91.58	-45.5	13.7	0.0001222	53.8
4	12	4a1	2e	* 1E	89.94	-47.1	15.4	0.0000594	26.2
3	12	4a1	2e	1E	89.04	-48.0	16.3	0.0001189	52.4
2	11	4a1	4a1	*1A1	81.40	-55.7	23.9	0.0000136	6.0
1	11	4a1	4a1	1A1	80.50	-56.6	24.8	0.0000272	12.0

```
Total Transition Rate(au) =     1.66348E-03
```

D.4.3. Hydrogen sulphide - S($L_{23}VV$)

```
     CALCULATIONS FOR SH2,geom. LB/15 p.114

   1       0.0000000       1.8172377       1.7515180
   1       0.0000000      -1.8172377       1.7515180
  16       0.0000000       0.0000000       0.0000000
 DEGENERACY OF OCCUPIED ORBITALS
1 1 1 1


      EIGENVECTORS
 -0.1931   -0.4118   -0.4135    0.0000
 -0.1931    0.4118   -0.4135    0.0000
 -0.9591    0.0000    0.2269    0.0000
  0.0000    0.0000    0.0000    1.0000
  0.0000   -0.8129    0.0000    0.0000
 -0.0744    0.0000   -0.7788    0.0000


      MOLECULAR J(PP,QQ) COULOMB INTEGRALS
  0.4669    0.4303    0.4290    0.4758
  0.4303    0.4440    0.4334    0.4206
  0.4290    0.4334    0.4652    0.4358
  0.4758    0.4206    0.4358    0.5262


      MOLECULAR K(PQ,PQ) EXCHANGE INTEGRALS
  0.4669    0.0563    0.0457    0.0752
  0.0563    0.4440    0.0679    0.0094
  0.0457    0.0679    0.4652    0.0230
  0.0752    0.0094    0.0230    0.5262


                          MOLECULE: H2S 2p          ATOM: Sulphur

                                AUGER SPECTRUM

                    CORE AND VALENCE I.P.S USED

                     2p3/2   170.360
                     4a1 22.800   2b2 15.500   5a1 13.300   2b1 10.500

SPIN - ORBIT  SPLITTING =      1.20 eV

CONTRIBUTIONS FROM 2p1/2 INITIAL HOLE ARE MARKED WITH *
```

PEAK NR.	MO.INDEX	MO.NAME	SYM	ABS.ENERGY	REL.ENERGY		ABS.RATE	REL.INT.
32	34	5a1 2b1	* 3X	136.53	-33.8	0.0	0.0001282	47.2
31	44	2b1 2b1	*1A1	136.24	-34.1	0.3	0.0001175	43.3
30	34	5a1 2b1	3X	135.33	-35.0	1.2	0.0002564	94.4
29	34	5a1 2b1	* 1X	135.28	-35.1	1.3	0.0000670	24.7
28	44	2b1 2b1	1A1	135.04	-35.3	1.5	0.0002350	86.5
27	24	2b2 2b1	* 3X	134.37	-36.0	2.2	0.0001358	50.0
26	34	5a1 2b1	1X	134.08	-36.3	2.5	0.0001340	49.3
25	24	2b2 2b1	* 1X	133.86	-36.5	2.7	0.0000691	25.4
24	24	2b2 2b1	3X	133.17	-37.2	3.4	0.0002716	100.0
23	23	2b2 5a1	* 3X	132.81	-37.5	3.7	0.0000847	31.2
22	24	2b2 2b1	1X	132.66	-37.7	3.9	0.0001382	50.9
21	33	5a1 5a1	*1A1	132.30	-38.1	4.2	0.0000495	18.2
20	23	2b2 5a1	3X	131.61	-38.7	4.9	0.0001694	62.4
19	33	5a1 5a1	1A1	131.10	-39.3	5.4	0.0000991	36.5
18	23	2b2 5a1	* 1X	129.12	-41.2	7.4	0.0000443	16.3
17	22	2b2 2b2	*1A1	128.48	-41.9	8.0	0.0000513	18.9
16	23	2b2 5a1	1X	127.92	-42.4	8.6	0.0000886	32.6
15	14	4a1 2b1	* 3X	127.36	-43.0	9.2	0.0000641	23.6
14	22	2b2 2b2	1A1	127.28	-43.1	9.2	0.0001026	37.8
13	14	4a1 2b1	3X	126.16	-44.2	10.4	0.0001283	47.2
12	13	4a1 5a1	* 3X	125.03	-45.3	11.5	0.0000400	14.7
11	13	4a1 5a1	3X	123.83	-46.5	12.7	0.0000799	29.4
10	14	4a1 2b1	* 1X	123.27	-47.1	13.3	0.0000647	23.8
9	12	4a1 2b2	* 3X	123.08	-47.3	13.4	0.0000424	15.6
8	13	4a1 5a1	* 1X	122.54	-47.8	14.0	0.0000382	14.1
7	14	4a1 2b1	1X	122.07	-48.3	14.5	0.0001293	47.6
6	12	4a1 2b2	3X	121.88	-48.5	14.6	0.0000848	31.2
5	13	4a1 5a1	1X	121.34	-49.0	15.2	0.0000764	28.1
4	12	4a1 2b2	* 1X	120.02	-50.3	16.5	0.0000427	15.7

3	12	4a1	2b2	1X	118.82	-51.5	17.7	0.0000855	31.5
2	11	4a1	4a1	*1A1	113.25	-57.1	23.3	0.0000175	6.5
1	11	4a1	4a1	1A1	112.05	-58.3	24.5	0.0000351	12.9

Total Transition Rate(au) = 3.17136E-03

D.4.4. Hydrogen chloride - Cl($L_{23}VV$)

```
    CALCULATIONS FOR HCl, geom. Gordy, TCH, vol.18, p.76

   17       0.0000000       0.0000000       0.0000000
    1       0.0000000       0.0000000       2.4086442
  DEGENERACY OF OCCUPIED ORBITALS
 1 1 2 2


      EIGENVECTORS
   0.9772  -0.1681   0.0000   0.0000
   0.0000   0.0000   1.0000   0.0000
   0.0000   0.0000   0.0000   1.0000
   0.0625   0.8116   0.0000   0.0000
   0.2028   0.5595   0.0000   0.0000


      MOLECULAR J(PP,QQ) COULOMB INTEGRALS
   0.5391   0.4801   0.5441   0.5441
   0.4801   0.5273   0.4724   0.4724
   0.5441   0.4724   0.5847   0.5363
   0.5441   0.4724   0.5363   0.5847


      MOLECULAR K(PQ,PQ) EXCHANGE INTEGRALS
   0.5391   0.0639   0.1038   0.1038
   0.0639   0.5273   0.0171   0.0171
   0.1038   0.0171   0.5847   0.0242
   0.1038   0.0171   0.0242   0.5847

                                MOLECULE: HCl 2p          ATOM: Chlorine

                                      AUGER SPECTRUM

                           CORE AND VALENCE I.P.S USED

                            2p3/2   207.400
                            4si 29.830   5si 16.600   2pi 12.800   2pi 12.800

 SPIN - ORBIT  SPLITTING =      1.63000
  CONTRIBUTIONS FROM 2p1/2 INITIAL HOLE ARE MARKED WITH *
```

PEAK NR.	MO.INDEX	MO.NAME		SYM	ABS.ENERGY	REL.ENERGY		ABS.RATE	REL.INT.
22	34	2pi	2pi	*3A2	169.49	-37.9	0.0	0.0002148	37.4
21	34	2pi	2pi	* 1E	168.18	-39.2	1.3	0.0002187	38.1
20	34	2pi	2pi	3A2	167.86	-39.5	1.6	0.0004296	74.9
19	23	5si	2pi	* 3E	167.24	-40.2	2.3	0.0002869	50.0
18	33	2pi	2pi	*1A1	166.86	-40.5	2.6	0.0001371	23.9
17	34	2pi	2pi	1E	166.55	-40.9	2.9	0.0004374	76.2
16	23	5si	2pi	* 1E	166.31	-41.1	3.2	0.0001481	25.8
15	23	5si	2pi	3E	165.61	-41.8	3.9	0.0005738	100.0
14	33	2pi	2pi	1A1	165.23	-42.2	4.3	0.0002743	47.8
13	23	5si	2pi	1E	164.68	-42.7	4.8	0.0002963	51.6
12	22	5si	5si	*1A1	161.48	-45.9	8.0	0.0000574	10.0
11	22	5si	5si	1A1	159.85	-47.5	9.6	0.0001148	20.0
10	13	4si	2pi	* 3E	154.42	-53.0	15.1	0.0001347	23.5
9	13	4si	2pi	3E	152.79	-54.6	16.7	0.0002693	46.9
8	12	4si	5si	* 3X	151.27	-56.1	18.2	0.0000450	7.8
7	12	4si	5si	3X	149.64	-57.8	19.9	0.0000899	15.7
6	13	4si	2pi	* 1E	148.77	-58.6	20.7	0.0001383	24.1
5	12	4si	5si	* 1X	147.80	-59.6	21.7	0.0000447	7.8
4	13	4si	2pi	1E	147.14	-60.3	22.4	0.0002765	48.2
3	12	4si	5si	1X	146.17	-61.2	23.3	0.0000895	15.6
2	11	4si	4si	*1A1	134.70	-72.7	34.8	0.0000201	3.5
1	11	4si	4si	1A1	133.07	-74.3	36.4	0.0000402	7.0

```
Total Transition Rate(au) =     4.33730E-03
```

D.5.1. Carbonyl sulphide - S(L_{23}VV)

```
     CALCULATIONS FOR OCS, geom.  LBII/15 p.214

   16       0.0000000       0.0000000       2.9533219
    8       0.0000000       0.0000000      -2.1785338
    6       0.0000000       0.0000000       0.0000000
  DEGENERACY OF OCC ORBITALS
 1 1 1 2 2 1 2 2

       EIGENVECTORS
  -0.0479   0.8926   0.3063   0.0000   0.0000  -0.2861   0.0000   0.0000
   0.0000   0.0000   0.0000   0.2541   0.0000   0.0000   0.9429   0.0000
   0.0000   0.0000   0.0000   0.0000   0.2541   0.0000   0.0000   0.9429
   0.0377  -0.1387   0.2685   0.0000   0.0000  -0.5637   0.0000   0.0000
  -0.7879  -0.1230   0.4474   0.0000   0.0000   0.1792   0.0000   0.0000
   0.0000   0.0000   0.0000   0.7638   0.0000   0.0000  -0.3321   0.0000
   0.0000   0.0000   0.0000   0.0000   0.7638   0.0000   0.0000  -0.3321
  -0.2259   0.0432  -0.6235   0.0000   0.0000  -0.5020   0.0000   0.0000
  -0.4556   0.2969  -0.4945   0.0000   0.0000   0.2859   0.0000   0.0000
   0.0000   0.0000   0.0000   0.5933   0.0000   0.0000   0.0238   0.0000
   0.0000   0.0000   0.0000   0.0000   0.5933   0.0000   0.0000   0.0238
   0.3419   0.2810  -0.0263   0.0000   0.0000   0.4843   0.0000   0.0000


       MOLECULAR J(PP,QQ) COULOMB INTEGRALS
   0.6489   0.3339   0.5575   0.5999   0.5999   0.3769   0.3102   0.3102
   0.3339   0.4339   0.3426   0.3500   0.3500   0.3987   0.4057   0.4057
   0.5575   0.3426   0.6312   0.5604   0.5604   0.3923   0.3248   0.3248
   0.5999   0.3500   0.5604   0.6023   0.5731   0.3874   0.3222   0.3147
   0.5999   0.3500   0.5604   0.5731   0.6023   0.3874   0.3147   0.3222
   0.3769   0.3987   0.3923   0.3874   0.3874   0.4394   0.3875   0.3875
   0.3102   0.4057   0.3248   0.3222   0.3147   0.3875   0.4439   0.4139
   0.3102   0.4057   0.3248   0.3147   0.3222   0.3875   0.4139   0.4439


       MOLECULAR K(PQ,PQ) EXCHANGE INTEGRALS
   0.6489   0.0121   0.0548   0.0634   0.0634   0.0133   0.0138   0.0138
   0.0121   0.4339   0.0548   0.0137   0.0137   0.0522   0.0455   0.0455
   0.0548   0.0548   0.6312   0.0316   0.0316   0.0953   0.0190   0.0190
   0.0634   0.0137   0.0316   0.6023   0.0146   0.0102   0.0653   0.0037
   0.0634   0.0137   0.0316   0.0146   0.6023   0.0102   0.0037   0.0653
   0.0133   0.0522   0.0953   0.0102   0.0102   0.4394   0.0245   0.0245
   0.0138   0.0455   0.0190   0.0653   0.0037   0.0245   0.4439   0.0150
   0.0138   0.0455   0.0190   0.0037   0.0653   0.0245   0.0150   0.4439

      SPECIAL J(PQ,RS) AND K(PS,RQ) INTEGRALS
         4    5    7    8   0.0037   0.0037
         4    5    8    7   0.0037   0.0578

                              MOLECULE: OCS            ATOM: Sulphur 2p

                                      AUGER SPECTRUM

                          CORE AND VALENCE I.P.S USED

                          2p3/2   170.650
                           6si 35.800   7si 27.400   8si 18.000   2pi 15.500   2pi 15.500
                           9si 16.000   3pi 11.200   3pi 11.200

SPIN - ORBIT  SPLITTING =     1.20000

CONTRIBUTIONS FROM 2p1/2 INITIAL HOLE ARE MARKED WITH *

 PEAK NR.  MO.INDEX   MO.NAME     SYM     ABS.ENERGY      REL.ENERGY      ABS.RATE   REL.INT.

   88        78       3pi  3pi    *3A2     138.60          -32.1           0.0      0.0001625    49.1
   87        47       2pi  3pi    *3A1     138.16          -32.5           0.4      0.0000000     0.0
   86        47       2pi  3pi    *1A2     138.16          -32.5           0.4      0.0000109     3.3
   85        47       2pi  3pi    * 3E     138.16          -32.5           0.4      0.0000000     0.0
   84        78       3pi  3pi    * 1E     137.78          -32.9           0.8      0.0001653    50.0
   83        78       3pi  3pi     3A2     137.40          -33.3           1.2      0.0003250    98.3
   82        77       3pi  3pi    *1A1     136.96          -33.7           1.6      0.0001031    31.2
   81        47       2pi  3pi     1A2     136.96          -33.7           1.6      0.0000218     6.6
   80        47       2pi  3pi      3E     136.96          -33.7           1.6      0.0000000     0.0
   79        47       2pi  3pi     3A1     136.96          -33.7           1.6      0.0000000     0.0
   78        78       3pi  3pi      1E     136.58          -34.1           2.0      0.0003306   100.0
   77        77       3pi  3pi     1A1     135.76          -34.9           2.8      0.0002062    62.4
```

76	47	2pi	3pi	*3A2	135.22	-35.4	3.4	0.0000236	7.1
75	47	2pi	3pi	* 1E	134.81	-35.8	3.8	0.0000023	0.7
74	67	9si	3pi	* 3E	134.77	-35.9	3.8	0.0001261	38.1
73	47	2pi	3pi	*1A1	134.40	-36.2	4.2	0.0000257	7.8
72	37	8si	3pi	* 3E	134.33	-36.3	4.3	0.0000378	11.4
71	47	2pi	3pi	3A2	134.02	-36.6	4.6	0.0000472	14.3
70	47	2pi	3pi	1E	133.61	-37.0	5.0	0.0000047	1.4
69	67	9si	3pi	3E	133.57	-37.1	5.0	0.0002522	76.3
68	67	9si	3pi	* 1E	133.44	-37.2	5.2	0.0000692	20.9
67	37	8si	3pi	* 1E	133.29	-37.4	5.3	0.0000250	7.6
66	47	2pi	3pi	1A1	133.20	-37.4	5.4	0.0000514	15.6
65	37	8si	3pi	3E	133.13	-37.5	5.5	0.0000755	22.8
64	67	9si	3pi	1E	132.24	-38.4	6.4	0.0001385	41.9
63	37	8si	3pi	1E	132.09	-38.6	6.5	0.0000501	15.1
62	46	2pi	9si	* 3X	130.09	-40.6	8.5	0.0000092	2.8
61	36	8si	9si	* 3X	129.77	-40.9	8.8	0.0000006	0.2
60	46	2pi	9si	* 1X	129.53	-41.1	9.1	0.0000050	1.5
59	46	2pi	9si	3X	128.89	-41.8	9.7	0.0000183	5.5
58	36	8si	9si	3X	128.57	-42.1	10.0	0.0000013	0.4
57	46	2pi	9si	1X	128.33	-42.3	10.3	0.0000101	3.0
56	66	9si	9si	*1A1	127.89	-42.8	10.7	0.0000172	5.2
55	66	9si	9si	1A1	126.69	-44.0	11.9	0.0000344	10.4
54	45	2pi	2pi	*3A2	125.65	-45.0	12.9	0.0000009	0.3
53	45	2pi	2pi	* 1E	124.86	-45.8	13.7	0.0000009	0.3
52	36	8si	9si	* 1X	124.58	-46.1	14.0	0.0000116	3.5
51	45	2pi	2pi	3A2	124.45	-46.2	14.1	0.0000017	0.5
50	44	2pi	2pi	*1A1	124.06	-46.6	14.5	0.0000005	0.2
49	34	8si	2pi	* 3E	123.96	-46.7	14.6	0.0000027	0.8
48	45	2pi	2pi	1E	123.66	-47.0	14.9	0.0000017	0.5
47	27	7si	3pi	* 3E	123.45	-47.2	15.1	0.0001041	31.5
46	36	8si	9si	1X	123.38	-47.3	15.2	0.0000233	7.0
45	44	2pi	2pi	1A1	122.86	-47.8	15.7	0.0000011	0.3
44	34	8si	2pi	3E	122.76	-47.9	15.8	0.0000055	1.7
43	27	7si	3pi	3E	122.25	-48.4	16.3	0.0002081	62.9
42	34	8si	2pi	* 1E	122.24	-48.4	16.4	0.0000018	0.5
41	34	8si	2pi	1E	121.04	-49.6	17.6	0.0000036	1.1
40	27	7si	3pi	* 1E	120.97	-49.7	17.6	0.0001023	30.9
39	24	7si	2pi	* 3E	119.80	-50.9	18.8	0.0000076	2.3
38	27	7si	3pi	1E	119.77	-50.9	18.8	0.0002046	61.9
37	24	7si	2pi	* 1E	119.05	-51.6	19.5	0.0000074	2.2
36	26	7si	9si	* 3X	119.02	-51.6	19.6	0.0000202	6.1
35	33	8si	8si	*1A1	118.67	-52.0	19.9	0.0000021	0.6
34	23	7si	8si	* 3X	118.62	-52.0	20.0	0.0000055	1.6
33	24	7si	2pi	3E	118.60	-52.1	20.0	0.0000151	4.6
32	24	7si	2pi	1E	117.85	-52.8	20.7	0.0000149	4.5
31	26	7si	9si	3X	117.82	-52.8	20.8	0.0000404	12.2
30	33	8si	8si	1A1	117.47	-53.2	21.1	0.0000043	1.3
29	23	7si	8si	3X	117.42	-53.2	21.2	0.0000109	3.3
28	17	6si	3pi	* 3E	116.78	-53.9	21.8	0.0000008	0.2
27	26	7si	9si	* 1X	116.18	-54.5	22.4	0.0000165	5.0
26	17	6si	3pi	* 1E	116.03	-54.6	22.6	0.0000005	0.2
25	23	7si	8si	* 1X	115.64	-55.0	23.0	0.0000047	1.4
24	17	6si	3pi	3E	115.58	-55.1	23.0	0.0000016	0.5
23	26	7si	9si	1X	114.98	-55.7	23.6	0.0000330	10.0
22	17	6si	3pi	1E	114.83	-55.8	23.8	0.0000011	0.3
21	23	7si	8si	1X	114.44	-56.2	24.2	0.0000094	2.8
20	16	6si	9si	* 3X	110.16	-60.5	28.4	0.0000001	0.0
19	16	6si	9si	* 1X	109.43	-61.2	29.2	0.0000001	0.0
18	16	6si	9si	3X	108.96	-61.7	29.6	0.0000002	0.1
17	16	6si	9si	1X	108.23	-62.4	30.4	0.0000002	0.1
16	14	6si	2pi	* 3E	105.95	-64.7	32.6	0.0000001	0.0
15	22	7si	7si	*1A1	105.24	-65.4	33.4	0.0000155	4.7
14	14	6si	2pi	3E	104.75	-65.9	33.8	0.0000001	0.0
13	13	6si	8si	* 3X	104.37	-66.3	34.2	0.0000000	0.0
12	22	7si	7si	1A1	104.04	-66.6	34.6	0.0000310	9.4
11	13	6si	8si	3X	103.17	-67.5	35.4	0.0000001	0.0
10	14	6si	2pi	* 1E	102.50	-68.1	36.1	0.0000000	0.0
9	13	6si	8si	* 1X	101.39	-69.3	37.2	0.0000000	0.0
8	14	6si	2pi	1E	101.30	-69.3	37.3	0.0000001	0.0
7	13	6si	8si	1X	100.19	-70.5	38.4	0.0000000	0.0
6	12	6si	7si	* 3X	99.89	-70.8	38.7	0.0000000	0.0
5	12	6si	7si	* 1X	99.23	-71.4	39.4	0.0000002	0.1
4	12	6si	7si	3X	98.69	-72.0	39.9	0.0000001	0.0
3	12	6si	7si	1X	98.03	-72.6	40.6	0.0000004	0.1
2	11	6si	6si	*1A1	82.59	-88.1	56.0	0.0000000	0.0
1	11	6si	6si	1A1	81.39	-89.3	57.2	0.0000000	0.0

Total Transition Rate(au) = 3.26971E-03

D.5.2. Carbonyl sulphide - C(KVV)*

```
       CALCULATIONS FOR OCS, geom. LBII/15 p.214

  16       0.0000000       0.0000000       2.9533219
   8       0.0000000       0.0000000      -2.1785338
   6       0.0000000       0.0000000       0.0000000
 DEGENERACY OF OCC ORBITALS
1 1 1 2 2 1 2 2


     EIGENVECTORS
-0.0490   0.7513   0.4003   0.0000   0.0000   0.4918   0.0000   0.0000
 0.0000   0.0000   0.0000   0.2057   0.0000   0.0000   0.9085   0.0000
 0.0000   0.0000   0.0000   0.0000   0.2057   0.0000   0.0000   0.9085
 0.0497  -0.2162   0.1134   0.0000   0.0000   0.5222   0.0000   0.0000
-0.7862  -0.2097   0.4458   0.0000   0.0000  -0.0872   0.0000   0.0000
 0.0000   0.0000   0.0000   0.7848   0.0000   0.0000  -0.3751   0.0000
 0.0000   0.0000   0.0000   0.0000   0.7848   0.0000   0.0000  -0.3751
-0.2252   0.1218  -0.7015   0.0000   0.0000   0.3839   0.0000   0.0000
-0.4591   0.4551  -0.3340   0.0000   0.0000  -0.3640   0.0000   0.0000
 0.0000   0.0000   0.0000   0.5847   0.0000   0.0000   0.1839   0.0000
 0.0000   0.0000   0.0000   0.0000   0.5847   0.0000   0.0000   0.1839
 0.3397   0.3506   0.1563   0.0000   0.0000  -0.4449   0.0000   0.0000


     MOLECULAR J(PP,QQ) COULOMB INTEGRALS
 0.6489   0.3339   0.5575   0.5999   0.5999   0.3769   0.3102   0.3102
 0.3339   0.4339   0.3426   0.3500   0.3500   0.3987   0.4057   0.4057
 0.5575   0.3426   0.6312   0.5604   0.5604   0.3923   0.3248   0.3248
 0.5999   0.3500   0.5604   0.6023   0.5731   0.3874   0.3222   0.3147
 0.5999   0.3500   0.5604   0.5731   0.6023   0.3874   0.3147   0.3222
 0.3769   0.3987   0.3923   0.3874   0.3874   0.4394   0.3875   0.3875
 0.3102   0.4057   0.3248   0.3222   0.3147   0.3875   0.4439   0.4139
 0.3102   0.4057   0.3248   0.3147   0.3222   0.3875   0.4139   0.4439


     MOLECULAR K(PQ,PQ) EXCHANGE INTEGRALS
 0.6489   0.0121   0.0548   0.0634   0.0634   0.0133   0.0138   0.0138
 0.0121   0.4339   0.0548   0.0137   0.0137   0.0522   0.0455   0.0455
 0.0548   0.0548   0.6312   0.0316   0.0316   0.0953   0.0190   0.0190
 0.0634   0.0137   0.0316   0.6023   0.0146   0.0102   0.0653   0.0037
 0.0634   0.0137   0.0316   0.0146   0.6023   0.0102   0.0037   0.0653
 0.0133   0.0522   0.0953   0.0102   0.0102   0.4394   0.0245   0.0245
 0.0138   0.0455   0.0190   0.0653   0.0037   0.0245   0.4439   0.0150
 0.0138   0.0455   0.0190   0.0037   0.0653   0.0245   0.0150   0.4439


   SPECIAL J(PQ,RS) AND K(PS,RQ) INTEGRALS
     4    5    7    8   0.0037   0.0037
     4    5    8    7   0.0037   0.0578

                    MOLECULE: OCS 1s          ATOM: Carbon

                                   AUGER SPECTRUM

                    CORE AND VALENCE I.P.S USED

                    1s  295.430
                    6si  35.800  7si  27.400  8si  18.000  2pi  15.500  2pi  15.500
                    9si  16.000  3pi  11.200  3pi  11.200

PEAK NR.  MO.INDEX   MO.NAME    SYM   ABS.ENERGY      REL.ENERGY       ABS.RATE   REL.INT.

  44        78      3pi  3pi    3A2     262.17        -33.3        0.0     0.0000000     0.0
  43        47      2pi  3pi    3A1     261.74        -33.7        0.4     0.0000000     0.0
  42        47      2pi  3pi    1A2     261.74        -33.7        0.4     0.0000000     0.0
  41        47      2pi  3pi     3E     261.74        -33.7        0.4     0.0000000     0.0
  40        78      3pi  3pi     1E     261.36        -34.1        0.8     0.0000024     1.0
  39        77      3pi  3pi    1A1     260.54        -34.9        1.6     0.0000007     0.3
  38        47      2pi  3pi    3A2     258.80        -36.6        3.4     0.0000000     0.0
  37        47      2pi  3pi     1E     258.39        -37.0        3.8     0.0000487    19.8
  36        67      9si  3pi     3E     258.35        -37.1        3.8     0.0000019     0.8
  35        47      2pi  3pi    1A1     257.98        -37.4        4.2     0.0000143     5.8
  34        37      8si  3pi     3E     257.91        -37.5        4.3     0.0000016     0.6
  33        67      9si  3pi     1E     257.02        -38.4        5.2     0.0000196     8.0
  32        37      8si  3pi     1E     256.87        -38.6        5.3     0.0000064     2.6
  31        46      2pi  9si     3X     253.67        -41.8        8.5     0.0000188     7.6
```

30	36	8si	9si	3X	253.35	-42.1	8.8	0.0000088	3.6
29	46	2pi	9si	1X	253.11	-42.3	9.1	0.0001984	80.6
28	66	9si	9si	1A1	251.47	-44.0	10.7	0.0000624	25.3
27	45	2pi	2pi	3A2	249.23	-46.2	12.9	0.0000000	0.0
26	45	2pi	2pi	1E	248.44	-47.0	13.7	0.0002462	100.0
25	36	8si	9si	1X	248.16	-47.3	14.0	0.0000501	20.4
24	44	2pi	2pi	1A1	247.64	-47.8	14.5	0.0000724	29.4
23	34	8si	2pi	3E	247.54	-47.9	14.6	0.0000158	6.4
22	27	7si	3pi	3E	247.03	-48.4	15.1	0.0000029	1.2
21	34	8si	2pi	1E	245.82	-49.6	16.4	0.0000646	26.2
20	27	7si	3pi	1E	244.55	-50.9	17.6	0.0000174	7.1
19	24	7si	2pi	3E	243.38	-52.1	18.8	0.0000294	11.9
18	24	7si	2pi	1E	242.64	-52.8	19.5	0.0001758	71.4
17	26	7si	9si	3X	242.60	-52.8	19.6	0.0000012	0.5
16	33	8si	8si	1A1	242.25	-53.2	19.9	0.0000127	5.2
15	23	7si	8si	3X	242.20	-53.2	20.0	0.0000074	3.0
14	17	6si	3pi	3E	240.36	-55.1	21.8	0.0000030	1.2
13	26	7si	9si	1X	239.76	-55.7	22.4	0.0001199	48.7
12	17	6si	3pi	1E	239.62	-55.8	22.6	0.0000170	6.9
11	23	7si	8si	1X	239.22	-56.2	23.0	0.0000573	23.3
10	16	6si	9si	3X	233.73	-61.7	28.4	0.0000223	9.1
9	16	6si	9si	1X	233.01	-62.4	29.2	0.0001244	50.5
8	14	6si	2pi	3E	229.53	-65.9	32.6	0.0000299	12.2
7	22	7si	7si	1A1	228.82	-66.6	33.4	0.0000635	25.8
6	13	6si	8si	3X	227.95	-67.5	34.2	0.0000004	0.1
5	14	6si	2pi	1E	226.08	-69.3	36.1	0.0001720	69.8
4	13	6si	8si	1X	224.97	-70.5	37.2	0.0000551	22.4
3	12	6si	7si	3X	223.48	-72.0	38.7	0.0000207	8.4
2	12	6si	7si	1X	222.81	-72.6	39.4	0.0001324	53.8
1	11	6si	6si	1A1	206.17	-89.3	56.0	0.0000627	25.5

Total Transition Rate (in au) = 1.96038E-03

D.5.3. Carbonyl sulphide - O(KVV)

```
        CALCULATIONS FOR OCS geom. LBII/15 p.214

  16       0.0000000       0.0000000       2.9533219
   8       0.0000000       0.0000000      -2.1785338
   6       0.0000000       0.0000000       0.0000000
 DEGENERACY OF OCC ORBITALS
1 1 1 2 2 1 2 2


     EIGENVECTORS
  0.0176   0.7067  -0.3923   0.0000   0.0000   0.5615   0.0000   0.0000
  0.0000   0.0000   0.0000   0.1308   0.0000   0.0000   0.8361   0.0000
  0.0000   0.0000   0.0000   0.0000   0.1308   0.0000   0.0000   0.8361
 -0.0282  -0.2227  -0.0046   0.0000   0.0000   0.5185   0.0000   0.0000
  0.8528  -0.1921  -0.3506   0.0000   0.0000   0.0015   0.0000   0.0000
  0.0000   0.0000   0.0000   0.8872   0.0000   0.0000  -0.3385   0.0000
  0.0000   0.0000   0.0000   0.0000   0.8872   0.0000   0.0000  -0.3385
  0.1787   0.2335   0.7746   0.0000   0.0000   0.2696   0.0000   0.0000
  0.3613   0.5345   0.1991   0.0000   0.0000  -0.4578   0.0000   0.0000
  0.0000   0.0000   0.0000   0.4424   0.0000   0.0000   0.4316   0.0000
  0.0000   0.0000   0.0000   0.0000   0.4424   0.0000   0.0000   0.4316
 -0.3303   0.2718  -0.2889   0.0000   0.0000  -0.3653   0.0000   0.0000


     MOLECULAR J(PP,QQ) COULOMB INTEGRALS
  0.6489   0.3339   0.5575   0.5999   0.5999   0.3769   0.3102   0.3102
  0.3339   0.4339   0.3426   0.3500   0.3500   0.3987   0.4057   0.4057
  0.5575   0.3426   0.6312   0.5604   0.5604   0.3923   0.3248   0.3248
  0.5999   0.3500   0.5604   0.6023   0.5731   0.3874   0.3222   0.3147
  0.5999   0.3500   0.5604   0.5731   0.6023   0.3874   0.3147   0.3222
  0.3769   0.3987   0.3923   0.3874   0.3874   0.4394   0.3875   0.3875
  0.3102   0.4057   0.3248   0.3222   0.3147   0.3875   0.4439   0.4139
  0.3102   0.4057   0.3248   0.3147   0.3222   0.3875   0.4139   0.4439


     MOLECULAR K(PQ,PQ) EXCHANGE INTEGRALS
  0.6489   0.0121   0.0548   0.0634   0.0634   0.0133   0.0138   0.0138
  0.0121   0.4339   0.0548   0.0137   0.0137   0.0522   0.0455   0.0455
  0.0548   0.0548   0.6312   0.0316   0.0316   0.0953   0.0190   0.0190
  0.0634   0.0137   0.0316   0.6023   0.0146   0.0102   0.0653   0.0037
  0.0634   0.0137   0.0316   0.0146   0.6023   0.0102   0.0037   0.0653
  0.0133   0.0522   0.0953   0.0102   0.0102   0.4394   0.0245   0.0245
  0.0138   0.0455   0.0190   0.0653   0.0037   0.0245   0.4439   0.0150
  0.0138   0.0455   0.0190   0.0037   0.0653   0.0245   0.0150   0.4439


   SPECIAL J(PQ,RS) AND K(PS,RQ) INTEGRALS
     4    5    7    8   0.0037   0.0037
     4    5    8    7   0.0037   0.0578

                    MOLECULE: OCS 1s          ATOM: Oxygen


                                  AUGER SPECTRUM


                    CORE AND VALENCE I.P.S USED

                    1s   540.280
                    6si  35.800  7si  27.400  8si  18.000  2pi  15.500  2pi  15.500
                    9si  16.000  3pi  11.200  3pi  11.200

PEAK NR.  MO.INDEX   MO.NAME     SYM     ABS.ENERGY     REL.ENERGY          ABS.RATE  REL.INT.

  44        78       3pi  3pi     3A2      507.03       -33.3     0.0     0.0000000      0.0
  43        47       2pi  3pi     3A1      506.59       -33.7     0.4     0.0000000      0.0
  42        47       2pi  3pi     1A2      506.59       -33.7     0.4     0.0000000      0.0
  41        47       2pi  3pi      3E      506.59       -33.7     0.4     0.0000000      0.0
  40        78       3pi  3pi      1E      506.21       -34.1     0.8     0.0000280      2.1
  39        77       3pi  3pi     1A1      505.39       -34.9     1.6     0.0000082      0.6
  38        47       2pi  3pi     3A2      503.65       -36.6     3.4     0.0000000      0.0
  37        47       2pi  3pi      1E      503.24       -37.0     3.8     0.0003844     29.1
  36        67       9si  3pi      3E      503.20       -37.1     3.8     0.0000000      0.0
  35        47       2pi  3pi     1A1      502.83       -37.4     4.2     0.0001132      8.6
  34        37       8si  3pi      3E      502.76       -37.5     4.3     0.0000056      0.4
  33        67       9si  3pi      1E      501.87       -38.4     5.2     0.0000177      1.3
  32        37       8si  3pi      1E      501.72       -38.6     5.3     0.0001641     12.4
```

31	46	2pi	9si	3X	498.52	-41.8	8.5	0.0000000	0.0
30	36	8si	9si	3X	498.20	-42.1	8.8	0.0000018	0.1
29	46	2pi	9si	1X	497.96	-42.3	9.1	0.0001219	9.2
28	66	9si	9si	1A1	496.32	-44.0	10.7	0.0000045	0.3
27	45	2pi	2pi	3A2	494.08	-46.2	12.9	0.0000000	0.0
26	45	2pi	2pi	1E	493.29	-47.0	13.7	0.0013202	100.0
25	36	8si	9si	1X	493.01	-47.3	14.0	0.0000794	6.0
24	44	2pi	2pi	1A1	492.49	-47.8	14.5	0.0003886	29.4
23	34	8si	2pi	3E	492.39	-47.9	14.6	0.0000386	2.9
22	27	7si	3pi	3E	491.88	-48.4	15.1	0.0000017	0.1
21	34	8si	2pi	1E	490.67	-49.6	16.4	0.0011273	85.4
20	27	7si	3pi	1E	489.40	-50.9	17.6	0.0000186	1.4
19	24	7si	2pi	3E	488.23	-52.1	18.8	0.0000116	0.9
18	24	7si	2pi	1E	487.48	-52.8	19.5	0.0001278	9.7
17	26	7si	9si	3X	487.45	-52.8	19.6	0.0000005	0.0
16	33	8si	8si	1A1	487.10	-53.2	19.9	0.0003598	27.3
15	23	7si	8si	3X	487.05	-53.2	20.0	0.0000009	0.1
14	17	6si	3pi	3E	485.21	-55.1	21.8	0.0000332	2.5
13	26	7si	9si	1X	484.61	-55.7	22.4	0.0000084	0.6
12	17	6si	3pi	1E	484.46	-55.8	22.6	0.0001120	8.5
11	23	7si	8si	1X	484.07	-56.2	23.0	0.0000798	6.0
10	16	6si	9si	3X	478.59	-61.7	28.4	0.0000105	0.8
9	16	6si	9si	1X	477.86	-62.4	29.2	0.0000370	2.8
8	14	6si	2pi	3E	474.38	-65.9	32.6	0.0002281	17.3
7	22	7si	7si	1A1	473.67	-66.6	33.4	0.0000048	0.4
6	13	6si	8si	3X	472.80	-67.5	34.2	0.0001042	7.9
5	14	6si	2pi	1E	470.93	-69.3	36.1	0.0007692	58.3
4	13	6si	8si	1X	469.82	-70.5	37.2	0.0004611	34.9
3	12	6si	7si	3X	468.32	-72.0	38.7	0.0000109	0.8
2	12	6si	7si	1X	467.66	-72.6	39.4	0.0000740	5.6
1	11	6si	6si	1A1	451.02	-89.3	56.0	0.0004561	34.5

Total Transition Rate (in au) = 6.71371E-03

D.6.1.1. Carbon tetrafluoride - C(KVV)

```
    CALCULATIONS FOR CF4, geom. LBII/15 p.152

   6       0.0000000       0.0000000       0.0000000
   9       1.4393502       1.4393502       1.4393502
   9      -1.4393502      -1.4393502       1.4393502
   9       1.4393502      -1.4393502      -1.4393502
   9      -1.4393502       1.4393502      -1.4393502
 DEGENERACY OF OCCUPIED ORBITALS
1 3 3 3 1 3 3 3 2 2 3 3 3 3 3 3


      EIGENVECTORS
-0.6018   0.0000   0.0000   0.0000  -0.5152   0.0000   0.0000   0.0000   0.0000   0.0000   0.0000
 0.0000   0.4081   0.0000   0.0000   0.0000   0.4756   0.0000   0.0000   0.0000   0.0000   0.0000
 0.0000   0.0000   0.4081   0.0000   0.0000   0.0000   0.4756   0.0000   0.0000   0.0000   0.0000
 0.0000   0.0000   0.0000   0.4081   0.0000   0.0000   0.0000   0.4756   0.0000   0.0000   0.0000
-0.3761   0.4477   0.4477   0.4477   0.3112  -0.1875  -0.1875  -0.1875   0.0000   0.0000   0.0000
 0.0775   0.0211  -0.0611  -0.0611   0.1701   0.1000  -0.2723  -0.2723  -0.2041  -0.3536   0.0000
 0.0775  -0.0611   0.0211  -0.0611   0.1701  -0.2723   0.1000  -0.2723  -0.2041   0.3536  -0.3536
 0.0775  -0.0611  -0.0611   0.0211   0.1701  -0.2723  -0.2723   0.1000   0.4082   0.0000  -0.3536
-0.3761  -0.4477  -0.4477   0.4477   0.3112   0.1875   0.1875  -0.1875   0.0000   0.0000   0.0000
-0.0775   0.0211  -0.0611   0.0611  -0.1701   0.1000  -0.2723   0.2723   0.2041   0.3536   0.0000
-0.0775  -0.0611   0.0211   0.0611  -0.1701  -0.2723   0.1000   0.2723   0.2041  -0.3536   0.3536
 0.0775   0.0611   0.0611   0.0211   0.1701   0.2723   0.2723   0.1000   0.4082   0.0000   0.3536
-0.3761   0.4477  -0.4477  -0.4477   0.3112  -0.1875   0.1875   0.1875   0.0000   0.0000   0.0000
 0.0775   0.0211   0.0611   0.0611   0.1701   0.1000   0.2723   0.2723  -0.2041  -0.3536   0.0000
-0.0775   0.0611   0.0211  -0.0611  -0.1701   0.2723   0.1000  -0.2723   0.2041  -0.3536  -0.3536
-0.0775   0.0611  -0.0611   0.0211  -0.1701   0.2723  -0.2723   0.1000  -0.4082   0.0000  -0.3536
-0.3761  -0.4477   0.4477  -0.4477   0.3112   0.1875  -0.1875   0.1875   0.0000   0.0000   0.0000
-0.0775   0.0211   0.0611  -0.0611  -0.1701   0.1000   0.2723  -0.2723   0.2041   0.3536   0.0000
 0.0775   0.0611   0.0211   0.0611   0.1701   0.2723   0.1000   0.2723  -0.2041   0.3536   0.3536
-0.0775  -0.0611   0.0611   0.0211  -0.1701  -0.2723   0.2723   0.1000  -0.4082   0.0000   0.3536
 0.0000   0.0000   0.0000   0.0000   0.0000
 0.0000   0.0000   0.2766   0.0000   0.0000
 0.0000   0.0000   0.0000   0.2766   0.0000
 0.0000   0.0000   0.0000   0.0000   0.2766
 0.0000   0.0000  -0.0438  -0.0438  -0.0438
-0.3536  -0.3536  -0.4782  -0.0123  -0.0123
 0.0000  -0.3536  -0.0123  -0.4782  -0.0123
-0.3536   0.0000  -0.0123  -0.0123  -0.4782
 0.0000   0.0000   0.0438   0.0438  -0.0438
 0.3536  -0.3536  -0.4782  -0.0123   0.0123
 0.0000  -0.3536  -0.0123  -0.4782   0.0123
 0.3536   0.0000   0.0123   0.0123  -0.4782
 0.0000   0.0000  -0.0438   0.0438   0.0438
 0.3536   0.3536  -0.4782   0.0123   0.0123
 0.0000   0.3536   0.0123  -0.4782  -0.0123
 0.3536   0.0000   0.0123  -0.0123  -0.4782
 0.0000   0.0000   0.0438  -0.0438   0.0438
-0.3536   0.3536  -0.4782   0.0123  -0.0123
 0.0000   0.3536   0.0123  -0.4782   0.0123
-0.3536   0.0000  -0.0123   0.0123  -0.4782


   MOLECULAR J(PP,QQ) COULOMB INTEGRALS
 0.4282   0.4205   0.4205   0.4205   0.4041   0.4097   0.4097   0.4097   0.4110   0.4110   0.4114
 0.4205   0.4217   0.4160   0.4160   0.4095   0.4083   0.4149   0.4149   0.4151   0.4153   0.4152
 0.4205   0.4160   0.4217   0.4160   0.4095   0.4149   0.4083   0.4149   0.4151   0.4153   0.4151
 0.4205   0.4160   0.4160   0.4217   0.4095   0.4149   0.4149   0.4083   0.4154   0.4150   0.4151
 0.4041   0.4095   0.4095   0.4095   0.4463   0.4296   0.4296   0.4296   0.4111   0.4111   0.4147
 0.4097   0.4083   0.4149   0.4149   0.4296   0.4391   0.4143   0.4143   0.4130   0.4170   0.4174
 0.4097   0.4149   0.4083   0.4149   0.4296   0.4143   0.4391   0.4143   0.4130   0.4170   0.4146
 0.4097   0.4149   0.4149   0.4083   0.4296   0.4143   0.4143   0.4391   0.4191   0.4109   0.4146
 0.4110   0.4151   0.4151   0.4154   0.4111   0.4130   0.4130   0.4191   0.4330   0.4140   0.4219
 0.4110   0.4153   0.4153   0.4150   0.4111   0.4170   0.4170   0.4109   0.4140   0.4330   0.4188
 0.4114   0.4152   0.4151   0.4151   0.4147   0.4174   0.4146   0.4146   0.4219   0.4188   0.4330
 0.4114   0.4151   0.4152   0.4151   0.4147   0.4146   0.4174   0.4146   0.4219   0.4188   0.4188
 0.4114   0.4151   0.4151   0.4152   0.4147   0.4146   0.4146   0.4174   0.4172   0.4235   0.4188
 0.4114   0.4155   0.4144   0.4144   0.4189   0.4112   0.4199   0.4199   0.4156   0.4203   0.4135
 0.4114   0.4144   0.4155   0.4144   0.4189   0.4199   0.4112   0.4199   0.4156   0.4203   0.4223
 0.4114   0.4144   0.4144   0.4155   0.4189   0.4199   0.4199   0.4112   0.4226   0.4132   0.4223
 0.4114   0.4114   0.4114   0.4114   0.4114
 0.4151   0.4151   0.4155   0.4144   0.4144
 0.4152   0.4151   0.4144   0.4155   0.4144
 0.4151   0.4152   0.4144   0.4144   0.4155
 0.4147   0.4147   0.4189   0.4189   0.4189
 0.4146   0.4146   0.4112   0.4199   0.4199
 0.4174   0.4146   0.4199   0.4112   0.4199
 0.4146   0.4174   0.4199   0.4199   0.4112
```

0.4219	0.4172	0.4156	0.4156	0.4226
0.4188	0.4235	0.4203	0.4203	0.4132
0.4188	0.4188	0.4135	0.4223	0.4223
0.4330	0.4188	0.4223	0.4135	0.4223
0.4188	0.4330	0.4223	0.4223	0.4135
0.4223	0.4223	0.4308	0.4137	0.4137
0.4135	0.4223	0.4137	0.4308	0.4137
0.4223	0.4135	0.4137	0.4137	0.4308

MOLECULAR K(PQ,PQ) EXCHANGE INTEGRALS

0.4282	0.1085	0.1085	0.1085	0.0224	0.0261	0.0261	0.0261	0.0297	0.0297	0.0334
0.1085	0.4217	0.1163	0.1163	0.0440	0.0284	0.0423	0.0423	0.0369	0.0389	0.0387
0.1085	0.1163	0.4217	0.1163	0.0440	0.0423	0.0284	0.0423	0.0369	0.0389	0.0395
0.1085	0.1163	0.1163	0.4217	0.0440	0.0423	0.0423	0.0284	0.0398	0.0360	0.0395
0.0224	0.0440	0.0440	0.0440	0.4463	0.0849	0.0849	0.0849	0.0168	0.0168	0.0504
0.0261	0.0284	0.0423	0.0423	0.0849	0.4391	0.0216	0.0216	0.0314	0.0696	0.0726
0.0261	0.0423	0.0284	0.0423	0.0849	0.0216	0.4391	0.0216	0.0314	0.0696	0.0884
0.0261	0.0423	0.0423	0.0284	0.0849	0.0216	0.0216	0.4391	0.0887	0.0123	0.0884
0.0297	0.0369	0.0369	0.0398	0.0168	0.0314	0.0314	0.0887	0.4330	0.0095	0.0836
0.0297	0.0389	0.0389	0.0360	0.0168	0.0696	0.0696	0.0123	0.0095	0.4330	0.0539
0.0334	0.0387	0.0395	0.0395	0.0504	0.0726	0.0884	0.0884	0.0836	0.0539	0.4330
0.0334	0.0395	0.0387	0.0395	0.0504	0.0884	0.0726	0.0884	0.0836	0.0539	0.0539
0.0334	0.0395	0.0395	0.0387	0.0504	0.0884	0.0884	0.0726	0.0391	0.0984	0.0539
0.0320	0.0362	0.0356	0.0356	0.0702	0.0131	0.0817	0.0817	0.0312	0.0752	0.0114
0.0320	0.0356	0.0362	0.0356	0.0702	0.0817	0.0131	0.0817	0.0312	0.0752	0.0956
0.0320	0.0356	0.0356	0.0362	0.0702	0.0817	0.0817	0.0131	0.0971	0.0093	0.0956
0.0334	0.0334	0.0320	0.0320	0.0320						
0.0395	0.0395	0.0362	0.0356	0.0356						
0.0387	0.0395	0.0356	0.0362	0.0356						
0.0395	0.0387	0.0356	0.0356	0.0362						
0.0504	0.0504	0.0702	0.0702	0.0702						
0.0884	0.0884	0.0131	0.0817	0.0817						
0.0726	0.0884	0.0817	0.0131	0.0817						
0.0884	0.0726	0.0817	0.0817	0.0131						
0.0836	0.0391	0.0312	0.0312	0.0971						
0.0539	0.0984	0.0752	0.0752	0.0093						
0.0539	0.0539	0.0114	0.0956	0.0956						
0.4330	0.0539	0.0956	0.0114	0.0956						
0.0539	0.4330	0.0956	0.0956	0.0114						
0.0956	0.0956	0.4308	0.0183	0.0183						
0.0114	0.0956	0.0183	0.4308	0.0183						
0.0956	0.0114	0.0183	0.0183	0.4308						

SPECIAL J(PQ,RS) AND K(PS,RQ) INTEGRALS

2	3	6	7	0.0248	0.0152
4	2	8	6	0.0248	0.0152
3	4	7	8	0.0248	0.0152
2	3	7	6	0.0248	0.0078
2	4	8	6	0.0248	0.0078
3	4	8	7	0.0248	0.0078
2	3	9	10	0.0000	0.0000
2	3	10	9	0.0000	0.0000
2	3	11	12	0.0705	0.0211
4	2	13	11	0.0705	0.0211
3	4	12	13	0.0705	0.0211
2	3	12	11	0.0705	0.0192
2	4	13	11	0.0705	0.0192
3	4	13	12	0.0705	0.0192
2	3	14	15	0.0319	0.0094
4	2	16	14	0.0319	0.0094
3	4	15	16	0.0319	0.0094
2	3	15	14	0.0319	0.0088
2	4	16	14	0.0319	0.0088
3	4	16	15	0.0319	0.0088
6	7	9	10	0.0000	0.0000
6	7	10	9	0.0000	0.0000
6	7	11	12	0.0208	0.0748
8	6	13	11	0.0208	0.0748
7	8	12	13	0.0208	0.0748
6	7	12	11	0.0208	0.0332
6	8	13	11	0.0208	0.0332
7	8	13	12	0.0208	0.0332
6	7	14	15	0.0124	0.0667
8	6	16	14	0.0124	0.0667
7	8	15	16	0.0124	0.0667
6	7	15	14	0.0124	0.0068
6	8	16	14	0.0124	0.0068
7	8	16	15	0.0124	0.0068
9	10	11	12	0.0000	-0.0229
9	10	12	11	0.0000	0.0229

9	10	14	15	0.0000	0.0000
9	10	15	14	0.0000	0.0000
11	12	14	15	0.0193	0.0037
13	11	16	14	0.0193	0.0037
12	13	15	16	0.0193	0.0037
11	12	15	14	0.0193	0.0022
11	13	16	14	0.0193	0.0022
12	13	16	15	0.0193	0.0022

MOLECULE: CF4 ATOM: Carbon

AUGER SPECTRUM

CORE AND VALENCE I.P.S USED

1s	301.800								
3a1	43.800	2t2	40.300	2t2	40.300	2t2	40.300	4a1	25.100
3t2	22.200	3t2	22.200	3t2	22.200	1e	18.500	1e	18.500
1t1	16.100	1t1	16.100	1t1	16.100	4t2	17.400	4t2	17.400
4t2	17.400								

PEAK NR.	MO.INDEX	MO.NAME		SYM	ABS.ENERGY	REL.ENERGY		ABS.RATE	REL.INT.
107	1114	1t1	4t2	3T1	259.88	-41.9	0.0	0.0000000	0.0
106	1112	1t1	1t1	3T1	259.67	-42.1	0.2	0.0000000	0.0
105	1111	1t1	1t1	1E	259.29	-42.5	0.6	0.0000000	0.0
104	1114	1t1	4t2	3T2	258.94	-42.9	0.9	0.0000000	0.0
103	1114	1t1	4t2	3E	257.78	-44.0	2.1	0.0000000	0.0
102	911	1e	1t1	3T2	257.42	-44.4	2.5	0.0000000	0.0
101	1114	1t1	4t2	1E	257.36	-44.4	2.5	0.0000000	0.0
100	611	3t2	1t1	3A1	257.06	-44.7	2.8	0.0000000	0.0
99	911	1e	1t1	3T1	257.01	-44.8	2.9	0.0000000	0.0
98	1112	1t1	1t1	1T2	256.74	-45.1	3.1	0.0000000	0.0
97	1114	1t1	4t2	3A1	256.51	-45.3	3.4	0.0000000	0.0
96	1415	4t2	4t2	3T1	256.24	-45.6	3.6	0.0000000	0.0
95	914	1e	4t2	3T1	255.97	-45.8	3.9	0.0000000	0.0
94	914	1e	4t2	3T2	255.97	-45.8	3.9	0.0000000	0.0
93	1414	4t2	4t2	1E	255.78	-46.0	4.1	0.0000123	5.2
92	1114	1t1	4t2	1A1	255.49	-46.3	4.4	0.0000000	0.0
91	1415	4t2	4t2	1T2	255.24	-46.6	4.6	0.0000185	7.8
90	611	3t2	1t1	3T2	254.96	-46.8	4.9	0.0000000	0.0
89	1111	1t1	1t1	1A1	254.88	-46.9	5.0	0.0000000	0.0
88	1114	1t1	4t2	1T1	254.79	-47.0	5.1	0.0000000	0.0
87	911	1e	1t1	1T1	254.51	-47.3	5.4	0.0000000	0.0
86	911	1e	1t1	1T2	254.40	-47.4	5.5	0.0000000	0.0
85	614	3t2	4t2	3A1	254.32	-47.5	5.6	0.0000000	0.0
84	611	3t2	1t1	3T1	254.28	-47.5	5.6	0.0000000	0.0
83	1414	4t2	4t2	1A1	254.28	-47.5	5.6	0.0000024	1.0
82	910	1e	1e	3A2	253.79	-48.0	6.1	0.0000000	0.0
81	1114	1t1	4t2	1T2	253.62	-48.2	6.3	0.0000000	0.0
80	914	1e	4t2	1T2	253.57	-48.2	6.3	0.0000000	0.0
79	910	1e	1e	1E	253.28	-48.5	6.6	0.0000000	0.0
78	614	3t2	4t2	3T1	253.15	-48.6	6.7	0.0000000	0.0
77	914	1e	4t2	1T1	253.08	-48.7	6.8	0.0000000	0.0
76	614	3t2	4t2	3T2	252.84	-49.0	7.0	0.0000000	0.0
75	614	3t2	4t2	1E	252.81	-49.0	7.1	0.0000760	31.9
74	611	3t2	1t1	1E	252.77	-49.0	7.1	0.0000000	0.0
73	99	1e	1e	1A1	252.76	-49.0	7.1	0.0000000	0.0
72	611	3t2	1t1	3E	252.65	-49.2	7.2	0.0000000	0.0
71	611	3t2	1t1	1T1	251.28	-50.5	8.6	0.0000000	0.0
70	69	3t2	1e	3T1	251.18	-50.6	8.7	0.0000000	0.0
69	69	3t2	1e	3T2	251.18	-50.6	8.7	0.0000000	0.0
68	511	4a1	1t1	3T2	250.69	-51.1	9.2	0.0000000	0.0
67	614	3t2	4t2	3E	249.89	-51.9	10.0	0.0000000	0.0
66	514	4a1	4t2	3T2	249.81	-52.0	10.1	0.0000127	5.3
65	614	3t2	4t2	1T1	249.07	-52.7	10.8	0.0000000	0.0
64	69	3t2	1e	1T1	248.43	-53.4	11.4	0.0000000	0.0
63	69	3t2	1e	1T2	248.43	-53.4	11.4	0.0000000	0.0
62	611	3t2	1t1	1T2	248.34	-53.5	11.5	0.0000000	0.0
61	614	3t2	4t2	1T2	248.03	-53.8	11.9	0.0001094	45.9
60	511	4a1	1t1	1T2	247.94	-53.9	11.9	0.0000000	0.0
59	59	4a1	1e	3E	247.47	-54.3	12.4	0.0000000	0.0
58	67	3t2	3t2	3T1	246.71	-55.1	13.2	0.0000000	0.0
57	59	4a1	1e	1E	246.56	-55.2	13.3	0.0000000	0.0
56	614	3t2	4t2	1A1	246.35	-55.5	13.5	0.0000139	5.9
55	66	3t2	3t2	1E	246.04	-55.8	13.8	0.0001078	45.3
54	514	4a1	4t2	1T2	245.99	-55.8	13.9	0.0000376	15.8
53	67	3t2	3t2	1T2	245.54	-56.3	14.3	0.0001617	67.9
52	56	4a1	3t2	3T2	245.12	-56.7	14.8	0.0000374	15.7

51	611	3t2	1t1	1A1	244.96	-56.8	14.9	0.0000000	0.0
50	66	3t2	3t2	1A1	244.28	-57.5	15.6	0.0000206	8.7
49	56	4a1	3t2	1T2	240.50	-61.3	19.4	0.0001111	46.6
48	55	4a1	4a1	1A1	239.46	-62.3	20.4	0.0000604	25.4
47	211	2t2	1t1	3T1	236.57	-65.2	23.3	0.0000000	0.0
46	211	2t2	1t1	3E	236.50	-65.3	23.4	0.0000000	0.0
45	211	2t2	1t1	1E	235.54	-66.3	24.3	0.0000000	0.0
44	211	2t2	1t1	1T1	235.47	-66.3	24.4	0.0000000	0.0
43	214	2t2	4t2	3T1	234.42	-67.4	25.5	0.0000000	0.0
42	214	2t2	4t2	3E	234.39	-67.4	25.5	0.0000000	0.0
41	211	2t2	1t1	3T2	233.78	-68.0	26.1	0.0000000	0.0
40	214	2t2	4t2	3T2	233.16	-68.6	26.7	0.0000000	0.0
39	214	2t2	4t2	1T1	232.96	-68.8	26.9	0.0000000	0.0
38	214	2t2	4t2	1E	232.93	-68.9	26.9	0.0000559	23.5
37	29	2t2	1e	3T1	232.73	-69.1	27.1	0.0000000	0.0
36	29	2t2	1e	3T2	232.73	-69.1	27.1	0.0000000	0.0
35	214	2t2	4t2	3A1	232.55	-69.2	27.3	0.0000000	0.0
34	211	2t2	1t1	3A1	232.47	-69.3	27.4	0.0000000	0.0
33	111	3a1	1t1	3T2	231.62	-70.2	28.3	0.0000000	0.0
32	214	2t2	4t2	1T2	230.75	-71.1	29.1	0.0000805	33.8
31	29	2t2	1e	1T2	230.67	-71.1	29.2	0.0000000	0.0
30	29	2t2	1e	1T1	230.67	-71.1	29.2	0.0000000	0.0
29	211	2t2	1t1	1T2	230.59	-71.2	29.3	0.0000000	0.0
28	114	3a1	4t2	3T2	230.28	-71.5	29.6	0.0000173	7.2
27	111	3a1	1t1	1T2	229.80	-72.0	30.1	0.0000000	0.0
26	26	2t2	3t2	3T1	229.62	-72.2	30.3	0.0000000	0.0
25	214	2t2	4t2	1A1	229.56	-72.2	30.3	0.0000103	4.3
24	26	2t2	3t2	3E	229.22	-72.6	30.7	0.0000000	0.0
23	19	3a1	1e	3E	229.12	-72.7	30.8	0.0000000	0.0
22	26	2t2	3t2	3T2	228.70	-73.1	31.2	0.0000000	0.0
21	114	3a1	4t2	1T2	228.53	-73.3	31.3	0.0000512	21.5
20	26	2t2	3t2	1E	228.50	-73.3	31.4	0.0001654	69.4
19	26	2t2	3t2	3A1	228.44	-73.4	31.4	0.0000000	0.0
18	211	2t2	1t1	1A1	228.06	-73.7	31.8	0.0000000	0.0
17	26	2t2	3t2	1T1	227.74	-74.1	32.1	0.0000000	0.0
16	19	3a1	1e	1E	227.51	-74.3	32.4	0.0000000	0.0
15	25	2t2	4a1	3X	226.45	-75.3	33.4	0.0000275	11.6
14	26	2t2	3t2	1T2	225.97	-75.8	33.9	0.0002381	100.0
13	16	3a1	3t2	3T2	225.36	-76.4	34.5	0.0000510	21.4
12	26	2t2	3t2	1A1	225.24	-76.6	34.6	0.0000304	12.7
11	25	2t2	4a1	1X	224.06	-77.7	35.8	0.0000818	34.3
10	16	3a1	3t2	1T2	223.94	-77.9	35.9	0.0001515	63.6
9	15	3a1	4a1	3X	222.51	-79.3	37.4	0.0000000	0.0
8	15	3a1	4a1	1X	221.30	-80.5	38.6	0.0001648	69.2
7	23	2t2	2t2	3T1	213.05	-88.8	46.8	0.0000000	0.0
6	22	2t2	2t2	1E	212.89	-88.9	47.0	0.0000584	24.5
5	12	3a1	2t2	3T2	209.21	-92.6	50.7	0.0000376	15.8
4	23	2t2	2t2	1T2	206.71	-95.1	53.2	0.0000877	36.8
3	22	2t2	2t2	1A1	203.39	-98.4	56.5	0.0000112	4.7
2	12	3a1	2t2	1T2	203.31	-98.5	56.6	0.0001115	46.8
1	11	3a1	3a1	1A1	202.55	-99.3	57.3	0.0001124	47.2

Total Transition Rate (in au) = 2.32618E-03

D.6.1.2. Carbon tetrafluoride - F(KVV)*

```
        CALCULATIONS FOR CF4

   6      0.0000000      0.0000000      0.0000000
   9     -1.4393502     -1.4393502      1.4393502
   9      1.4393502     -1.4393502     -1.4393502
   9      1.4393502      1.4393502      1.4393502
   9     -1.4393502      1.4393502     -1.4393502
 DEGENERACY OF OCCUPIED ORBITALS
1 3 3 3 1 3 3 3 2 2 3 3 3 3 3 3


     EIGENVECTORS
 0.5298   0.0000   0.0000   0.0000  -0.4200   0.0000   0.0000   0.0000   0.0000   0.0000   0.0000
 0.0000   0.4031   0.0000   0.0000   0.0000   0.3890   0.0000   0.0000   0.0000   0.0000   0.0000
 0.0000   0.0000   0.4031   0.0000   0.0000   0.0000   0.3890   0.0000   0.0000   0.0000   0.0000
 0.0000   0.0000   0.0000   0.4031   0.0000   0.0000   0.0000   0.3890   0.0000   0.0000   0.0000
 0.4052  -0.4482  -0.4482   0.4482   0.2534   0.1750   0.1750  -0.1750   0.0000   0.0000   0.0000
 0.0722   0.0279  -0.0621   0.0621  -0.2173   0.1104  -0.2910   0.2910   0.2041   0.3536   0.0000
 0.0722  -0.0621   0.0279   0.0621  -0.2173  -0.2910   0.1104   0.2910   0.2041  -0.3536  -0.3536
-0.0722   0.0621   0.0621   0.0279   0.2173   0.2910   0.2910   0.1104   0.4083   0.0000   0.3535
 0.4052   0.4482  -0.4482  -0.4482   0.2534  -0.1750   0.1750   0.1750   0.0000   0.0000   0.0000
-0.0722   0.0279   0.0621   0.0621   0.2173   0.1104   0.2910   0.2910  -0.2041  -0.3536   0.0000
 0.0722   0.0621   0.0279  -0.0621  -0.2173   0.2910   0.1104  -0.2910   0.2041  -0.3535   0.3536
 0.0722   0.0621  -0.0621   0.0279  -0.2173   0.2910  -0.2910   0.1104  -0.4082   0.0000  -0.3535
 0.4052   0.4482   0.4482   0.4482   0.2534  -0.1750  -0.1750  -0.1750   0.0000   0.0000   0.0000
-0.0722   0.0279  -0.0621  -0.0621   0.2173   0.1104  -0.2910  -0.2910  -0.2041  -0.3536   0.0000
-0.0722  -0.0621   0.0279  -0.0621   0.2173  -0.2910   0.1104  -0.2910  -0.2041   0.3535   0.3535
-0.0722  -0.0621  -0.0621   0.0279   0.2173  -0.2910  -0.2910   0.1104   0.4082   0.0000  -0.3535
 0.4052  -0.4482   0.4482  -0.4482   0.2534   0.1750  -0.1750   0.1750   0.0000   0.0000   0.0000
 0.0722   0.0279   0.0621  -0.0621  -0.2173   0.1104   0.2910  -0.2910   0.2041   0.3536   0.0000
-0.0722   0.0621   0.0279   0.0621   0.2173   0.2910   0.1104   0.2910  -0.2041   0.3536  -0.3536
 0.0722  -0.0621   0.0621   0.0279  -0.2173  -0.2910   0.2910   0.1104  -0.4083   0.0000   0.3536
 0.0000   0.0000   0.0000   0.0000   0.0000
 0.0000   0.0000   0.1776   0.0000   0.0000
 0.0000   0.0000   0.0000   0.1776   0.0000
 0.0000   0.0000   0.0000   0.0000   0.1776
 0.0000   0.0000   0.0249   0.0249  -0.0249
-0.3536   0.3535  -0.4852  -0.0549   0.0549
 0.0000   0.3535  -0.0549  -0.4852   0.0549
 0.3535   0.0000   0.0549   0.0549  -0.4852
 0.0000   0.0000  -0.0249   0.0249   0.0249
-0.3536  -0.3535  -0.4852   0.0549   0.0549
 0.0000  -0.3536   0.0549  -0.4853  -0.0549
 0.3536   0.0000   0.0549  -0.0549  -0.4853
 0.0000   0.0000  -0.0249  -0.0249  -0.0249
 0.3536   0.3536  -0.4853  -0.0549  -0.0549
 0.0000   0.3536  -0.0549  -0.4853  -0.0549
-0.3535   0.0000  -0.0549  -0.0549  -0.4853
 0.0000   0.0000   0.0249  -0.0249   0.0249
 0.3536  -0.3536  -0.4853   0.0549  -0.0549
 0.0000  -0.3535   0.0549  -0.4852   0.0549
-0.3535   0.0000  -0.0549   0.0549  -0.4852


     MOLECULAR J(PP,QQ) COULOMB INTEGRALS
 0.4282   0.4205   0.4205   0.4205   0.4041   0.4097   0.4097   0.4097   0.4110   0.4110   0.4114
 0.4205   0.4217   0.4160   0.4160   0.4095   0.4083   0.4149   0.4149   0.4151   0.4153   0.4152
 0.4205   0.4160   0.4217   0.4160   0.4095   0.4149   0.4083   0.4149   0.4151   0.4153   0.4151
 0.4205   0.4160   0.4160   0.4217   0.4095   0.4149   0.4149   0.4083   0.4154   0.4150   0.4151
 0.4041   0.4095   0.4095   0.4095   0.4463   0.4296   0.4296   0.4296   0.4111   0.4111   0.4147
 0.4097   0.4083   0.4149   0.4149   0.4296   0.4391   0.4143   0.4143   0.4130   0.4170   0.4174
 0.4097   0.4149   0.4083   0.4149   0.4296   0.4143   0.4391   0.4143   0.4130   0.4170   0.4146
 0.4097   0.4149   0.4149   0.4083   0.4296   0.4143   0.4143   0.4391   0.4191   0.4109   0.4146
 0.4110   0.4151   0.4151   0.4154   0.4111   0.4130   0.4130   0.4191   0.4330   0.4140   0.4219
 0.4110   0.4153   0.4153   0.4150   0.4111   0.4170   0.4170   0.4109   0.4140   0.4330   0.4188
 0.4114   0.4152   0.4151   0.4151   0.4147   0.4174   0.4146   0.4146   0.4219   0.4188   0.4330
 0.4114   0.4151   0.4152   0.4151   0.4147   0.4146   0.4174   0.4146   0.4219   0.4188   0.4188
 0.4114   0.4151   0.4151   0.4152   0.4147   0.4146   0.4146   0.4174   0.4172   0.4235   0.4188
 0.4114   0.4155   0.4144   0.4144   0.4189   0.4112   0.4199   0.4199   0.4156   0.4203   0.4135
 0.4114   0.4144   0.4155   0.4144   0.4189   0.4199   0.4112   0.4199   0.4156   0.4203   0.4223
 0.4114   0.4144   0.4144   0.4155   0.4189   0.4199   0.4199   0.4112   0.4226   0.4132   0.4223
 0.4114   0.4114   0.4114   0.4114   0.4114
 0.4151   0.4151   0.4155   0.4144   0.4144
 0.4152   0.4151   0.4144   0.4155   0.4144
 0.4151   0.4152   0.4144   0.4144   0.4155
 0.4147   0.4147   0.4189   0.4189   0.4189
 0.4146   0.4146   0.4112   0.4199   0.4199
 0.4174   0.4146   0.4199   0.4112   0.4199
 0.4146   0.4174   0.4199   0.4199   0.4112
```

0.4219	0.4172	0.4156	0.4156	0.4226
0.4188	0.4235	0.4203	0.4203	0.4132
0.4188	0.4188	0.4135	0.4223	0.4223
0.4330	0.4188	0.4223	0.4135	0.4223
0.4188	0.4330	0.4223	0.4223	0.4135
0.4223	0.4223	0.4308	0.4137	0.4137
0.4135	0.4223	0.4137	0.4308	0.4137
0.4223	0.4135	0.4137	0.4137	0.4308

MOLECULAR K(PQ,PQ) EXCHANGE INTEGRALS

0.4282	0.1085	0.1085	0.1085	0.0224	0.0261	0.0261	0.0261	0.0297	0.0297	0.0334
0.1085	0.4217	0.1163	0.1163	0.0440	0.0284	0.0423	0.0423	0.0369	0.0389	0.0387
0.1085	0.1163	0.4217	0.1163	0.0440	0.0423	0.0284	0.0423	0.0369	0.0389	0.0395
0.1085	0.1163	0.1163	0.4217	0.0440	0.0423	0.0423	0.0284	0.0398	0.0360	0.0395
0.0224	0.0440	0.0440	0.0440	0.4463	0.0849	0.0849	0.0849	0.0168	0.0168	0.0504
0.0261	0.0284	0.0423	0.0423	0.0849	0.4391	0.0216	0.0216	0.0314	0.0696	0.0726
0.0261	0.0423	0.0284	0.0423	0.0849	0.0216	0.4391	0.0216	0.0314	0.0696	0.0884
0.0261	0.0423	0.0423	0.0284	0.0849	0.0216	0.0216	0.4391	0.0887	0.0123	0.0884
0.0297	0.0369	0.0369	0.0398	0.0168	0.0314	0.0314	0.0887	0.4330	0.0095	0.0836
0.0297	0.0389	0.0389	0.0360	0.0168	0.0696	0.0696	0.0123	0.0095	0.4330	0.0539
0.0334	0.0387	0.0395	0.0395	0.0504	0.0726	0.0884	0.0884	0.0836	0.0539	0.4330
0.0334	0.0395	0.0387	0.0395	0.0504	0.0884	0.0726	0.0884	0.0836	0.0539	0.0539
0.0334	0.0395	0.0395	0.0387	0.0504	0.0884	0.0884	0.0726	0.0391	0.0984	0.0539
0.0320	0.0362	0.0356	0.0356	0.0702	0.0131	0.0817	0.0817	0.0312	0.0752	0.0114
0.0320	0.0356	0.0362	0.0356	0.0702	0.0817	0.0131	0.0817	0.0312	0.0752	0.0956
0.0320	0.0356	0.0356	0.0362	0.0702	0.0817	0.0817	0.0131	0.0971	0.0093	0.0956
0.0334	0.0334	0.0320	0.0320	0.0320						
0.0395	0.0395	0.0362	0.0356	0.0356						
0.0387	0.0395	0.0356	0.0362	0.0356						
0.0395	0.0387	0.0356	0.0356	0.0362						
0.0504	0.0504	0.0702	0.0702	0.0702						
0.0884	0.0884	0.0131	0.0817	0.0817						
0.0726	0.0884	0.0817	0.0131	0.0817						
0.0884	0.0726	0.0817	0.0817	0.0131						
0.0836	0.0391	0.0312	0.0312	0.0971						
0.0539	0.0984	0.0752	0.0752	0.0093						
0.0539	0.0539	0.0114	0.0956	0.0956						
0.4330	0.0539	0.0956	0.0114	0.0956						
0.0539	0.4330	0.0956	0.0956	0.0114						
0.0956	0.0956	0.4308	0.0183	0.0183						
0.0114	0.0956	0.0183	0.4308	0.0183						
0.0956	0.0114	0.0183	0.0183	0.4308						

SPECIAL J(PQ,RS) AND K(PS,RQ) INTEGRALS

2	3	6	7	0.0248	0.0152
4	2	8	6	0.0248	0.0152
3	4	7	8	0.0248	0.0152
2	3	7	6	0.0248	0.0078
2	4	8	6	0.0248	0.0078
3	4	8	7	0.0248	0.0078
2	3	9	10	0.0000	0.0000
2	3	10	9	0.0000	0.0000
2	3	11	12	0.0705	0.0211
4	2	13	11	0.0705	0.0211
3	4	12	13	0.0705	0.0211
2	3	12	11	0.0705	0.0192
2	4	13	11	0.0705	0.0192
3	4	13	12	0.0705	0.0192
2	3	14	15	0.0319	0.0094
4	2	16	14	0.0319	0.0094
3	4	15	16	0.0319	0.0094
2	3	15	14	0.0319	0.0088
2	4	16	14	0.0319	0.0088
3	4	16	15	0.0319	0.0088
6	7	9	10	0.0000	0.0000
6	7	10	9	0.0000	0.0000
6	7	11	12	0.0208	0.0748
8	6	13	11	0.0208	0.0748
7	8	12	13	0.0208	0.0748
6	7	12	11	0.0208	0.0332
6	8	13	11	0.0208	0.0332
7	8	13	12	0.0208	0.0332
6	7	14	15	0.0124	0.0667
8	6	16	14	0.0124	0.0667
7	8	15	16	0.0124	0.0667
6	7	15	14	0.0124	0.0068
6	8	16	14	0.0124	0.0068
7	8	16	15	0.0124	0.0068
9	10	11	12	0.0000	-0.0229
9	10	12	11	0.0000	0.0229

9	10	14	15	0.0000	0.0000
9	10	15	14	0.0000	0.0000
11	12	14	15	0.0193	0.0037
13	11	16	14	0.0193	0.0037
12	13	15	16	0.0193	0.0037
11	12	15	14	0.0193	0.0022
11	13	16	14	0.0193	0.0022
12	13	16	15	0.0193	0.0022

MOLECULE: CF4 ATOM: Fluorine 1

AUGER SPECTRUM

CORE AND VALENCE I.P.S USED

1s	695.200								
3a1	43.800	2t2	40.300	2t2	40.300	2t2	40.300	4a1	25.100
3t2	22.200	3t2	22.200	3t2	22.200	1e	18.500	1e	18.500
1t1	16.100	1t1	16.100	1t1	16.100	4t2	17.400	4t2	17.400
4t2	17.400								

PEAK NR.	MO.INDEX	MO.NAME		SYM	ABS.ENERGY	REL.ENERGY		ABS.RATE	REL.INTENS.
107	1114	1t1	4t2	3T1	653.28	-41.9	0.0	0.0000000	0.0
106	1112	1t1	1t1	3T1	653.07	-42.1	0.2	0.0000000	0.0
105	1111	1t1	1t1	1E	652.69	-42.5	0.6	0.0000988	32.0
104	1114	1t1	4t2	3T2	652.34	-42.9	0.9	0.0000001	0.0
103	1114	1t1	4t2	3E	651.18	-44.0	2.1	0.0000000	0.0
102	911	1e	1t1	3T2	650.82	-44.4	2.5	0.0000000	0.0
101	1114	1t1	4t2	1E	650.76	-44.4	2.5	0.0000427	13.8
100	611	3t2	1t1	3A1	650.46	-44.7	2.8	0.0000029	1.0
99	911	1e	1t1	3T1	650.41	-44.8	2.9	0.0000000	0.0
98	1112	1t1	1t1	1T2	650.14	-45.1	3.1	0.0002264	73.3
97	1114	1t1	4t2	3A1	649.91	-45.3	3.4	0.0000001	0.0
96	1415	4t2	4t2	3T1	649.64	-45.6	3.6	0.0000000	0.0
95	914	1e	4t2	3T1	649.37	-45.8	3.9	0.0000000	0.0
94	914	1e	4t2	3T2	649.37	-45.8	3.9	0.0000002	0.1
93	1414	4t2	4t2	1E	649.18	-46.0	4.1	0.0001165	37.7
92	1114	1t1	4t2	1A1	648.89	-46.3	4.4	0.0001550	50.2
91	1415	4t2	4t2	1T2	648.64	-46.6	4.6	0.0001907	61.7
90	611	3t2	1t1	3T2	648.36	-46.8	4.9	0.0000066	2.1
89	1111	1t1	1t1	1A1	648.28	-46.9	5.0	0.0000577	18.7
88	1114	1t1	4t2	1T1	648.19	-47.0	5.1	0.0002792	90.3
87	911	1e	1t1	1T1	647.91	-47.3	5.4	0.0000857	27.7
86	911	1e	1t1	1T2	647.80	-47.4	5.5	0.0002033	65.8
85	614	3t2	4t2	3A1	647.72	-47.5	5.6	0.0000016	0.5
84	611	3t2	1t1	3T1	647.68	-47.5	5.6	0.0000022	0.7
83	1414	4t2	4t2	1A1	647.68	-47.5	5.6	0.0000298	9.6
82	910	1e	1e	3A2	647.19	-48.0	6.1	0.0000000	0.0
81	1114	1t1	4t2	1T2	647.02	-48.2	6.3	0.0002377	76.9
80	914	1e	4t2	1T2	646.97	-48.2	6.3	0.0001997	64.6
79	910	1e	1e	1E	646.68	-48.5	6.6	0.0001317	42.6
78	614	3t2	4t2	3T1	646.55	-48.6	6.7	0.0000025	0.8
77	914	1e	4t2	1T1	646.48	-48.7	6.8	0.0000931	30.1
76	614	3t2	4t2	3T2	646.24	-49.0	7.0	0.0000047	1.5
75	614	3t2	4t2	1E	646.21	-49.0	7.1	0.0000465	15.1
74	611	3t2	1t1	1E	646.17	-49.0	7.1	0.0001752	56.7
73	99	1e	1e	1A1	646.16	-49.0	7.1	0.0000385	12.5
72	611	3t2	1t1	3E	646.05	-49.2	7.2	0.0000015	0.5
71	611	3t2	1t1	1T1	644.68	-50.5	8.6	0.0000216	7.0
70	69	3t2	1e	3T1	644.58	-50.6	8.7	0.0000015	0.5
69	69	3t2	1e	3T2	644.58	-50.6	8.7	0.0000044	1.4
68	511	4a1	1t1	3T2	644.09	-51.1	9.2	0.0000092	3.0
67	614	3t2	4t2	3E	643.29	-51.9	10.0	0.0000028	0.9
66	514	4a1	4t2	3T2	643.21	-52.0	10.1	0.0000080	2.6
65	614	3t2	4t2	1T1	642.47	-52.7	10.8	0.0002192	71.0
64	69	3t2	1e	1T1	641.83	-53.4	11.4	0.0000777	25.2
63	69	3t2	1e	1T2	641.83	-53.4	11.4	0.0001653	53.5
62	611	3t2	1t1	1T2	641.74	-53.5	11.5	0.0003090	100.0
61	614	3t2	4t2	1T2	641.43	-53.8	11.8	0.0001703	55.1
60	511	4a1	1t1	1T2	641.34	-53.9	11.9	0.0001857	60.1
59	59	4a1	1e	3E	640.87	-54.3	12.4	0.0000062	2.0
58	67	3t2	3t2	3T1	640.11	-55.1	13.2	0.0000019	0.6
57	59	4a1	1e	1E	639.96	-55.2	13.3	0.0000947	30.6
56	614	3t2	4t2	1A1	639.75	-55.5	13.5	0.0001055	34.1
55	66	3t2	3t2	1E	639.44	-55.8	13.8	0.0000809	26.2
54	514	4a1	4t2	1T2	639.39	-55.8	13.9	0.0001683	54.5
53	67	3t2	3t2	1T2	638.94	-56.3	14.3	0.0001303	42.2

52	56	4a1	3t2	3T2	638.52	-56.7	14.8	0.0000040	1.3
51	611	3t2	1t1	1A1	638.36	-56.8	14.9	0.0000604	19.5
50	66	3t2	3t2	1A1	637.68	-57.5	15.6	0.0000138	4.5
49	56	4a1	3t2	1T2	633.90	-61.3	19.4	0.0001395	45.1
48	55	4a1	4a1	1A1	632.86	-62.3	20.4	0.0000255	8.3
47	211	2t2	1t1	3T1	629.97	-65.2	23.3	0.0000145	4.7
46	211	2t2	1t1	3E	629.90	-65.3	23.4	0.0000096	3.1
45	211	2t2	1t1	1E	628.94	-66.3	24.3	0.0000394	12.8
44	211	2t2	1t1	1T1	628.87	-66.3	24.4	0.0000480	15.5
43	214	2t2	4t2	3T1	627.82	-67.4	25.5	0.0000219	7.1
42	214	2t2	4t2	3E	627.79	-67.4	25.5	0.0000140	4.5
41	211	2t2	1t1	3T2	627.18	-68.0	26.1	0.0000434	14.0
40	214	2t2	4t2	3T2	626.56	-68.6	26.7	0.0000348	11.3
39	214	2t2	4t2	1T1	626.36	-68.8	26.9	0.0000777	25.1
38	214	2t2	4t2	1E	626.33	-68.9	26.9	0.0000497	16.1
37	29	2t2	1e	3T1	626.13	-69.1	27.1	0.0000096	3.1
36	29	2t2	1e	3T2	626.13	-69.1	27.1	0.0000289	9.4
35	214	2t2	4t2	3A1	625.95	-69.2	27.3	0.0000139	4.5
34	211	2t2	1t1	3A1	625.87	-69.3	27.4	0.0000193	6.2
33	111	3a1	1t1	3T2	625.02	-70.2	28.3	0.0000236	7.7
32	214	2t2	4t2	1T2	624.15	-71.1	29.1	0.0001225	39.6
31	29	2t2	1e	1T2	624.07	-71.1	29.2	0.0001013	32.8
30	29	2t2	1e	1T1	624.07	-71.1	29.2	0.0000351	11.4
29	211	2t2	1t1	1T2	623.99	-71.2	29.3	0.0001543	49.9
28	114	3a1	4t2	3T2	623.68	-71.5	29.6	0.0000233	7.6
27	111	3a1	1t1	1T2	623.20	-72.0	30.1	0.0000941	30.5
26	26	2t2	3t2	3T1	623.02	-72.2	30.3	0.0000155	5.0
25	214	2t2	4t2	1A1	622.96	-72.2	30.3	0.0000483	15.6
24	26	2t2	3t2	3E	622.62	-72.6	30.7	0.0000147	4.8
23	19	3a1	1e	3E	622.52	-72.7	30.8	0.0000158	5.1
22	26	2t2	3t2	3T2	622.10	-73.1	31.2	0.0000273	8.8
21	114	3a1	4t2	1T2	621.93	-73.3	31.3	0.0000903	29.2
20	26	2t2	3t2	1E	621.90	-73.3	31.4	0.0000399	12.9
19	26	2t2	3t2	3A1	621.84	-73.4	31.4	0.0000100	3.2
18	211	2t2	1t1	1A1	621.46	-73.7	31.8	0.0000649	21.0
17	26	2t2	3t2	1T1	621.14	-74.1	32.1	0.0000718	23.2
16	19	3a1	1e	1E	620.91	-74.3	32.4	0.0000596	19.3
15	25	2t2	4a1	3X	619.85	-75.3	33.4	0.0000194	6.3
14	26	2t2	3t2	1T2	619.37	-75.8	33.9	0.0001369	44.3
13	16	3a1	3t2	3T2	618.76	-76.4	34.5	0.0000202	6.5
12	26	2t2	3t2	1A1	618.64	-76.6	34.6	0.0000676	21.9
11	25	2t2	4a1	1X	617.46	-77.7	35.8	0.0001235	40.0
10	16	3a1	3t2	1T2	617.34	-77.9	35.9	0.0000934	30.2
9	15	3a1	4a1	3X	615.91	-79.3	37.4	0.0000065	2.1
8	15	3a1	4a1	1X	614.70	-80.5	38.6	0.0000367	11.9
7	23	2t2	2t2	3T1	606.45	-88.8	46.8	0.0000006	0.2
6	22	2t2	2t2	1E	606.29	-88.9	47.0	0.0000042	1.4
5	12	3a1	2t2	3T2	602.61	-92.6	50.7	0.0000012	0.4
4	23	2t2	2t2	1T2	600.11	-95.1	53.2	0.0002068	66.9
3	22	2t2	2t2	1A1	596.79	-98.4	56.5	0.0000990	32.1
2	12	3a1	2t2	1T2	596.71	-98.5	56.6	0.0001723	55.8
1	11	3a1	3a1	1A1	595.95	-99.3	57.3	0.0000240	7.8

Total Transition Rate (in au) = 6.885946728E-03

D.6.2.1. Silicon tetrafluoride - Si(L_{23}VV)

```
      CALCULATIONS FOR SiF4, geom. LBII/15 p.96

  14       0.0000000       0.0000000       0.0000000
   9      -2.3978181       0.0000000      -1.6955135
   9       0.0000000      -2.3978181       1.6955135
   9       2.3978181       0.0000000      -1.6955135
   9       0.0000000       2.3978181       1.6955135
 DEGENERACY OF OCCUPIED ORBITALS
1 3 3 3 3 3 3 1 2 2 3 3 3 3 3 3

     EIGENVECTORS
-0.4262  0.0000  0.0000  0.0000  0.0000  0.0000  0.0000  0.6778  0.0000  0.0000  0.0000
 0.0000  0.2607  0.0000  0.0000  0.3630  0.0000  0.0000  0.0000  0.0000  0.0000  0.0000
 0.0000  0.0000  0.2607  0.0000  0.0000  0.3630  0.0000  0.0000  0.0000  0.0000  0.0000
 0.0000  0.0000  0.0000  0.2607  0.0000  0.0000  0.3630  0.0000  0.0000  0.0000  0.0000
-0.4488 -0.4816  0.4816  0.4816  0.0804 -0.0804 -0.0804 -0.1997  0.0000  0.0000  0.0000
-0.0325  0.0122  0.0218  0.0218  0.2291  0.2812  0.2812  0.1782  0.2041 -0.3536  0.0000
 0.0325  0.0218  0.0122 -0.0218  0.2812  0.2291 -0.2812 -0.1782 -0.2041 -0.3536  0.3536
 0.0325  0.0218 -0.0218  0.0122  0.2812 -0.2812  0.2291 -0.1782  0.4082  0.0000  0.3536
-0.4488  0.4816  0.4816 -0.4816 -0.0804 -0.0804  0.0804 -0.1997  0.0000  0.0000  0.0000
 0.0325  0.0122 -0.0218  0.0218  0.2291 -0.2812  0.2812 -0.1782 -0.2041  0.3536  0.0000
 0.0325 -0.0218  0.0122  0.0218 -0.2812  0.2291  0.2812 -0.1782 -0.2041 -0.3536 -0.3536
-0.0325  0.0218  0.0218  0.0122  0.2812  0.2812  0.2291  0.1782 -0.4082  0.0000 -0.3536
-0.4488 -0.4816 -0.4816 -0.4816  0.0804  0.0804  0.0804 -0.1997  0.0000  0.0000  0.0000
-0.0325  0.0122 -0.0218 -0.0218  0.2291 -0.2812 -0.2812  0.1782  0.2041 -0.3536  0.0000
-0.0325 -0.0218  0.0122 -0.0218 -0.2812  0.2291 -0.2812  0.1782  0.2041  0.3536  0.3536
-0.0325 -0.0218 -0.0218  0.0122 -0.2812 -0.2812  0.2291  0.1782 -0.4083  0.0000  0.3536
-0.4488  0.4816 -0.4816  0.4816 -0.0804  0.0804 -0.0804 -0.1997  0.0000  0.0000  0.0000
 0.0325  0.0122  0.0218 -0.0218  0.2291  0.2812 -0.2812 -0.1782 -0.2041  0.3536  0.0000
-0.0325  0.0218  0.0122  0.0218  0.2812  0.2291  0.2812  0.1782  0.2041  0.3536 -0.3536
 0.0325 -0.0218  0.0218  0.0122 -0.2812  0.2812  0.2291 -0.1782  0.4083  0.0000 -0.3536
 0.0000  0.0000  0.0000  0.0000  0.0000
 0.0000  0.0000  0.3063  0.0000  0.0000
 0.0000  0.0000  0.0000  0.3063  0.0000
 0.0000  0.0000  0.0000  0.0000  0.3063
 0.0000  0.0000  0.0415 -0.0415 -0.0415
 0.3536  0.3536 -0.4405  0.1241  0.1241
 0.0000 -0.3536  0.1241 -0.4405 -0.1241
-0.3536  0.0000  0.1241 -0.1241 -0.4405
 0.0000  0.0000 -0.0415 -0.0415  0.0415
 0.3536 -0.3536 -0.4405 -0.1241  0.1241
 0.0000  0.3536 -0.1241 -0.4405  0.1241
-0.3536  0.0000  0.1241  0.1241 -0.4405
 0.0000  0.0000  0.0415  0.0415  0.0415
-0.3536 -0.3536 -0.4405 -0.1241 -0.1241
 0.0000  0.3536 -0.1241 -0.4405 -0.1241
 0.3536  0.0000 -0.1241 -0.1241 -0.4405
 0.0000  0.0000 -0.0415  0.0415 -0.0415
-0.3536  0.3536 -0.4405  0.1241 -0.1241
 0.0000 -0.3536  0.1241 -0.4405  0.1241
 0.3536  0.0000 -0.1241  0.1241 -0.4405

   MOLECULAR J(PP,QQ) COULOMB INTEGRALS
 0.3812  0.3824  0.3824  0.3824  0.3778  0.3778  0.3778  0.3725  0.3856  0.3856  0.3856
 0.3824  0.5439  0.2249  0.3840  0.3716  0.3885  0.3807  0.3755  0.3880  0.3880  0.5592
 0.3824  0.2249  0.5439  0.3840  0.3885  0.3716  0.3807  0.3755  0.3880  0.3880  0.2168
 0.3824  0.3840  0.3840  0.3848  0.3807  0.3807  0.3793  0.3755  0.3880  0.3880  0.3880
 0.3778  0.3716  0.3885  0.3807  0.3909  0.3726  0.3727  0.3760  0.3815  0.3874  0.3842
 0.3778  0.3885  0.3716  0.3807  0.3726  0.3909  0.3727  0.3760  0.3815  0.3874  0.3867
 0.3778  0.3807  0.3807  0.3793  0.3727  0.3727  0.3908  0.3760  0.3903  0.3786  0.3810
 0.3725  0.3755  0.3755  0.3755  0.3760  0.3760  0.3760  0.3852  0.3744  0.3744  0.3792
 0.3856  0.3880  0.3880  0.3880  0.3815  0.3815  0.3903  0.3744  0.4052  0.3862  0.3988
 0.3856  0.3880  0.3880  0.3880  0.3874  0.3874  0.3786  0.3744  0.3862  0.4052  0.3862
 0.3856  0.5592  0.2168  0.3880  0.3842  0.3867  0.3810  0.3792  0.3988  0.3862  0.6018
 0.3856  0.2169  0.5591  0.3880  0.3984  0.3751  0.3794  0.3760  0.3904  0.3988  0.2085
 0.3856  0.3880  0.3880  0.3880  0.3879  0.3786  0.3855  0.3792  0.3894  0.3957  0.3862
 0.3838  0.4672  0.3054  0.3861  0.3814  0.3812  0.3851  0.3836  0.3861  0.3893  0.4705
 0.3838  0.3054  0.4672  0.3861  0.3812  0.3814  0.3851  0.3836  0.3861  0.3893  0.3004
 0.3838  0.3861  0.3861  0.3865  0.3851  0.3851  0.3775  0.3836  0.3908  0.3845  0.4010
 0.3856  0.3856  0.3838  0.3838  0.3838
 0.2169  0.3880  0.4672  0.3054  0.3861
 0.5591  0.3880  0.3054  0.4672  0.3861
 0.3880  0.3880  0.3861  0.3861  0.3865
 0.3984  0.3879  0.3814  0.3812  0.3851
 0.3751  0.3786  0.3812  0.3814  0.3851
 0.3794  0.3855  0.3851  0.3851  0.3775
 0.3760  0.3792  0.3836  0.3836  0.3836
```

0.3904	0.3894	0.3861	0.3861	0.3908
0.3988	0.3957	0.3893	0.3893	0.3845
0.2085	0.3862	0.4705	0.3004	0.4010
0.6018	0.3988	0.3067	0.4693	0.3900
0.3988	0.4052	0.4020	0.3845	0.3855
0.3067	0.4020	0.4452	0.3431	0.3873
0.4693	0.3845	0.3431	0.4452	0.3873
0.3900	0.3855	0.3873	0.3873	0.4011

MOLECULAR K(PQ,PQ) EXCHANGE INTEGRALS

0.3812	0.1548	0.1548	0.1548	0.0362	0.0362	0.0362	0.0316	0.0397	0.0397	0.0401
0.1548	0.5439	0.0004	0.1595	0.0374	0.0383	0.0399	0.0381	0.0415	0.0417	0.0835
0.1548	0.0004	0.5439	0.1595	0.0383	0.0374	0.0399	0.0381	0.0415	0.0417	0.0000
0.1548	0.1595	0.1595	0.3848	0.0399	0.0399	0.0358	0.0381	0.0419	0.0413	0.0415
0.0362	0.0374	0.0383	0.0399	0.3909	0.0090	0.0092	0.0508	0.0379	0.0955	0.2205
0.0362	0.0383	0.0374	0.0399	0.0090	0.3909	0.0092	0.0508	0.0379	0.0955	0.0087
0.0362	0.0399	0.0399	0.0358	0.0092	0.0092	0.3908	0.0508	0.1243	0.0091	0.0333
0.0316	0.0381	0.0381	0.0381	0.0508	0.0508	0.0508	0.3852	0.0094	0.0094	0.0566
0.0397	0.0415	0.0415	0.0419	0.0379	0.0379	0.1243	0.0094	0.4052	0.0095	0.1342
0.0397	0.0417	0.0417	0.0413	0.0955	0.0955	0.0091	0.0094	0.0095	0.4052	0.0095
0.0401	0.0835	0.0000	0.0415	0.2205	0.0087	0.0333	0.0566	0.1342	0.0095	0.6018
0.0398	0.0006	0.0829	0.0414	0.1239	0.0798	0.0172	0.0251	0.0511	0.2038	0.0000
0.0401	0.0421	0.0413	0.0416	0.1765	0.0091	0.0769	0.0566	0.0407	0.1031	0.0095
0.0387	0.0598	0.0207	0.0401	0.0822	0.0088	0.0815	0.1026	0.0249	0.0560	0.0435
0.0387	0.0207	0.0598	0.0401	0.0088	0.0822	0.0815	0.1026	0.0249	0.0560	0.0047
0.0387	0.0401	0.0401	0.0405	0.0815	0.0815	0.0095	0.1026	0.0716	0.0093	0.1721
0.0398	0.0401	0.0387	0.0387	0.0387						
0.0006	0.0421	0.0598	0.0207	0.0401						
0.0829	0.0413	0.0207	0.0598	0.0401						
0.0414	0.0416	0.0401	0.0401	0.0405						
0.1239	0.1765	0.0822	0.0088	0.0815						
0.0798	0.0091	0.0088	0.0822	0.0815						
0.0172	0.0769	0.0815	0.0815	0.0095						
0.0251	0.0566	0.1026	0.1026	0.1026						
0.0511	0.0407	0.0249	0.0249	0.0716						
0.2038	0.1031	0.0560	0.0560	0.0093						
0.0000	0.0095	0.0435	0.0047	0.1721						
0.6018	0.1342	0.0671	0.0237	0.0635						
0.1342	0.4052	0.1922	0.0093	0.0188						
0.0671	0.1922	0.4452	0.0069	0.0510						
0.0237	0.0093	0.0069	0.4452	0.0510						
0.0635	0.0188	0.0510	0.0510	0.4011						

SPECIAL J(PQ,RS) AND K(PS,RQ) INTEGRALS

2	3	5	6	-0.0007	-0.0007
4	2	7	5	-0.0085	0.0009
3	4	6	7	-0.0085	0.0009
2	3	6	5	-0.0007	-0.0033
2	4	7	5	-0.0085	-0.0017
3	4	7	6	-0.0085	-0.0017
2	3	9	10	0.0000	-0.0002
2	3	10	9	0.0000	-0.0002
2	3	11	12	0.0000	0.0000
4	2	13	11	0.0000	0.0000
3	4	12	13	0.1397	0.0337
2	3	12	11	0.0000	-0.0002
2	4	13	11	0.0000	0.0000
3	4	13	12	0.1397	0.0337
2	3	14	15	0.0002	0.0002
4	2	16	14	0.0809	0.0195
3	4	15	16	0.0809	0.0195
2	3	15	14	0.0002	0.0002
2	4	16	14	0.0809	0.0196
3	4	16	15	0.0809	0.0196
5	6	9	10	-0.0050	-0.0499
5	6	10	9	-0.0050	-0.0499
5	6	11	12	0.0000	0.0000
7	5	13	11	0.0000	0.0000
6	7	12	13	-0.0066	0.0003
5	6	12	11	0.0000	-0.0436
5	7	13	11	0.0000	0.0000
6	7	13	12	-0.0066	0.0003
5	6	14	15	-0.0038	-0.0038
7	5	16	14	0.0001	0.0689
6	7	15	16	0.0001	0.0689
5	6	15	14	-0.0038	-0.0682
5	7	16	14	0.0001	0.0045
6	7	16	15	0.0001	0.0045
9	10	11	12	0.0000	0.0000
9	10	12	11	0.0000	0.0000

9	10	14	15	-0.0027	-0.0270
9	10	15	14	-0.0027	-0.0270
11	12	14	15	0.0000	0.0000
13	11	16	14	0.0000	0.0000
12	13	15	16	0.0687	0.0037
11	12	15	14	0.0000	-0.0061
11	13	16	14	0.0000	0.0000
12	13	16	15	0.0687	0.0037

MOLECULE: SiF4 ATOM: Silicon 2p

AUGER SPECTRUM

CORE AND VALENCE I.P.S USED

2p3/2 111.700

4a1 40.600	3t2 39.300	3t2 39.300	3t2 39.300	4t2 19.500
4t2 19.500	4t2 19.500	5a1 21.500	1e 18.100	1e 18.100
1t1 16.400	1t1 16.400	1t1 16.400	5t2 17.500	5t2 17.500
5t2 17.500				

SPIN - ORBIT SPLITTING = 0.60 eV
CONTRIBUTIONS FROM 2p1/2 INITIAL HOLE ARE MARKED WITH *

PEAK NR.	MO.INDEX	MO.NAME		SYM	ABS.ENERGY	REL.ENERGY		ABS.RATE	REL.INT.
214	1112	1t1	1t1	*3T1	71.79	-39.9	0.0	0.0000000	0.0
213	1114	1t1	5t2	*3T1	71.44	-40.3	0.3	0.0000000	0.0
212	1112	1t1	1t1	3T1	71.19	-40.5	0.6	0.0000000	0.0
211	1114	1t1	5t2	3T1	70.84	-40.9	0.9	0.0000000	0.0
210	1114	1t1	5t2	*3T2	70.16	-41.5	1.6	0.0000000	0.0
209	911	1e	1t1	*3T2	69.90	-41.8	1.9	0.0000000	0.0
208	511	4t2	1t1	*3A1	69.56	-42.1	2.2	0.0000000	0.0
207	1114	1t1	5t2	3T2	69.56	-42.1	2.2	0.0000000	0.0
206	511	4t2	1t1	* 3E	69.38	-42.3	2.4	0.0000000	0.0
205	911	1e	1t1	3T2	69.30	-42.4	2.5	0.0000000	0.0
204	1112	1t1	1t1	*1T2	69.18	-42.5	2.6	0.0000000	0.0
203	514	4t2	5t2	*3A1	69.03	-42.7	2.8	0.0000000	0.0
202	511	4t2	1t1	3A1	68.96	-42.7	2.8	0.0000000	0.0
201	511	4t2	1t1	3E	68.78	-42.9	3.0	0.0000000	0.0
200	1112	1t1	1t1	1T2	68.58	-43.1	3.2	0.0000000	0.0
199	514	4t2	5t2	3A1	68.43	-43.3	3.4	0.0000000	0.0
198	1415	5t2	5t2	*3T1	68.15	-43.5	3.6	0.0000047	17.8
197	911	1e	1t1	*3T1	68.06	-43.6	3.7	0.0000000	0.0
196	511	4t2	1t1	*3T1	67.92	-43.8	3.9	0.0000000	0.0
195	914	1e	5t2	*3T1	67.91	-43.8	3.9	0.0000000	0.0
194	1114	1t1	5t2	* 3E	67.75	-44.0	4.0	0.0000000	0.0
193	1415	5t2	5t2	3T1	67.55	-44.1	4.2	0.0000094	35.6
192	911	1e	1t1	3T1	67.46	-44.2	4.3	0.0000000	0.0
191	511	4t2	1t1	3T1	67.32	-44.4	4.5	0.0000000	0.0
190	914	1e	5t2	3T1	67.31	-44.4	4.5	0.0000000	0.0
189	59	4t2	1e	*3T1	67.27	-44.4	4.5	0.0000000	0.0
188	511	4t2	1t1	*3T2	67.25	-44.4	4.5	0.0000000	0.0
187	1114	1t1	5t2	3E	67.15	-44.6	4.6	0.0000000	0.0
186	914	1e	5t2	*3T2	67.03	-44.7	4.8	0.0000000	0.0
185	514	4t2	5t2	*3T1	66.92	-44.8	4.9	0.0000132	50.0
184	1114	1t1	5t2	*1T1	66.78	-44.9	5.0	0.0000000	0.0
183	59	4t2	1e	3T1	66.67	-45.0	5.1	0.0000000	0.0
182	511	4t2	1t1	3T2	66.65	-45.0	5.1	0.0000000	0.0
181	1414	5t2	5t2	* 1E	66.57	-45.1	5.2	0.0000016	6.0
180	914	1e	5t2	3T2	66.43	-45.3	5.4	0.0000000	0.0
179	911	1e	1t1	*1T1	66.41	-45.3	5.4	0.0000000	0.0
178	514	4t2	5t2	3T1	66.32	-45.4	5.5	0.0000264	100.0
177	1114	1t1	5t2	* 1E	66.26	-45.4	5.5	0.0000000	0.0
176	1111	1t1	1t1	* 1E	66.21	-45.5	5.6	0.0000000	0.0
175	1114	1t1	5t2	1T1	66.18	-45.5	5.6	0.0000000	0.0
174	1415	5t2	5t2	*1T2	66.17	-45.5	5.6	0.0000024	9.0
173	1114	1t1	5t2	*3A1	65.98	-45.7	5.8	0.0000000	0.0
172	1414	5t2	5t2	1E	65.97	-45.7	5.8	0.0000032	12.0
171	514	4t2	5t2	*3T2	65.91	-45.8	5.9	0.0000000	0.0
170	910	1e	1e	*3A2	65.85	-45.9	5.9	0.0000000	0.0
169	911	1e	1t1	1T1	65.81	-45.9	6.0	0.0000000	0.0
168	914	1e	5t2	*1T2	65.72	-46.0	6.1	0.0000000	0.0
167	1114	1t1	5t2	1E	65.66	-46.0	6.1	0.0000000	0.0
166	814	5a1	5t2	*3T2	65.65	-46.0	6.1	0.0000083	31.5
165	59	4t2	1e	*3T2	65.65	-46.1	6.1	0.0000000	0.0
164	811	5a1	1t1	*3T2	65.62	-46.1	6.2	0.0000000	0.0
163	1111	1t1	1t1	1E	65.61	-46.1	6.2	0.0000000	0.0

162	1114	1t1	5t2	*1T2	65.58	-46.1	6.2	0.0000000	0.0
161	1415	5t2	5t2	1T2	65.57	-46.1	6.2	0.0000048	18.0
160	1114	1t1	5t2	3A1	65.38	-46.3	6.4	0.0000000	0.0
159	910	1e	1e	* 1E	65.33	-46.4	6.5	0.0000000	0.0
158	514	4t2	5t2	3T2	65.31	-46.4	6.5	0.0000000	0.0
157	514	4t2	5t2	* 3E	65.29	-46.4	6.5	0.0000004	1.4
156	910	1e	1e	3A2	65.25	-46.5	6.5	0.0000000	0.0
155	914	1e	5t2	1T2	65.12	-46.6	6.7	0.0000000	0.0
154	814	5a1	5t2	3T2	65.05	-46.6	6.7	0.0000166	63.0
153	59	4t2	1e	3T2	65.05	-46.7	6.7	0.0000000	0.0
152	811	5a1	1t1	3T2	65.02	-46.7	6.8	0.0000000	0.0
151	1114	1t1	5t2	1T2	64.98	-46.7	6.8	0.0000000	0.0
150	99	1e	1e	*1A1	64.82	-46.9	7.0	0.0000000	0.0
149	910	1e	1e	1E	64.73	-47.0	7.1	0.0000000	0.0
148	511	4t2	1t1	*1T2	64.69	-47.0	7.1	0.0000000	0.0
147	514	4t2	5t2	3E	64.69	-47.0	7.1	0.0000007	2.8
146	514	4t2	5t2	* 1E	64.56	-47.1	7.2	0.0000004	1.5
145	911	1e	1t1	*1T2	64.54	-47.2	7.3	0.0000000	0.0
144	1114	1t1	5t2	*1A1	64.29	-47.4	7.5	0.0000000	0.0
143	914	1e	5t2	*1T1	64.24	-47.5	7.6	0.0000000	0.0
142	99	1e	1e	1A1	64.22	-47.5	7.6	0.0000000	0.0
141	511	4t2	1t1	1T2	64.09	-47.6	7.7	0.0000000	0.0
140	514	4t2	5t2	1E	63.96	-47.7	7.8	0.0000008	3.0
139	911	1e	1t1	1T2	63.94	-47.8	7.9	0.0000000	0.0
138	514	4t2	5t2	*1T2	63.87	-47.8	7.9	0.0000006	2.4
137	511	4t2	1t1	*1T1	63.79	-47.9	8.0	0.0000000	0.0
136	1114	1t1	5t2	1A1	63.69	-48.0	8.1	0.0000000	0.0
135	914	1e	5t2	1T1	63.64	-48.1	8.2	0.0000000	0.0
134	1414	5t2	5t2	*1A1	63.61	-48.1	8.2	0.0000011	4.0
133	56	4t2	4t2	*3T1	63.41	-48.3	8.4	0.0000093	35.1
132	514	4t2	5t2	1T2	63.27	-48.4	8.5	0.0000013	4.8
131	511	4t2	1t1	1T1	63.19	-48.5	8.6	0.0000000	0.0
130	1414	5t2	5t2	1A1	63.01	-48.7	8.8	0.0000021	8.1
129	59	4t2	1e	*1T2	62.92	-48.8	8.9	0.0000000	0.0
128	55	4t2	4t2	* 1E	62.91	-48.8	8.9	0.0000031	11.8
127	56	4t2	4t2	*1T2	62.91	-48.8	8.9	0.0000047	17.7
126	56	4t2	4t2	3T1	62.81	-48.9	9.0	0.0000186	70.2
125	89	5a1	1e	* 3E	62.77	-48.9	9.0	0.0000000	0.0
124	514	4t2	5t2	*1T1	62.73	-49.0	9.1	0.0000060	22.8
123	511	4t2	1t1	*1A1	62.71	-49.0	9.1	0.0000000	0.0
122	811	5a1	1t1	*1T2	62.54	-49.2	9.3	0.0000000	0.0
121	511	4t2	1t1	* 1E	62.54	-49.2	9.3	0.0000000	0.0
120	58	4t2	5a1	* 3X	62.45	-49.2	9.3	0.0000117	44.2
119	59	4t2	1e	1T2	62.32	-49.4	9.5	0.0000000	0.0
118	55	4t2	4t2	1E	62.31	-49.4	9.5	0.0000063	23.7
117	56	4t2	4t2	1T2	62.31	-49.4	9.5	0.0000094	35.5
116	1111	1t1	1t1	*1A1	62.30	-49.4	9.5	0.0000000	0.0
115	89	5a1	1e	* 1E	62.26	-49.4	9.5	0.0000000	0.0
114	55	4t2	4t2	*1A1	62.17	-49.5	9.6	0.0000021	7.9
113	89	5a1	1e	3E	62.17	-49.5	9.6	0.0000000	0.0
112	514	4t2	5t2	1T1	62.13	-49.6	9.7	0.0000121	45.7
111	511	4t2	1t1	1A1	62.11	-49.6	9.7	0.0000000	0.0
110	811	5a1	1t1	1T2	61.94	-49.8	9.9	0.0000000	0.0
109	511	4t2	1t1	1E	61.94	-49.8	9.9	0.0000000	0.0
108	58	4t2	5a1	3X	61.85	-49.8	9.9	0.0000234	88.4
107	1111	1t1	1t1	1A1	61.70	-50.0	10.1	0.0000000	0.0
106	89	5a1	1e	1E	61.66	-50.0	10.1	0.0000000	0.0
105	55	4t2	4t2	1A1	61.57	-50.1	10.2	0.0000042	15.9
104	514	4t2	5t2	*1A1	61.02	-50.7	10.8	0.0000070	26.5
103	59	4t2	1e	*1T1	60.93	-50.8	10.9	0.0000000	0.0
102	514	4t2	5t2	1A1	60.42	-51.3	11.4	0.0000140	53.1
101	59	4t2	1e	1T1	60.33	-51.4	11.5	0.0000000	0.0
100	814	5a1	5t2	*1T2	60.07	-51.6	11.7	0.0000081	30.6
99	58	4t2	5a1	* 1X	59.68	-52.0	12.1	0.0000113	42.9
98	814	5a1	5t2	1T2	59.47	-52.2	12.3	0.0000162	61.1
97	58	4t2	5a1	1X	59.08	-52.6	12.7	0.0000227	85.8
96	88	5a1	5a1	*1A1	58.82	-52.9	13.0	0.0000030	11.4
95	88	5a1	5a1	1A1	58.22	-53.5	13.6	0.0000060	22.7
94	211	3t2	1t1	*3T1	49.31	-62.4	22.5	0.0000000	0.0
93	211	3t2	1t1	3T1	48.71	-63.0	23.1	0.0000000	0.0
92	211	3t2	1t1	*1T1	48.41	-63.3	23.4	0.0000000	0.0
91	211	3t2	1t1	1T1	47.81	-63.9	24.0	0.0000000	0.0
90	214	3t2	5t2	*3T1	47.75	-63.9	24.0	0.0000068	25.8
89	211	3t2	1t1	*3T2	47.39	-64.3	24.4	0.0000000	0.0
88	214	3t2	5t2	3T1	47.15	-64.5	24.6	0.0000136	51.6
87	211	3t2	1t1	3T2	46.79	-64.9	25.0	0.0000000	0.0
86	214	3t2	5t2	*1T1	46.64	-65.1	25.2	0.0000031	11.8
85	214	3t2	5t2	* 3E	46.09	-65.6	25.7	0.0000002	0.7
84	214	3t2	5t2	1T1	46.04	-65.7	25.8	0.0000062	23.6
83	111	4a1	1t1	*3T2	45.90	-65.8	25.9	0.0000000	0.0
82	211	3t2	1t1	* 3E	45.79	-65.9	26.0	0.0000000	0.0
81	214	3t2	5t2	*3T2	45.53	-66.2	26.3	0.0000000	0.0

80	214	3t2	5t2	3E	45.49	-66.2	26.3	0.0000004	1.4
79	29	3t2	1e	*3T1	45.48	-66.2	26.3	0.0000000	0.0
78	29	3t2	1e	*3T2	45.47	-66.2	26.3	0.0000000	0.0
77	111	4a1	1t1	3T2	45.30	-66.4	26.5	0.0000000	0.0
76	211	3t2	1t1	*1T2	45.27	-66.4	26.5	0.0000000	0.0
75	211	3t2	1t1	3E	45.19	-66.5	26.6	0.0000000	0.0
74	214	3t2	5t2	3T2	44.93	-66.8	26.9	0.0000000	0.0
73	29	3t2	1e	3T1	44.88	-66.8	26.9	0.0000000	0.0
72	29	3t2	1e	3T2	44.87	-66.8	26.9	0.0000000	0.0
71	114	4a1	5t2	*3T2	44.81	-66.9	27.0	0.0000033	12.4
70	211	3t2	1t1	1T2	44.67	-67.0	27.1	0.0000000	0.0
69	25	3t2	4t2	*3A1	44.66	-67.0	27.1	0.0000000	0.0
68	25	3t2	4t2	*3T2	44.24	-67.5	27.6	0.0000000	0.0
67	114	4a1	5t2	3T2	44.21	-67.5	27.6	0.0000066	24.9
66	19	4a1	1e	* 3E	44.19	-67.5	27.6	0.0000000	0.0
65	25	3t2	4t2	* 3E	44.15	-67.5	27.6	0.0000003	1.0
64	25	3t2	4t2	3A1	44.06	-67.6	27.7	0.0000000	0.0
63	25	3t2	4t2	*3T1	44.04	-67.7	27.8	0.0000096	36.2
62	214	3t2	5t2	* 1E	43.89	-67.8	27.9	0.0000002	0.8
61	111	4a1	1t1	*1T2	43.72	-68.0	28.1	0.0000000	0.0
60	25	3t2	4t2	3T2	43.64	-68.1	28.2	0.0000000	0.0
59	19	4a1	1e	3E	43.59	-68.1	28.2	0.0000000	0.0
58	25	3t2	4t2	3E	43.55	-68.1	28.2	0.0000005	2.0
57	25	3t2	4t2	3T1	43.44	-68.3	28.4	0.0000192	72.4
56	214	3t2	5t2	1E	43.29	-68.4	28.5	0.0000004	1.6
55	29	3t2	1e	*1T2	43.21	-68.5	28.6	0.0000000	0.0
54	29	3t2	1e	*1T1	43.20	-68.5	28.6	0.0000000	0.0
53	111	4a1	1t1	1T2	43.12	-68.6	28.7	0.0000000	0.0
52	214	3t2	5t2	*1T2	42.98	-68.7	28.8	0.0000003	1.2
51	15	4a1	4t2	*3T2	42.90	-68.8	28.9	0.0000046	17.5
50	211	3t2	1t1	*3A1	42.90	-68.8	28.9	0.0000000	0.0
49	214	3t2	5t2	*3A1	42.74	-69.0	29.0	0.0000000	0.0
48	114	4a1	5t2	*1T2	42.70	-69.0	29.1	0.0000032	12.1
47	211	3t2	1t1	* 1E	42.62	-69.1	29.2	0.0000000	0.0
46	25	3t2	4t2	*1A1	42.61	-69.1	29.2	0.0000051	19.2
45	29	3t2	1e	1T2	42.61	-69.1	29.2	0.0000000	0.0
44	29	3t2	1e	1T1	42.60	-69.1	29.2	0.0000000	0.0
43	214	3t2	5t2	1T2	42.38	-69.3	29.4	0.0000007	2.5
42	28	3t2	5a1	* 3X	42.32	-69.4	29.5	0.0000060	22.8
41	15	4a1	4t2	3T2	42.30	-69.4	29.5	0.0000092	35.0
40	211	3t2	1t1	3A1	42.30	-69.4	29.5	0.0000000	0.0
39	25	3t2	4t2	*1T2	42.22	-69.5	29.6	0.0000005	1.8
38	25	3t2	4t2	* 1E	42.16	-69.5	29.6	0.0000003	1.1
37	214	3t2	5t2	3A1	42.14	-69.6	29.6	0.0000000	0.0
36	114	4a1	5t2	1T2	42.10	-69.6	29.7	0.0000064	24.2
35	19	4a1	1e	* 1E	42.03	-69.7	29.8	0.0000000	0.0
34	211	3t2	1t1	1E	42.02	-69.7	29.8	0.0000000	0.0
33	25	3t2	4t2	1A1	42.01	-69.7	29.8	0.0000102	38.4
32	25	3t2	4t2	*1T1	41.78	-69.9	30.0	0.0000044	16.5
31	28	3t2	5a1	3X	41.72	-70.0	30.1	0.0000121	45.6
30	25	3t2	4t2	1T2	41.62	-70.1	30.2	0.0000009	3.5
29	25	3t2	4t2	1E	41.56	-70.1	30.2	0.0000006	2.2
28	19	4a1	1e	1E	41.43	-70.3	30.4	0.0000000	0.0
27	25	3t2	4t2	1T1	41.18	-70.5	30.6	0.0000087	33.1
26	15	4a1	4t2	*1T2	40.93	-70.8	30.9	0.0000045	17.0
25	18	4a1	5a1	* 3X	40.92	-70.8	30.9	0.0000000	0.0
24	15	4a1	4t2	1T2	40.33	-71.4	31.5	0.0000090	33.9
23	18	4a1	5a1	3X	40.32	-71.4	31.5	0.0000000	0.0
22	28	3t2	5a1	* 1X	40.24	-71.5	31.5	0.0000059	22.1
21	28	3t2	5a1	1X	39.64	-72.1	32.1	0.0000117	44.3
20	18	4a1	5a1	* 1X	39.20	-72.5	32.6	0.0000024	9.0
19	18	4a1	5a1	1X	38.60	-73.1	33.2	0.0000048	18.0
18	214	3t2	5t2	*1A1	38.42	-73.3	33.4	0.0000036	13.7
17	211	3t2	1t1	*1A1	37.90	-73.8	33.9	0.0000000	0.0
16	214	3t2	5t2	1A1	37.82	-73.9	34.0	0.0000072	27.4
15	211	3t2	1t1	1A1	37.30	-74.4	34.5	0.0000000	0.0
14	23	3t2	3t2	*3T1	27.59	-84.1	44.2	0.0000025	9.3
13	23	3t2	3t2	3T1	26.99	-84.7	44.8	0.0000049	18.7
12	12	4a1	3t2	*3T2	26.21	-85.5	45.6	0.0000024	9.0
11	12	4a1	3t2	3T2	25.61	-86.1	46.2	0.0000048	18.0
10	22	3t2	3t2	* 1E	23.24	-88.5	48.6	0.0000008	3.1
9	22	3t2	3t2	1E	22.64	-89.1	49.2	0.0000017	6.3
8	23	3t2	3t2	*1T2	21.80	-89.9	50.0	0.0000012	4.7
7	23	3t2	3t2	1T2	21.20	-90.5	50.6	0.0000025	9.4
6	11	4a1	4a1	*1A1	20.73	-91.0	51.1	0.0000005	1.8
5	11	4a1	4a1	1A1	20.13	-91.6	51.7	0.0000009	3.6
4	12	4a1	3t2	*1T2	17.78	-93.9	54.0	0.0000023	8.8
3	12	4a1	3t2	1T2	17.18	-94.5	54.6	0.0000046	17.5
2	22	3t2	3t2	*1A1	14.55	-97.2	57.2	0.0000006	2.1
1	22	3t2	3t2	1A1	13.95	-97.8	57.8	0.0000011	4.2

Total Transition Rate(au) = 5.20512E-04

D.6.2.2. Silicon tetrafluoride - F(KVV)*

```
        CALCULATIONS FOR SiF4, geom. LBII/15 p.96

  14       0.0000000       0.0000000       0.0000000
   9      -2.3978182       0.0000000      -1.6955135
   9       0.0000000      -2.3978182       1.6955135
   9       2.3978182       0.0000000      -1.6955135
   9       0.0000000       2.3978182       1.6955135
 DEGENERACY OF OCCUPIED ORBITALS
1 3 3 3 3 3 3 1 2 2 3 3 3 3 3 3


      EIGENVECTORS
-0.3165  0.0000  0.0000  0.0000  0.0000  0.0000  0.0000 -0.4392  0.0000  0.0000  0.0000
 0.0000  0.2558  0.0000  0.0000  0.3513  0.0000  0.0000  0.0000  0.0000  0.0000  0.0000
 0.0000  0.0000  0.2558  0.0000  0.0000  0.3513  0.0000  0.0000  0.0000  0.0000  0.0000
 0.0000  0.0000  0.0000  0.2558  0.0000  0.0000  0.3513  0.0000  0.0000  0.0000  0.0000
-0.4725 -0.6821  0.0000 -0.4823  0.1085  0.0000  0.0767  0.1112  0.0000  0.0000  0.0000
-0.0334 -0.0064  0.0000 -0.0284 -0.1214  0.0000 -0.4255 -0.3553 -0.2887  0.0000  0.0000
 0.0000  0.0000  0.0337  0.0000  0.0000  0.4804  0.0000  0.0000  0.0000  0.5000  0.0000
-0.0236 -0.0284  0.0000  0.0137 -0.4255  0.0000  0.1795 -0.2513  0.4082  0.0000 -0.7071
-0.4725  0.0000 -0.6821  0.4823  0.0000  0.1085 -0.0767  0.1112  0.0000  0.0000  0.0000
 0.0000  0.0337  0.0000  0.0000  0.4804  0.0000  0.0000  0.0000  0.0000  0.5000  0.0000
-0.0334  0.0000 -0.0064  0.0284  0.0000 -0.1214  0.4255 -0.3553 -0.2887  0.0000  0.0000
 0.0236  0.0000  0.0284  0.0137  0.0000  0.4255  0.1795  0.2513 -0.4083  0.0000  0.0000
-0.4725  0.6821  0.0000 -0.4823 -0.1085  0.0000  0.0767  0.1112  0.0000  0.0000  0.0000
 0.0334 -0.0064  0.0000  0.0284 -0.1214  0.0000  0.4255  0.3553  0.2887  0.0000  0.0000
 0.0000  0.0000  0.0337  0.0000  0.0000  0.4804  0.0000  0.0000  0.0000 -0.5000  0.0000
-0.0236  0.0284  0.0000  0.0137  0.4255  0.0000  0.1795 -0.2513  0.4082  0.0000  0.7071
-0.4725  0.0000  0.6821  0.4823  0.0000 -0.1085 -0.0767  0.1112  0.0000  0.0000  0.0000
 0.0000  0.0337  0.0000  0.0000  0.4804  0.0000  0.0000  0.0000  0.0000 -0.5000  0.0000
 0.0334  0.0000 -0.0064 -0.0284  0.0000 -0.1213 -0.4255  0.3553  0.2887  0.0000  0.0000
 0.0236  0.0000 -0.0284  0.0137  0.0000 -0.4255  0.1795  0.2513 -0.4082  0.0000  0.0000
 0.0000  0.0000  0.0000  0.0000  0.0000
 0.0000  0.0000  0.1644  0.0000  0.0000
 0.0000  0.0000  0.0000  0.1644  0.0000
 0.0000  0.0000  0.0000  0.0000  0.1644
 0.0000  0.0000  0.0254  0.0000  0.0179
 0.0000 -0.5000 -0.5792  0.0000 -0.1596
 0.0000  0.0000  0.0000 -0.3535  0.0000
 0.0000  0.0000 -0.1596  0.0000 -0.4663
 0.0000  0.0000  0.0000  0.0254 -0.0179
-0.5774  0.5000 -0.3535  0.0000  0.0000
 0.0000  0.0000  0.0000 -0.5792  0.1596
-0.4082  0.0000  0.0000  0.1596 -0.4663
 0.0000  0.0000 -0.0254  0.0000  0.0179
 0.0000 -0.5000 -0.5792  0.0000  0.1596
 0.0000  0.0000  0.0000 -0.3535  0.0000
 0.0000  0.0000  0.1596  0.0000 -0.4663
 0.0000  0.0000  0.0000 -0.0254 -0.0179
 0.5773  0.5000 -0.3535  0.0000  0.0000
 0.0000  0.0000  0.0000 -0.5792 -0.1596
 0.4082  0.0000  0.0000 -0.1596 -0.4663


   MOLECULAR J(PP,QQ) COULOMB INTEGRALS
 0.3812  0.3824  0.3824  0.3824  0.3778  0.3778  0.3778  0.3725  0.3856  0.3856  0.3856
 0.3824  0.5439  0.2249  0.3840  0.3716  0.3885  0.3807  0.3755  0.3880  0.3880  0.5592
 0.3824  0.2249  0.5439  0.3840  0.3885  0.3716  0.3807  0.3755  0.3880  0.3880  0.2168
 0.3824  0.3840  0.3840  0.3848  0.3807  0.3807  0.3793  0.3755  0.3880  0.3880  0.3880
 0.3778  0.3716  0.3885  0.3807  0.3909  0.3726  0.3727  0.3760  0.3815  0.3874  0.3842
 0.3778  0.3885  0.3716  0.3807  0.3726  0.3909  0.3727  0.3760  0.3815  0.3874  0.3867
 0.3778  0.3807  0.3807  0.3793  0.3727  0.3727  0.3908  0.3760  0.3903  0.3786  0.3810
 0.3725  0.3755  0.3755  0.3755  0.3760  0.3760  0.3760  0.3852  0.3744  0.3744  0.3792
 0.3856  0.3880  0.3880  0.3880  0.3815  0.3815  0.3903  0.3744  0.4052  0.3862  0.3988
 0.3856  0.3880  0.3880  0.3880  0.3874  0.3874  0.3786  0.3744  0.3862  0.4052  0.3862
 0.3856  0.5592  0.2168  0.3880  0.3842  0.3867  0.3810  0.3792  0.3988  0.3862  0.6018
 0.3856  0.2169  0.5591  0.3880  0.3984  0.3751  0.3794  0.3760  0.3904  0.3988  0.2085
 0.3856  0.3880  0.3880  0.3880  0.3879  0.3786  0.3855  0.3792  0.3894  0.3957  0.3862
 0.3838  0.4672  0.3054  0.3861  0.3814  0.3812  0.3851  0.3836  0.3861  0.3893  0.4705
 0.3838  0.3054  0.4672  0.3861  0.3812  0.3814  0.3851  0.3836  0.3861  0.3893  0.3004
 0.3838  0.3861  0.3861  0.3865  0.3851  0.3851  0.3775  0.3836  0.3908  0.3845  0.4010
 0.3856  0.3856  0.3838  0.3838  0.3838
 0.2169  0.3880  0.4672  0.3054  0.3861
 0.5591  0.3880  0.3054  0.4672  0.3861
 0.3880  0.3880  0.3861  0.3861  0.3865
 0.3984  0.3879  0.3814  0.3812  0.3851
 0.3751  0.3786  0.3812  0.3814  0.3851
 0.3794  0.3855  0.3851  0.3851  0.3775
 0.3760  0.3792  0.3836  0.3836  0.3836
```

```
0.3904   0.3894   0.3861   0.3861   0.3908
0.3988   0.3957   0.3893   0.3893   0.3845
0.2085   0.3862   0.4705   0.3004   0.4010
0.6018   0.3988   0.3067   0.4693   0.3900
0.3988   0.4052   0.4020   0.3845   0.3855
0.3067   0.4020   0.4452   0.3431   0.3873
0.4693   0.3845   0.3431   0.4452   0.3873
0.3900   0.3855   0.3873   0.3873   0.4011
```

MOLECULAR K(PQ,PQ) EXCHANGE INTEGRALS

```
0.3812   0.1548   0.1548   0.1548   0.0362   0.0362   0.0362   0.0316   0.0397   0.0397   0.0401
0.1548   0.5439   0.0004   0.1595   0.0374   0.0383   0.0399   0.0381   0.0415   0.0417   0.0835
0.1548   0.0004   0.5439   0.1595   0.0383   0.0374   0.0399   0.0381   0.0415   0.0417   0.0000
0.1548   0.1595   0.1595   0.3848   0.0399   0.0399   0.0358   0.0381   0.0419   0.0413   0.0415
0.0362   0.0374   0.0383   0.0399   0.3909   0.0090   0.0092   0.0508   0.0379   0.0955   0.2205
0.0362   0.0383   0.0374   0.0399   0.0090   0.3909   0.0092   0.0508   0.0379   0.0955   0.0087
0.0362   0.0399   0.0399   0.0358   0.0092   0.0092   0.3908   0.0508   0.1243   0.0091   0.0333
0.0316   0.0381   0.0381   0.0381   0.0508   0.0508   0.0508   0.3852   0.0094   0.0094   0.0566
0.0397   0.0415   0.0415   0.0419   0.0379   0.0379   0.1243   0.0094   0.4052   0.0095   0.1342
0.0397   0.0417   0.0417   0.0413   0.0955   0.0955   0.0091   0.0094   0.0095   0.4052   0.0095
0.0401   0.0835   0.0000   0.0415   0.2205   0.0087   0.0333   0.0566   0.1342   0.0095   0.6018
0.0398   0.0006   0.0829   0.0414   0.1239   0.0798   0.0172   0.0251   0.0511   0.2038   0.0000
0.0401   0.0421   0.0413   0.0416   0.1765   0.0091   0.0769   0.0566   0.0407   0.1031   0.0095
0.0387   0.0598   0.0207   0.0401   0.0822   0.0088   0.0815   0.1026   0.0249   0.0560   0.0435
0.0387   0.0207   0.0598   0.0401   0.0088   0.0822   0.0815   0.1026   0.0249   0.0560   0.0047
0.0387   0.0401   0.0401   0.0405   0.0815   0.0815   0.0095   0.1026   0.0716   0.0093   0.1721
0.0398   0.0401   0.0387   0.0387   0.0387
0.0006   0.0421   0.0598   0.0207   0.0401
0.0829   0.0413   0.0207   0.0598   0.0401
0.0414   0.0416   0.0401   0.0401   0.0405
0.1239   0.1765   0.0822   0.0088   0.0815
0.0798   0.0091   0.0088   0.0822   0.0815
0.0172   0.0769   0.0815   0.0815   0.0095
0.0251   0.0566   0.1026   0.1026   0.1026
0.0511   0.0407   0.0249   0.0249   0.0716
0.2038   0.1031   0.0560   0.0560   0.0093
0.0000   0.0095   0.0435   0.0047   0.1721
0.6018   0.1342   0.0671   0.0237   0.0635
0.1342   0.4052   0.1922   0.0093   0.0188
0.0671   0.1922   0.4452   0.0069   0.0510
0.0237   0.0093   0.0069   0.4452   0.0510
0.0635   0.0188   0.0510   0.0510   0.4011
```

SPECIAL J(PQ,RS) AND K(PS,RQ) INTEGRALS

```
 2    3    5    6   -0.0007   -0.0007
 4    2    7    5   -0.0085    0.0009
 3    4    6    7   -0.0085    0.0009
 2    3    6    5   -0.0007   -0.0033
 2    4    7    5   -0.0085   -0.0017
 3    4    7    6   -0.0085   -0.0017
 2    3    9   10    0.0000   -0.0002
 2    3   10    9    0.0000   -0.0002
 2    3   11   12    0.0000    0.0000
 4    2   13   11    0.0000    0.0000
 3    4   12   13    0.1397    0.0337
 2    3   12   11    0.0000   -0.0002
 2    4   13   11    0.0000    0.0000
 3    4   13   12    0.1397    0.0337
 2    3   14   15    0.0002    0.0002
 4    2   16   14    0.0809    0.0195
 3    4   15   16    0.0809    0.0195
 2    3   15   14    0.0002    0.0002
 2    4   16   14    0.0809    0.0196
 3    4   16   15    0.0809    0.0196
 5    6    9   10   -0.0050   -0.0499
 5    6   10    9   -0.0050   -0.0499
 5    6   11   12    0.0000    0.0000
 7    5   13   11    0.0000    0.0000
 6    7   12   13   -0.0066    0.0003
 5    6   12   11    0.0000   -0.0436
 5    7   13   11    0.0000    0.0000
 6    7   13   12   -0.0066    0.0003
 5    6   14   15   -0.0038   -0.0038
 7    5   16   14    0.0001    0.0689
 6    7   15   16    0.0001    0.0689
 5    6   15   14   -0.0038   -0.0682
 5    7   16   14    0.0001    0.0045
 6    7   16   15    0.0001    0.0045
 9   10   11   12    0.0000    0.0000
 9   10   12   11    0.0000    0.0000
```

9	10	14	15	-0.0027	-0.0270
9	10	15	14	-0.0027	-0.0270
11	12	14	15	0.0000	0.0000
13	11	16	14	0.0000	0.0000
12	13	15	16	0.0687	0.0037
11	12	15	14	0.0000	-0.0061
11	13	16	14	0.0000	0.0000
12	13	16	15	0.0687	0.0037

MOLECULE: SiF4 ATOM: Fluorine 1

AUGER SPECTRUM

CORE AND VALENCE I.P.S USED

1s 695.100
4a1 40.600 3t2 39.300 3t2 39.300 3t2 39.300 4t2 19.500
4t2 19.500 4t2 19.500 5a1 21.500 1e 18.100 1e 18.100
1t1 16.400 1t1 16.400 1t1 16.400 5t2 17.500 5t2 17.500
5t2 17.500

PEAK NR.	MO.INDEX	MO.NAME		SYM	ABS.ENERGY	REL.ENERGY		ABS.RATE	REL.INT.
107	1112	1t1	1t1	3T1	654.59	-40.5	0.0	0.0000000	0.0
106	1114	1t1	5t2	3T1	654.24	-40.9	0.3	0.0000000	0.0
105	1114	1t1	5t2	3T2	652.96	-42.1	1.6	0.0000000	0.0
104	911	1e	1t1	3T2	652.70	-42.4	1.9	0.0000000	0.0
103	511	4t2	1t1	3A1	652.36	-42.7	2.2	0.0000005	0.2
102	511	4t2	1t1	3E	652.18	-42.9	2.4	0.0000009	0.4
101	1112	1t1	1t1	1T2	651.98	-43.1	2.6	0.0001317	50.9
100	514	4t2	5t2	3A1	651.83	-43.3	2.8	0.0000004	0.2
99	1415	5t2	5t2	3T1	650.95	-44.1	3.6	0.0000000	0.0
98	911	1e	1t1	3T1	650.86	-44.2	3.7	0.0000000	0.0
97	511	4t2	1t1	3T1	650.72	-44.4	3.9	0.0000006	0.2
96	914	1e	5t2	3T1	650.71	-44.4	3.9	0.0000000	0.0
95	1114	1t1	5t2	3E	650.55	-44.6	4.0	0.0000001	0.0
94	59	4t2	1e	3T1	650.07	-45.0	4.5	0.0000003	0.1
93	511	4t2	1t1	3T2	650.05	-45.0	4.5	0.0000006	0.2
92	914	1e	5t2	3T2	649.83	-45.3	4.8	0.0000001	0.0
91	514	4t2	5t2	3T1	649.72	-45.4	4.9	0.0000002	0.1
90	1114	1t1	5t2	1T1	649.58	-45.5	5.0	0.0002525	97.6
89	1414	5t2	5t2	1E	649.37	-45.7	5.2	0.0001184	45.8
88	911	1e	1t1	1T1	649.21	-45.9	5.4	0.0000658	25.4
87	1114	1t1	5t2	1E	649.06	-46.0	5.5	0.0001130	43.7
86	1111	1t1	1t1	1E	649.01	-46.1	5.6	0.0001921	74.2
85	1415	5t2	5t2	1T2	648.97	-46.1	5.6	0.0001892	73.1
84	1114	1t1	5t2	3A1	648.78	-46.3	5.8	0.0000000	0.0
83	514	4t2	5t2	3T2	648.71	-46.4	5.9	0.0000009	0.4
82	910	1e	1e	3A2	648.65	-46.5	5.9	0.0000000	0.0
81	914	1e	5t2	1T2	648.52	-46.6	6.1	0.0001859	71.8
80	814	5a1	5t2	3T2	648.45	-46.6	6.1	0.0000014	0.5
79	59	4t2	1e	3T2	648.45	-46.7	6.1	0.0000008	0.3
78	811	5a1	1t1	3T2	648.42	-46.7	6.2	0.0000018	0.7
77	1114	1t1	5t2	1T2	648.38	-46.7	6.2	0.0001880	72.6
76	910	1e	1e	1E	648.13	-47.0	6.5	0.0001317	50.9
75	514	4t2	5t2	3E	648.09	-47.0	6.5	0.0000006	0.2
74	99	1e	1e	1A1	647.62	-47.5	7.0	0.0000385	14.9
73	511	4t2	1t1	1T2	647.49	-47.6	7.1	0.0002518	97.3
72	514	4t2	5t2	1E	647.36	-47.7	7.2	0.0001000	38.7
71	911	1e	1t1	1T2	647.34	-47.8	7.3	0.0002103	81.3
70	1114	1t1	5t2	1A1	647.09	-48.0	7.5	0.0001531	59.2
69	914	1e	5t2	1T1	647.04	-48.1	7.6	0.0000830	32.1
68	514	4t2	5t2	1T2	646.67	-48.4	7.9	0.0001481	57.2
67	511	4t2	1t1	1T1	646.59	-48.5	8.0	0.0001102	42.6
66	1414	5t2	5t2	1A1	646.41	-48.7	8.2	0.0000528	20.4
65	56	4t2	4t2	3T1	646.21	-48.9	8.4	0.0000005	0.2
64	59	4t2	1e	1T2	645.72	-49.4	8.9	0.0001598	61.8
63	55	4t2	4t2	1E	645.71	-49.4	8.9	0.0000990	38.3
62	56	4t2	4t2	1T2	645.71	-49.4	8.9	0.0001487	57.5
61	89	5a1	1e	3E	645.57	-49.5	9.0	0.0000012	0.5
60	514	4t2	5t2	1T1	645.53	-49.6	9.1	0.0002468	95.4
59	511	4t2	1t1	1A1	645.51	-49.6	9.1	0.0000584	22.6
58	811	5a1	1t1	1T2	645.34	-49.8	9.3	0.0001943	75.1
57	511	4t2	1t1	1E	645.34	-49.8	9.3	0.0001992	77.0
56	58	4t2	5a1	3X	645.25	-49.8	9.3	0.0000011	0.4
55	1111	1t1	1t1	1A1	645.10	-50.0	9.5	0.0000687	26.6
54	89	5a1	1e	1E	645.06	-50.0	9.5	0.0001036	40.0
53	55	4t2	4t2	1A1	644.97	-50.1	9.6	0.0000176	6.8
52	514	4t2	5t2	1A1	643.82	-51.3	10.8	0.0001025	39.6
51	59	4t2	1e	1T1	643.73	-51.4	10.9	0.0000943	36.4
50	814	5a1	5t2	1T2	642.87	-52.2	11.7	0.0002070	80.0

49	58	4t2	5a1	1X	642.48	-52.6	12.1	0.0001556	60.2
48	88	5a1	5a1	1A1	641.62	-53.5	13.0	0.0000314	12.2
47	211	3t2	1t1	3T1	632.11	-63.0	22.5	0.0000223	8.6
46	211	3t2	1t1	1T1	631.21	-63.9	23.4	0.0000733	28.3
45	214	3t2	5t2	3T1	630.55	-64.5	24.0	0.0000169	6.5
44	211	3t2	1t1	3T2	630.19	-64.9	24.4	0.0000223	8.6
43	214	3t2	5t2	1T1	629.44	-65.7	25.2	0.0000553	21.4
42	214	3t2	5t2	3E	628.89	-66.2	25.7	0.0000217	8.4
41	111	4a1	1t1	3T2	628.70	-66.4	25.9	0.0000322	12.4
40	211	3t2	1t1	3E	628.59	-66.5	26.0	0.0000372	14.4
39	214	3t2	5t2	3T2	628.33	-66.8	26.3	0.0000378	14.6
38	29	3t2	1e	3T1	628.28	-66.8	26.3	0.0000112	4.3
37	29	3t2	1e	3T2	628.27	-66.8	26.3	0.0000335	12.9
36	211	3t2	1t1	1T2	628.07	-67.0	26.5	0.0000739	28.6
35	114	4a1	5t2	3T2	627.61	-67.5	27.0	0.0000314	12.1
34	25	3t2	4t2	3A1	627.46	-67.6	27.1	0.0000081	3.1
33	25	3t2	4t2	3T2	627.04	-68.1	27.6	0.0000284	11.0
32	19	4a1	1e	3E	626.99	-68.1	27.6	0.0000214	8.3
31	25	3t2	4t2	3E	626.95	-68.1	27.6	0.0000195	7.5
30	25	3t2	4t2	3T1	626.84	-68.3	27.8	0.0000302	11.7
29	214	3t2	5t2	1E	626.69	-68.4	27.9	0.0000717	27.7
28	111	4a1	1t1	1T2	626.52	-68.6	28.1	0.0001064	41.1
27	29	3t2	1e	1T2	626.01	-69.1	28.6	0.0001098	42.4
26	29	3t2	1e	1T1	626.00	-69.1	28.6	0.0000389	15.0
25	214	3t2	5t2	1T2	625.78	-69.3	28.8	0.0001247	48.2
24	15	4a1	4t2	3T2	625.70	-69.4	28.9	0.0000278	10.8
23	211	3t2	1t1	3A1	625.70	-69.4	28.9	0.0000186	7.2
22	214	3t2	5t2	3A1	625.54	-69.6	29.0	0.0000214	8.3
21	114	4a1	5t2	1T2	625.50	-69.6	29.1	0.0001039	40.1
20	211	3t2	1t1	1E	625.42	-69.7	29.2	0.0001221	47.2
19	25	3t2	4t2	1A1	625.41	-69.7	29.2	0.0000345	13.3
18	28	3t2	5a1	3X	625.12	-70.0	29.5	0.0000258	10.0
17	25	3t2	4t2	1T2	625.02	-70.1	29.6	0.0000986	38.1
16	25	3t2	4t2	1E	624.96	-70.1	29.6	0.0000660	25.5
15	19	4a1	1e	1E	624.83	-70.3	29.8	0.0000707	27.3
14	25	3t2	4t2	1T1	624.58	-70.5	30.0	0.0001030	39.8
13	15	4a1	4t2	1T2	623.73	-71.4	30.9	0.0000972	37.6
12	18	4a1	5a1	3X	623.72	-71.4	30.9	0.0000085	3.3
11	28	3t2	5a1	1X	623.04	-72.1	31.5	0.0000977	37.8
10	18	4a1	5a1	1X	622.00	-73.1	32.6	0.0000316	12.2
9	214	3t2	5t2	1A1	621.22	-73.9	33.4	0.0000702	27.1
8	211	3t2	1t1	1A1	620.70	-74.4	33.9	0.0000609	23.5
7	23	3t2	3t2	3T1	610.39	-84.7	44.2	0.0000001	0.0
6	12	4a1	3t2	3T2	609.01	-86.1	45.6	0.0000002	0.1
5	22	3t2	3t2	1E	606.04	-89.1	48.6	0.0000901	34.8
4	23	3t2	3t2	1T2	604.60	-90.5	50.0	0.0001799	69.5
3	11	4a1	4a1	1A1	603.53	-91.6	51.1	0.0000414	16.0
2	12	4a1	3t2	1T2	600.58	-94.5	54.0	0.0002588	100.0
1	22	3t2	3t2	1A1	597.35	-97.8	57.2	0.0001340	51.8

Total Transition Rate (in au) = 7.406341799383E-03